DOCTOR OF PHILOSOPHY

Characterisation of human PRDM9 and TEX19 as potential oncogenic cancer testis genes

Alsulami, Afrah

Award date:
2020

Awarding institution:
Bangor University

Link to publication

Characterisation of human *PRDM9* and *TEX19* as potential oncogenic cancer testis genes

Ph.d. Thesis 2019
Afrah A. Alsulami

Declaration and Consent

Details of the Work

I hereby agree to deposit the following item in the digital repository maintained by Bangor University and/or in any other repository authorized for use by Bangor University.

Author Name:

…………………………………………………………………………………………………

Title:

……………………………………………………………………………………….………

Supervisor/Department:

....

Funding body (if any):

....

Qualification/Degree obtained:

……………………………………………………………………

This item is a product of my own research endeavours and is covered by the agreement below in which the item is referred to as "the Work". It is identical in content to that deposited in the Library, subject to point 4 below.

Non-exclusive Rights

Rights granted to the digital repository through this agreement are entirely non-exclusive. I am free to publish the Work in its present version or future versions elsewhere.

I agree that Bangor University may electronically store, copy or translate the Work to any approved medium or format for the purpose of future preservation and accessibility. Bangor University is not under any obligation to reproduce or display the Work in the same formats or resolutions in which it was originally deposited.

Bangor University Digital Repository

I understand that work deposited in the digital repository will be accessible to a wide variety of people and institutions, including automated agents and search engines via the World Wide Web.

I understand that once the Work is deposited, the item and its metadata may be incorporated into public access catalogues or services, national databases of

electronic theses and dissertations such as the British Library's EThOS or any service provided by the National Library of Wales.

I understand that the Work may be made available via the National Library of Wales Online Electronic Theses Service under the declared terms and conditions of use (http://www.llgc.org.uk/index.php?id=4676). I agree that as part of this service the National Library of Wales may electronically store, copy or convert the Work to any approved medium or format for the purpose of future preservation and accessibility. The National Library of Wales is not under any obligation to reproduce or display the Work in the same formats or resolutions in which it was originally deposited.

Statement 1:

This work has not previously been accepted in substance for any degree and is not being concurrently submitted in candidature for any degree unless as agreed by the University for approved dual awards.

Signed …………………………………….. (candidate)

Date …………………………………………..

Statement 2:

This thesis is the result of my own investigations, except where otherwise stated. Where correction services have been used, the extent and nature of the correction is clearly marked in a footnote(s).

All other sources are acknowledged by footnotes and/or a bibliography.

Signed …………………………………………. (candidate)

Date ………………………………………….

Statement 3:

I hereby give consent for my thesis, if accepted, to be available for photocopying, for inter-library loan and for electronic storage (subject to any constraints as defined in statement 4), and for the title and summary to be made available to outside organisations.

Signed …………………………………………. (candidate)

Date ………………………………………….

NB: Candidates on whose behalf a bar on access has been approved by the Academic Registry should use the following version of **Statement 3:**

<u>**Statement 3 (bar):**</u>

I hereby give consent for my thesis, if accepted, to be available for photocopying, for inter-library loans and for electronic storage (subject to any constraints as defined in statement 4), after expiry of a bar on access.

Signed ………………………………………… (candidate)

Date ………………………………………………

<u>**Statement 4:**</u>

Choose **one** of the following options

a) I agree to deposit an electronic copy of my thesis (the Work) in the Bangor University (BU) Institutional Digital Repository, the British Library ETHOS system, and/or in any other repository authorized for use by Bangor University and where necessary have gained the required permissions for the use of third party material.	
b) I agree to deposit an electronic copy of my thesis (the Work) in the Bangor University (BU) Institutional Digital Repository, the British Library ETHOS system, and/or in any other repository authorized for use by Bangor University when the approved **bar on access** has been lifted.	
c) I agree to submit my thesis (the Work) electronically via Bangor University's e-submission system, however I **opt-out** of the electronic deposit to the Bangor University (BU) Institutional Digital Repository, the British Library ETHOS system, and/or in any other repository authorized for use by Bangor University, due to lack of permissions for use of third party material.	

Options B should only be used if a bar on access has been approved by the University.

In addition to the above I also agree to the following:

1. That I am the author or have the authority of the author(s) to make this agreement and do hereby give Bangor University the right to make available the Work in the way described above.

2. That the electronic copy of the Work deposited in the digital repository and covered by this agreement, is identical in content to the paper copy of the Work deposited in the Bangor University Library, subject to point 4 below.

3. That I have exercised reasonable care to ensure that the Work is original and, to the best of my knowledge, does not breach any laws – including those relating to defamation, libel and copyright.

4. That I have, in instances where the intellectual property of other authors or copyright holders is included in the Work, and where appropriate, gained explicit permission for the inclusion of that material in the Work, and in the electronic form of the Work as accessed through the open access digital repository, *or* that I have identified and removed that material for which adequate and appropriate permission has not been obtained and which will be inaccessible via the digital repository.

5. That Bangor University does not hold any obligation to take legal action on behalf of the Depositor, or other rights holders, in the event of a breach of intellectual property rights, or any other right, in the material deposited.

6. That I will indemnify and keep indemnified Bangor University and the National Library of Wales from and against any loss, liability, claim or damage, including without limitation any related legal fees and court costs (on a full indemnity bases), related to any breach by myself of any term of this agreement.

Signature: …………………………………………………… Date :

…………………………………………….

Abstract

Cancer is a complex disease that is considered one of the leading causes of the world-wide death. Through genetic and/or epigenetic changes, cancer cells acquire many abnormal characteristics that trigger tumour growth, spread and avoidance of immunologic and therapeutic targeting. One of the key features that characterises many cancers is the re-activation of a group of genes that are normally only expressed during distinct developmental processes, including germline genes. Cancer/testis (CT) genes are a group of germline genes that have expression normally restricted to testicular germ cells but are aberrantly activated in a wide range of tumours. The activation of CT genes in cancer cells has been reported to contribute to oncogenic function. Given this, understanding this class of genes is important in the field of cancer biology. This current study focused on exploring the functional roles of two germ-cell specific genes that are activated in a variety of tumours, *PRDM9* and *TEX19*.

PRDM9 is a histone methyltransferase activator of meiotic recombination hotspots. Its murine orthologue, *Meisetz*, activates meiotic recombination and acts as a transcriptional regulator for many meiosis genes. Human *PRDM9* is a meiosis-specific gene that is normally expressed in the early stages of the meiotic prophase. Data obtained in this study suggests that human *PRDM9* may influence cellular proliferation and acts as a transcriptional regulator for other germline genes in cancerous cells.

TEX19 is a mammalian specific gene. TEX19 plays important roles in pluripotency and the self-renewal potential of germ cells, although its exact function remains unclear. More recently, human TEX19 has been reported to potentially serve to maintain the proliferative state in cancer cells. In this study, we found that depletion of TEX19 had a significant influence on cancer cell proliferation. Furthermore, we suggest that TEX19 may regulate histone acetylation.

Acknowledgement

I am thrilled to have had the opportunity to complete this work. I would like to thank ALLAH for giving me the power and patience to complete this important step in my educational and professional life.

I owe my deepest gratitude to my supervisor Dr Ramsay McFarlane. Without his continuous optimism concerning this work, and his enthusiasm, guidance and support throughout the research and during the writing of this thesis, this study would probably have never been completed. Nobody could have wished for better supervision. Special thanks and appreciation to Dr Jane Wakeman for sharing her experience, constructive advice and firm support during my study.

I am grateful to all members of the McFarlane laboratory, past and present, who have shared scientific knowledge and technical support as well as good company with me along the way, particularly to, Dr Natalia Gomez-Escobar and Dr Ellen Vernon who was always already to offer friendly and generous discussion and for their effort in results assessment.

I am deeply grateful to my husband Mishal, for his constant love and endless support, encouragement and patience. My love to you and our boy, Abdulaziz. Last but not least, it gives me great pleasure to acknowledge the help and support of my mother, father and my sibling. I am very grateful to my friends for their unwavering belief in me and for supporting my dreams and my goals.

Without these people, I could never have completed this project. I really appreciate their help, most deeply and sincerely.

Thank you all.

Afrah A. Alsulami

List of abbreviations

°C	Degrees Centigrade
3'	Three prime end of DNA
5'	Five prime end of DNA
acetyl-CoA	acetyl coenzyme A
ACRBP	Acrosin-binding protein
ActB	Beta Actin
AEs	The axial elements
ALT	alternative lengthening of telomere
amp	Ampicillin
ASC	Adult stem cells
ATCC	the American Type Culture Collection
BBB	Blood-brain barrier
BCA	Bicinchoninic acid
BLAST	Basic Local Alignment Search Tool
BLM	Bloom syndrome protein
bp	Base pair
BRCA1	Breast cancer susceptibility 1
BRCA2	Breast cancer susceptibility 2
BSA	Bovine serum albumin
BSP	bisulphite sequencing PCR
BTB	Blood-testis barrier
C-terminal	Carboxy-terminal domain
CD	Cluster of Differentiation
CDK	Cyclin dependent kinase
cDNA	Complementary DNA
CDS	Coding DNA sequence
CE	Central element
CG	Cancer germline genes
CNS	Central nervous system
CO	Crossover event
CpG	-Cytosine-phosphate-guanine-
Cq	Quantification cycle
CRC	Colorectal Cancer
CSC	Cancer Stem Cell

CT	Cancer-testis
CTA	Cancer testis antigen
CTLs	Cytotoxic T lymphocytes
D-loop	Disassociation loop
dH2O	Distilled water
dHJ	Double-Holliday junction
DMC1	Disrupted meiotic cDNA1
DMEM	Dulbecco's Modified Eagle Medium
DMSO	Dimethyl sulphoxide
DNA	Deoxyribonucleic acid
DNMT	DNA methyltransferase
DNMTi	DNA methyltransferase inhibitor
DPBS	Dulbecco's phosphate-buffered
DSB	Double-strand break
EB	Elution buffer
ECACC	European Collection of Cell Cultures
ECL	Enhanced chemiluminescence
ES/ESC	Embryonic stem cells
EST	Expressed sequence tag
F	Forward
FBS	Foetal bovine serum
g	Gram
G0	quiescent phase
G1	Gap-1 phase
G2	Gap-2 phase
G418	Geneticin
GAPDH	Glyceraldehyde 3-phosphate dehydrogenase
GNAT	The Gcn5-related N-acetyltransferase
GOI	gene of interest
GTEx	Genotype Tissue Expression
H3K36	Histone 3 lysine 36
H3K36me3	Trimethylation of lysine 36 of histone 3
H3K4	Histone 3 lysine 4
H3K4me3	Trimethylation of lysine 4 of histone 3
H3K9	H3 Histone 3 lysine 9
HATs	Histone acetylransferases

HCT116	Colon carcinoma
HDACs	Histone deacetylases
HDMs	Histone demethylases
HEK	human embryonic kidney
Hela	Henrietta Lacks
HMTs	Histone methyltransferases
HR	Homologous recombination
IF	Immunofluorescence
IHC	Immunohistochemistry
indel	insertions/deletions
K562	Leukaemia
KATs	lysine (K) acetyltransferases
kb	Kilobase
KDa	Kilodalton
KRAB	Kruppel-association box
L	Litter
LB	Luria bertani
Le	The lateral elements
M	Mitosis phase
M-PER	Mammalian protein extraction reagent
mA	Milliamperes
MAGE	melanoma-associated antigens
MAGE-A	Melanoma antigen family A
MCF7	breast cancer cell line
MCS	Multiple cloning site
MHC	Major histocompatibility complex
mL	Milliliter
MMP	matrix metalloproteinase
mRNA	Messenger RNA
MW	Molecular weight
N-terminal	Amino-terminal domain
NATs	N-acetyltransferases
NCBI	National Centre for Biotechnology Information
NCO	Non-crossover
NDRs	nucleosome-depleted regions
NEAA	Non-Essential Amino Acids Solution

ng	Nanogram
NHEJ	Non-homologous end-joining
nM	Nanomolar
non X-CT	Non chromosome cancer testis genes
NRC	nuclear receptor coactivators
NSCLC	non-small cell lung cancer
NTERA-2	Embryonal carcinoma
NY-ESO-1	New York oesophageal squamous cell carcinoma-1
Oct4	Octamer-binding transcription factor 4
ORF	Open reading frame
PCR	Polymerase chain reaction
PRDM9	PR domain zinc finger protein 9
PTMs	Post translation modifications
PVDF	polyvinylidene difluoride
R	Reverse
r.p.m	Rotation per minute
RDA	representational difference analysis
RNA	Ribonucleic acid
RPA	protein A
RT	Room temperature
RT-PCR	Reverse transcription-polymerase chain reaction
RT-qPCR	Quantitative, real time-polymerase chain reaction
S	Synthesis-phase
SAGE1	Sarcoma antigen 1
SAGE1	Sarcoma antigen 1
SAM	S-Adenosylmethionine
SC	Synaptonemal complex
SCC	Sister chromatid cohesion
SDS	Sodium dodecyl sulphate
SDS-PAGE	Sodium dodecyl sulphate polyacrylamide gel electrophoresis
SDSA	Synthesis-dependent strand annealing
siRNA	Small interfering RNA
SMC	the structural maintenance of chromosome
SMC1β	Structural Maintenance of Chromosomes 1β
SNV	single nucleotide variation

SOC	Super Optimal broth with Catabolite repression
ssDNA	Single strand DNA
SSX-2	the synovial sarcoma X member 2
STAG3	Stromal Antigen 3
SW480	Colon adenocarcinoma
SYCP1	Synaptonemal complex protein 1
TAAs	Tumour associated antigens
TBE	Tris-borate-EDTA
TBS	Tris buffered saline
TCGA	The Cancer Genomic Atlas
TE	Transposable Element
TEX19	Testis expressed 19
TFs	Transcription factors
TM	Melting temperature
TRE	tetracycline responsive element
Tris	Tris (hydroxymethyl) aminomethane
TS	Testis-specific
TSGs	Tumour suppressor genes
TSS	transcription start sites
UPD	uniparent disomy
UV	Ultraviolet light
V	Volts
W	Whole cell extract
WB	Western Blot
WHO	World Health Organization
X-CT	X- chromosome cancer testis genes
ZF	Zinc-finger
µg	Microgram
µL	Microliter

Table of Contents

List of Figures

List of Tables

Chapter 1:
Introduction

1. INTRODUCTION

1.1 Human Cancer

1.1.1 Cancer overview

Cancer consists of a large group of diseases characterized by the abnormal proliferation of cells. Cancer is the second major cause of death from disease in the world, and there were 17 million cancer incidents with more than 9 million deaths in 2018, according to the International Agency for Research on Cancer (IARC) (cancer.org) and (http://www.who.int/cancer/en/). There were more than 1,600,000 new cancer cases and more than 600,000 cancer deaths in the United States in 2017, and it is estimated to be 20% higher in men than in women (Siegel et al., 2017). In United Kingdom, the records of cancer deaths have exceeded 164,000 in 2017 (cancerresearchuk.org). However, there are also distinctions in cancer deaths between males and females; for instance, the second cause of cancer deaths in females in the United Kingdom is breast cancer (Jemal et al., 2010). Leukaemia and brain cancer are both continual causes of death among children in the United States (Siegel et al., 2012).

1.1.2 Cancer classification and types

Human cancers can be categorised according to the tissue affected (Stratton et al., 2009). The main types of cancers include carcinoma, sarcoma, leukaemia and lymphoma (Roy et al., 2017). Carcinoma is a type of cancer linked with the epithelium and endothelium of tissues (e.g., breast, colon and skin). Sarcomas typically originate from connective and supportive tissues, such as cartilage, bones, muscles, and blood vessels (Souhami, 2008). Leukaemias are a group of cancers found in tissues associated with the creation of blood cells, while lymphomas are the cancers in B and T lymphocytes.

Tumours are generally described as either benign or malignant. Benign tumours consist of non-cancerous cells that are not able to invade or spread to other tissues. However, malignant tumours are comprised of cancerous cells that have the ability to migrate and spread through the blood stream to distant tissues and organs in a process called metastasis.

1.1.3 The causes of human cancer and the hallmarks of tumorigenesis

Identifying the causes of cancer disease is difficult (Washio et al., 2016). Many studies indicate that cancer is a result of genetic and environmental factors (Clapp et al., 2008; Flavahan et al., 2017). The purpose of studying environmental factors is to reveal all non-genetic factors, including diet, lifestyle and infection. Exposure to carcinogens, such as chemicals, air pollution and radiation, is involved in the development of cancer. About 30% of cancers are caused by smoking, and 35% are a result of diet, while infection from viruses comprises about 15% (Katzke et al., 2015; Weiderpass, 2010). Another related factor that contributes to cancer development is age; for example, men over 40 years old are more likely to develop prostate and colon tumours, and women are susceptible to breast cancer from the age of 50 onwards (Autier, 2016). Based on data from the United Kingdom, about 50% of malignancies are diagnosed in 70-year-old patients, but 52% of cancer cases result in death for patients are over 75 years old, suggesting a strong correlation between age and cancer mortality and morbidity (Moller et al., 2011).Genetic and/or epigenetic factors induce and maintain the development of tumours. Alterations to tumour suppressor genes (TSGs) and oncogenes play fundamental roles in tumorigenesis as they contribute to tumour cell proliferation, spreading and invasion (Gnoni et al., 2013). Nevertheless, some data have shown that cancer has a common basis in a polyclonal epigenetic disruption of progenitor or stem cells, which is mediated by cancer stem cell genes that drive the alterations in gene expression that commonly participate in cancer initiation and development (Feinberg et al., 2006; Vogelstein & Kinzler, 2004).

Weinberg and Hanahan have described a total of ten key charcteristcs that allow cancer cells to transform into malignant cells during a process of carcinogenesis; these charateristics termed as The Hallmarks of Cancer (Hanahan & Weinberg, 2000; 2011). In the vast majority of tumours, each tumour cell acquire a succession of functional features that enable cells to survive, proliferate and disseminate through several mechanisms and at different times in a multistep process.

Hanahan & Weinberg (2000) first proposed six major hallmarks: sustaining proliferative signalling, avoiding growth suppressors, permitting replicative potential, encouraging angiogenesis, fighting cell death and tissue invasion and metastasis. In 2011, the same authors also proposed that the process of tumorigenesis is probably furthered by four additional emerging components, which include genomic instability,

the tumour-promoting inflammatory condition of premalignant damage and malignant cells, avoiding immune destruction and metabolic passage abnormalities. The latter are suggested as an additional hallmark group (Figure 1.1) (Hanahan & Weinberg, 2011).

In 2013, Sinneschein and Soto criticized the notion that cancer hallmarks must be present in any carcinogenic process. These authors criticized the list of features and examined the postulate that cancer is not only cell-based in terms of uncontrolled cell proliferation, but it is also a tissue-based disease, where there is interaction between cells in a microenvironment and their intricate signalling system during tumorigenesis (Sonnenschein & Soto, 2013). The authors argue that Hanahan and Weinberg rely on single mutation theory (SMT) of carcinogenesis and a cancer is a result of genetic defects within cell circuit. However, Sonnenschein and Soto provide evident that support the tissue organisation field theory (TOFT) proposing that carcinogenesis results from the faulty interaction between stroma and epithelium (Sonnenschein & Soto, 2013). Furthermore, the authors also criticise the premise adopted by H and W that the default state of cells is the quiescence state, which contradicts with the evolutionary theory perspective, the proliferation is the default state of cell, the author said.
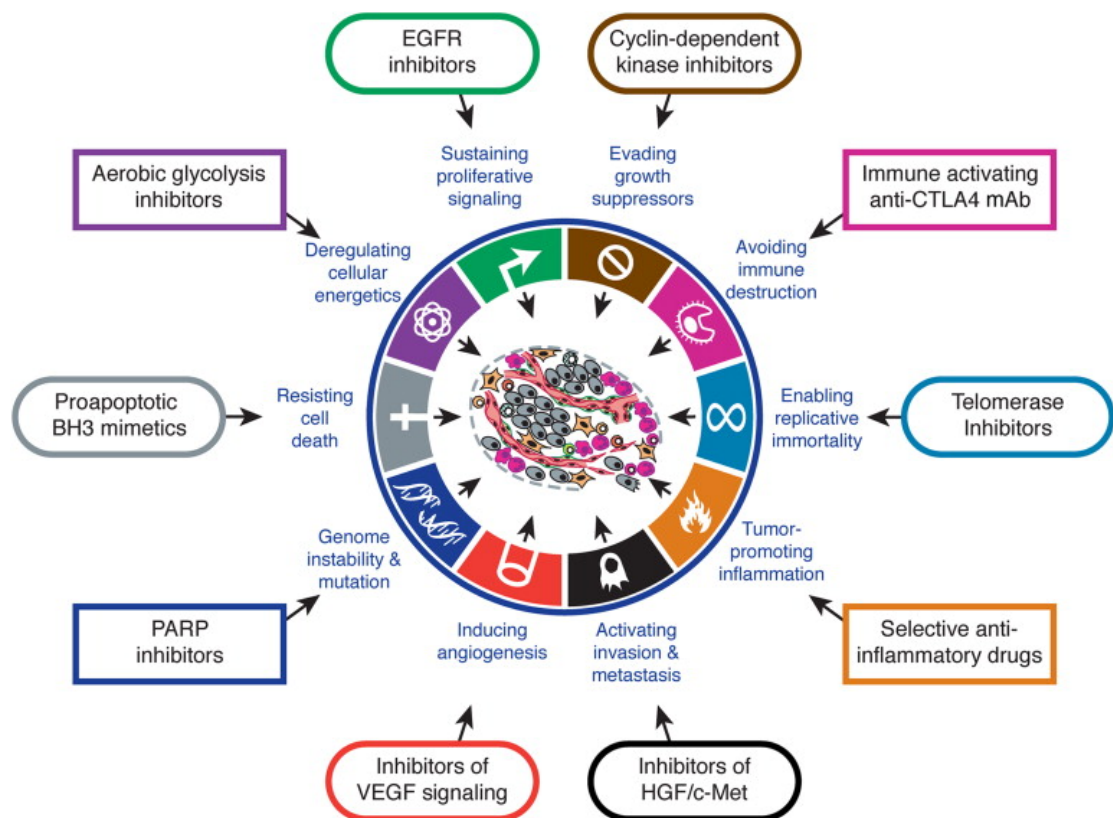
Figure 1.1: A diagram demonstrates cancer hallmarks with their therapeutic agent classes. The figure shows a summary for the ten characteristics of cancer cells that lead to the immortality of cancer cells (Adapted from Hanahan & Weinberg, 2011).

1.1.4 Genetic alterations in cancer development

Many studies have revealed that there are three categories of genes that contribute to cancer initiation and progression. TSGs, oncogenes and genomic stability genes all play key roles in regulatory processes such as cell cycle control, DNA repair and chromosome segregation. These genes participate in the hallmarks of cancer, and they are responsible for cell division interruption and, thereafter, cancer development. Oncogenes have the potential to drive tumorigenesis because they can promote cell proliferation, while TSG are engaged in cell growth inhibition and cell apoptotic activation. Thus, a combination of TSG mutation or dysfunction with aberrant expression of oncogenes can enable tumorigenesis (Vogelstein & Kinzler, 2004; Negrini et al., 2010; Morris & Chan, 2015; Ferguson et al., 2015; Hanahan & Weinberg, 2011).

1.1.4.1 The roles of TSGs

TSGs are growth inhibitory factors during normal cell division, and a dysfunction in TSGs leads to uncontrolled cell growth proliferation and avoidance of cell apoptosis, key cancer hallmarks (Thoma et al., 2011; Weinberg, 2013). This class of genes have capabilities to protect normal cells from transformation into cancerous cells. The mutations and dysfunction of TSGs are likely causes that direct normal cells into tumourigenesis (Thoma et al., 2011; Weinberg, 2013). TSGs are phenotypically recessive, so both copies must be functionally altered to promote cancer, and are responsible for inherited cancer syndromes. TP53 protein is one example of a tumour suppressor that plays a fundamental role in the maintaining cell cycle and apoptosis processes; in addition it has a critical function in anti-angiogenesis mechanisms. The loss of function of TP53 has been identified regularly in various types of cancers, including colon cancer (Prabhu et al., 2016). Deactivation of TP53 has also been observed to promote metastasis and evasion (Surget et al., 2014; Zhang et al., 2015). Active TP53 is able to differentiate stem cells from progenitor cells via regulated differentiation and specific pathways. Conversely, the absence of TP53 is reported to lead the continuous of stem cell replication which subsequently results in the maintenance and/or activation of oncogenic epigenetic cascades (Levine et al., 2016).

1.1.4.2 The roles of oncogenes

Oncogenes are derived from mutated class of normal cellular genes (proto-oncogenes) that regulate cell proliferation, survival and invasion. The expression of proto-oncogenes in healthy cells is highly orchestrated to avoid uncontrolled cell growth. In cancerous cells, mutated proto-oncogenes result in restrain apoptosis, promote survival, uncontrolled cell division and dissemination. Mutation changes in proto-oncogene regulatory systems can result in aberrant expressions of oncogenes that are apparently observed in a wide range of cancers (Croce, 2008; Bagci & Kurtgöz, 2015). Oncogenes are defined as phynotypically dominant by which a single mutation in one copy of proto-oncogene is sufficient to initiate carcinogenesis, and are not correlated with inherited cancer syndrome. The activation of oncogenes can be triggered by many factors, such as gene amplification, mutations in the gene, chromosomal translocation and epigenetic dysregulation leading to changes in structures of encoded proteins and subsequently change their function. (Croce, 2008; Bagci & Kurtgöz, 2015). Examples of an oncogene is the *RAS* family of genes, which include *HRAS*, *NRAS* and *KRAS.* Mutations in different oncogenes lead to different types of cancer; for instance, mutated *KRAS* oncogene has been identified in pancreatic, bowel and lung cancers (Rodenhuis. 1992); however, mutations in *NRAS* oncogene have been detected in myelodysplastic syndrome and myelogenous leukaemia (Beaupre & Kurzrock, 1999). Moreover, the *BRAF* gene, which has been found to be activated in several tumours such as bowel cancers, liver carcinomas and melanomas (Davies et al., 2002; Solit, et al., 2006; Bagci & Kurtgöz, 2015).

In addition, there are subclasses of oncogenes that can become activated without mutation. For instance, cancer testis antigen (CTA) genes that can derive an immunogenic response in cancer tissues, but they are not activated in normal tissues (Whitehurst, 2014; Yang et al., 2015).

1.1.4.3. Genome stability genes

Genome stability genes are a group of genes that have been identified to play roles in regulating DNA repair, segregating chromosomes and maintaining genetic modifications. However, genetic alterations or changes of these genes have been linked to tumour initiation (Negrini et al., 2010). For instance, the *NBS1* gene is required and implicated in repairing DNA double-strand breaks (DSBs). Furthermore,

mutations in *NBS1* is linked with a congenital disease, Nijmegen Breakage Syndrome (NBS) (Tauchi, 2000), however, the overexpression of *NBS1* is associated with oesophageal carcinoma (Kuo et al., 2012), liver cancer (Wang et al., 2014) and prostate cancer (Berlin et al., 2014). Moreover, tumour suppressor genes, *BRCA1* and *BRCA2,* have functions in DNA repair and genome stability. Mutations in *BRCA1* and/or *BRCA2* are considered as a cancer risk indicator, and their inactivation is associated with breast and ovarian cancers in women (Yoshida & Miki, 2004; Trego et al., 2016). A functional reduction of the mouse double minute 2 homolog (MDM2) protein, which is encoded by *MDM2* gene in humans, has been related to DSB DNA repair inhibition. It has been indicated that *MDM2* is overexpressed in certain types of tumours by which it acts as an oncogene, however, its expression is downregulated in other cancers acting as TSG. This leads to the suggestion that *MDM2* has ability to act as oncogene and TSG, this is based on the relevant cellular situation (Małuszek, 2015).

1.1.5. Epigenetic Alterations in Cancers

One of the most vital area of medicinal chemistry and chemoprotection of cancer is epigenetics, which refers to the study of alterations of genomic regulation without changing the nucleotide sequence. Among these alterations is DNA methylation and histone modification and both have been reported to be linked with several kinds of cancers (Hatzimichael & Crook, 2013).

Transcription factor accessibility to DNA can be changed by chromatin remodelling or histone modifications such as histone acetylation and histone deacetylation, thereby regulating gene expression. For example, genes expression such as, expression of *BAX*, *CDKN1A* and *TP53* has been shown to modulate cancer development by influencing several processes such as signalling pathways, apoptosis, cell cycle arrest, cellular migration and cell growth. Cancer treatment can make use of the strategy of manipulation of gene expression (Hatzimichael & Crook, 2013; Qiu et al., 2018).

1.1.5.1 DNA methylation

DNA methylation is a major modification of the genome in which a methyl group is covalently added to the carbon atom at the 5´ carbon of the cytosine bases in CpG dinucleotides. This process is catalysed by DNA methyltransferase (DNMT) enzymes, and it plays an essential role in gene expression regulation (Ballestar, 2011). Gene promoter hypermethylation is mostly linked with gene silencing, it has been reported that human gene promoters contain about 76% of CpG islands, which are presented at the 5´ end of the genes and which regularly remain unmethylated through processes such as differentiation and development (Davuluri et al., 2001; Mariño-Ramírez et al., 2004).

DNA hypermethylation in the promoter sequence and hypomethylation in the non-promoter region of genes are often detected in different tumour cells, which results in the transcription silencing of genes, such as TSGs and DNA repair genes (Akhavan-Niaki & Samadani, 2013). Furthermore, hypermethylation is also reported to affect cell cycle regulation, apoptosis and the DNA repair process, leading to genomic instability and, subsequently, cancer development (Esteller & Herman, 2002; Wu & Bekaii-Saab, 2012). The activity and levels of DNMTs are observed to be increased in a range of human cancers in comparison to normal tissues (Ibrahim et al., 2011).

1.1.5.2. Histone and Histone Modification

In eukaryotic cells, DNA is tightly packaged in chromatin by both histone and non-histone proteins within the nucleus. Nucleosomes, which are basic subunits of chromatin, are made up of 146 base pairs of DNA wrapped around four core histones that form an octamer. The histone octamer is highly conserved, composed of two copies of the core histones H2A, H2B, H3 and H4 to make the nucleosomal core (Figure 1.2). It has been found that from each nucleosome, 8 flexible lysine-rich histone tails are extended, which are responsible for mediating internucleosomal contacts. These tails also serve as binding sites for non-histone proteins. In the context of gene transcription, chromatin can be categorized into two forms namely euchromatin and heterochromatin (Kouzarides, 2007). The euchromatin refers to an open form of chromatin which allows transcription factors to readily access the DNA leading to activation of genes. The later refers to a closed form of chromatin which

does not permit interaction between transcription factors and DNA, thereby causing repression of genes. Multiple histone modifications that may occur in sequential or combinatorial manner on one or more histone tails, lead to specific downstream functions (Strahl & Allis, 2000). Numerous histone post-translational modifications have been identified (PTMs), including acetylation, methylation, sumoylation, ubiquitination, and phosphorylation (Tessarz & Kouzarides, 2014). Therefore, PTMs comprise a unique code to regulate the interactions between histone and other proteins. In this way, the intrinsic histone barrier to transcription and other DNA regulatory mechanisms is modified (either accessible or inaccessible).
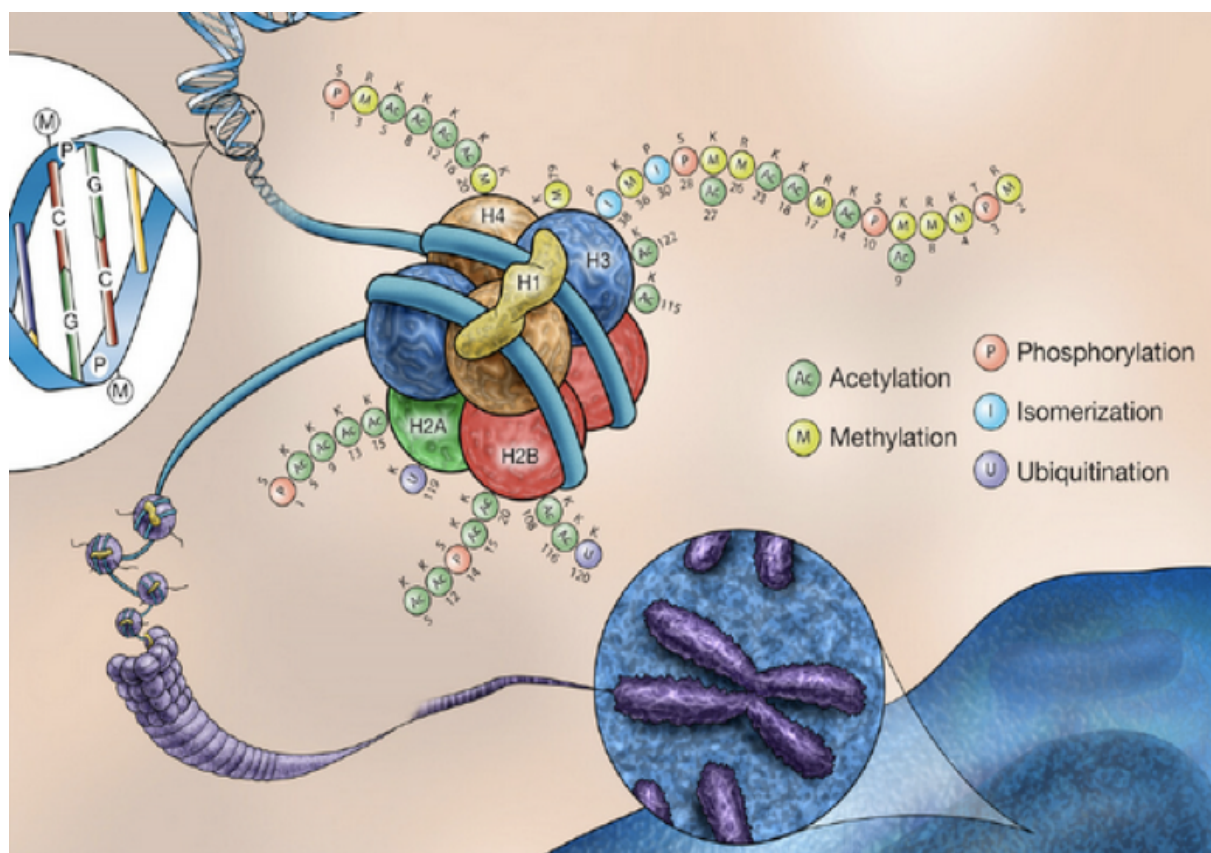
Figure 1. 2. Chromatin structure. DNA is wrapped twice around a histone octamer. The histone octamer is highly conserved, comprised of two copies of the core histone H2A, H2B, H3 and H4 (Barber Rastegar, 2010)**.**

1.1.5.2.1. Histone Acetylation and Deacetylation

A crucial event of regulation of gene expression is histone acetylation. This process is catalysed by histone acetyltransferases (HATs) that interact with lysine residues present inside the extended N-terminal tail from the histone core (Grunstein, 1997). In particular, acetyl groups are transferred by HATs to epsilon-amino groups of lysine present in histone tail N-termini resulting in neutralization of the positive charge. The cofactor acetyl-CoA is used in this process. Because of neutralization, the interaction between negatively charged DNA and histones is decreased that leads to loosening of the structure of chromatin. As a result, transcription factors can more readily access the DNA and hence gene expression is activated (Zhang & Dent, 2005) On the basis of structure and function, HATs can be categorized into four groups. The Gcn5-related N-acetyltransferase (GNAT) family contains bromodomain and has been reported to be involved in acetylation of lysine residues on histones H2B, H3 and H4 (Lee et al., 2007). As indicated by the name, the p300/CBP family contains metazoan-specific p300 as well as CBP (Yuan & Marmorstein, 2013). Presence of a catalytic HAT domain, a bromodomain and numerous zinc finger regions, these HATs have been reported to be involved in acetylation of histones H2A, H2B, H3 and H4 (Roth et al., 2001) The MYST family contains chromodomains and zinc fingers and has been reported to be involved in acetylation of lysine residues on histones H2A, H3 and H4. Finally, the nuclear receptor coactivators (NRC) family present in humans has been found to be involved in acetylation of histones H3 and H4 (Sterner & Berger, 2000).

Histone deacetylation is a process that catalysed by histone deacetylases (HDACs) and involves deacetylation of lysine residues present in the tail that extends from the N-terminal of the histone core (Grunstein, 1997). Unlike acetylation, acetyl groups are removed by HDACs from the epsilon-amino groups of lysine residues thereby making the DNA more compact as part of gene expression regulation. Therefore, transcription factors are unable to easily access the DNA leading to repression of certain genes (Choudhary et al., 2009). On the basis of domain structure and sequence homology, HDACs have been classified into four classes (Dokmanovic et al., 2007). Class I (e.g., HDACs 1, 2, 3, and 8), class II (e.g., HDACs 4, 5, 6, 7, 9, and 10), class III (e.g., SIRT1, SIRT2, SIRT3, SIRT4, SIRT5, SIRT6, and SIRT7), and class IV (e.g., HDAC11) (De Ruijter et al., 2003). Class I, class II and class IV of HDACs depend on zinc for

deacetylation, while class III HDACs are NAD+ dependent for deacetylation (Hrabeta et al., 2014; Marks & Xu, 2009).

Histone acetylation can also facilitate transcription by providing binding sites to proteins that contribute to gene activation (Filippakopoulos et al., 2012). Transcriptional activity in euchromatin is generally correlated with high levels of histone acetylation; however, silent heterochromatin is linked with a low level (Bannister & Kouzarides, 2011; Nakazawa et al., 2012). Additionally, the disturbance in the natural balance between acetylation and deacetylation has been linked with several human diseases, particularly, tumorigenesis (Sharma et al., 2010). For example, class I HDACs contribute to invasiveness regulation by increasing the expression of matrix metalloproteinase (MMP) so that the dysfunction of their activity is correlated with cancer metastasis (Ramakrishnan et al., 2016). Also, HDAC1 and HDAC2 have been identified to establish a transcriptional repressor complex with SNAIL to repress and inhibit the expression of E-cadherin in metastatic pancreatic cancers (Peinado et al., 2004).

1.1.5.2.2. Histone Methylation and Demethylation

The process that implies transferring of methyl groups to different amino acids of histone proteins by histone methyltransferases (HMTs) is termed histone methylation. Conversely, the process during which methyl groups are removed from amino acids of histone proteins by histone demethylases (HDMs) is termed as histone demethylation. HMTs have been reported to be responsible for transference of methyl groups to particularly arginine and lysine residues of H3 and H4 histones (Wood & Shilatifard, 2004). Accordingly, HMTs have been grouped as lysine-specific and arginine-specific (Sawan & Herceg, 2010). Moreover, it has been found that both lysine-specific and arginine-specific HMTs used S-Adenosyl methionine (SAM) as a cofactor methyl donor in this process (Wood et al., 2004; Pal & Sif, 2007; Strahl & Allis, 2000).

Histones methylation may be mono- (me1), di- (me2), or tri- (me3). Histone methylation is not thought to change the structure of chromatin, but rather enhances the binding sites for other proteins that may have an effect on chromatin. In addition,

different residues of lysine methylation may be linked to either transcription repression or activation (Nielsen et al., 2001). For example, it has been found that methylation of H3K79, H3K36 and H3K4 are involved in activation of genes. On the other hand, methylation of H3K56, H3K27, H3K20 and H3K9 are involved in silencing the transcription of certain genes and regions (Gao & Tollefsbol, 2015).

1.1.5.3. Histone Modification and Cancer

Considering the role played by epigenetic changes in regulation of gene expression, it can be expected that alterations in these modifications like acetylation and deacetylation of histones are involved in development of cancer. It has been reported that hyperacetylation of histones mediated by reduced HDAC or increased HAT activity leads to expression of genes and hypoacetylation of histones mediated by increased HDAC or reduced HAT activity results in silencing of gene expression (reviewed in Kim et al., 2003). Furthermore, many studies have shown that the development of cancer is regulated and maintained by the changes of expression of related genes termed tumour associated antigen (TAA) genes. These genes can produce antigens on cancer cell surface by which they can be targeted and recognised by the immune system making these gene products good candidates for cancer immunotherapy (Costa et al., 2007; Caballero & Chen, 2009). The abnormal expression of these genes is also used as a diagnostic biomarker for several types of cancers. Recent studies have focused on a specific class of tumour antigens that are promising targets for early detection of tumours and have good potentials in the fields of immunotherapy and vaccination. One such group of cancer related genes is cancer-testis antigen (CTA) genes that have the potentials to be involved in clinical studies (Mirandola et al., 2011).

1.2. Cancer testis antigen (CTA) genes

1.2.1. Overview of CTAs

CTAs are a subgroup of germline proteins that are encoded by cancer/testis (CT) genes (Chen et al., 1998). CTAs encode proteins whose production is normally restricted to germ cells in adult male testes, but not present in other normal tissues. However, CTA genes are aberrantly activated in different types of human malignancies (Whitehurst, 2014). In the early 1990s, melanoma antigen-1 (MAGE-1) was the first identified CTA using autologous typing with cytotoxic T lymphocytes obtained from a melanoma patient (van der Bruggen et al., 1991). Later, the synovial sarcoma X member 2 (*SSX-2*) and New York oesophageal squamous cell carcinoma-1 (*NY-ESO-1*) genes were also discovered using a serological analysis of recombinant tumour cDNA expression libraries with autologous serum (SEREX) (Chen et al., 1997; Türeci et al., 1998). In addition, the successful cloning of these genes has led to the use of SEREX to identify other novel CTAs, such as OY-TES-1, CAGE, cTAGE-1, MAGE-C1 and SCP-1, from several types of cancers (Chen et al., 1997; Chen et al., 1998; Li et al., 2004). The feature of CTA gene expression has allowed for the employment of other techniques, such as mRNA expression profiling, cDNA oligonucleotide array analysis, bioinformatics analysis, and representational difference analysis (RDA), to identify additional CTAs. To date, more than 850 new CTA genes are reported in databases, such as The Cancer Genome Atlas (TCGA) and Genotype Tissue Expression (GTEx) (Pagotto et al., 2013; Lai et al., 2016).

CTA genes can be categorised according to their chromosomal location on the X chromosome (X-CTA) genes and non-X chromosome (non-X-CTA) genes. (Figure 1.3) (Simpson et al., 2005). According to database, 228 CTAs have been identified of which 120 CTAs (52%) map to the X chromosome while the remaining are distributed on the 22 autosomes and the Y chromosome (http://www.cta.lncc.br/) (Rajagopalan et al., 2011). It has been also found that only one CTA is located on the Y chromosome (Rajagopalan et al., 2011). X-CTA genes encode proteins that are produced in the spermatogonia stage of spermatogenesis, although their functions are largely poorly understood. Some X-CTA genes are expressed in the placenta, as well as in the testes, such as; *XAGE-2*, *XAGE*-3, *MAGE-A3*, *MAGE-8* and *MAGE-A10* (Simpson et al., 2005). Meanwhile, others showed detectable transcripts in some somatic healthy

tissues, such as the pancreas, spleen and liver. However, a quantitative RT-PCR analysis determined that these levels of mRNA transcripts are normally less than 1% compared to their expressions in germ cells of the testis (Caballero & Chen, 2009). On the other hand, non-X-CTA genes encoded proteins are thought to functionally contribute to spermatocytes and spermatids during the spermatogenesis process. It has been proposed that they may play an essential role in meiotic cell division. For example, SPO11 and SCP1 are non-X-CT genes that composed Synaptonimal Complex (SC). SPO11 initiates double-strand DNA breaks (DSB) to commence recombination during meiosis (Keeney et al., 1997). SCP1 forms the transverse filaments of SC (Pousette et al., 1997). Other non-X-CT genes play important roles during spermatogenic processes, such as; ACRBP (acrosin-binding protein) and ADAM2 (Türeci et al., 1998; Kurashige et al., 2001; Chen et al., 2005). Thus, the expression of non-X-CT genes such as SPO11 and SCP1 in cancer cells is suggested to drive abnormal chromosomal segregation and anaploidy leading to genomic instability and cancer. Most of the non-X genes are activated during and/or after meiosis, but their activation is generally not observed in the pre-meiotic phase.

Hofmann and colleagues previously categorised approximately 153 CT genes into four main groups (Hofmann et al., 2008). First, testis-restricted genes that are only expressed in the testis and in the placenta. Second, testis/CNS-restricted genes can be expressed in the central nervous system (CNS) and in the adult testis. Third, testis-selective genes are expressed in the adult male testis with one or two other selective healthy tissues, other than the CNS. Lastly, testis/CNS-selective genes are expressed in the CNS, testis and no more than two additional normal tissues. The features of CT genes, which include normal activation in germ cells with silencing in healthy somatic tissues and abnormal activation in cancerous tissues, have led to the suggestion that these genes may play an important role in the soma-to-germline transition by which they may drive oncogenesis (McFarlane et al., 2014; McFarlane, Feichtinger & Larcombe, 2015). Furthermore, it has also been suggested that the activation of CT genes during meiosis and aberrant activation in cancers are associated with the essential function of these genes in important molecular events, such as chromosomal segregation instability in cancer cells (McFarlane & Wakeman, 2017).
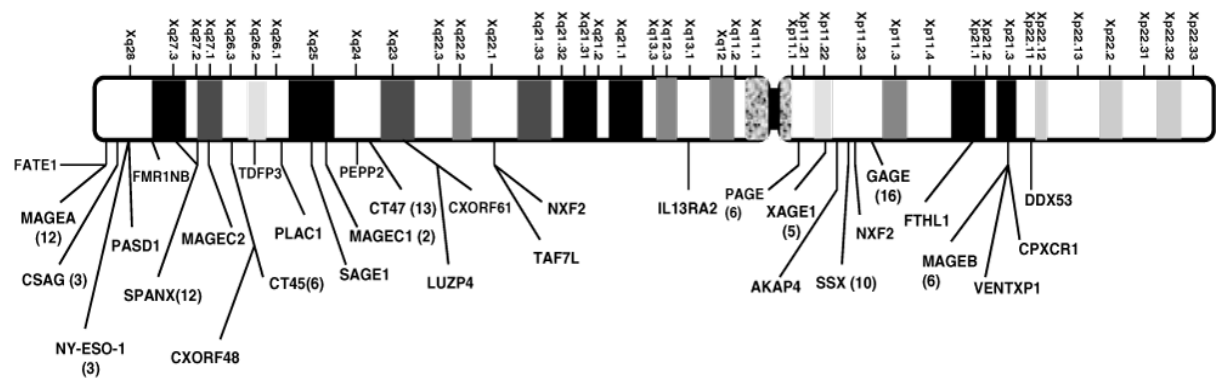
Figure 1. 3. Distribution of X-CTA genes present on the X-chromosome. Examples of X-CTA genes' families and their location on the X-chromosome are illustrated (Adapted from Caballero & Chen, 2009).

1.2.2. CTA genes expression and functional roles in normal and cancer cells
1.2.2.1. CT genes in normal tissue

CTAs are essentially present in the testis tissues of adult males. In brief, the testes are ovoid glands that have seminiferous tubules, which are separated by the septa into two compartments: basal and adluminal (Hess & De Franca, 2009). These structures are physically supported and maintained by connective tissues that contain Leydig cells. The seminiferous epithelium is composed of two types of cells, including germ cells and Sertoli cells. Germ cells are present in the basal compartment and arranged in a hierarchical structure by which the spermatogonia differentiate into spermatocytes and spermatocytes differentiate into spermatids that finally produce sperm in a process termed spermatogenesis. During this process, large spermatogonia cells are localised in contact with the basal membrane, while the differentiated spermatids are located near the lumen of the seminiferous tubule (Figure 1.4). Sertoli cells provide a physical support and facilitate the differentiation of germ cells into more functional and specialised cells. Furthermore, Sertoli cells separate the two compartments of seminiferous tubules by forming a physical wall, which generates the blood-testis barrier (BTB) (Mirandola et al., 2011; Sandor et al., 2012). This barrier separates the germ cells (undifferentiated cells) in the basal compartment from the differentiated cells in the adluminal compartment, where spermatogenesis occurs (Ovalle & Nahirney, 2013).

To date, the functional roles of CTAs in spermatogenesis remains largely unclear; however, knockout and gene-targeting studies have shown the important roles of some CTAs in the spermatogenesis process (Whitehurst, 2014). This is supported by the findings that mice lacking single CTA genes are associated with a reduced fertility (Brown et al., 2003; Fiedler et al., 2013; Whitehurst, 2014). Additionally, previous studies on some CTAs, including, NY-ESO-1 and MAGEA1, demonstrated that these proteins are produced during initial stages of spermatogenesis, suggesting that these CTAs are essentials for the initiation of spermatogenesis (Jungbluth et al., 2000; Whitehurst, 2014).

CTA genes are found to play essential roles that associated with molecular events during gametogenesis. For example, synaptonemal complex protein 1 (*SYCP1*) is a CTA gene which contributes to meiotic crossover control and deletion of this gene leads to sterility (Türeci et al., 1998; de Vries et al., 2005; Schramm et al., 2011). Moreover, SPO11 is a meiosis specific protein that initiates DSBs during meiotic cell division (Yamada & Ohta, 2013) and *SPO11* has been identified as a CTA gene (Koslowski et al., 2002).

The cohesin proteins plays important functions in tethering sister chromatids during cell division. Although the constitution of cohesin complexes vary between meiosis and mitosis, proteins such as RAD21L, REC8, Stormal Antigen 3 (STAG3) and Structural Maintenance of Chromosomes 1β (SMC1β) are meiosis-specific cohesin proteins (Chambers et al., 2003; Lee et al., 2011; Ishiguro et al., 2011; Ward et al, 2016). These proteins were reported as CTAs that present in various tumour types (Feichtinger et al., 2012; Rosa et al., 2012; Lindsey et al., 2013).

1.2.2.2. CT genes in cancer tissue

Cancerous cells acquire some biological features such as self-renewal and activation of germline genes suggesting that these cells may acquire germ-like state (McFarlane et al., 2014; Nassar & Blanpain, 2016) . This has led to the postulate that the key factor of the carcinogenesis process is a soma-to-germline transition that is regulated and maintained by the activation of germline genes in these somatic cells (Nielsen & Gjerstorff, 2016; Koslowski, et al, 2004; McFarlane et al., 2014; Nassar & Blanpain, 2016; Feichtinger et al., 2015). The idea is supported by the evidence that a large group of germline genes were re-expressed during oncogenesis in *Drosophila*. The inactivation of these germline genes resulted in tumour repression suggesting the essential roles of these genes during oncogenesis (Janic et al., 2010; Altemose et al., 2017). Many studies also reported that CTAs might have a critical role in the evolution of genetic instability within cancer cells and tumour heterogeneity, leading to cancer development and drug resistance (Rousseaux et al., 2013; Lafta et al., 2014; Whitehurst, 2014; McFarlane et al., 2015).

A)
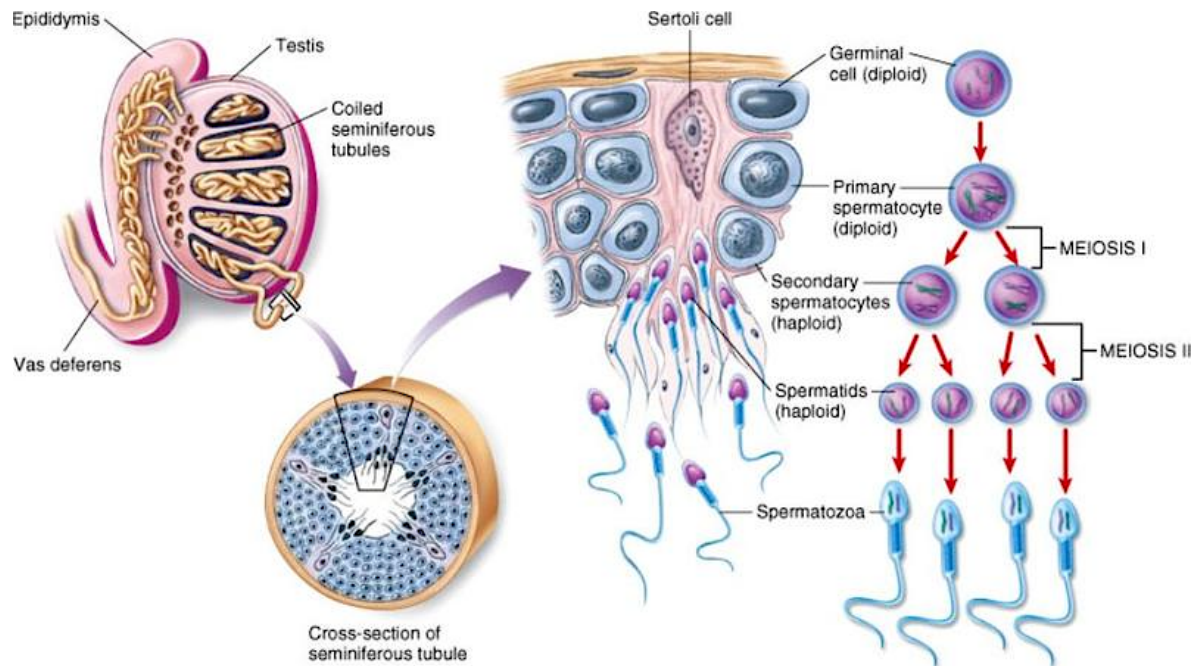
B)
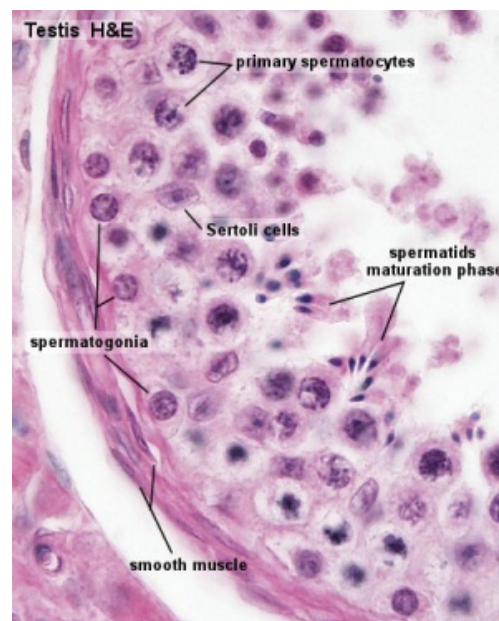
Figure 1. 4. Spermatogenesis process and the histology of testis. A) Spermatogonia stem cells (SSCs) are located at the edge of basal compartments of the Seminiferous tubules and divide mitotically to produce new stem cells. Half of SSCs undergo to differentiate into spermatocytes. Primary spermatocytes destined to produce mature spermatids through meiosis I and II. **B)** Testis H&E histology showing spermatogonia, spermatocytes, spermatids and the Sertoli cells (adapted from Ovalle & Nahirney, 2013).

CTA genes are expressed variably and extensively in several types of tumours. The majority of studies are based on RT-PCR/qRT-PCR analyses and some CTAs have been examined at the protein level by immunohistochemistry (IHC) analysis. Fratta and co-workers (2011) summarised all identified CTAs and their frequency of expression in different types of cancer. For example, CTAs have been differentially expressed in melanoma, lung and prostate cancers. Interestingly, CTA genes were reported to be co-expressed in some tumours (Scanlan et al., 2000). This supports the idea that cancer cells undergo a reprogramming and re-activation of germline machinery during oncogenesis.

Extensive research has been conducted in recent years to determine the roles and functions of CT genes during cancer progression and development, and the emerging data support the idea that the reactivation of CTA genes in cancers may contribute to the hallmarks of cancers. Some CTA genes play key roles in the sustained growth of cancer cells, which is one of the main features of tumours. For example, the depletion of *SSX2* gene mRNA levels in melanoma cells leads to the significant inhibition of cell proliferation (Greve et al., 2015). Furthermore, a knockdown experiment of some *MAGE* family genes, such as *MAGE-A, MAGE-B and MAGE-C* in melanoma cells, resulted in an increase in TP53 activity and apoptosis (Soriano et al., 2007) (Figure 1.5).
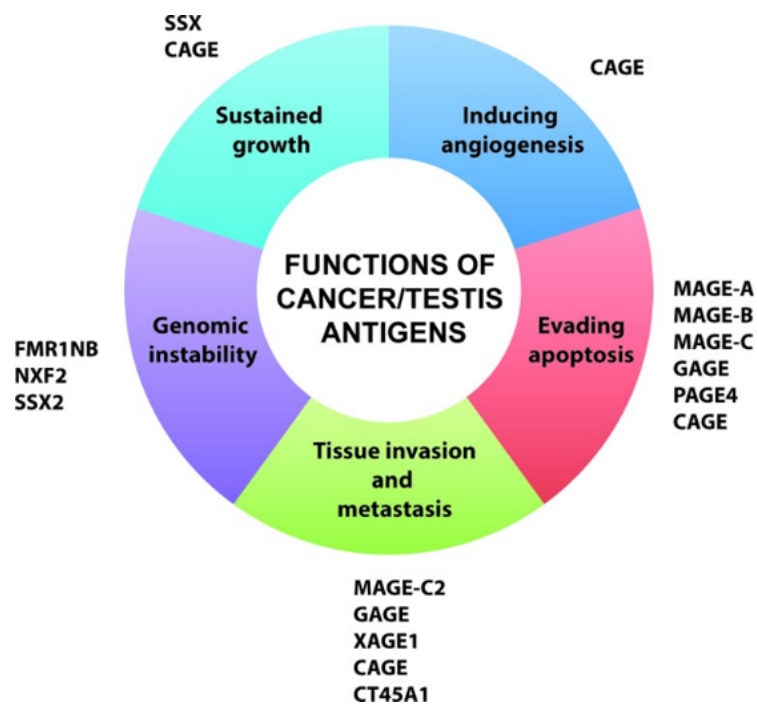
Figure 1. 5. The identified functions of some CTA genes. The diagram illustrates examples of CTAs with roles linked to cancer characteristics (Gjerstorff et al., 2015).

1.2.3. CT gene regulation

The expression of CTA genes are regulated and controlled by DNA methylation and histone modification (De Smet & Loriot, 2013; Kim et al., 2013; Almatrafi et al., 2014) (see section 1.1.5). In healthy somatic cells, majority of CTA genes are normally silent and not expressed due to the presence of CpG islands that are usually methylated at their promoter sequence (Simpson, et al, 2005). In many cancer types, global DNA hypomethylation is the most frequently reported mechanism that is responsible for gene activation (Zhao, et al, 2004). Therefore, DNA hypomethylation reportedly leads to the activation of some CT genes in cancers, such as the cancer-associated gene (*CAGE*) in gastric cancer (Lee et al., 2006) and the melanoma-associated antigen (*MAGE-A1*) gene in different cancer cells (De Smet & Loriot, 2013). Consistent with this, it has been found that the hypermethylation of the *MAGE-A1* family promoter has led to gene repression (Wischnewski et al., 2007).

Transcription can be inhibited either by the methylated recognition sequence that prevents transcription factors (TFs) from binding to the promoter region or by the binding of methyl-CpG-binding proteins that stop gene activation (Fratta et al., 2011). Additionally, some CTA genes, such as *NY-ESO-1* and *SSX2*, showed over-expression in cancer cell lines post treatment with DNA methyl-transferase 1 inhibitor (DNMTi) (Zhao et al., 2004).

The inhibition of HDACs leads to the upregulation of many CTA genes (Akers et al., 2010; Barneda-Zahonero & Parra, 2012), indicating a regulatory role for histone acetylation. Both histone deacetylation and/or DNA hypermethylation can result in some CTA genes being silenced, such as *MAGE-A9* and *MAGE-A11* in breast cancers (Hou et al., 2014).

1.2.4. Clinical Application of CTAs

1.2.4.1. CTA genes and cancer diagnosis

CTAs have distinct potentials in areas of cancer prognosis and diagnosis (Lai et al., 2016). In diagnosis, CTAs have the ability to distinguish malignant tumour samples from benign tumours. For instance, analysis of blood sample, has revealed that patient with lung cancer have increased levels of anti-STAG9 antibody in comparison to healthy persons. Hence, STAG9 CTA can act as a diagnostic biomarker for lung cancer specifically (Ren et al., 2016). During another study, researchers analysed around 200 clinical samples collected from patients of colorectal cancer (CRC) from different grades and stages. It was found in this study that most of the specimens had showed expression of the CT gene *AKAP4* which implies that this gene can be utilized as a tool for diagnosis of CRC at early stages (Jagadish et al., 2016). In the case of prostate cancer, the levels of PSA protein in blood sample is currently being used for diagnosis with other pathological and clinical investigations, such as assessment of concentration of the CTA BORIS. BORIS is a CTA gene, expression of which correlates with aggressive prostate cancer (Cheema et al., 2014). It has been revealed that the presence of some CTAs gives an indication (a prognostic marker) for poor clinical outcomes, for example, such as EBI3 (Rousseaux et al., 2013) and MAGEA1 (Zou et al., 2012). Additionally, among four different CTAs (CTCFL, XAGE3, ACTL8 and OIP5) in glioblastoma patients, studies demonstrated that patients with OIP5-positive have significantly higher overall survival period than OIP5-negative ones (Freitas et al., 2013). The expression of CTA genes may give impressions for the patient response to treatment after chemotherapy. For example, NY-ESO-1 is determined as a good marker for the response to the chemotherapy treatment of non-small lung cancer patients (NSLC) and the reports demonstrated that NY-ESO-1 is associated with downstaging and better survival outcomes following chemotherapy treatments (John et al., 2013). Thus, CTA genes possess intriguing features make these genes of high interest in the field of cancer diagnosis and prognosis.

1.2.4.2. CTAs and cancer treatment

Utilization of CTAs as promising tools for cancer diagnosis, vaccination and immunotherapy has been reported by numerous studies (Houghton et al., 2001; Mellman et al., 2011; Rosa et al., 2012) . Majority of the tumour specific markers contain a small peptide of the antigenic protein. Major histocompatibility complex (MHC) molecules present these antigenic peptides on the surface of tumour cells. Cytotoxic T lymphocytes (CTL) have ability to recognise the MCH by which it ultimately kills the cancerous cells (Adair & Hogan, 2009). CTAs provide good candidates for immunotherapy because they able to target cancer cells with highly efficient and less toxicity to the surrounding healthy cells. CTAs are immunologically targeted as they are recognised as non-self-antigens. The germ cells of adult male testis are not targeted by the immune system because of: firstly, MHC class I being not expressed on the testis germ cells surface (Ghafouri-Fard & Modarressi, 2012) and secondly, the existence of blood-testis barrier (BTB) (Ghafouri-Fard & Modarressi, 2012; Li et al., 2012). Thus, normal germ cells are protected from immune system targeting (Kalejs & Erenpreisa, 2005). These features make CTAs of high interest to be used in cancer therapeutic fields.

Cancer treatment using radiotherapy and chemotherapy has proven to have side effects such as toxicity and are inefficient to some extent. In this regard, immunotherapy can be of great help as it can specifically target cancerous cells without damaging healthy cells(Aly, 2012). Nowadays, immunotherapy has turned into a promising method of cancer treatment (Mellman et al., 2011; O'Shea et al., 2014). For instance, autologous CD4+ T cells were isolated from an individual diagnosed with metastatic melanoma using NY-ESO-1 peptide, which is an immune reactive CTA. The isolated cells were expanded *in vitro* before being injected back into the patient resulting in reduction of the tumour mass. When CT scan examination was performed after two months of this therapy, it was found that the metastasised tumours were undetectable. Moreover, the patient lived free of the disease for more than two years following reception of the adoptive therapy (Hunder et al., 2008). Additionally, another emerging and promising cancer immunotherapeutic strategy by which the T cells can be derived from a patient and ex vivo engineered with chimeric antigen receptors (CARs) (Maus et al., 2016; Jacoby et al 2016). These adoptive CAR T cells have ability

to evoke immune response and the production of cytokines to target tumour cells 3. However, many studies have faced many limitations when using CAR T-cells-based immunotherapy (Tokarew et al., 2019; Siciliano et al., 2019). For instance, on-target off-tumour toxicity is a highly dangerous because CAR Tcells may recognise and target healthy cells expressing low levels of target antigens (Morgan et al., 2010). In addition to this limitaion, side effects may appear following a large dose of CAR T cells such as; tumour lysis syndrome and cytokines release syndrome (Ramos et al .,2014). Furthermore, it still remains a challenge to identify good target antigens for this strategy. Thus, These example best describe the needs of adoptive treatment to employ CTAs as promising targets for immunologically reactive cancers.

Vaccination using CTAs is considered to be a promising method for cancer treatment (Renkvist et al., 2001; Blanchard et al., 2013). CD8+ cytotoxic T lymphocytes are unable to recognize CTAs on germ cells of testes and placenta because these cells lack MHC class I (Jungbluth et al., 2005). The majority of the vaccines developed for cancer treatment contain antigens presented by cancer cells which are recognized by CD4+ and CD8+ T cells in humans (Greten & Jaffee 1999., Blanchard et al., 2013). At present, clinical trials of cancer vaccines developed from CT genes; *NY-ESO-1* and *MAGE-A1* are in progress with the aim to trigger T cells against tumour (Caballero & Chen, 2009). These CTAs are potential targets for cancer vaccination (Campos-Perez, et al, 2013).

1.3. Cell Cycle

1.3.1. Cell Cycle Overview

In eukaryotes, there are two types of cell division: mitosis and meiosis. In mitotic cell division, two identical diploid daughter cells, that have a similar number of chromosomes, are produced from a single parental cell. As a part of tissue homeostasis, somatic cells divide mitotically to maintain cellular levels and repair damaged tissues (Marston & Amon 2005; Walczak et al., 2010; Silkworth & Cimini, 2012). Mitosis is characterised by an equational chromosomal segregation which produces two genetically identical cells.

Meiosis is needed for sexual reproduction in eukaryotes. Meiosis involves the production of four haploid gametes, sperm or egg, from a diploid cell of the gonads in male testes and female ovaries respectively (Marston & Amon, 2005). The main and unique feature of meiosis is the genetic diversity generated by homologous genetic recombination resulting in changes to genetic information through generations (Ségurel, 2013). Both cell division types are highly regulated, and the disruption of either mitosis or meiosis may result in serious genetic diseases including cancers (Miller et al., 2013).

1.3.1.1. Mitosis

The mitotic cell cycle is a regulated set of stages consisting of a cellular growth and division. These stages are sequentially ordered, with the initiation of the late stages being dependent on successful completion of the early stages. The normal mitotic cell cycle involves the completion of four stages: Gap-1 (G1), Synthesis (S), Gap-2 (G2) and Mitosis (M) (Figure 1.6). The G1 phase is a gap growth phase that separates the M phase of the preceding cell cycle and prepares the cell to undergo DNA synthesis (S phase), where the chromosomes are duplicated. This is followed by the G2 phase. M phase involves the accurate separation of the duplicated sister chromatids to generate two new daughter cells (Kronja et al., 2011). M phase is also divided into four distinct sub-phases when the cell achieves the appropriate reorganisation of chromosomes which are prophase, metaphase, anaphase and telophase. Following M phase, the cytoplasm of the dividing cell is separated during cytokinesis to generate two daughter cells (Petronczki et al., 2003; Walczak et al., 2010). Moreover, there is

an additional phase that is termed as the quiescent state or G0 phase. The G0 phase promotes the cell to exit the cell cycle in response to external triggers (Singh & Dalton, 2014; Kronja et al., 2011).

In eukaryotes, the cell cycle is conserved and tightly regulated by a series of checkpoints and proteins that control the progression between phases (Stubbs & Suleyman, 2015). The progression of the cell cycle is essential to maintain the integrity of the genome. For example, when DNA damage occurs, the checkpoint proteins and cyclin-dependent kinases (CDKs) stall the progression of the cell cycle until the damaged DNA is repaired. Additionally, defective cell cycle regulators may lead to uncontrolled cell growth and/or avoidance of cell apoptosis, which are hallmarks of cancer (Aarts et al., 2013).
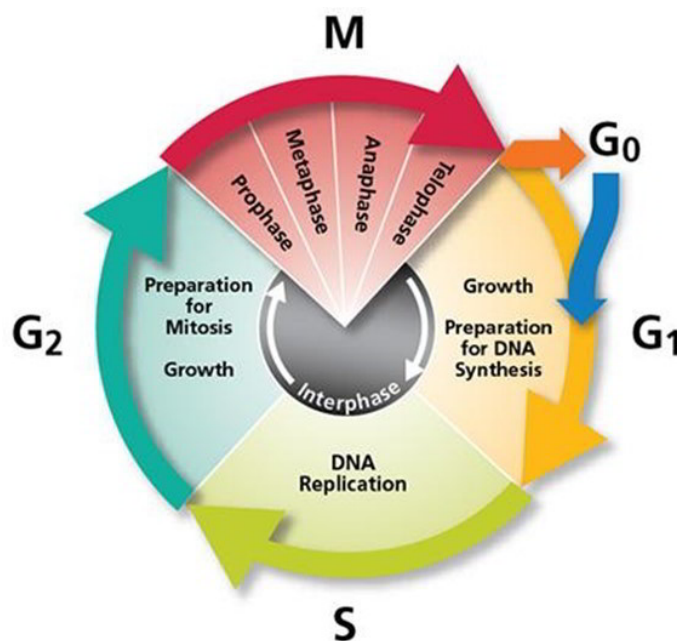
Figure 1. 6. Schematic diagram represents the cell cycle of eukaryotes. Two main stages in the cell cycle: interphase and mitosis (M). Interphase has three sub-phases: Gap-1 (G1), synthesis (S) and Gap-2 (G2). In G1 phase, the cell grows and prepared for next stage of DNA synthesis (S) in which the chromosomes are duplicated. Followed by G2 phase, when the cells grow, synthesize protein and prepare for dividing. M phase is consisted of nuclear division (mitosis) and cytoplasmic division (cytokinesis). Mitosis is divided into four distinct sub-phases to achieve the appropriate reorganisation of chromosomes which are, prophase, metaphase, anaphase and telophase. G0 is a quiescent state or resting phase.

1.3.1.2. Meiosis

Meiotic cell division is a key step in sexual reproduction in eukaryotes. Meiotic cell division is especially for generating haploid gamete cells (ovum and sperm) that each have a haploid set of chromosomes (Gerton & Hawley, 2005; Longhese et al., 2008). Meiosis is initiated with a single round of DNA replication (pre-meiotic S-phase) that is followed by two successive rounds of chromosomal segregations, known as meiosis I and meiosis II. Meiosis I is termed reductional because the number of chromosomes is reduced to the haploid state. The second round of meiosis, meiosis II, is termed equational because of the segregation of sister chromatids, ultimately produces four individual gametes (Clift & Marston, 2011; Marston & Amon, 2005).

Both meiosis I and meiosis II are divided into four different stages including prophase, metaphase, anaphase and telophase (Figure 1.7) (Page & Hawley, 2004; Zickler & Kleckner, 1998). Although these four stages have some similarities with the mitosis phases, they are substantially different. The main feature that distinguishes meiotic division is the occurrence of an inter-homologous interaction event, which is responsible for genetic diversity.

During prophase I, homologous chromosomes become connected together in a process called synapsis. The connection allows segment exchanges and the initiation of crossover (CO) events in a homologous recombination process. Prophase I is considered one of the longest and most complex phases that involves several biological events specific to meiosis. Based on the cytological landmarks of chromosome structure, prophase I consists of five sub-phases: leptotene, zygotene, pachytene, diplotene and diakinesis, (summarised in Table 1.1), (Zickler & Kleckner, 1998; Zickler, 2006). During metaphase I, the homologous chromosome pairs are aligned and attached to spindles along the metaphase plate at the centre of the cell (Petronczki et al., 2003). At anaphase I, the homologous chromosomes are segregated as the cohesin is resolved from the chromosome arms, allowing the chromosomes to migrate to opposite poles, hence reducing division. At this stage inter-sister cohesion is maintained at centromeres driving the monopolar attachments of sister centromeres to the meiosis I spindle (Egel & Lankenau, 2007).

The cells then enter meiosis II which has sub-phases similar to those in mitosis (Figure 1.7). Sister chromatids stay conjoined via centromere-associated cohesion in metaphase II. This alignment is followed by loss of centromeric cohesion and sister segregation to opposite poles during anaphase II. Telophase II involves the complete separation of sister chromatids which form into four haploid cells that are genetically different (Handel & Schimenti, 2010; Miller et al., 2013).

Table 1. 1. Summary of prophase I substages.

Substages in prophase I	Description of meiosis events
Leptotene	Chromosomes become apparently condensed and thin (thread-like). Telomere start to cluster and the recombination of homologous chromosomes takes place during this stage.
Zygotene	"bouquet structure" is formed as a result of telomer clustering at the nuclear envelop. Homologous chromosomes are completely paired and synapsed by a highly proteinaceous complex termed as the synaptonemal complex (SC).
Pachytene	Synapsis is completed, and chromosomes become thick and short. Chiasmata is formed and resolution of crossing over occurs. Pachytene checkpoints are activated to arrest meiosis in case of errors that occur during recombination and/or synapsis processes, to be repaired or to promote apoptosis.
Diplotene	The release of SC begins to separate the homologs although the physical linkage remains by the chiasmata.
Diakinesis	Further condensation of chromatids prior to metaphase I. Centrioles/spindle pole bodies start to move to opposite poles of the nucleus leading in breakdown of nuclear membrane.
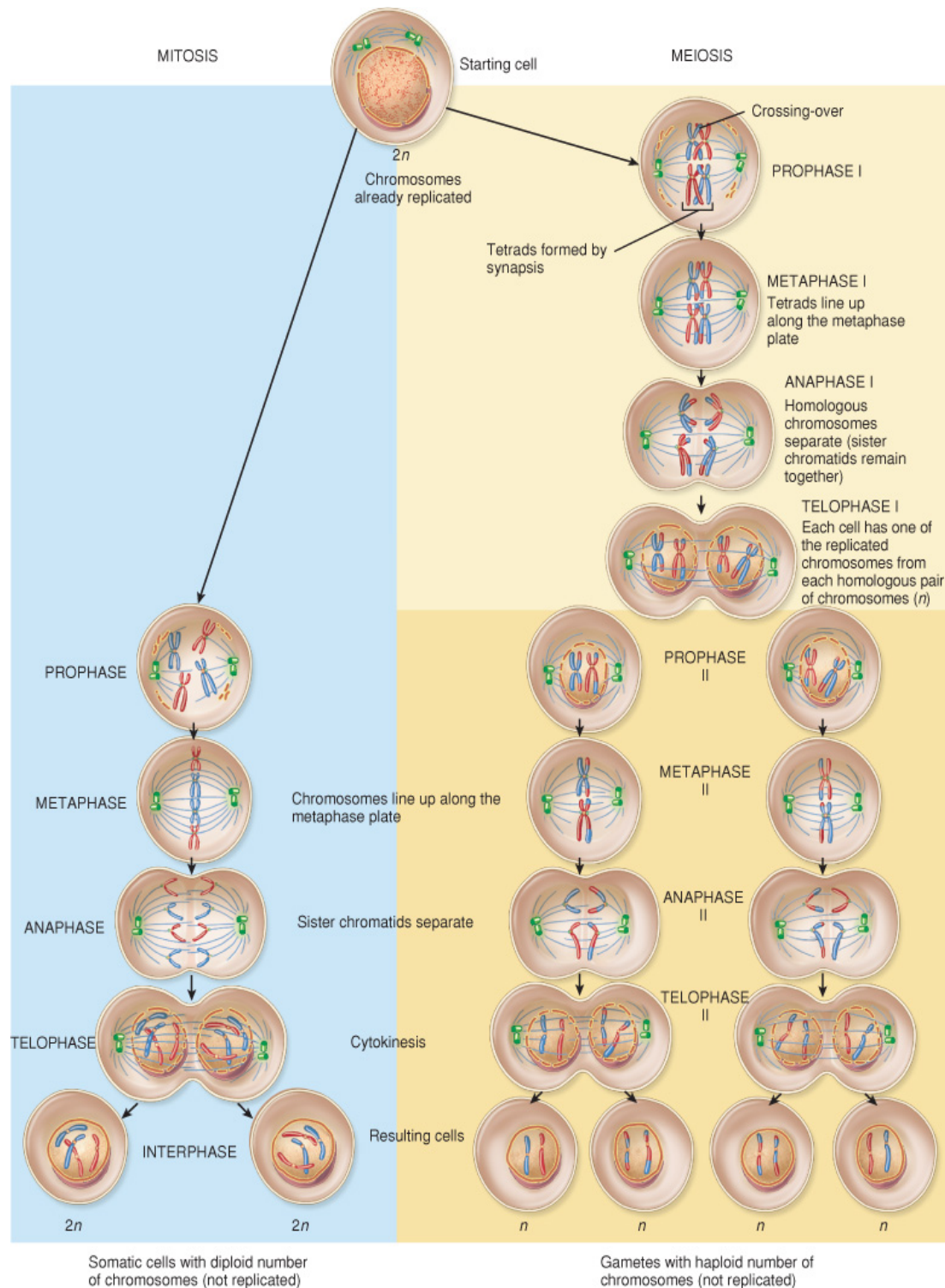
Figure 1. 7. Stages of meiotic and mitotic cell division. Four haploid cells are produced during meiotic cell division, while two genetically identical diploid cells are produced by end of mitosis. Meiosis contain two segregation rounds; meiosis I and meiosis II. Meiosis I is a reductional division because the number of chromosomes is reduced into two halves of homologous chromosomes and separated into two nuclei. Meiosis II is equational division without DNA replication prior to the segregation. Sister chromatids are separated each in different nucleus which ultimately produces four individual gametes. Mitosis and meiosis have similar sub-phases (Tortora & Derrickson, 2008).

1.3.2. Meiotic Recombination

Meiotic recombination is considered as a distinct feature of meiosis I, occurring during early prophase I. It is also an important source of exchanging genetic information, by which new combinations of alleles in the population are established. Homologous recombination (HR) is important for many events during meiosis such as chiasmata formation, prevention of chromosomal non-disjunction, and chromosome segregation (Romanienko et al., 2000; Storlazzi, et al., 2003; Henderson & Keeney, 2004). Many molecular events occur during meiotic recombination starting from the generation of DSBs, 5′ end resection at the breaks, invasion of 3′ end strand with homologous chromosome, establishment of Holliday junctions and subsequent resolution (Handel & Schimenti, 2010). Two separate results are attained for recombination products: crossover (CO) and non-crossover (NCO), where meiosis needs at least a single obligated crossover event per chromosome arm to ensure correct connections between homologues are established in meiosis I (Baudat et al., 2013).

1.3.2.1. Homologous recombination (HR) repair

DSBs are the most dangerous kind of genomic DNA damages. They are induced by various factors, which include endogenous factors, for example, problem arises from DNA replication or DNA damage due to external factors, for example, exposure to ionising radiation (Abbotts et al., 2014). DSBs are initiated as a vital event in meiosis following DNA duplication to ensure proper homologous chromosomes segregation via inter homologue events (Longhese et al., 2009).

The meiotic recombination is initiated by the formation of DSB in one chromatid of the homologues (Bergerat et al., 1997; Keeney et al., 1997; Hunter 2015; Gray & Cohen 2016). DSBs are catalysed by a highly conserved protein complex, topoisomerase VI-like complex, which is composed of SPO11 and TOPOVIBL (Robert et al., 2016). In mammalians, the catalytic tyrosine of SPO11 generates a covalent SPO11 attachment to DNA, forming SPO11-DNA complex at the 5′ end of a break. MRN complex (MRE11-RAD50-NBS1) protein in mammals and yeast, is recruited to DSB site to remove SPO11. This process results in 3′ single-stranded DNA (ssDNA) overhang (Figure 1.8) (De Massy, 2013). RecA family members, RAD51 and DMC1 (in meiosis) recombinases are loaded to create nucleoprotein filaments and initiate strand invasion

into a homologue (Holthausen et al., 2010). The meiosis-specific RAD51 paralogue, DMC1, also associates with RAD51 to search for a homologous pair template in a process named strand invasion. Generation of a displacement loop (D-loop) occurs between the invading 3' ssDNA and its homologue during strand invasion. This is followed by DNA synthesis from the invading 3' end and extension of the D-loop. The extended D-loop is dissociated and repaired by synthesis-dependent strand annealing (SDSA), which results in non-crossover, thus avoiding loss of heterozygosity; this occurs mostly in somatic cells. During SDSA, the disruption of extended D-loop is followed by annealing with the other end of the DSB (Pâques & Haber, 1999; Wright et al., 2018). Alternatively, second-end capture or invasion could occur on the extended D-loop forming a double Holliday junction (dHJ). This may either lead to a crossover or noncrossover outcome (Wright et al., 2018).

The recombination events do not occur throughout the genome randomly, in fact, they seem to be distributed in certain regions, termed as hotspots. Hotspots refer to kilobase-size segments of DNA where the recombination rates tend to be thousands of times higher than in nearby areas of the genome (Paigen & Petkov, 2010; Myers et al., 2005).
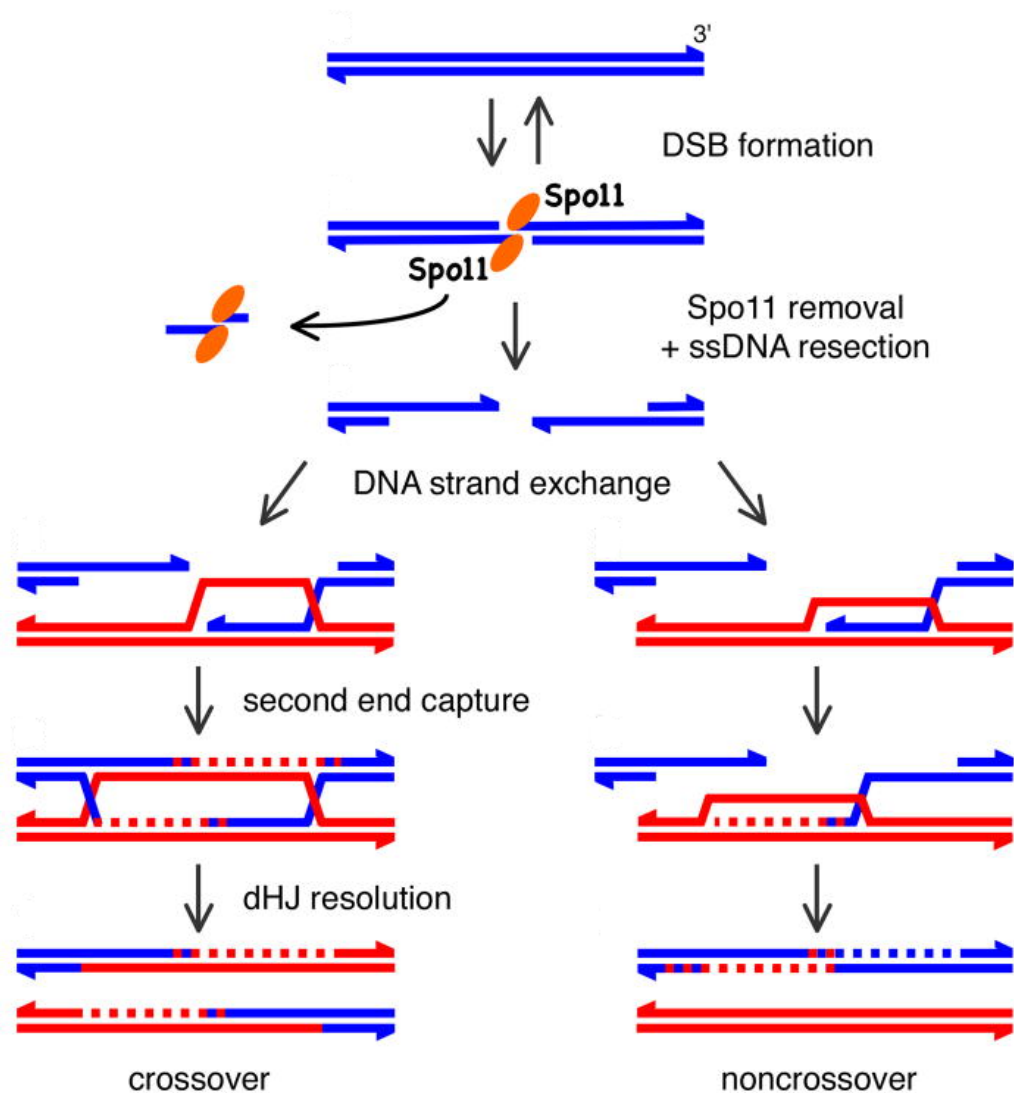
Figure 1. 8. Diagram of DSB mechanism during meiotic recombination. ssDNAs are represented in blue and red horizontal lines. The DSB is induced by cleavage of both strands of the DNA at the 5' ends by SPO11, followed by loading MRN/MRX protein complex to removal of SPO11 and generate 3' ssDNA overhangs. Then, a single 3' end overhang invades the other homologue to create a D-loop by which the other homologues are used as a template to synthesize DNA. The two major recombination pathways are presented: crossover (CO) on the left and non-crossover (NCO) on the right. In the CO pathway, double holiday junctions (dHJs), can be resolved to establish CO products (chiasmata). The non-crossover pathway also termed as synthesis-dependent strand annealing (SDSA) that does not generate chiasmata, instead leads to a phenomenon known as gene conversion. (Adapted from Neale & Keeney, 2006).

1.3.2.2 The synaptonemal complex (SC)

During meiosis I, the chromosome reorganised and form specialized meiosis-specific chromosome structures by which the homologous chromosomes pairs align and assemble in a structure named the Synaptonemal complex (SC). The SC structure consists of axial elements along the pairs of sister chromatids, known as lateral elements (LEs), and the central region (CR) of the SC that is composed of a group of proteins that connect the homologue axes (reviewed in Cahoon & Hawley, 2016). These SC-CR proteins are normally required for the meiosis and play functional roles in stabilisation the distances between LEs.

In *Caenorhabditis elegans*, it has been identified that the SC protein forming the SC-CR is composed of four different proteins; SYP-1, SYP-2, SYP-3 and SYP-4. These proteins depend on each other for localization and stability and they are confined between the LEs (Schild-Prüfert et al., 2011). Additionally, SYP proteins function to stabilize homologous chromosomes and allow the formation of CO events during meiotic recombination (MacQueen et al., 2002; Colaiácovo et al., 2003; Smolikov et al., 2007; Smolikov et al., 2009) Studies on human, mice and *Saccharomyces cerevisiae* have reported that the mature SC functions mainly include its contribution to the formation of CO and completion of meiotic recombination (Hunter, 2015). If SC assembly is incomplete, this results in the failure of homologous chromosomes synapsis and impaired meiotic recombination and ultimately may lead to cell apoptosis (Page & Hawley, 2004). In mammals, the disruption in synapsis results in aneuploidy, infertility and miscarriages (Garcia-Cruz et al., 2009; Fraune et al., 2012).

In cancer cells, the aberrant expression of many proteins that are involved in SC structure was observed in many tumours, suggesting their functional roles in tumour maintenance and development. For example, the abnormal production of SYCP1 protein is detected in tumours such as, lung, brain, melanoma, gastric and pancreatic carcinoma (Meuwissen et al., 1992; Türeci et al., 1998; Nishikawa et al., 2012). Additionally, it has been reported that SYCP3 can interact with BRCA2 forming a complex that deactivates DNA repair pathway during the mitotic recombination leading to oncogenesis (Hosoya, et al, 2012).

1.3.2.3 The cohesin complex

Cohesin is a multiprotein ring structure that connects the newly formed sister chromatids together during pre-meiotic DNA replication. Cohesin has essential roles for accurate chromosomal segregation and initiating sister chromatid cohesion (SCC) (Choudhury et al., 2012). It plays a fundamental role in DSB initiation and repair events during mitosis (Sjögren & Nasmyth, 2001) and meiosis (Kim & Scott, 2010). During meiosis, cohesion is contributed to the assembly of axial elements (AEs) of SC structure to allow pairing of homologous chromosomes (Kim & Scott, 2010; Klein et al., 1999). In yeast, cohesion also works as a transcriptional activator (Lin et al., 2011).

 The complex of cohesin is mainly composed of two members of the structural maintenance of chromosome (SMC), SMC1 and SMC3, a member of α-klesin proteins and stromalin proteins (STAG) (Garcia-Cruz et al., 2009). In mammals, it has been found that there are two types of SMC1: SMC1α that is present in mitosis and SMC1β that is specifically produced during meiosis. The α-klesin subunits are made of three subunits: SSC1/RAD21 in mitosis or RAD21L and REC8 in meiosis. REC8 is essential for two reasons; firstly, it is vital for inter-homologue meiotic recombination and secondly, it is required during meiosis I to form sister centromere monopolarity to achieve correct reductional segregation. In mitosis, the defect of monopolarity onto sister centromeres may lead to uniparent disomy (UPD). Additionally, it has been recently found that the high frequencies of UDP during mitotic division is linked to the expression of at least one meiotic cohesin gene (Folco et al., 2017).

STAG3, SMC1β and RAD21L are meiosis-specific cohesin subunits and their gene expressions are restricted to the healthy male testes in humans. However, some cancers are characterised by the activation of the consequent cohesin genes (Feichtinger et al., 2012). Furthermore, it has been reported that mutation of cohesin subunit (*STAG2*) is linked with aneuploidy and tumourigenesis in mice (Remeseiro et al., 2012). Another study has identified that mutations of cohesin genes; *STAG2*, *RAD21*, *SMC1* and *SMC3* are associated with acute myeloid leukaemia (Welch et al., 2012) and other cohesinopathies (Skibbens, et al., 2013; Tock & Henderson, 2018).

1.3.2.4. Meiotic recombination Hotspots

In human, many studies have demonstrated that meiotic recombination occurs in specific and narrow regions within a range of 1 to 2 kb size (Jeffreys et al., 2001). In 1982, Orkin and co-workers were the first to describe human hotspots (Orkin et al., 1982). In 2005, the genome-wide maps of recombination hotspots were carried out for first time on human populations, resulting in the identification of over 30000 recombination hotspots (Myers et al., 2005). These findings open the door to a better understanding of the recombination process.

DSBs result in the exchange of the allelic sequence at breaks (active allele) (Lichten & Goldman, 1995; Petes, 2001). It is suggested that this conversion between alleles during recombination is faster in genomic areas that have recombination hotspots (Cooper et al., 2016). The genome-wide DSB landscape has defined genomic loci having high local chances of DNA cleavage by SPO11 as DSB hotspots (Pan et al., 2011).

Gene promoters have nucleosome-depleted regions (NDRs), in which there is frequent occurrence of hotspots, as suggested by genome-wide DSB maps for many species. Therefore, it is postulated that these loci undergo DSB formation due to local chromatin accessibility (Pan et al., 2011; Lam & Keeney 2015; He et al., 2017; Choi et al., 2018). Transcriptional regulation greatly depends on trimethylated lysine 4 on histone H3 and the histone variant H2A.Z (H3K4me3) (Deal & Henikoff, 2011; Coleman-Derr & Zilberman, 2012; Sura et al., 2017) which are present in great amounts in the nucleosomes that have gene promotors showing the highest crossover frequencies (Choi et al., 2013).

In 2010, it was revealed that DSBs are directed to many hotspot sites by PRDM9 protein in the mouse and human genomes (Myers, et al, 2010, Baudat, et al, 2010, Parvanov, Petkov & Paigen, 2010). Additionally, H3K4 methylation is reported to mark hotspot sites (Borde et al., 2009; Buard et al., 2009; Smagulova et al., 2011). Other studies reported a significant correlation between PRDM9 and H3K4-me3 (Hayashi et al., 2005; Baker et al., 2014). Although PRDM9 identifies recombination hotspots in humans (Pratto et al., 2014), and in mice (Brick et al., 2012), PRDM9 has many more

DNA binding sites in the genome than there are hotspots, suggesting other possible functions (Baudat, et al, 2010).

1.3.2.5. Meiotic recombination genes and cancer

Meiosis-specific genes are a subclass of CT genes that are normally present in germ cells but not expressed in healthy somatic tissues. Many cancers are characterized by the activation of meiosis-specific and CT genes (McFarlane et al., 2014, 2015; McFarlane & Wakeman, 2017). This has led to the suggestion that the re-activation of these genes may drive oncogenesis in somatic cells (Rousseaux et al., 2013; McFarlane et al., 2014, 2015; Whitehurst, 2014; McFarlane & Wakeman, 2017). Additionally, this activation may require specific molecular events that are harmful for somatic cells, for example, the formation of DSB, inaccurate repair of inter-homologue leading to loss of heterozygosity, changes of transcriptional activation of other genes and activation of recombination hotspot loci. Many investigations have been performed in recent years to discover the functional roles of meiosis-specific genes in cancer initiation and maintenance (McFarlane & Wakeman, 2017).

Meiosis-specific genes normally modulate a reductional segregation during meiotic division. In normal somatic cells, they are silent, however; re-activation of these genes is widely detected in many tumours, and may have oncogenic potential (McFarlane & Wakeman, 2017), this oncogenic function might be achieved through either the involvement of meiosis-specific genes in wider soma-to-germline transition or a specific contribution to oncogenic chromosomes dynamics (McFarlane & Wakeman, 2017). A function of meiosis-specific genes in tumour initiation was suggested based on seminal work in *Drosophila melanogaster* where it was shown that *l(3)mbt* brain tumor development required the aberrant expression of many germline genes, including meiosis-specific genes (Janic et al., 2010; Rossi et al., 2017). In the line with this, Feichtinger and co-workers reported that many human cancers showed similar gene expression profiles, suggesting that these germline genes were required for human oncogenesis (Feichtinger et al., 2014).

Many meiosis- specific genes are activated in a wide range of tumours. For example, *SPO11*, which encodes a protein that initiates the formation of DSB in meiosis. The oncogenic potentials of *SPO11* remain unclear, however, its orthologue in fly, *mei-W68* is required for *l(3)mbt* brain tumor formation (Rossi et al., 2017).

During meiosis, synaptonemal complex (SC) forms synapsis to connect homologus chromosomes for crossover (CO) events. SYCP3 is a component of SC structure which is consider as an indicator for meiotic progression in germ cell tumours (Jørgensen & Rajpert-De Meyts, 2014). In addition to SYCP3, other meiotic factors contribute to the formation of SC and inter-homologue recombination, such as; HORMA domain protein HORMAD1 (Wojtasz et al., 2009; Shin et al., 2010; Daniel et al., 2011). It has been revealed that both SYCP3 and HORMAD1 have the potential to initiate and maintain tumour progression. The re-activation of *SYCP3* in mitotic dividing cells has been shown to impair recombination via disrupting the activity of BRCA2, a tumour suppressor recombination regulator (Hosoya et al., 2012; McFarlane & Wakeman, 2017). In cancer cells, the upregulation of *SYCP3* also results in ploidy changes (Hosoya et al., 2012). HORMAD1 is important meiotic factor that is required for meiotic recombination control (Shin et al., 2010; Daniel et al., 2011). However, the abnormal activation of *HORMAD1* in cancer cells has been shown to modulate homologous recombination repair pathways (Watkins et al., 2015). Furthermore, the activation of meiotic recombination regulators play roles in the maintenance of cancer cells progression, for example; the recombinase, RAD51 and its orthologue DMC1 is activated in glioblastoma and is reported to promote cellular proliferation (Rivera et al., 2015).

Greenberg and colleagues have extensively studied the influence of meiosis genes in cancer chromosomal dynamics and they found that the two meiotic recombination regulators, MND1 and HOP2, contribute to oncogenesis. The study reported that these two meiosis factors assist cancerous cells to drive an alternative lengthening of telomere (ALT) mechanism during the absence of telomerase activity (Arnoult & Karlseder, 2014; Cho et al., 2014, McFarlane & Wakeman 2017).

PRDM9 is another meiosis-specific gene, which encodes as an initiator of meiotic recombination hotspots via a methyltransferase activity (Koslowski et al., 2002). *Meisetz*, the murine orthologue of *PRDM9*, activates meiotic recombination hot spots and acts as a transcriptional activator for many genes, including other meiosis genes (Hayashi et al., 2005). It was also discovered that several types of cancers activate *PRDM9* and it is reported as a CT gene (Feichtinger et al., 2012). A recent study has reported that the overexpression of human *PRDM9* in HEK293T cells resulted in the upregulation of many human genes, suggesting it can function as a transcription activator factor in cancer cells (Altemose et al., 2017).

In addition, recent study in mice has found that mammalian-specific gene, *Tex19.1* has functional roles in the initiation of meiotic recombination (Crichton et al., 2017). Its human ortholog, *TEX19*, is defined as CT gene, which is normally expressed in testis and embryonic stem cells but is also broadly re-activated in many types of cancers (Feichtinger et al., 2012; Planells-Palop et al., 2017). More focusses insight into, PRDM9 and TEX19, and their identified functions in normal and cancer cells are provided below.

1.4. PRDM9

Our understanding about the interaction of PRDM9 with DNA has become stronger in recent years. Studies have also shown capability of PRDM9 for changing the structure of chromatin through methylation of histone H3 at lysine residues, K4 and K36. In addition to trimethylation of nucleosomes, PRDM9 marked hotspots in DNA loops with the axis of chromosome to initiate DSBs allowing genetic exchange (Paigen & Petkov, 2018). Moreover, it has reported that SPO11 is recruited at PRDM9 binding sites to generate DSBs (Neale & Keeney, 2006; Smagulova et al., 2011).

The structure of PRDM9 consists of a zinc finger domain, a SET domain, SSXRD nuclear localization signal and KRAB domain, which present at the N-terminal and is responsible for interaction with other proteins (Figure 1.9) (Parvanov et al., 2017; Imai et al., 2017). Histone methyltransferase activity is provided by the SET domain (Powers et al., 2016; Hayashi et al., 2005; Wu et al., 2013; Eram et al., 2014). The zinc finger domain possesses a proximal zinc finger, which is distant from the terminal C2H2 zinc finger array that may comprised of 8 to more than 20 fingers (Berg et al.,

2011; Fledel-Alon et al., 2011; Parvanov et al., 2010; Hinch et al., 2011; Berg et al., 2010; Sandor et al., 2012; Ma et al., 2015). The structure of PRDM9 protein has been found to be highly conserved among different species except for the terminal zinc finger array. This terminal zinc finger array is very polymorphic in number of fingers contained in it and/or in the three amino acids of every finger that determine DNA-binding specificity of PRDM9 (Paigen & Petkov, 2018).

Studies on germline cells of male juvenile mice that undergo the first round of meiosis have provided some detailed mechanisms and functions of Prdm9 protein. It has been identified by cytological assays that Prdm9 is active during the stages preleptotene to leptotene and is localized in the nucleus. By the end of zygotene, Prdm9 disappears (Sun et al., 2015; Parvanov et al., 2017).

Human PRDM9
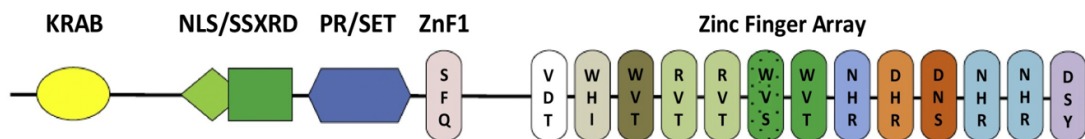
Mouse Prdm9
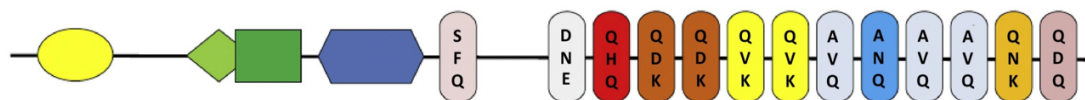
Figure 1. 9. Comparison of the Molecular Structure of PRDM9 in human and mouse. The unique structure of the PRDM9 protein is composed of a KRAB-like, SSXRD, SET, and zinc finger array domains. The amino acid residues in each finger are responsible for the contact with DNA. Zinc fingers array are polymorphic; differ in number and the three amino acids in human and mouse. Figure is adapted from (Paigen & Petkov, 2018).

Every variant of PRDM9 protein binds to specific DNA sites depending on a common recognition motif. The composition of zinc finger domain determines these motifs allowing DNA binding (Billings et al., 2013; Berg et al., 2011; Hinch et al., 2011). DNA binding involves the use of all fingers of PRDM9, however, a subset of only 4-6 fingers have significant roles in recognition motif (Patel et al., 2016; Patel et al., 2017). The remaining fingers have a secondary role in sequence specificity (Baker et al., 2015)

and also function to further stabilize DNA binding (Billings et al., 2013). PRDM9 acts as a multimer *in vivo* (Patel et al., 2016; Altemose et al., 2017). This is important in determining hotspots in individuals heterozygous for PRDM9 alleles that have different DNA binding affinity (Flachs et al., 2012). Trimethylation H3K4 and H3K36 are catalysed by the SET domain of the protein that reorganizes the nearby nucleosomes and alters the structure of chromatin facilitating recombination (Baker et al., 2014). Another study also reported that PRDM9 contributes to automethylation of its own lysine sequences (Koh-Stenta et al., 2017), although the importance of this activity still needs to be determined. It is possible that methylated and unmethylated PRDM9 may demonstrate distinct potentials for DNA binding or histone methylation. Additionally, it is also possible that automethylation may influence *in vivo* stability of PRDM9 since it disappears suddenly at the end of zygotene phase (Paigen & Petkov, 2018).

During homologous recombination, it has been suggested that the extent of Holliday junction migration away from the origin of DSB is restricted to the area containing nucleosomes subjected to methylation by PRDM9, thereby limiting the final location of the crossover event (Baker et al., 2014).

When PRDM9 is absent, DSBs are initiated at other H3K4me3 sites located in the open chromatin regions, specifically the sites that are regulated by other elements like promoters of genes (Brick et al., 2012). These DSBs are not repaired efficiently leading cells to undergo pachytene arrest and subsequently apoptosis. This results in infertility as a consequence of failure of gamete production. Given that, Power and co-workers proposed that the presence of only H3K4me3 is unable to differentiate hotspots from other H3K4me3 sites, but it requires involvement of other factors. It is highly likely that H3K36me3 is also involved since H3K4me3 and H3K36me3 are found to co-exist at hotspots only in germ cells (Powers et al., 2016). Other possible factors involved can be PRDM9 and its association with other proteins or some combination of these factors (Paigen & Petkov, 2018). The interactions of PRDM9 protein with phosphorylated meiotic cohesin protein REC8 and SC proteins such as; SYCP1 and SYCP3 were reported, (for example, see Parvanov et al., 2017). Germ cells lacking PRDM9 show defects in homology recognition and synapsis, in addition to failure DSB repairs and transcriptional abnormality features of meiotic silencing of unsynapsed chromatin (Sun et al., 2015).

It has been demonstrated that duplication of *PRDM9* in primates has resulted in the evolution of *PRDM7*, a primate-specific gene (Fumasoni et al., 2007). Because they share similar DNA sequences, *PRDM7* is highly homologous with *PRDM9*. Both genes encode proteins that share 97% of amino acids across the PR domain sequence and 41% of overall amino acids. The differences between PRDM7 and PRDM9 proteins are three divergent amino acids in the PR domain sequence and the number of zinc finger repeats that each displays. PRDM7 has only 0–4 zinc finger repeats (depends on isoforms) as compared to 14 zinc finger repeats in PRDM9. *PRDM7* also has major structural rearrangements in the zinc finger sequence, including modified gene splicing. *PRDM7* and *PRDM9* are both members of the *PRDM* family and have expressions that are normally restricted to germ cells (Hayashi et al., 2005). Fumasoni and colleagues found that the expression of *PRDM7* is restricted to melanocytes, suggesting that *PRDM7* has tissue-specificity (Fumasoni et al., 2007). PRDM7 is thought to be involved in cell progressive and specialization functions and/or it may have tight regulatory functions (Fumasoni et al., 2007). Recently PRDM7 has also been shown to be an efficient methyletransferase, which could catalyze H3K4 *in vivo* and *in vitro* (Blazer et al., 2016).

1.5. Testis Expressed 19 (TEX19)

TEX19 is a gene specific to mammalians that was initially identified in mouse germ cells. The *Tex19* orthologue has been duplicated, resulting in two different paralogues in rodents, *Tex19.1* and *Tex19.2.* Only one version of *TEX19* exists in humans. In mice, both forms of *Tex19* are located on chromosome 11, whereas the human *TEX19* is present on chromosome 17. It has been suggested that the human *TEX19* is the human orthologue for the mouse *Tex19.1* gene, since the two are closely related in terms of their genome loci, and they have a similar orientation and separation distance from the *UTS2R* gene (see Figure 1.10) (Kuntz et al., 2008).

In mice, the two paralogues have different expression profiles. While the expression of *Tex19.1* is detected in germ cells and placentas, the expression of *Tex19.2* has been found in testes and is broadly expressed in somatic tissues (Kuntz et al., 2008). *Tex19.1* expression is reported to be restricted to male germ cells and the early stages

of mouse embryonic stem cells (mESC) (Kuntz et al., 2008). Interestingly, it has been reported that this paralogue and *Oct4* expression patterns are parallel during the early stages of embryogenesis and that their transcript levels are reduced upon embryonic stem cell differentiation. This suggests that *Tex19.1* might play a functional role in stemness. Moreover, human *TEX19* showed an expression pattern similar to that of mouse *Tex19.1*. The expression of human *TEX19* has been detected in unfertilised oocytes, placentas and adult male testis tissues (Celebi et al., 2012). A recent study reported that TEX19 protein is only produced in testes and in no other normal tissues (Zhong et al., 2016). The lack of *Tex19.1* has been demonstrated to cause defects in meiotic chromosomal synapsis (Yang et al., 2010) and in spermatogenesis, subsequently resulting in male infertility (Öllinger et al., 2008a). Furthermore, the loss of *Tex19.1* in germ cells has led to consistent alterations in meiosis-specific genes that are involved in meiotic recombination, for example, Spo11, synaptonemal complex genes *Sycp1*, *Sycp2* and *Sycp3*, as well as in cohesion complex Rec8 and *Smc1β* (Öllinger et al., 2008). Tex19.1 also interacts with Ubr2 (Yang et al., 2010). This interaction was observed to play a role in regulating meiotic recombination (Reichmann et al., 2017) and retrotransposon activities (MacLennan et al., 2017). Hence, *Tex19.1* mutants demonstrate an arrest in meiosis (Bourc'his & Bestor, 2004; Soper et al., 2008; Öllinger et al., 2008). Many findings have established that *Tex19.1* is involved in the genomic instability of germ cells, since it regulates transposable elements (Öllinger et al., 2008; Reichmann et al., 2017).

Recent studies have developed two bioinformatic pipelines to identify new cancer-testis (CT) genes (Feichtinger et al., 2012; Sammut et al., 2014). *TEX19* was one of the genes defined as a CT gene, although the functions of human *TEX19* is still unclear (Wang et al., 2001; Kuntz et al., 2008). *TEX19* is classifies as a testis-selective CT gene, because its expression profile was detected in adult male testes and thymus tissues (Hofmann, et al, 2008). The expression of human *TEX19* has been detected in a wide range of cancers (Feichtinger et al., 2012), suggesting its functional role in oncogenesis. A recent study also found that *TEX19* expression is restricted to testes and tumour tissues (Zhong et al., 2016), confirming that it is a CT gene. Additionally, *TEX19* transcript levels were detected in 60% of bladder carcinoma samples. The TEX19 protein was also present in significantly greater amounts in late stage cancer samples as compared to early stage tumours (Zhong et al., 2016).

Planells-Palop et al. found that the depletion of TEX19 in many cancer cell lines limits cellular proliferation and self-renewal. Moreover, the downregulation of *TEX19* results in changes to the transcript levels of many tumour-associated genes. This indicates that TEX19 might have the potential to drive proliferation in cancer cells (Planells-Palop, et al, 2017).

All these findings suggest that *TEX19* has the potential to drive cancer progression and act as an oncogene. Moreover, as a CT gene, *TEX19* might be used as a cancer biomarker for prognostic and diagnostic approaches, as well as a good target for immunotherapeutic applications.
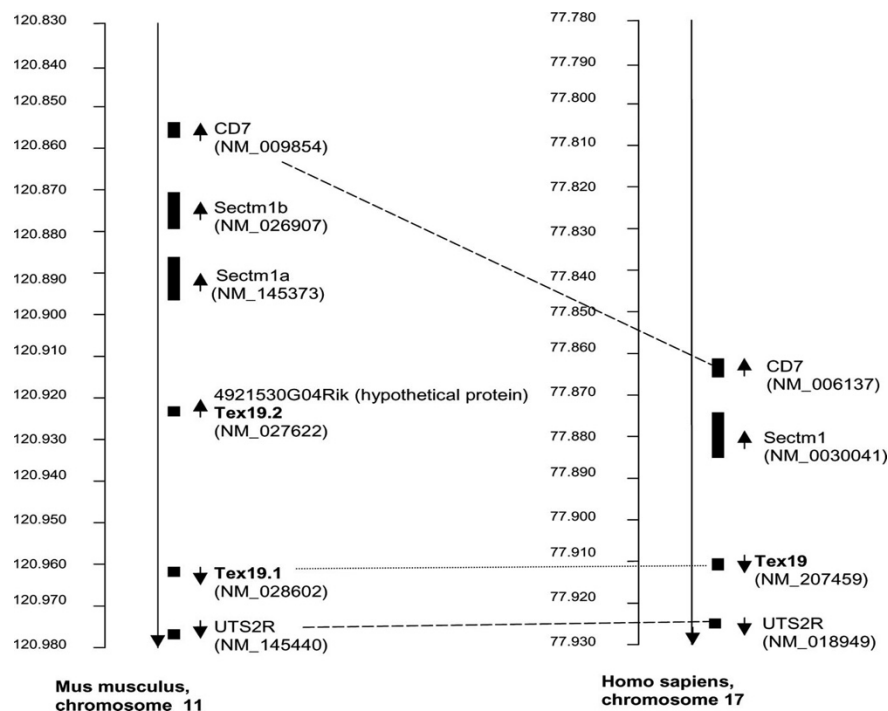
Figure 1. 10. The genomic location of *Tex19*. This scheme shows the conserved region of both human and mice genomes in order to compare human chromosome 17 and mouse chromosome 11. Human *TEX19* is closely related to mouse *Tex19.1*, since they are oriented in a similar direction and separated from the *UTS2R* gene by a similar distance (Kuntz et al., 2008).

1.6. The aim of study

PRDM9 and TEX19 are both CTA genes that play important roles in meiosis and ferltility in germinal cells, however, their re-activations in cancer cells have been proposed to maintain the process of oncogenesis. The roles of those genes during oncogenesis are still not clear.

This project aims to elucidate the functional roles of PRDM9 and TEX19 in human cancer cells.

The main goals of this project were to:

1. Investigate the function of PRDM9 as transcriptional activator of several meiosis-specific genes that are re-activated in human cancer cells.

2. Examine the epigenetic roles of PRDM9 and its influence on histone modifications and methyletransferase activities in cancer cells.

3. Study the effects of TEX19 depletion on the proliferation of different types of cancer cells.

4. Check whether TEX19 has influence on the epigenetic mechanisms in cancer cells.

Chapter 2:

Materials and Methods

2. Materials and Methods

2.1. Sources of Human Cancer Cell Lines

The sources of the cells used in this study as following; H460 cells were purchased from the American Type Culture Collection (ATCC). K562, SW480, MCF7 and HCT116 cell lines were obtained from the European Collection of Cell Cultures (ECACC). Prof. P.W. Andrews (University of Sheffield) provided the embryonal carcinoma NTERA-2 (clone D1). The HeLa Tet-On® 3G cell line, which was transfected with pCMV-Tet3G, was obtained from Clontech. More details on theis cell lines are demonstrated in table 2.1. The Laboratory of the Government Chemist (LGC Standards^{TM}) was used for verifying the authenticity of all cancer cell lines every year (authentication tracking number SO0409759).

2.2. Cell Culture Growth Maintenance

Appropriate medium (as shown in Table 2.1) with Foetal Bovine Serum (FBS) (Invitrogen; GIBCO 10270) was used for culturing the cancer cell lines. The Tet System Approved FBS medium (Clontech; 631106) was used for culturing HeLa Tet-On® 3G cells. The medium also contained 100 µg/ml Geneticin G418 (Invitrogen; GIBCO 10131035). For incubation of the cancer cell lines, humidified incubators with 5% CO_2 were used and cells were incubated at 37°C. For NTERA-2 (clone D1) 10% CO_2 was used during incubation. The LookOut® Mycoplasma PCR Detection kit (Sigma Aldrich; MP0035) was utilized for checking the cell lines for mycoplasma infection according to manufacturer's instruction. Table 2.1 summarizes the media composition and culture conditions used for culturing cell lines.

2.3. Preparation of Cancer Cell Line Stocks

Phosphate buffered saline (1X) (PBS) buffer was used for washing the confluent cells twice. Following these cells were trypsinized using 1x trypsin Ethylenediamineteraacetic acid EDTA (Invitrogen, GIBCO 1370163). This was followed by counting of cells through automated cell counter (Bio-Rad) or a haemocytometer slide and centrifugation of cells for five minutes at 100 x*g*. The pellet thus obtained was re-suspended in a freezing medium containing 1:9 dimethyl sulphoxide (DMSO): FBS. Finally, the cells were kept in labelled cryotubes then they

were stored at   -80°C for one day (short term storage). Alternatively, cells were stored in liquid nitrogen for long-term storage.

Table 2. 1. Description and growth conditions for the human cancer cell lines used in this study.

Cell line	Description	Media	CO_2
HCT116	Human colon carcinoma	McCoy's 5A medium + GLUTAMAXTM (Invitrogen, GIBCO 36600) supplemented with 10% FBS	5%
HA-HCT116	Human colon carcinoma with HA tag		
MCF7	Human Caucasian breast adenocarcinoma	DMEM + GLATAMAXTM + supplemented with 10% FBS and 1xNEAA (non-essential amino acids)	5%
NTERA-2	Human Caucasian pluripotent embryonal carcinoma	Dulbecco's modified Eagle's medium (DMEM) + GLUTAMAXTM (Invitrogen, GIBCO 61965) supplemented with 10% FBS	10%
SW480	Human colon adenocarcinoma		5%
HeLa Tet-On® 3G	Stably transfected Human cervical cancer with pCMV- Tet3G vector		5%
K562	Leukaemia	RPMI 1640 + GLUTAMAXTM + 10% FBS and 2 mM sodium pyruvate	5%

2.4. Thawing of Stored Cancer Cell Lines

The vials containing cells were kept in a water bath set at 37°C and were agitated gently for thawing. An appropriate prewarmed medium (5 ml) was then added to the vial and mixed thoroughly for diluting the cell suspension. The cell suspension was then centrifuged for five minutes at 100 xg. After discarding the supernatant, cells were suspended in 10 ml of growth medium. Cells obtained in this way were divided into two halves and kept in separate T25 cm^3 flasks. These flasks were incubated in a humidified incubator at 37°C for one day with suitable concentration of CO_2.

2.5. RNA Extraction

The RNeasy plus Mini Kit (Qiagen; #74136) was used for extracting RNA following the procedure described by the manufacturer. In particular, trypsin activity was inactivated by washing cells with 5 ml of PBS. This was followed by aspiration of the PBS and addition of an adequate quantity of RLT plus buffer for cell lysis and inactivation of RNases. In order to eliminate genomic DNA, the cell lysates were transferred to a gDNA Eliminator spin column. The flow through thus obtained was transferred to an RNeasy spin column for isolating RNA. A NanoDrop 2000c (NanoDrop; Thermo Scientific) was finally used to evaluate the concentration and quality of the isolated RNA.

2.6. cDNA Synthesis

SuperScript III First-Strand Synthesis System (ThermoFisher Scientific; #1808-051) was used for creating first strand of cDNA as manufacturer's instructions. With the help of an oligo-dT primer, 1 µg of total RNA was transcribed giving rise to a single strand of cDNA. In order to get pure single-strand cDNA, RNA was degraded by adding RNase H to all specimens. The reverse transcriptase enzyme (SSIII provided with the kit) was added to all test specimens but not the control specimen as an internal negative control, which is non reverse transcriptase (NRT) control. DNAse/RNAse free water was added to every sample to obtain the final cDNA dilution at 1:8. Finally, qualitative RT-PCR was conducted using *β-ACT* primers for analysing the quality of cDNA obtained.

2.7. Polymerase Chain Reaction (PCR)

The required gene sequences were taken from the database maintained at the National Centre for Biotechnology Information (NCBI; http://www.ncbi.nlm.nih.gov). Next step was designing of primers that can span multiple introns when possible. Primers were designed by both manual procedure and by Primer 3 software (available at http://primer3.ut.ee/) and all primers are listed in Table 2.2 and Table 2.3.

PCR amplification was carried out using the following protocol. 25 µl of BioMix^{TM}Red (Bioline; BIO-25006) was added to 2 µl of diluted cDNA. The mixture was then added with 1 µl (10 pmol) of forward primer and 1 µl of reverse primer. ddH$_2$O was then added to make up the final volume to 50 µl. All samples were subjected to pre-cycling melting step for five minutes at 96°C. 40 cycles of denaturation were carried out for 30 seconds at 96°C. Next annealing was conducted for 30 seconds at a temperature between 58°C and 62°C (specific annealing temperature can be found in table 2.2 and 2.3). Extension lasted for 30 seconds at 72°C followed by final extension period of 5 minutes at 72°C.

2.8. DNA Purification Method

2.8.1. Direct RT-PCR product purification
A quantity of 50 µl of PCR reaction mixtures were subjected to purification conducted with the High Pure PCR Product Purification Kit (Roche Applied Science; 11732676001). For this purpose, the protocol provided with the kit was followed.

2.8.2. Purification of DNA from Agarose Gel
The prepared 1% agarose gels were loaded with PCR products for purification. Particular fragments of the gel were taken out with the help of a sterilized scalpel. The excised gel was then used for purification which was conducted using Geneclean (MP; 111102400) or PCR purification Kit (Roche; 11732676001) following the protocol provided by the manufacturer.

2.8.3. DNA sequencing
The Eurofins MWG Company (Germany) conducted the DNA sequencing. A NanoDrop was used to evaluate the purified DNA concentration. A sufficient concentration (75 ng of purified DNA, or 1 µg in case of plasmid DNA) was adjusted with DNase/RNase free sterile water to a final volume of 15 µl for each sequencing reaction. Only one primer (forward or reverse) at a concentration of 10 µM were added to its respective tube and sent Eurofins MWG for sequencing. The resulted sequence of gene was then aligned to identify the gene identity. For this purpose, the Basic Local Alignment Search Tool (BLAST) (http://blast.ncbi.nlm.nih.gov/Blast.cgi) and EMBL European Bioinformatics Institute Website (http://www.ebi.ac.uk/) were used.

Table 2. 2. Primer sequences of studied genes with their product sizes (bp)

Gene	Primer	Primer Sequence (5′ to 3′)	Annealing Temp (°C)	Predicted Product Size (bp)
MORC1	F	CAGGAGCTGTGCAATGATGT	58.4	455
	R	CATTGCCCCAGAGAGATTTC		
MORC2	F	TGACCTGCCTCTTCCTGTCT	60.5	776
	R	GAACATGCCATCCAGATCCC		
MORC3	F	CAAGAAGCAGGAAAGGATGG	58.4	562
	R	TTTCCGCCACTTTAGACAGG		
MORC4	F	ACCCAGATGATTGCCAAGAG	58.4	614
	R	GGCATCTTCTTCTTCTCCTC		
DMC1	F	GAACCAGGATTCTTGACTGC	58.4	518
	R	TGGAGTCGTGACAACATCTG		
HORMAD1	F	GCCCAGGATCTACACAGTTA	60.5	486
	R	CCATTCGTTCTCTCTCAGTG		
HORMAD2	F	GAGAGCTCTTATGGAGAACG	60.5	707
	R	CTGGAGCACTCAGAACTTTG		
RAD21	F	TTGGAACTTGCACCTCCTAC	58.4	627
	R	GCCAGCTGTTTCTTTAGGAC		
SPO11	F	AAACGTCGAAGAACGAGGCC	55.0	625
	R	GCACCACAGGTACAATTCAC		
STAG3	F	CTCTTCCATCAGGACAAGCA	60.5	495
	R	CTCTTCTTCCTCGTCCTCTT		
STRA8	F	TGGCAGGTTCTGAATAAGGC	58.4	723
	R	GAAGCTTGCCACATCAAAGG		
SYCO1	F	GGTCAGCAGAAAGCAAGCAA	61.0	509
	R	GGCAGATGTCCACAGATAGT		
SYCO3	F	GTCTTCTGCAGGAGTAGTTG	58.4	645
	R	CACTTGCTATCTCTTGCTGC		
SYCE1	F	CTGCTCAAGGAAGAGAAGCT	60.5	318
	R	CTCTTCCTCTTGTGTGCTCT		
SYCE2	F	CTTCTCCTCTCTGGACTCAA	60.5	3339
	R	CATCTGAGTCTTAGGCTCTG		
PRDM1	F	CAGTGCCTTCTCCTTTACCG	60.5	768
	R	ATGTCATCCTCCACGTCCTC		
PRDM4	F	GGGGACAGGTCATGTAGATG	55.4	714
	R	TGTCCCTGGGTAGGAAGATG		
PRDM6	F	GCACCTGGATTGGACCTTTC	60.5	384
	R	CTTGTCTGCACATGGCTTCC		
PRDM7	F	CTTCATTGACAGCTGTGCTG	60.5	607
	R	AGTTCCTGGCCATACTCATC		
PRDM11	F	AAAGCTTCCAGCAAGTGGAC	60.5	680
	R	TACATCCCCCTCATCAAAGC		
ARRDC5	F	CAACAAGGCAGACTACGTGC	60.5	628
	R	GCGAGTGTGCATGATCTCAC		
C12ORF12	F	CAGCGTACAATAGACCGCAC	60.5	748
	R	CACACCTCCTGGTCATACTC		
DDX4	F	GTGCTACTCCTGGAAGACTG	60.5	756
	R	CCAACCATGCAGGAACATCC		
NT5C1B	F	CGGCAGGAAAATCTACGAGC	60.5	647
	R	CTGTAACCAGGTAGGTCCTG		
NUT	F	CACCACCAGTTGCTCAACTG	60.5	623
	R	CTCCTTCACAGCTTCTGGTG		
ODF4	F	GACAAGATGGGAGACTGCTG	60.5	602
	R	GGTGTCTGTGATCGTCTGTG		

Gene	Primer	Primer Sequence (5′ to 3′)	Annealing Temp (°C)	Predicted Product Size (bp)
SEPT12	F	CTGCAGCTGCATTCACTGAC	60.5	608
	R	CGGATAAGCAGGTCTCTCAG		
TDRD12	F	GAGCTAAAGTGCTGGTGCAG	60.5	641
	R	CTGAGGTCACCGACAATACC		
GAGE1	F	TAGACCAAGGCGCTATGTAC	58.4	245
	R	CATCAGGACCATCTTCACAC		
MAGEA1	F	CCCACTACCATCAACTTCAC	58.4	676
	R	CTCTTGCACTGACCTTGATC		
MAGE-B5	F	CCTCCACTGAGAGTTCATGC	60.5	655
	R	CTTGGGCTCTCTTCCTCATC		
TDRD5	F	GATCCAAAGTGGTCCAACCC	60.5	610
	R	GGATCTCTGGTGAGCTTTCC		
PIWIL1	F	GACCAGAATCCCAAGAGCAC	60.5	350
	R	CAGTCTCGAAGCTCCCTTTG		
TEX19	F	GCTTCAACATGGAGATCAGC	58.0	386
	R	GAAGCTCCTCAAATCTCCAG		
SYCP2	F	CTTGGGAGACCTGGCAAAAT	60.5	354
	R	GATGAAGCCTCTGTTGTTCG		

Table 2. 3. Primer sequences were designed for genes and their expected sizes (bp)

Gene	Primer	Primer Sequence (5′ to 3′)	Annealing Temp (°C)	Predicted Product Size (bp)
KRT5	F	TCTCGCCAGTCAAGTGTGTC	60.0	
	R	ACCAAATCCACTACCGGCAC		315
KRT9	F	GCTCCTGGCAAAGATCTCAC	60.0	214
	R	GCAGCTCAATCTCCAACTCC		
LGALS7	F	GGTCTTCAACAGCAAGGAGC	60.0	230
	R	AGAAGATCCTCACGGAGTCC		
RNASE1	F	TCCTGATACTGCTGGTGCTG	60.0	333
	R	ATGCACAGTTGGGGTACCTG		
LGALS9C	F	GACTTTCAGACGGGCTTCAG	60.0	369
	R	GAAACAGACAGGCTGGGAGA		
SH3TC1	F	ATGCTCTCGGCTTCACTCAT	58.4	376
	R	AGAGCCCACTGATGAAATGG		
TH	F	GTGTTCCAGTGCACCCAGTA	60.0	362
	R	TACGTCTGGTCTTGGTAGGG		
CTCFL	F	CTACAAGCTGAAACGCCACA	58.4	328
	R	GCAGTGTTTGCACTTGAACC		
CPNE6	F	TGCCAGATCAGCTTCACGGT	60.0	423
	R	ACCAGCAGCACCGAGTACTT		
CAPN8	F	TGCTGGAGAAAGCCTATGCC	60.0	335
	R	CACTTCACCCCATGGATTCC		

Gene	Primer	Primer Sequence (5′ to 3′)	Annealing Temp (°C)	Predicted Product Size (bp)
PAX5	F	TGCTCATCAAGGTGTCAGGC	60.0	420
	R	ATGCCGCTGATGGAGTACGA		
C1orf116	F	AGAGCAGTGTAGGGAAGCCA	60.0	314
	R	AACTGCTTCGGCTGCTCTTC		
ONECUT3	F	CGAGGAGATCAACACCAAGG	60.0	271
	R	CTTCTGCTGCTCCTGTTCCT		
LGALS1	F	CAAACCTGGAGAGTGCCTTC	60.0	349
	R	CTTGAAGTCACCGTCAGCTG		
PDGFB	F	GCCGAGTTGGACCTGAACAT	60.0	342
	R	CGTCACCGTGGCCTTCTTAA		
P2RX2	F	CAGCTGCTCATCCTGCTCTA	60.0	502
	R	CGATGTTGCCCTTGGAGAAG		
NGFR	F	CAAGACCTCATAGCCAGCAC	60.0	403
	R	CAGAGCCGTTGAGAAGCTTC		
SYT11	F	GGTGACCGTCTTTGTCTGGT	60.0	233
	R	CTTTGTCTCGGCTTAGCAGG		
PALM3	F	TAAGTCAGAGGGCAGTGCCA	60.0	337
	R	AATCTCCTGGAGCCTAGG		
HMOX1	F	CCTTCTTCACCTTCCCCAAC	60.0	327
	R	GTGTAAGGACCCATCGGAGA		
PRDM9	F1	AGGAAGAATGGGCAGAGATG	58.0	984
	R1	GTTCCTGGCCGTATTCATCC		
	F2	ATCACCAAGGGGAGAAACTG	60.0	831
	R2	CTGGTGAATGAGGAGGTGTG		
	F3	GTCAAGTATGGAGAGTGTGG	60.0	897
	R3	GTGTCTGAGGAGGTGTGACT		
TEX19	F	GCTTCAACATGGAGATCAGC	58.0	386
	R	GAAGCTCCTCAAATCTCCAG		

2.9. Real Time Quantitative qRT-PCR

Primers used in the qRT-PCR were either personally designed using Primer 3 software or as commercial primers obtained from Qiagen. These primers were utilized for conducting the SYBR® Green-based quantitative real time qRT-PCR.

The quantitative real-time PCR (qRT-PCR) was conducted using the Go Taq qPCR Master Mix purchased from (Promega; A6001) and employed as the instructions provided by the manufacturer. 1.5 μl of cDNA (contains 10 ng RNA) and 0.2 μM of primers were added to every well of a Hard-Shell® 96 well plate, from (BioRad; 9655). Sterile water was added to reach a final reaction volume of 20 μl in each well. Each reaction was performed in triplicates.

The PCR amplification steps were set up as following: the amplification started with a denaturing temperature at 95°C for 5 minutes. This was followed by 40 cycles and each cycle is composed of three steps: denaturation at 95°C for 15 seconds, primer annealing at 60°C for 30 seconds and an elongation step at 95°C for 10 seconds. Finally, melt curve analysis was obtained after a completion of the 40 cycles of reaction. The qPCR was performed using a quantitative Bio-Rad CFX instrument. Moreover, the Bio-Rad CFX Manager Software (Version 2) was used for data analysis. The relative fold change and the normalisation of target to reference genes was computed by the ΔΔCt method. Results for the PCR for required genes were then normalized against results for the reference genes given in Table 2.4. Depending on data analysis during this study,such as CT value and melting tempresure analysis, ACTB and GAPDH appeared to be stable reference genes.

Table 2. 4. Commercial qRT-PCR primers in this study and their sources

Tested Gene	Assay Name	Source
β-ACT	Hs_ACTB_1_SG	Qiagen; QT00095431
GAPDH	Hs_GAPDH_2_SG	Qiagen; QT01192646
PRDM9	Hs_PRDM9_1_SG	Qiagen; QT01023631
TEX19	Hs_TEX19_1_SG	Qiagen; QT00033047
MAGEA1	Hs_MAGEA1_1_SG	Qiagen; QT00012320

2.10. Western Blotting Protocol

2.10.1. Whole Cell Protein Extractions

Extraction of proteins from cell lysates was carried out using the M-PER® Mammalian Protein Extraction Reagent, obtained from (Thermo; 78503). In 6-well plates, roughly from 1.5×10^5 to 2×10^5 of cells were grown until become 80 % confluent and then washed using warm 1x Dulbecco's phosphate-buffered (DPBS). Trypsin was added for detachment of adherent cells for 3-5 minutes. After this, warm 1x DPBS buffer was again used for washing the cell suspension. The mixture was then centrifuged at $2500 \times g$ for 10 minutes. After removing the supernatant, weight of the wet pellet was determined. During next step, every 1 mg of cell pellet was added with M-PER lysis buffer (10 µl). This was followed by addition of Halt Phosphatase Inhibitor Cocktail (Thermo Scientific; 78420) and Halt Protease Inhibitor Cocktail (Thermo Scientific; 87785) in a ratio of 1 µl of inhibitor cocktail per 100 µl of lysis buffer. After mixing the mixture through shaking it gently, it was incubated for 10 minutes at room temperature. After incubation, the mixture was centrifuged at $14000 \times g$ for 15 minutes for getting rid of cell debris. The supernatant was stored in a separate labelled tube at -20°C.

2.10.2. Histone Protein Extraction

Histone proteins were extracted utilizing the Histone Extraction Kit (Abcam; ab113476). The cells were treated with pre-lysis, lysis, and balance buffers to extract total histone for immediate use or storage. According to manufacturer protocol, cell pellet were resuspended in 3 volumes (approximately 200 µL/10^7 cells or 100 mg of tissue) of lysis and then kept on ice for 30 minutes incubation. Followed by cold centrifugation at 4°C for 5 minutes at 12,000 xg. The supernatant fraction (containing acid-soluble proteins) were transferred into new vial and 0.3 volume of Balance-DTT Buffer was added. Finally, the protein concentration can be calculated BSA or stored at -80°C for long-term storage.

2.10.3. Protein Concentration Assay Using BCA

BCA Protein Assay Kit (Thermo Scientific; 23227) was utilized to determine the concentration of total extracted protein so that every well of the gel could be loaded with equivalent quantities of protein. As per the instructions given with the kit, the

bovine serum albumin given with the kit was used for preparation of a set of standards. Next step was preparation of working reagent, which involved addition of 50 ml of Reagent A to 1 ml of Reagent B. After adding the test specimens and standards to the working reagent, the mixture was incubated in darkness, at 37°C for half an hour. 1 μl of these specimens were tested with NanoDrop ND 2000c Spectrophotometer (Thermo; WZ-83061-12) followed by drawing the standard curve to determine the protein concentration.

2.10.4. SDS Page and Western Blotting

10x Bolt Sample Reducing Agent (Life Technologies; B0009) and 4x Bolt LDS Sample Buffer (Life Technologies; B0007) were added to around 30 μg from total protein lysates to abtain a final volume of 20 μL. For denaturation, samples were kept at 70°C in a heating block for 10 minutes before electrophoresis. Samples were then loaded on polyacrylamide gels and the first lane contains a protein ladder (Precision Plus Protein Dual Color Standards, Biorad; 161-0374). For electrophoresis, the NuPAGE MOPS SDS running buffer (ThermoFisher Scientific; #NP0001) was used after dilution with distilled water. Electrophoresis was performed utilizing NuPAGE Novex 4-12% Bis-Tris Gel (ThermoFisher Scientific; #NP0322) in a prepared running buffer and power supply was conducted at 100 V for 1 hour. At the end of run, gels contained separated proteins were moved onto a PVDF membrane (Millipore; #IPVH00010), which was incubated in absolute methanol for 2-3 minutes and then immersed in water for activation. Transfer step was performed utilizing a dry transfer system instrument (Trans-Blot® Turbo^TM from Bio-Rad; # 1704150) with a Trans-blot® Turbo^TM RTA Mini PVDF transfer Kit (Bio-Rad; # 1704272). The dry transfer buffer was prepared as following; (200 ml of 5x transfer buffer (BioRad; #10026938) were mixed with 200 ml 100% ethanol and 600 ml of Nano-pure H_2O) to obtain 1x transfer buffer. The dry transfer system instrument was operating at 2.5 A for 7 minutes.

Next step was washing of the membrane with distilled water for 5 minutes. Membrane was then blocked in 5% skimmed milk powder in a mixture of PBS 0.5% Tween 20 (milk solution) at room temperature for at least 1 hour. This was followed by probing of the blotted membrane with desired quantity of primary antibody which had been diluted in blocking solution (Table 2.5). The membrane was then incubated on a rocker plate at 4°C overnight.

After incubation, the membrane was washed three times with washing buffer (PBS 0.1% Tween 20) for 5 minutes. Washing was followed by incubation of the membrane with relevant secondary antibody diluted adequately (Table 2.6) at room temperature for 1 hour. The membrane was then washed again in washing buffer three times. The required protein was identified through incubation of the membrane with Signal-generating solution for 5 minutes. The solutions used were Super Signal West Pico Chemiluminescent Substrate (Thermo, #34080) and Chemiluminescent Peroxidase Substrate-3 (Sigma, #CPS3100-1KT). Following this the membrane was placed in an X-ray cassettes and exposure to CL-X Posure film (Thermo Scientific, 34091) with the help of optimal exposure times. Following the instructions provided by the manufacturer, the film was developed in a dark room using X-ray Film Processor. For histone trimethylation immunoblotting, we used blocking buffer from Abcam (Ab126587) and washing buffer from ThermoFisher (28358) following the same protocol.

Table 2. 5. Sources and dilutions of primary Antibodies in this study.

Antibody	Source	Cat #	optimum dilutions	Molecular weight MW kDa
Anti-PRDM9 antibody	Abcam	ab178531	1:500	103
Anti-PRDM9 antibody	Abcam	Ab85654	1:1000	103
Tri-Methyl Histone H3 (Lys4) Antibody	Cell signaling	9727	1:1000	17
Tri-Methyl Histone H3 (Lys36) Antibody	Cell signaling	9763	1:1000	17
Anti-Histone H3 antibody	Abcam	ab10799	1:1000	15
Anti-Histone H3 (acetyl K9) antibody	Abcam	ab12179	1:250	17
Anti-Histone H3 (tri methyl K36) antibody	Abcam	Ab9050	1:1000	17
Anti-Histone H3 (tri methyl K4) antibody	Abcam	Ab8580	1:1000	17
Monoclonal ANTI-FLAG® M2 antibody	Sigma	F1408	1:1000	---
Anti-FLAG® M2 Antibody	Cell Signaling	8146	1:500 1:1000	---
HA-Tag (6E2) Mouse mAb	Cell Signaling	2367	1:1000	---
Human TEX19 Antibody	R&D	AF6319	1:250	23
Anti-GAPDH Antibody	Santa Cruz	Sc-365062	1:5000	37

Table 2. 6. Sources and dilutions of secondary antibodies in this study.

Antibody	Source	Cat #	optimum dilutions
Anti- mouce IgG	Cell Signaling	7076S	1:1000
Anti-rabbit IgG	Cell Signaling	7074S	1:1000
Sheep IgG HRP-conjugated	R&D	HAF016	1:1000
anti-Mouse IgG (H + L), Alexa Fluor 488 conjugate	Life technologies	A-11029	1:1000
anti-Rabbit IgG (H + L), Alexa Fluor 568 conjugate	Life technologies	A-11011	1:2000

2.11. Gene Knockdown using Small Interfering RNA (siRNA)

Wells of a six-well plate were added with cells at a concentration of 1.5×10^5 or 2.0×10^5 cells/well followed by incubation to allow up to 40% confluent growth. In order to prepare the transfection complex, 6 µl of HiPerfect reagent (Qiagen; 301705) and 10 nM of siRNA (Qiagen) were added to 100 µl serum free medium and the mixture was incubated at room temperature for 25 minutes (specific information on siRNA is given in Table 2.8). Non-interference control (Qiagen; 1022076) was used as negative control during knockdown experiment. From transfection mixture, about 107 µL were introduced to every well drop by drop followed by gentle shaking of the plates. After 24 hours, the medium was replaced and a second application of siRNA was applied. The treated and untreated cells were harvested after 72 hours and obtaining at least 2-3 hits for further analysis.

2.12. Cell Proliferation

Wells of a six-well plate were established with equal densities of cells (1×10^5 cells/ml) followed by incubation for one day to allow attachment and recovery. Therefore, transfection was conducted every day for 6 days using the positive siRNAs in treated cultures along with a negative siRNA in negative control cultures. Untreated cells were kept under similar conditions but not transfected. After 3rd and 5th day, the medium was changed. In day of harvest, cells were subjected to trypsinization. Similarly, they were counted daily with the help of a Biorad TC 20 automated cell counter and trypan blue staining. Finally, western blot was conducted following cell harvesting in order to find out any change in the level of protein.

Table 2. 5. List of siRNAs used to knock down the *PRDM9* gene

Gene	siRNA Name	Source	Target sequencing (5′ to 3′)
PRDM9	Hs_PRDM9_5	Qiagen; SI04190900	TTCCCTTATCACTGAAGGCAA
	Hs_PRDM9_6	Qiagen; SI04287038	CACGGGAGACTGTGAAGAGCA
	Hs_PRDM9_7	Qiagen; SI04299890	CCACACAGCCGTAATGACAAA
	Hs_PRDM9_8	Qiagen; SI04338747	GTGGACAAGGTTTCAGTGTTA
	Hs_PRDM9_9	Qiagen; SI05105583	TTCCACCCAGTGGCGTAATGA
	Hs_PRDM9_10	Qiagen; SI05105590	GAAGAGAAATGTAAGATTCTA
TEX19	Hs_FLJ35767_6	Qiagen; SI04215176	AGGATTCACCATAGTCTCTTA
	Hs_FLJ35767_7	Qiagen; SI04247705	TTCAACATGGAGATCAGCTAA
Non-interfering siRNA	Negative Control siRNA	Qiagen; 1022076	-

2.13. Cloning of N-flag*::PRDM9*, C-flag*::PRDM9* and C-Myc*::PRDM9* into pTRE-3G vector

2.13.1. Primers Design for Cloning

The full *PRDM9* open reading frame was cloned into pGEM (Promega: A1360). Human cDNA was used as a template. The template (*PRDM9*) was amplified using primers containing tags, C-Myc, C-FLAG and N-FLAG and restriction sites (Table 2.9). *PRDM9* cDNA contained the C-Myc, C-FLAG and N-FLAG tags were cloned into pTRE-3G vectors. Forward and reverse primers containing sites of restriction enzymes for C-Myc/FLAG and N-FLAG tags were designed using Primer3 software. NheI and BamHI were the restriction enzymes used this cloning. Enzyme needs these extra bases to bind to the sites. All primers used in cloning were prepared by Eurofins MWG. primers were diluted to achieve a stock concentration of 100 pmol and then again diluted to a working concentration of 10 pmol.

Table 2. 6. List of primer genes used for cloning into pTRE-3G vectors.

Gene	Primer	Primer Sequence (5′ to 3′)	Annealing Temp (°C)	Product Size (bp)
PRDM9-N FLAG	F	TTCGCTAGCATGTACAAAGACGATGACGA CAAGATGAGCCCT	58	2685
PRDM9-N FLAG	R	GAAGGATCCTTACTCATCCTCCCTGCAGA	60	
PRDM9-C FLAG	F	TTCGCTAGCATGAGCCCTGAAAAGTCCCA	60	2685
PRDM9-C FLAG	R	GAAGGATCCTTACTTGTCGTCATCGTCTT TGTAGTCCTCATCCTC	60	
PRDM9-C MYC	F	TCCGCTAGCATGAGCCCTGAAAAGTCCC AAGA	58	2685
PRDM9-C MYC	R	GAAGGATCCTTACAGGTCCTCCTCGAAG ATCAGCTTCTGCTCCTC	58	

2.13.2. Purification and DNA Digestion

MyTaq^{TM} HS Red Mas (Bioline; MTHRX-41408) was used to carry out PCR. Total volume of the reaction mixture was 50 µl. The products obtained through PCR were mixed with 6x blue loading dye (NEB; B7021S) and run on 1% agarose gel. This was followed by extraction of particular bands. Later, Nucleospin Gel and PCR clean-up (MACHEREY-NAGEL;740609-250) were used for purification. Purification was carried out as per the instructions given by the manufacturer. Around 25 µl of purified PCR product was subjected to digestion. The digestion mixture (50 µl) contained the PCR product, 1 µl of each restriction enzymes, 18 µl of ddH$_2$O and 5 µl of Cutsmart^{TM} Buffer (Bioline; B7204S). The specimens were then incubated for 2 hours at 37°C followed by electrophoresis on 1% agarose gel. Dephosphorylation was carried out in case of pTRE-3G vector after the purification step. Dephosphorylation was conducted through addition of 17 µl of ddH$_2$O, 5 µl of cut smart buffer and 2 µl of shrimp alkaline phosphatase (SAP) (Bioline; M0371L). The mixture exhibiting a total volume of 50 µl was subjected to incubation 30 minutes at 37°C. The reaction was inactivated by heating at 56°C for 5 minutes.

2.13.3. Ligation and Transformation

The pTRE-3G plasmid was ligated with C-Myc/FLAG:PRDM9 and N-FLAG:PRDM9. NanoDrop (ND_1000) was used for determination of concentration of plasmid and insert DNA molecules. For optimizing the ligation, the molar ratio of vector to insert

was calculated with the help of in-silico calculator (http://www.insilico.uni-duesseldorf.de/Lig_Input.html). The molar ratio of the insert calculated in this way was mixed with 50 ng of vector, 1 µl of T4 DNA ligase (Promega; M180A) and 1 µl of 10x ligase buffer (Promega; C126B). Finally, 20 µl of sterile water (Sigma; W4502) was added to adjust the volume of DNA ligation mixture. After gentle mixing and short centrifugation of the ligation mixtures, they were kept for overnight incubation at 4°C. For transformation, a vial containing NEB 10-beta competent *E. coli* (BioLabs; C3019H) was thawed by keeping it on ice for 10 minutes. The procedure provided by the manufacturer was then followed. Serial dilutions of the transformation mixture were made and inoculated on petri plates containing LB agar added with 100 mg/ml ampicillin (Sigma; A9518). The plates were kept for overnight incubation at 37°C. Table 2.10 presents the composition of the LB agar.

Table 2. 7. Medium recipe for *E. coli* growth

Media	Amount
Luria Broth (LB)	
Tryptone	10 g
Yeast extract	5 g
NaCl	10 g
Water	up to 1 L
For LB agar plates add:	
Agar	14 g
Water	up to 1 L

2.13.4. Colony Screening

After overnight incubation, some colonies were picked at random using a micropipette. These were then suspended in 20 µl of ddH$_2$O. For detection of *PRDM9* positive clones in the picked colonies, PCR was conducted using internal primers presented in Table 2.9. The reaction mixture for PCR was containing 6 µl distilled water, 0.5 µl of each primer, 12.5 µl of 2x My Taq red Max and 5 µl of suspension containing the colony. The remaining suspension of the colonies found to be positive for *PRDM9* was inoculated into 5 ml of LB broth added with 100 mg/ml ampicillin followed by overnight incubation at 37°C.

2.13.5. Plasmid Isolation from *E. coli*

Plasmids were extracted from cells of *E. coli*. For this purpose, 5 ml of overnight culture of *E. coli* were used. Moreover, the QIAprep Spin Miniprep Kit (250) (Qiagen; 27106) was used and the instructions given with the kit were followed. In order to verify cloning, 3 µg of purified plasmid specimens were subjected to digestion with suitable restriction enzymes NheI and BamHI. This was followed by gene sequencing for verification of correct sequence of the cloned genes and to check for mutations.

2.13.6. Sequencing PCR Products

For sequencing, 1500 ng/µl of DNA specimens were added with 2 µl of 10 pmol of reverse or forward primer in a labelled vial followed by addition of sterile water to make up the final volume of the mixture to 17 µl. The pTRE-3G forward and reverse primers were used for sequencing to verify that the *PRDM9* containing desired tag was inserted correctly and there are not any mutations. These vials were then sent to Eurofins MUG for sequencing. Results for sequencing were then blasted and aligned with relevant genes using Basic Local Alignment Search Tool (BLAST) website https://blast.ncbi.nlm.nih.gov/Blast.cgi.

2.14. Establishment of Double Tet-On 3G Stable Cell Line
2.14.1. Puromycin Selection (Kill curve)

A six-well plate was inoculated with HeLa Tet-On 3G cell line grown in suitable medium (Table 2.1) added with 100 µg/ml G418. Once the cells demonstrated confluent growth, the wells were added with seven doses of puromycin. This was done for optimization of the smallest dose which could kill all cells within three to five days. It was found that the minimum dose for HeLa cells was 0.8 µg/ml.

2.14.2. Generation of Double Stable HeLa / HCT116 Tet-On 3G Stable Cell Lines

HeLa Tet-On 3G cell lines were grown in six well plate till they demonstrated confluent growth. This was done to develop double stable HeLa Tet-On 3G cell lines containing *N-FLAG::PRDM9* and *C-Myc/FLAG::PRDM9*. This was followed by transfection of the

cell lines with the help of Xfect transfection reagent (Clontech; PT5003-2) according to the procedure provided by the manufacturer. Every plate of the 4 x 10 cm dishes was added with 2.5 µg and 5 µg of recombinant vector pTRE-3G with *N-FLAG::PRDM9* and *C-Myc/FLAG::PRDM9*. Wells were also added with 100 ng of linear puromycin selection marker in a ratio of 20:1. After 48 hours, cells were inoculated into dishes containing fresh medium added with 100 µg/ml of Geneticin (G418) and suitable quantity of puromycin (Hela = 0.8 µg/ml). After every four days, fresh G418 and puromycin were added. After 6-8 days, single healthy colony was picked and inoculated into 24 well plate, which was added with appropriate quantity of selective antibiotic (G418 and puromycin). Once the cells became confluent, they were divided into 3 halves and transferred into T75 flasks. An aliquot of these cells was used for screening and rest of the suspension was kept in liquid nitrogen in order to store it for long time.

2.14.3. Screening of Double Stable HeLa Tet-On 3G Stable Cell Lines

Gene induction was promoted for every colony using Doxycycline (Sigma; D9891-5G). 10 cm dishes were inoculated with colonies. Positive plates were added with 1 µg/ml doxycycline. No doxycycline was added to negative plates. All plates were kept in 5% CO_2 at 37°C for incubation. After incubation, protein extraction was conducted to perform western blotting. Western blotting was conducted to detect induction and cloning of N-FLAG and C-MYc/FLAG tags.

Chapter 3:

Analysis of the role of PRDM9 in cancer cell proliferation

3. Analysis of the role of PRDM9 in cancer cell proliferation

3.1. Introduction

The PRDM family encodes about 19 transcription activators that contain a SET domain, which is characterised by histone methyltransferase activity. Several motifs of a zinc finger follow this domain, which facilitates the interactions of protein to protein, protein to DNA or protein to RNA. Interestingly, all members of PRDM family have oncogenic potentials. Research has revealed that many family members are altered leading to cancer development (Sorrentino et al., 2018).

PRDM9 (Meisetz in mice) contributes to activation of meiotic recombination hotspot sites (Baudat et al., 2010; Myers et al., 2010; Parvanov et al., 2010). It also serves as a transcriptionl activator in meiosis; expression of the testis-specific *RIK* gene (also known as *Morc2b*) is controlled by Prdm9 (Hayashi et al., 2005). In human, PRDM9 has been reported to be activated in wide ranges of cancer and is described as a CTA (Feichtinger et al., 2012).

Cellular overgrowth is a cancer hallmark by which the cell signalling system that regulates the cell cycle is disrupted. Over time, the cancerous cells start dividing in an uncontrolled fashion and succeed in avoiding programmed cell death. There is a significant correlation between expression of CTA genes and the proliferation rates in cancerous cells. Maxfield and co-workers (2015) revealed that CTA gene expression affects the viability of cancerous cells. For example, the knockdown of *FATE1* expression results in the reduction of cell viability in breast cancer, sarcoma, melanoma cancer cells and prostate cancer. Additionally, it has been shown that reduced *FATE1* mRNA levels also decreased cell viability in the colorectal cancer (HCT116) cell line (Maxfield et al., 2015). Another CTA gene expressed in breast cancer cells is *ZNF165* and reducing expression also decreases cancer cell viability (Maxfield et al., 2015). Moreover, another study demonstrated that depletion of *MAGEC2* expression in melanoma cells impairs their viability and proliferation rate (Lajmi et al., 2015). The oncogenic process can also be induced by the overexpression of the CTA gene *MAGE- A1,* this increases the proliferation of multiple myeloma cells; on the other hand, its depletion results in reduced melanoma cell proliferation (Wang et al., 2016). Further study has shown that the depletion of *NY-SAR-35* expression

inhibits the cellular proliferation of human embryonic kidney (HEK) 293 cells (Song, et al, 2016). Shang and his co-workers (2014) demonstrated that the upregulation of the *CT45A1* gene results in activation of other genes contributing to oncogenesis and metastasis of MCF7 cells. On the other hand, *CT45A1* knockdown decreases the migration and invasion features of MCF7 cell lines (Shang et al., 2014). These findings support the importance of CTA genes in the proliferation and survival of cancerous cells and demonstrates their oncogenic potentials (Cheng et al., 2011; Maxfield et al., 2015; Song et al., 2016).

The overexpression of *PRDM9* is detected in several cancer cell lines but not in healthy cells except testis germ cell (Feichtinger et al., 2012). Additionally, RT-PCR analysis found that the *PRDM9* gene is potentially a good CT gene biomarker, so PRDM9 is proposed to have potential to be used in many applications for cancer treatment, such as, cancer vaccination and/or immunotherapy. The findings from Feichtinger and co-workers' study showed that PRDM9 transcripts were expressed in variable intensities. Thus, some cell lines with strong signals have been chosen in this study, such as; MCF7, K562, and NTERA-2.

The main aim of this chapter was to investigate the biological roles of PRDM9 in these cancer cells. The effects of PRDM9 on cancer cell proliferation was examined in this work.

3.2. Results

3.2.1. Depletion of PRDM9 in MCF-7 cell line

The knockdown of *PRDM9* in the MCF-7 cell line was performed using different molecules of small interfering RNA (siRNAs). Six different siRNAs were obtained from Qiagen to target the *PRDM9* gene at different sites, as shown in Figure 3.1. Although, there is similarity of *PRDM7* and *PRDM9* sequences, these siRNAs should specifically target *PRDM9* only. Additionally, previous work in McFarlane lab reported that PRDM7 expression was not detected in MCF-7 cells (Almatrafi, PhD thesis, 2014). Negative siRNA was used a negative control for transfection. All siRNAs molecules were transfected for 72 hours followed by RNA extraction from all cultures. The efficiency of knockdown and the levels of *PRDM9* mRNA levels were analysed using qRT-PCR. Results in Figure 3.2 demonstrate that the cultures treated with siRNAs #6, #7, #8, and #10 showed significant changes in *PRDM9* mRNA levels compared to the negative control (non- interference siRNA) as determined by P values (P < 0.001). Moreover, transfection of anti-*PRDM9* siRNA #7 showed a consistent 80-90% reduction of *PRDM9* mRNA levels and P<0.001. Moreover, the reduction percentages of *PRDM9* transcript levels in each culture was calculated in comparison to negative siRNA transcript levels and showed that siRNA #6 was 80 %, siRNA #7 was 88%, siRNA #8 was 83% and siRNA #10 was 81%.

A) *PRDM9*
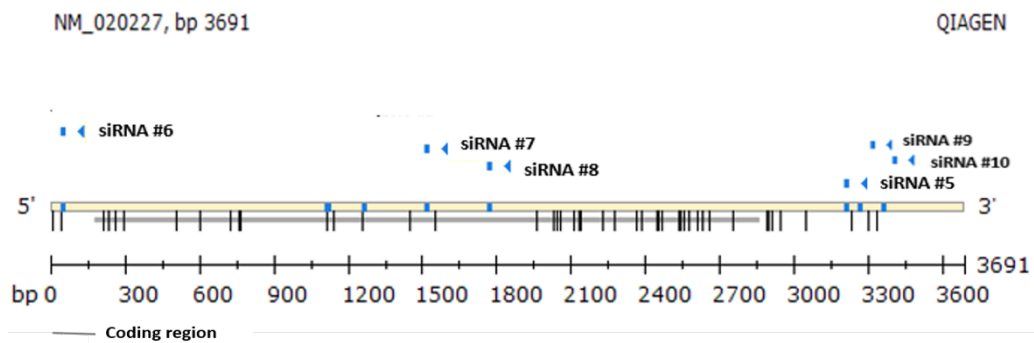
B) *PRDM7*
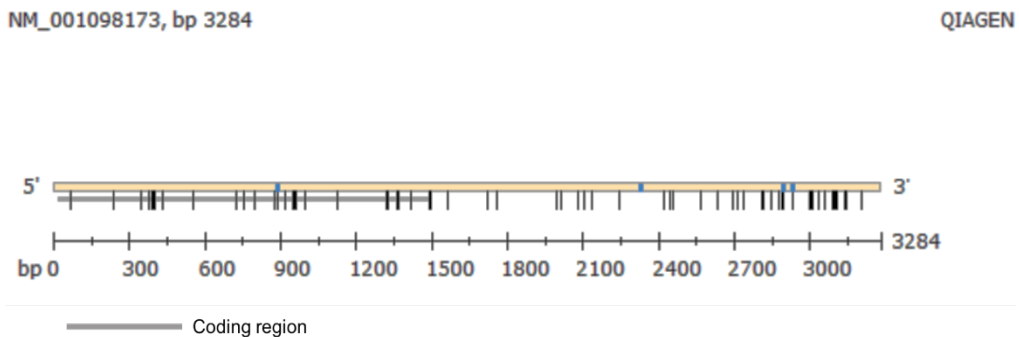
Figure 3. 1. schematic representation of *PRDM9* and *PRDM7*. A) *PRDM9* (NCBI accession number NM_020227, bP 3691) demonstrating the coding region and siRNA target sites. **B)** *PRDM7* (NCBI accession number NM_001098173, bP 3284) has sequence similar to PRDM9. The used siRNA molecules match with PRDM9 only. This figure adapted from Qiagen.
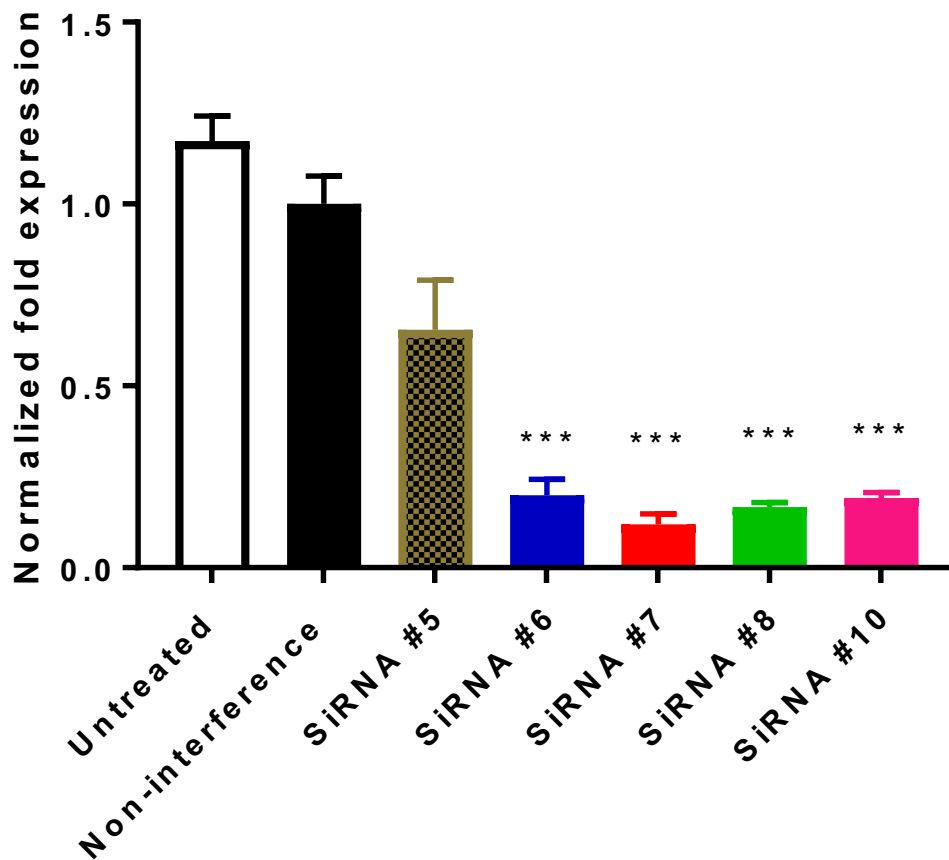
Figure 3. 2. Analysis of qRT-PCR for mRNA levels of *PRDM9* following siRNAs transfection in MCF-7 cells. Bar chart shows the mRNA transcript levels of *PRDM9*. Levels were normalised with two reference genes: *GAPDH* and *ACTβ*. Error bars denote the standard errors of the mean that are statistically obtained from three technical repeats in one of two biological repeats. P values were calculated to show significant changes compared to the negative control as (*** $P < 0.001$).

3.2.2. Protein analysis after the depletion of PRDM9 in MCF-7 cell line.

Western blot analysis was carried out to investigate the changes of PRDM9 protein after the siRNA treatment. Cultures were treated with siRNAs for 72 hours followed by harvesting and protein extraction. Anti-PRDM9 antibody from Abcam (# ab85654) was used to detect PRDM9 protein at the expected size of approximately 103 kDa and GAPDH was used as a loading control. Untreated and non-interference extracts show a clear band at approximately 103 kDa using the anti-PRDM9 antibody. This is also apparent using siRNAs 5,6 and 9, with no intensity reduction. siRNA #8 results in a strong depletion, with only a faint band at approximately 103 kDa, and siRNA #7 and #10 results in an almost total loss of detection of the 103 kDa band as shown in Figure 3.3.

3.2.3. The effects of *PRDM9* gene mRNA knockdown on MCF-7 cell proliferation.

The cell proliferation curve was established to check the changes of cell proliferation during 7 days of siRNA treatment. Two siRNAs (siRNA #7 and #10) were chosen in this experiment along with untreated and non-interference siRNA cultures as negative control for the treatment. The sequence of siRNA #7 targets *PRDM9* in the coding region. For each day, the cells were harvested and the cell counts were documented as shown in Figure 3.4 A. Furthermore, the qRT-PCR analysis was conducted to check the efficiency of *PRDM9* gene knockdown in siRNA #7 cultures only as shown in Figure 3.4 B. siRNA treatment resulted in a significant reduction ($P < 0.05$) in total cell counts and proliferation. This differs from siRNA 10, which did not cause any reduction in cell proliferation potential.
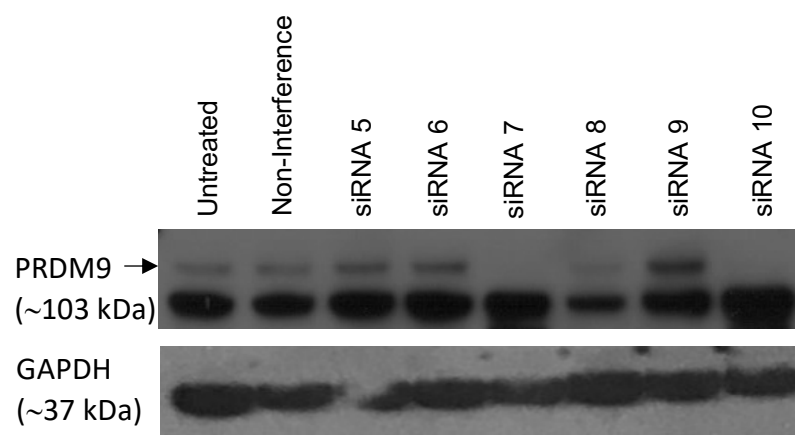
Figure 3. 3. Western blot analysis showing the levels of PRDM9 protein after siRNA treatment in MCF-7cells. Six different siRNAs (5, 6, 7, 8, 9 and 10) were used for three hits to deplete PRDM9. Anti-PRDM9 antibody was used to detect PRDM9. Untreated cells are positive controls, and cells treated with non-interfering siRNA are used as negative controls for transfection. Signals are apparent at the predicted size (approximately 103 kDa) and PRDM9 levels are deplated in cultures treated with siRNAs 7,8 and 10. GAPDH levels was used as a positive loading control. This figure is an example from three biological repeats.

A)
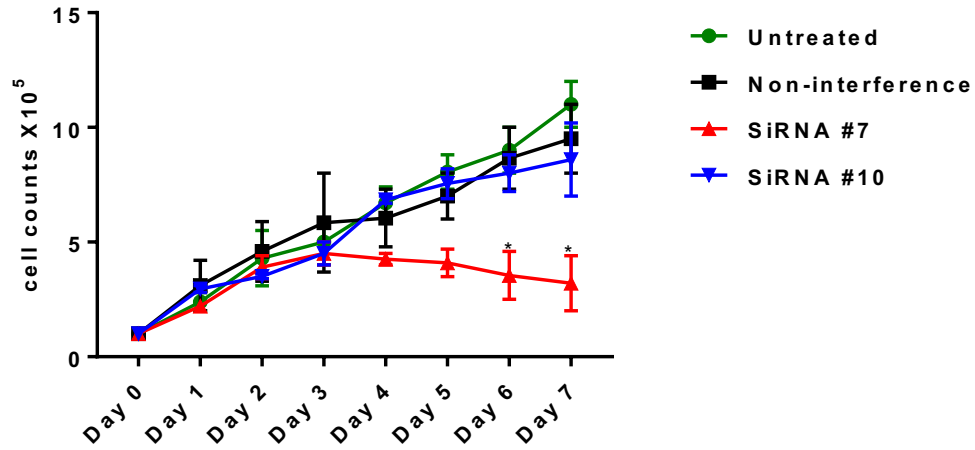
B)
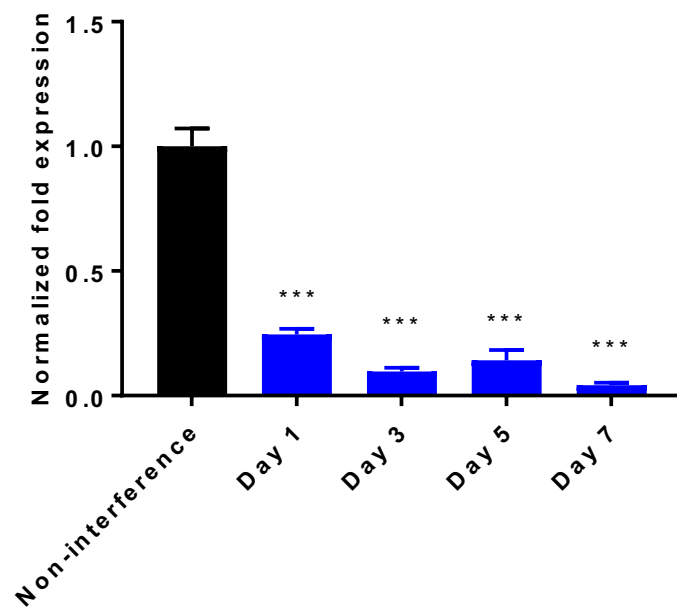
Figure 3. 4. MCF-7 cell proliferation curve was established for seven days of treatment with anti-PRDM9 siRNAs #7 and #10. A) The graph shows cell counts for each type of treatment for seven days. Significant changes in the cell counts were calculated from three biological repeats for the cells treated with siRNAs in comparison to (non-interference siRNA) the negative control (* P value < 0.05). B) The efficiency of knockdown was analysed using qRT-PCR in culture treated with siRNA #7 (***: P value < 0.001).

3.2.4. Depletion of *PRDM9* transcripts NTERA-2 cell line

The knockdown of *PRDM9* in NTERA-2 cell line was also carried out using siRNAs #5, #6, #7, #8 and #10. Non-interference siRNA was used as negative control for transfection. All siRNAs molecules were transfected for 72 hours followed by RNA extraction from all cultures. The efficiency of knockdown and the levels of PRDM9 mRNA levels were validated using qRT-PCR. Results in Figure 3.5 demonstrate that the cultures treated with siRNAs (#6, #7, #8, and #10) showed significant changes in *PRDM9* mRNA levels compared to negative control (non-interference siRNA) with P values as P < 0.001, P < 0.0001, P < 0.01 and P < 0.001 respectively. The efficiency of knockdown in *PRDM9* levels were calculated in each culture in comparison to negative control culture levels as; siRNA #6 was 70%, siRNA #7 was 80%, siRNA #8 was 30% and siRNA #10 was 51%.
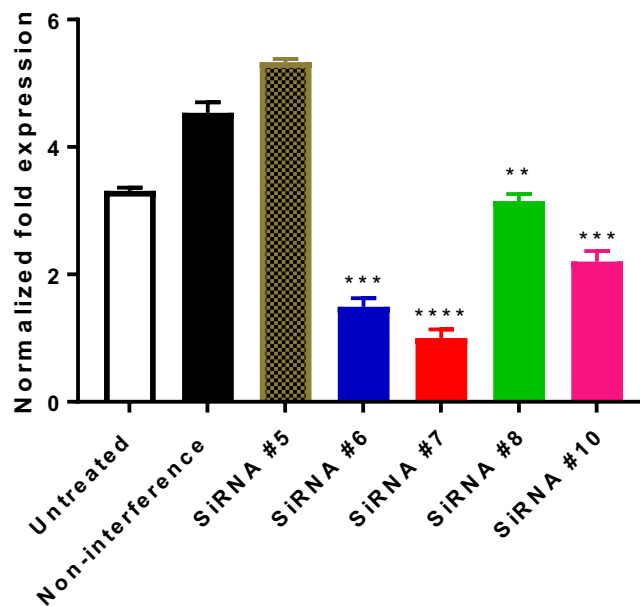
Figure 3. 3. Analysis of qRT-PCR for mRNA levels of *PRDM9* after siRNAs transfection in NTERA2 cells. Bar chart shows the levels of mRNA transcripts of the *PRDM9* gene. mRNA levels analysis was normalised with two reference genes: *GAPDH* and *ACTβ*. Error bars denote the standard errors of the mean that are statistically obtained from three technical repeats in one of two biological repeats. P values were calculated to show significant changes compared to the non-interference siRNA as (**** *P* < 0.0001, *** *P* < 0.001, and **P* < 0.01).

3.2.5. Protein analysis after attempted depletion of PRDM9 in NTERA-2 cell line.

Western blot analysis was conducted to examine the changes of PRDM9 protein after the siRNA treatment of NTERA-2 cells. Cultures were treated with siRNAs for 72 hours followed by harvesting and protein extraction. Anti-PRDM9 antibody from Abcam (# ab85654) was used to detect PRDM9 protein at expected size of approximately 103 kDa and GAPDH was used for load control. The results showed no changes of PRDM9 protein at the expected size 103 kDa as shown in Figure 3.6.

3.2.6. The effects of *PRDM9* gene mRNA knockdown on NTERA-2 cell proliferation.

The cell proliferation curve was established to check the changes of cell proliferation after the depletion of *PRDM9* mRNA in NTERA-2 cell line during 7 days of treatment. Two siRNAs (siRNA #7 and #10) were chosen in this experiment along with untreated and non-interfering siRNA cultures as negative control for the treatment. For each day, the cells were harvested, and the cell counts were documented as shown in Figure 3.7 A. Furthermore, the qRT-PCR analysis was applied to check the efficiency of *PRDM9* mRNA levels in NTERA-2 cultures treated with siRNA #7, as shown in Figure 3.7 B. As for MCF7 cells, depletion of PRDM9 mRNA with siRNA7 results in reduced cell proliferation (P < 0.001), but siRNA10 resulted in no statistically meaningful change, although proliferation does appear to be slowing at day 7.
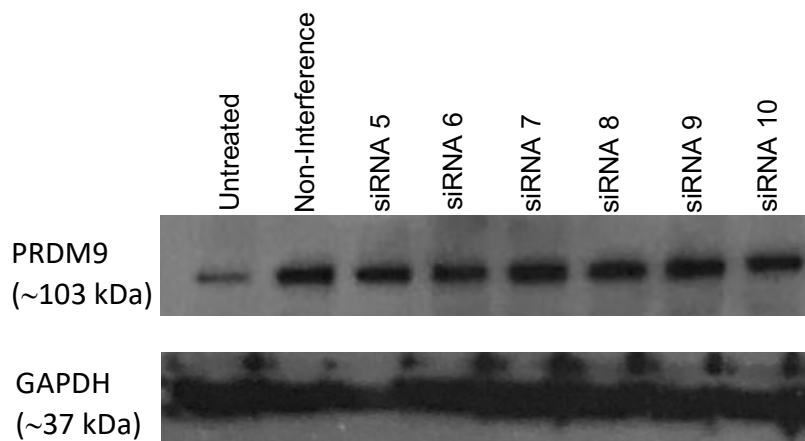
Figure 3. 6. Western blot analysis showing the levels of PRDM9 protein after siRNA treatment in NTERA2 cells. Six different siRNAs (5, 6, 7, 8, 9 and 10) were used for three hits to deplete PRDM9. Anti-PRDM9 antibody was used to detect PRDM9. Untreated cells are positive controls, and cells treated with non-interfering siRNA are used as negative controls for transfection. No apperant reduction of PRDM9 levels can be seen. GAPDH levels was used as a positive loading control. This figure is an example of two biological repeats.
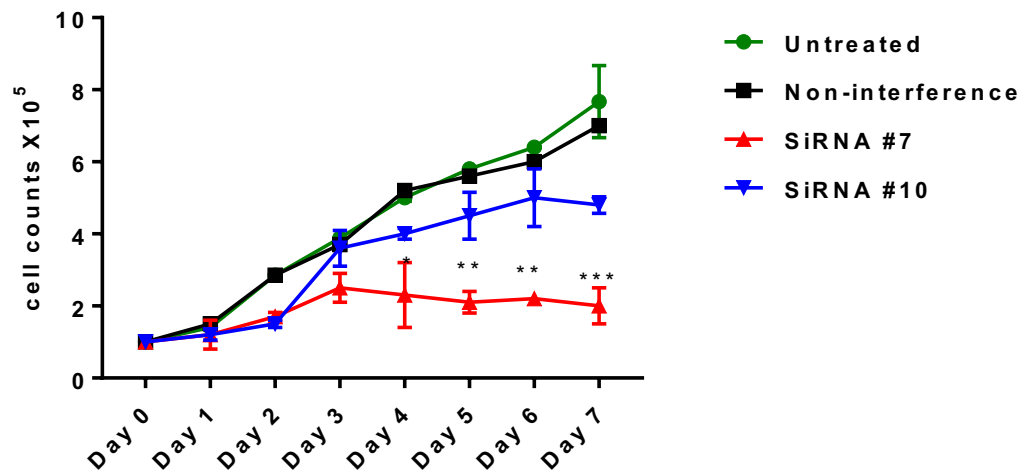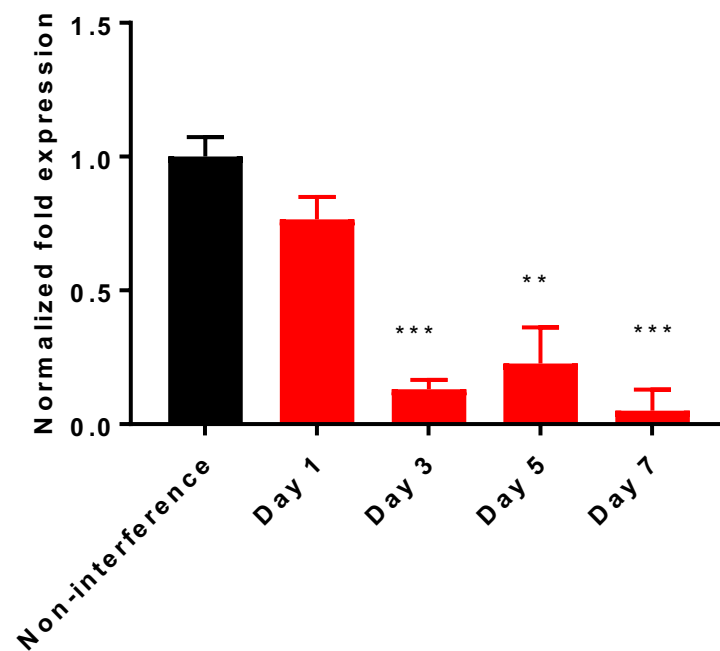
Figure 3. 7. NTERA-2 cell proliferation curve was established for seven days of treatment with anti-PRDM9 siRNAs #7 and #10. A) The graph demonstrates the cell counts for each type of treatment for seven days. Significant changes in the cell counts were calculated from three biological repeats for the cells treated with siRNAs in comparison to the negative control (**: $P < 0.01$ and ***: $P < 0.001$). B) The efficiency of knockdown was analysed using qRT-PCR in culture treated with siRNA #7 (**: $P < 0.01$ and ***: $P < 0.001$).

3.2.7. Depletion of PRDM9 in the K562 cell line

The knockdown of PRDM9 in K562 cell line was performed using siRNAs #5, #6, #7, #8, #9 and #10. Negative siRNA was used as a control for transfection. All siRNAs molecules were transfected for 72 hours followed by RNA extraction from all cultures. The efficiency of knockdown and the PRDM9 mRNA levels were assessed using qRT-PCR. Results in Figure 3.8 demonstrate that the cultures treated with siRNA #6, #7, #8 and #10 showed significant changes in *PRDM9* mRNA levels compared to negative control (non-interference siRNA) as determined by P values: P < 0.0001, P < 0.0001, P < 0.01 and P < 0.001 respectively. The efficiency of knockdown in *PRDM9* levels were calculated in each culture in comparison to negative control culture levels as; siRNA #6 was 55%, siRNA #7 was 70%, siRNA #8 was 45% and siRNA #10 was 45%.
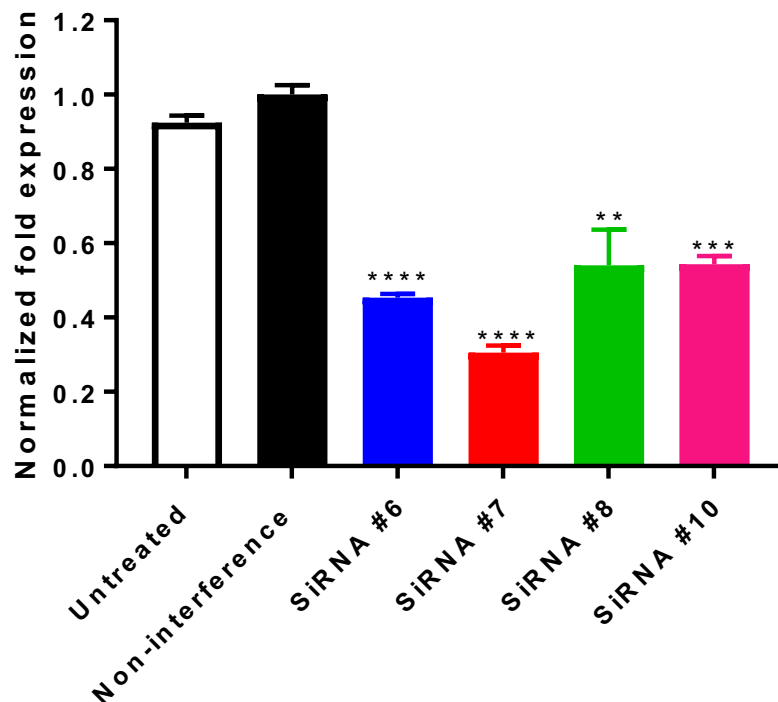

Figure 3. 4. Analysis of qRT-PCR for mRNA levels of *PRDM9* mRNA after siRNAs transfection experiment in K562 cells. Bar charts show the levels of mRNA transcripts of the *PRDM9* gene. mRNA levels analysis was normalised with two reference genes: *GAPDH* and *ACTβ*. Error bars denote the standard errors of the mean and are statistically obtained from three technical repeats. P values were calculated to show significant changes compared to the negative control (**** *P* < 0.0001, *** *P* < 0.001 and ** *P* < 0.01).

3.2.8. Protein analysis after the attempted depletion of PRDM9 in the K562 cell line.

Western blot analysis was conducted to examine the changes of PRDM9 protein after siRNA treatment. Cultures were treated with siRNAs for 72 hours followed by harvest and protein extraction. Anti-PRDM9 antibody from Abcam (# ab85654) was used to detect PRDM9 protein at expected size 103 of approximately kDa and GAPDH was used for load control. The results showed no changes of PRDM9 protein at the expected size of approximately 103 kDa as shown in Figure 3.9.
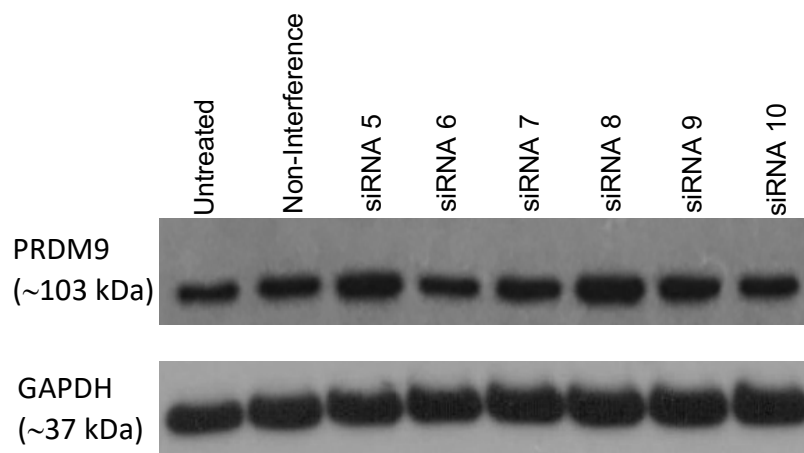

Figure 3. 5. Western blot analysis showing the levels of PRDM9 protein after siRNA treatment in K-562 cells. Six different siRNAs (5, 6, 7, 8, 9 and 10) were used for three hits to deplete PRDM9. Anti-PRDM9 antibody was used to detect PRDM9. Untreated cells are positive controls, and cells treated with non-interfering siRNA are used as negative controls for transfection. No apperant reduction of PRDM9 levels can be seen. GAPDH levels was used as a positive loading control.

3.3. Discussion

3.3.1. The influence of *PRDM9* gene expression in cancer cells.

PRDM family of proteins are aberrantly produced in many cancers such as leukaemia, cervical cancer, breast cancer, and colorectal cancer, and their production is linked with cancer development (Hohenauer & Moore, 2012). PRDM9 is the only member of PRDM family that is a meiosis-specific protein and it has been reported to specify the locations of meiotic recombination hotspots (Myers et al., 2010). Feichtinger and co-workers described the *PRDM9* gene as a CT gene that is abnormally activated in wide ranges of tumours including, breast cancer, colon cancer, ovarian cancer, and melanoma (Feichtinger et al., 2012).

Genes of *PRDM* family have been shown to regulate cell proliferation in healthy and cancer cells (Hohenauer & Moore, 2012). PRDM1 (also known as BLIMP1), for example, has been found to regulate cell proliferation and survival because it acts as a transcriptional activator that regulates *TP53* expression (Yan et al., 2007). The co-expression of *PRDM1* and *PRDM14* has been reported to play important function in the development of the germ cell lineage (Yamaji, et al, 2008, Di Zazzo, et al, 2013).

PRDM1 is expressed in different cancer cells and downregulation of *PRDM1* was observed to direct HCT116 cells to apoptosis and/or cell cycle arrest (Yan, et al, 2007). Additionally, (Nishikawa, et al, 2007) reported that several types of breast cancers show upregulation of *PRDM14* expression, and when the gene expression is downregulated using small interference transfection method, this results in cell proliferation reduction, apoptosis activation and chemotherapeutic drugs sensitivity of breast tumours (Nishikawa, et al, 2007). PRDM9 has an important function in designating hotspot activity during meiosis (Baudat, et al, 2010, Myers, et al, 2010, Parvanov, Petkov & Paigen, 2010). For this reason, it might be linked with genomic rearrangement abnormalities when present outside the meiotic context (Hussin, et al, 2013).

In this study, *PRDM9* transcripts were downregulated successfully in a number of cell lines, including MCF-7, NTERA-2 and K562. Moreover, the cultures of MCF-7 and NTERA-2 cells that were treated with anti-PRDM9 siRNA #7 showed reduced cell proliferation. For this reason, the efficiency of PRDM9 knockdown was confirmed

using qRT-PCR from these cultures, suggesting that PRDM9 is possibly contributing to cancer cell proliferation. conversely, cultures that were treated with siRNA #10 did not show changes in cellular proliferation. According to the sequence of siRNA #10, it does not target the coding region of *PRDM9*, and the reduction of its protein resulted from severe downregulation of its mRNA levels. However, the unchanged proliferation of these cultures was unexpected. The reason for this discrepancy of cellular proliferation between cells treated with siRNA #7 and siRNA #10 may referred to technical issues, for example, siRNA #10 mixture may become inefficient as a result of repeated thawing and freezing, or another vial was purchased but mistakes may occur in preparation or storage. Additionally, siRNA #7 reduced cell proliferation but siRNA #10 does not. However, for MCF7 at least, both give a reduction in protein levels. The explanation for this discrepancy could be that siRNA #7 is having off target effects and that is stopping the cellular proliferation, which is not actually caused by the reduction in PRDM9 levels. Indeed, siRNA #10 appears to give strong protein reduction, but no clear inhibition of proliferation, thus indicating that reduction of PRDM9 protein may not inhibit cell proliferation.

Moreover, other reasons for the apparent discrepancy could be due to the antibody specificity and reproducibility. Because of the similarity in sequences of PRDM7 and PRDM9, it might be argued that the antibody may bind PRDM7 not PRDM9. In this regard, we checked that the antibody target epitope amino acids match with PRDM9 only (see Appendix 9.1). Likewise, we checked whether siRNAs #7 and #10 could also target *PRDM9* not *PRDM7*. However, we have experienced some discrepancies with different batches of the antibody. The MCF-7 lysates in Figure 3.4 were probed against an antibody with different lot number (batch) from the next experiments on NTERA2 and K562 cell lines. We postulate that the new antibody did not work efficiently. This antibody is a polyclonal and we suggest that this issue might relate to a lack specificity of this antibody. Although the specificity of polyclonal antibodies can be 100% for any protein detection, there is a possibility that polyclonal antibodies may bind and detect other proteins. Serious issues surrounding antibody validation have recently been discussed (Bordeaux et al., 2010; Baker et al., 2015). To improve the reproducibility and reliability of antibodies, it has been argued that spicifity of these antibodies must be defined by using expressed recombinant proteins in cell lines (Bradbury & Plückthun, 2015). Given that, our reasonable explanation is that the antibody used

during this study might not be specific. To address this issue, a monoclonal antibody that targets PRDM9 protein should be used. Furthermore, the reduction of PRDM9 protein needs to be verified using different anti-PRDM9 antibodies but the main obstacle during this study was that the only antibody in the market was a polyclonal antibody purchased from Abcam.

3.3.2. Conclusion

The expression of the *PRDM9* gene in cancer cells is suggested to play functional roles although the molecular mechanisms of PRDM9 function in oncogenesis process remains unclear. However, a group of germline genes have been demonstrated to be required for the oncogenic process in *Drosophila melanogaster* and their human orthologues of these genes have also observed to be reactivated in several human tumours (Janic et al., 2010; Feichtinger et al., 2014). The functional roles of the activation of these germline genes in cancers remain not fully understood.

Interestingly, many studies found that CT genes, which are a subclass of germline family, have critical roles in cancer cell proliferation and the knockdown of these genes has led to the cellular proliferation disruption (Cappell et al., 2012; Linley et al., 2012).

This evidence support the suggestion that the activation of germline genes are needed for tumour sustainability as it has recently been postulated that cancers become 'addicted' to their reactivation (Rousseaux et al., 2013; McFarlane et al., 2014; McFarlane & Wakeman, 2017).

All these findings support the postulate that PRDM9 protein may have important oncogenic functions that maintain the cellular proliferation in cancer cell although the molecular pathway is still unknown.

To summarize the work in this chapter, PRDM9 transcripts were successfully reduced using different anti-PRDM9 small interference molecules. Further investigation proposed that PRDM9 might play important function in the cellular proliferation of some cancer cells. This is supported by the finding that PRDM9 is expressed in several types of tumours. Moreover, the attempts to investigate the levels of PRDM9 protein

were not successful. It is not clear if the PRDM9 protein is affected and subsequently leads to reduced cell proliferation or not. The used antibody was unable to answer this question clearly. To resolve this issue, in next chapter we tried to clone the full-length human PRDM9 open reading frame, which has a predicted size of 2685 bp. The primers used in this amplification contain tagged sequence to detect the production of PRDM9 protein and assess whether it can influence expression of other genes in tumour cells.

Chapter 4

Characterisation of PRDM9 functions in HeLa Tet-on 3G cell lines

4. Characterisation of PRDM9 functions in HeLa Tet-on 3G cell lines

4.1. Introduction

For fertility and genome evolution, homologous recombination is an important process. Through this process, paternal and maternal chromosomes exchange genetic information during meiosis. In several eukaryotes, hotspots – genomic loci of elevated levels of meiotic recombination – have a defining feature of accessible chromatin. In several vertebrates, these recombination sites are determined by PR domain-containing protein 9 (PRDM9). The different activities of PRDM9, including interactions with other proteins, histone methyltransferase activity and DNA binding, are responsible for initiating meiotic recombination hotspots.

The PRDM9 protein is strictly produced in spermatocytes and oocytes (Hayashi et al., 2005) and is a transcription factor belonging to the PRDM family (Hohenauer et al., 2012; Vervoort et al., 2015). This protein can be divided into three parts that include conserved domains with specific molecular functions as follows:

- The amino terminal part is made up of two domains that are intended to facilitate protein interactions. These domains are synovial sarcoma, the X breakpoint repression domain (SSXRD) and Kruppel-associated box (KRAB)–related domain (Birtle et al., 2006).

- The central part of the protein is made up of retinoblastoma protein-interacting zinc finger gene 1, which is also called PRDM2 (RIZ1) homology, and the PR/SET domain, which is named after positive regulatory domain I-binding factor 1 (PRDI-BF1). It has been reported that this domain relates to the family of suppressors of variegation 3-9, enhancers of Trithorax (SET) and Zeste domains present in several histone methyltransferases (Dillon et al., 2005).

- The carboxy-terminal part of the protein is a DNA-binding domain made up of an array of cysteine (2), histidine (2) (C2H2) zinc fingers in tandem. A single exon is responsible for encoding this part (Fumasoni et al., 2007). The PRDM

family is characterised by the link between the PR/SET domain and C2H2 zinc fingers (Hohenauer et al., 2012; Vervoort et al., 2015).

Because the domains of the PRDM9 protein are involved in transcription regulation, this protein has been considered to be a transcription factor (Hohenauer et al., 2012; Hayashi et al., 2005; Hayashi et al., 2006; Mihola et al., 2009; Nowick et al., 2013).

The PRDM9 domains play a role in regulating transcription, although how PRDM9 is involved in gene expression is not fully understood yet. Meisetz (a PRDM9 orthologue in mice) is a histone methyltransferase that plays a crucial role in the progression of prophase during meiotic early stages. The transcripts of *Meisetz* are found to be present only in germ cells at the early prophase of meiosis in postnatal testis and female foetal gonads (Hayashi et al., 2005; Hayashi & Matsui, 2006). The disruption of the *Meisetz* gene in mice has led to sterility in males and females because of impairment of the double-stranded break (DSB) repair pathway, impaired pairing of homologous chromosomes and disturbed sex body formation (Hayashi et al., 2005). Attenuation of trimethylation of lysine 4 of H3 and changes in the transcription of meiosis-specific genes have also been reported in *Meisetz*-deficient testis (Hayashi et al., 2005). Therefore, it can be stated that proper progression of meiosis in mammals essentially requires meiosis-specific epigenetic events.

Studies have reported that the PR/SET domain is related to the SET domains found in several histone methyltransferases (Hohenauer et al., 2012; Fog et al., 2012). Initially, it was found that the trimethylation of H3K4me2 is catalysed by the PRDM9 protein (Hayashi et al., 2005). Later, it was demonstrated *in vitro* that the mono-, di- and tri-methylation of H3K4 and H3K36 can be catalysed in the presence of isolated full-length mouse PRDM9 and mouse or human PRDM9 PR/SET domains (Eram et al., 2014; Wu et al., 2013).

Many reports have shown that PRDM9 binds to particular DNA motifs, thereby promoting histone trimethylation at lysine K4 and K36 (H3K4me3 and H3K36me3) via the action of methyltransferases that are mediated by the PR/SET domain. This results in the recruitment of proteins needed for the initiation of DSBs in close proximity to its binding site. Hence, the PRDM9 protein determines the meiotic recombination sites.

PRDM9's histone methyltransferase activity demonstrated *in vitro* has been verified *in vivo* by the enrichment of H3K4me3 and H3K36me3 at the recombination hotspots specified by PRDM9 (Powers et al., 2016; Buard et al., 2009; Grey et al., 2017; Baker et al., 2014; Smagulova et al., 2011; Pratto et al., 2014; Davies et al., 2016; Grey et al., 2011). This enrichment has been found to be independent of SPO11 (Buard et al., 2009; Grey et al., 2017) and has not been found in transgenic mice, which demonstrate a Y357F mutation in the SET domain of the PRDM9 protein. This implies that the catalytic activity of PRDM9 is needed for the deposition of these marks (Diagouraga et al., 2018). A strong correlation has been identified between the distribution of PRDM9-dependet H3K4me3 and H3K36me3. Moreover, the highest enrichment is detected at the nucleosomes found just next to the site of the binding of PRDM9 (Powers et al., 2016; Yamada et al., 2017).

The aim of the work in this chapter was to investigate the influence of human *PRDM9* on the expression of other human genes including meiosis-specific genes and cancer testis genes. This study used the previously constructed clones (clone A and clone B) (by McFarlane group), which are HeLa Tet-on 3G cell lines transfected with pTRE3G::PRDM9. Doxycycline inducible system was firstly induced to validate the overexpression of transfected *PRDM9* into HeLa Tet-on 3G cell lines. Because of that HeLa cells (Wildtype) are not expressing *PRDM9.* Therefore, RT-PCR was employed to check whether the overexpression of PRDM9 has influence on other human genes at transcriptional levels or not. Further analyses were performed on these clones including, genomic sequencing analysis, showing that the PRDM9 sequence contained two-point mutations (messence). These mutations have led to change in amino acids sequence and the produced protein. It has been questioned if these mutations have impacts on the expression of other genes at the transcription level or not.

4.2. Results

4.2.1. Validating the expression profile of *PRDM9* in constructed clones

PRDM9 was previously integrated into HeLa Tet-on 3G cells (inducible system) in the McFarlane lab (Almatrafi, PhD thesis, 2014). This was performed to create a double-stable cell line containing the pTRE3G::*PRDM9* vector and the Tet-on 3G transactivator protein that could undergo a conformational alteration in the presence of doxycycline to control for the expression of the *PRDM9* gene. Two colonies were previously constructed (clone A and clone B) for further analysis of *PRDM9*'s functional roles.

The induction of *PRDM9* was validated using conventional RT-PCR and quantitative real-time qRT-PCR in clones A and B, along with a negative control colony that contained pTRE3G only (Figure 4.1). Each colony was grown independently and induced with 1 µg/ml doxycycline for 24 hours. A fraction from each clone was also grown in the absence of doxycycline as a negative control for the treatment. From each culture, the total RNA was extracted to synthesise cDNA and to investigate the expression of *PRDM9* in the presence and absence of doxycycline.

Using conventional RT-PCR, *PRDM9* expression was examined in an independent colony containing the integration of the pTRE3G vector only. No expression of *PRDM9* was apparent in the negative control (clone transfected with HeLa Tet-on 3G cells with pTRE3G plasmids) either in the absence or presence of doxycycline for 24 hours. Moreover, the analysis showed that *PRDM9* was expressed following doxycycline treatment in clones A and B but no expression of *PRDM9* was observed in the untreated clones (Figure 4.1 A). In this experiment, the total RNA from the testis was used as a positive control for *PRDM9* expression. Analysis of *ACTB* expression was carried out to check the quality of the synthesised cDNA, and sample containing water only was run to check for contaminated primers.

Further analysis was performed using qRT-PCR to measure the levels of *PRDM9* expression in both colonies (A) and (B) before and after doxycycline induction. Commercial qRT-PCR primers for *PRDM9* that were purchased from (Qiagen) were used to carry out SYBR Green-based real-time run. Two reference genes – *ActB* and

GAPDH – were used to normalise the expression of *PRDM9*; the results are shown in Figure 4.1 B. The qRT-PCR results demonstrated no expression of *PRDM9* in the absence of doxycycline; however, high levels of *PRDM9* expression, particularly in clone (B), were detected after 24 hours of doxycycline treatment.

A)
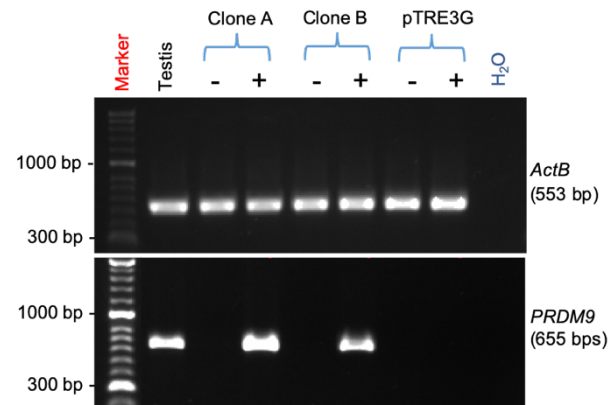
B)
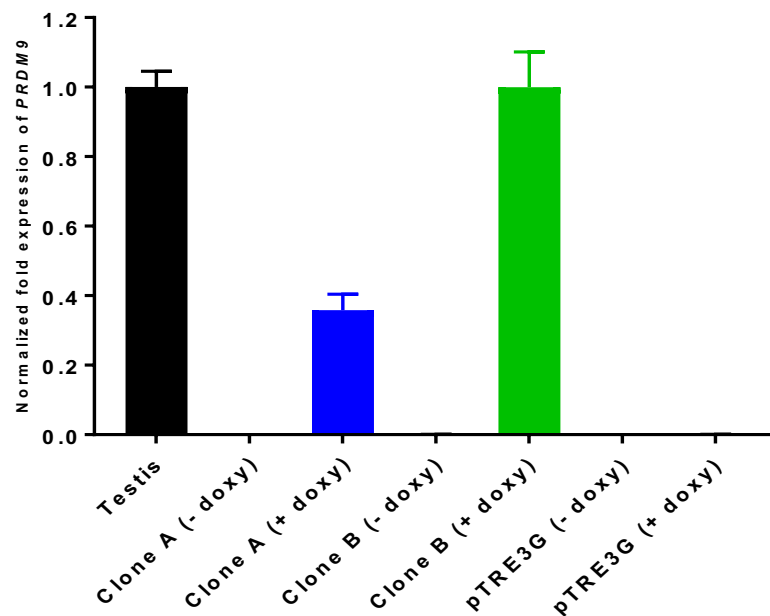
Figure 4. 1. Analysis using RT-PCR and qRT-PCR to confirm *PRDM9* expression in two independent clones. Clones A and B containing transfected *PRDM9* in HeLa Tet-on 3G were cultured and treated with 1 µg/ml doxycycline for 24 hours to overexpress *PRDM9*. A) RT-PCR analysis demonstrates the *PRDM9* expression profile in the presence/absence of doxycycline induction in each clone. The above agarose gel shows the constant expression of *ACTB* as a positive control for the cDNA quality. The testis is used as a positive control for *PRDM9* expression, and the pTRE3G clone is used as a negative control. The 1% agarose gels were run and stained with a pic-green stain to visualise the PCR products, predicted PCR product sizes are shown in parentheses. B) qRT-PCR analysis shows the mRNA levels of *PRDM9* before and after doxycycline inductions for all clones. Bar charts show the levels of mRNA transcripts of the *PRDM9* gene. The levels were normalised with two reference genes: *GAPDH* and *ActB*. The error bars denoted the standard errors of the mean that are statistically obtained from three technical repeats in one of three biological repeats.

4.2.2. PRDM9 acts as a transcriptional activator for other genes

4.2.2.1. The influence of *PRDM9* expression on *MAGEA1* gene expression

PRDM9 is a meiosis- specific gene that encodes histone methyltransferase activity and plays important roles in early meiosis progression. This was investigated in mice when the transcripts of *Meisetz*, an orthologue of human *PRDM9*, were detected in the germ cells of male and female gonads at early meiotic stages. Additionally, mice with Meisetz$^{-/-}$ showed an impairment of DSB repair that led to numerous consequences, such as sterility, homologous chromosome pairing abnormalities and meiosis arrest (Hayashi et al., 2005). Importantly, mouse deficiency of Meisetz demonstrated changes in the expression of other meiosis genes, indicating its transcriptional regulatory activities.

MAGEA1 is a member of melanoma-associated antigens (*MAGE*) family, which were the first CTA genes discovered by (Powers et al., 2016; van der Bruggen et al., 1991). *MAGEA1* is a well characterised CTA gene that is expressed in various tumour tissues, including non-small cell lung cancer (NSCLC), (Zhang et al., 2015; Mecklenburg et al., 2017) laryngeal squamous cell carcinoma, (Liu et al., 2016) breast cancer (Hou et al., 2014) bladder carcinoma (Mengus et al., 2013) and glioma (Guo et al., 2013).

Here, we investigated the influence of *PRDM9* overexpression on *MAGEA1* expression using an RT-PCR analysis, as shown in Figure 4.2, and qRT-PCR, as shown in Figure 4.3. Total RNA was extracted from two independent colonies of HeLa Tet-on 3G cells containing the pTRE3G::*PRDM9* vector, and one colony had pTRE3G only. Each colony was grown in the absence or presence of 1 µg/ml doxycycline for 24, 48 and 72 hours. The cDNA was created from each clone, and *ActB* was run first to evaluate the cDNA quality.

The results shown in Figure 4.2 demonstrate that the expression of *MAGEA1* was slightly increased in clone A following the overexpression of *PRDM9*. Additionally, *MAGEA1* had a clear expression that shows a strong band after a 24 hours of doxycycline induction in clone B, which is correlated with the overexpression of

PRDM9. The same primer set was conducted in two different annealing temperature settings and showed similar results.

These results were further confirmed, and the *MAGEA1* mRNA levels were quantified using a qRT-PCR analysis (Figure 4.3). The results confirm that *MAGEA1* mRNAs were significantly upregulated following doxycycline induction in correlation with the *PRDM9* mRNA levels. This indicates that PRDM9 may activate the expression of *MAGEA1*. Thus, PRDM9 could be a transcription activator for the *MAGEA1* gene.
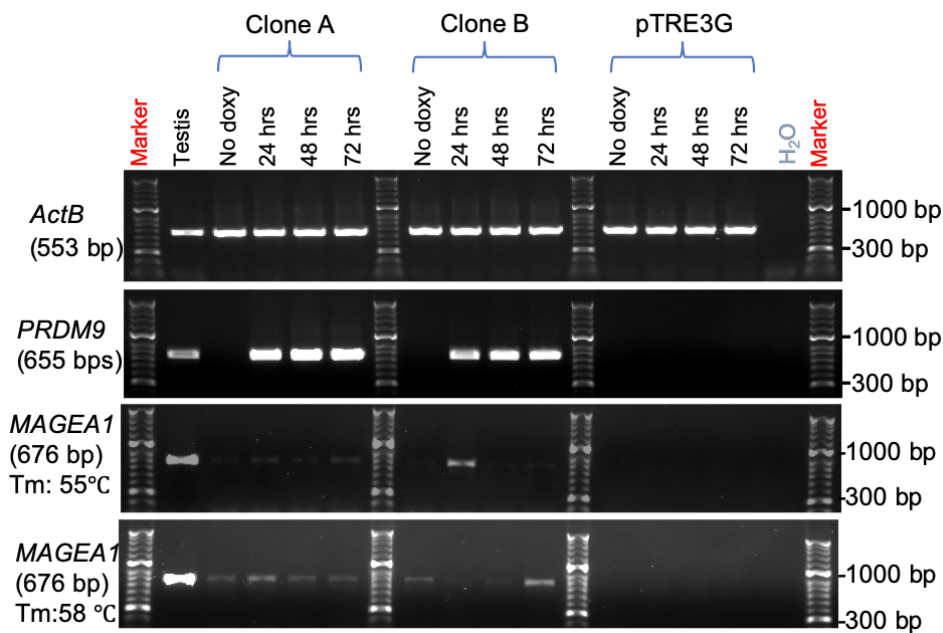
Figure 4. 2. Analysis using RT-PCR demonstrates the expression profile of the *MAGEA1* gene after *PRDM9* overexpression in the HeLa Tet-on 3G system. The expression of *ActB* was carried out as a positive control for the quality of the cDNA. *PRDM9* was overexpressed after doxycycline induction in clones A and B, but no expression was observed in the absence of doxycycline. Cultures of clone pTRE3G were used as a negative control for *PRDM9* expression. The testis sample was run as a positive control for the expression of *PRDM9* and *MAGEA1*. *MAGEA1* primers were run in two different settings of annealing temperature. The *MAGEA1* expression profile showed a significant correlation with *PRDM9* expression. The 1% agarose gels were run and stained with a pic-green stain to visualise the PCR products, predicted PCR product sizes are shown in parentheses.
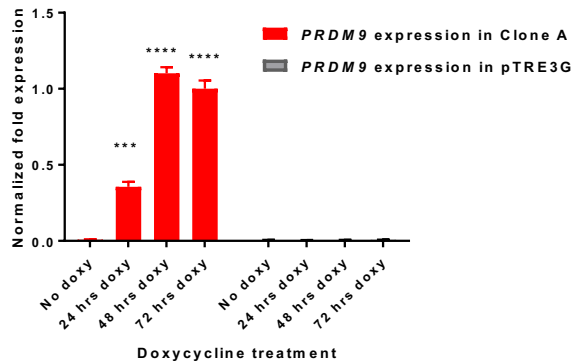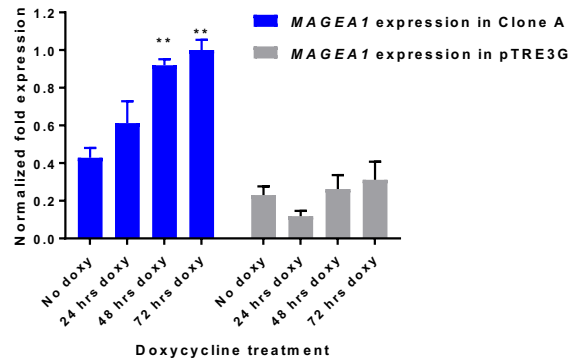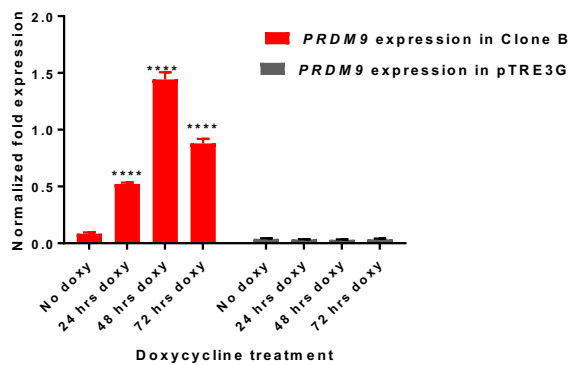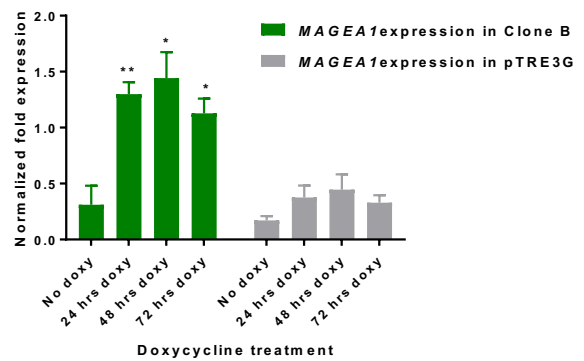
Figure 4. 3. Analysis of qRT-PCR for the mRNA levels of *PRDM9* and *MAGEA1* following doxycycline in HeLa Tet-on 3G cells. The bar charts show the levels of mRNA transcripts. The levels were normalised with two reference genes: *GAPDH* and *ACTβ*. The fold change was computed using the ΔΔCt method. The error bars refer to the standard errors of the mean and are statistically obtained from three technical repeats. A) *PRDM9* transcript levels in Clone A. B) *MAGEA1* expression in Clone A. C) *PRDM9* expression levels in Clone B. D) *MAGEA1* expression in Clone B. The P values were calculated to show significant changes compared with the negative control (* *P* value < 0.05, ** *P* value < 0.01, *** *P* value < 0.001 and **** *P* value < 0.0001).

4.2.2.2. The influence of *PRDM9* expression on *MORC* family genes

It has been proposed that through their transcriptional factors, the PRDM family proteins play a critical role in oncogenesis through their ability to modify the accessibility to chromatin (Hohenauer et al., 2012). This suggestion increases the possibility that the PRDM proteins may target the promoter of different genes, subsequently influencing their expression (Hohenauer et al., 2012; Fog et al., 2012). Hayashi et al. identified that mouse *Prdm9* has implications in the expression regulation of other genes, including *RiK* (*morc2b*) genes (Hayashi et al., 2005).

The current study was carried out to explore the influence of human *PRDM9* expression on the expression of human orthologues of *MORC* family members.

The total RNA was extracted from two independent colonies of HeLa Tet-on 3G cells containing the pTRE3G::*PRDM9* vector and one colony with pTRE3G only. Each colony was grown in the absence or presence of 1 µg/ml doxycycline for 24, 48 and 72 hours. The cDNA was created from each clone, and *ActB* was run first to evaluate the cDNA quality.

RT-PCR analyses were used to investigate the effects of *PRDM9* overexpression on human *MORC* members, including *MORC1*, *MORC2*, *MORC3* and *MORC4,* as shown in Figure 4.4*.* The results show that *MORC3* and *MORC4* had a slight increase in their expression in clone A after doxycycline induction for 72 hours and in a similar pattern of *PRDM9* expression; however, both genes were expressed in uninduced cultures in addition to their constant expressions in the pTRE3G clone. This may indicate that *MORC3* and *MORC4* are expressed in HeLa cells and that their expression might be influenced by *PRDM9* overexpression. The expression profiles of *MORC1* and *MORC2* showed no significant correlations with *PRDM9* overexpression.
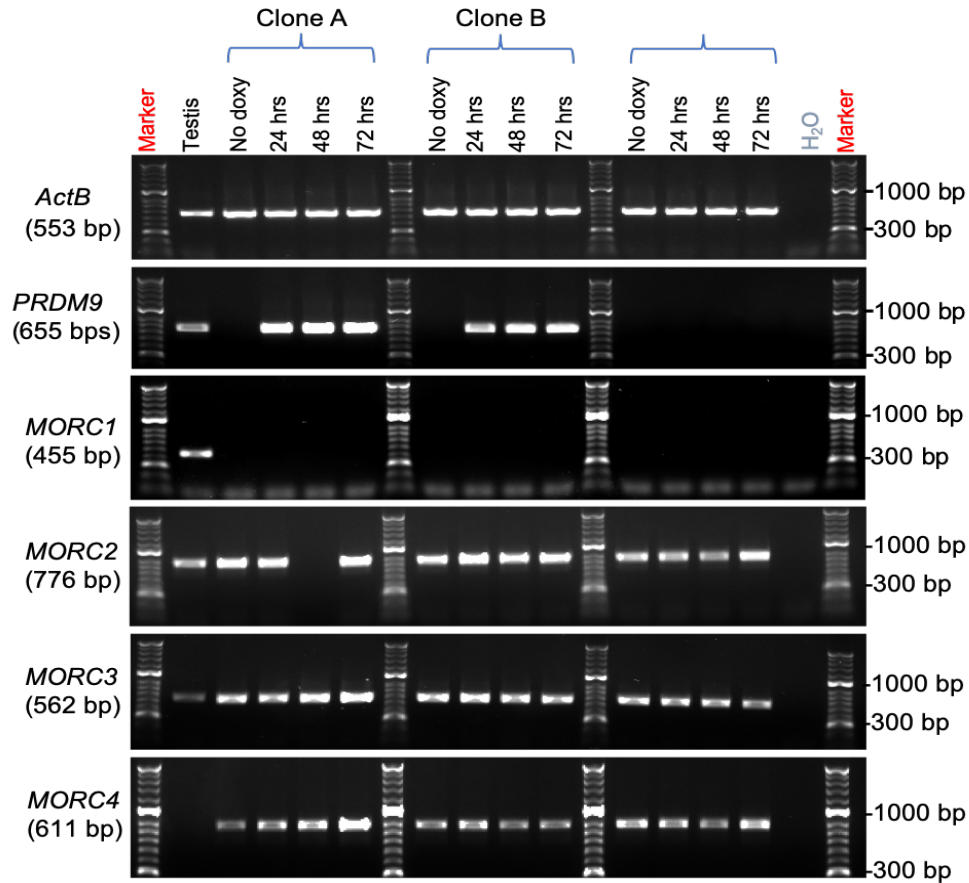
Figure 4. 4. Analysis using RT-PCR demonstrates the expression profile of four *MORC* family genes after *PRDM9* overexpression in the HeLa Tet-on 3G system. The expression of *ActB* was carried out as a positive control for the quality of cDNA. *PRDM9* was overexpressed after doxycycline induction in clones A and B, but no expression was observed in the absence of doxycycline. The cultures of the clone pTRE3G were used as a negative control for *PRDM9* expression. The testis sample was run as a positive control for the expression of *PRDM9* and the examined genes. The 1% agarose gels were run and stained with a pic-green stain to visualise the PCR products, predicted PCR product sizes are shown in parentheses.

4.2.2.3. The influence of *PRDM9* expression on other *PRDM* family genes

A further analysis was carried out to investigate the correlation between the expression of *PRDM9* and other members of the *PRDM* gene family. The primers of *PRDM1*, *PRDM4*, *PRDM6*, *PRDM7* and *PRDM11* were designed and run using RT-PCR on the three clones (A, B and pTRE3G) prior- and post-induction with doxycycline. The results are shown in (Figure 4.5) and demonstrate that the expression of *PRDM7* has a significant correlation with *PRDM9* expression. Moreover, *PRDM11* showed a significant increase of its expression after 24 and 72 hours of induction in clone B, only with very faint bands being found in clone pTRE3G. Other members (*PRDM4* and *PRDM6*) showed no changes in their expression profiles.

4.2.2.4. The influence of *PRDM9* expression on synaptonemal complex genes

The formation of a synaptonemal complex (SC) is a vital molecular process during meiosis that stabilises homologous chromosomes to ensure the occurrence of a crossover. Many meiosis genes encode function which contribute to the formation of SC, such as *SYCE1*, *SYCE2*, *SYCP1* and *SYCP3*. The expression of *PRDM9* has been reported as regulating other meiosis genes. Here, we also conducted a RT-PCR using primers that target SC genes, as shown in (Figure 4.6). The results showed that the expression of SC genes displayed no changes correlated to the overexpression of *PRDM9*.

Figure 4. 5. Analysis using RT-PCR demonstrates the expression profile of five *PRDM* family genes after *PRDM9* overexpression in the HeLa Tet-on 3G system. The expression of *ActB* was carried out as a positive control for the quality of cDNA. *PRDM9* was overexpressed after doxycycline induction in clones A and B, but no expression was observed in the absence of doxycycline. The cultures of clone pTRE3G were used as a negative control for *PRDM9* expression. The testis sample was run as a positive control for the expression of *PRDM9* and the examined genes. The 1% agarose gels were run and stained with a pic-green stain to visualise the PCR products, predicted PCR product sizes are shown in parentheses.
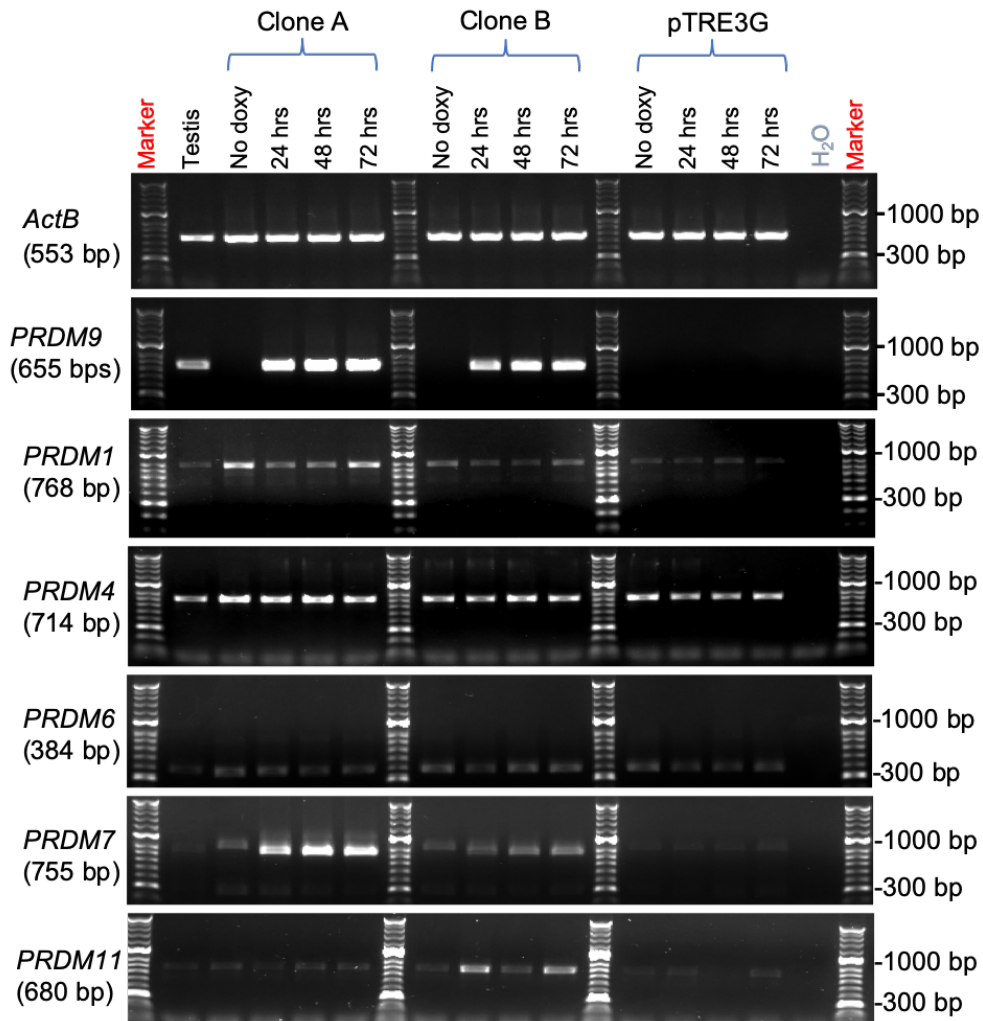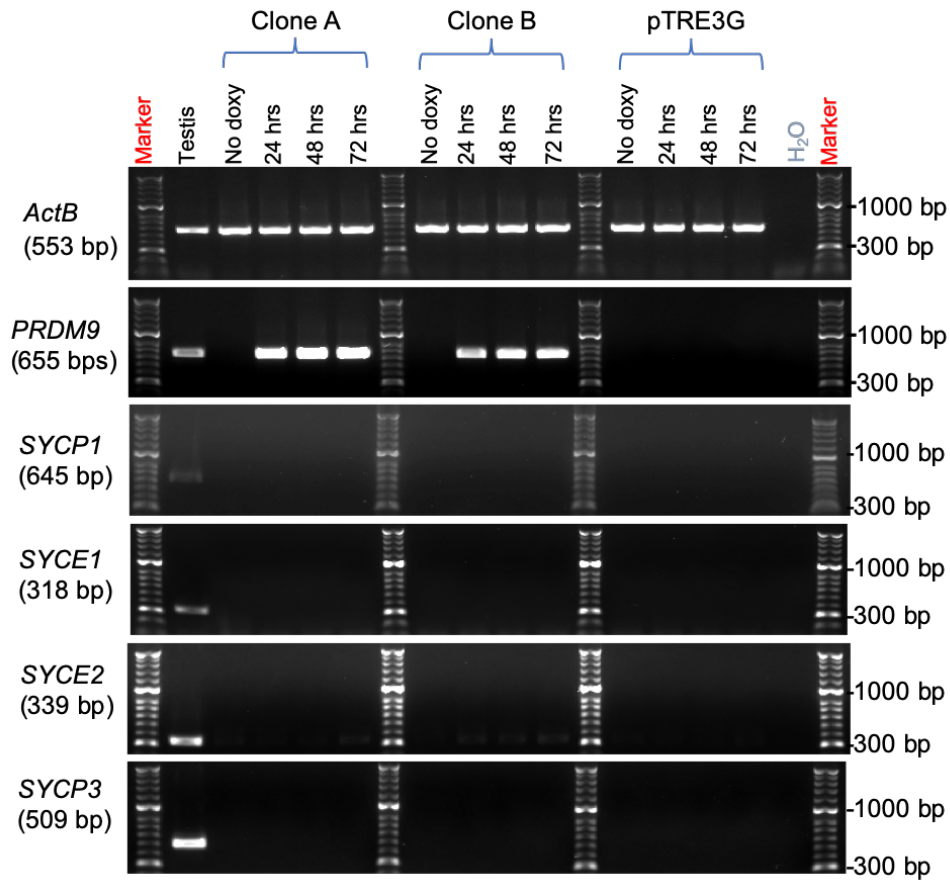
Figure 4. 6. Analysis using RT-PCR demonstrates the expression profile of four meiosis-specific genes after *PRDM9* overexpression in the HeLa Tet-on 3G system. The expression of *ActB* was carried out as a positive control for the quality of the cDNA. *PRDM9* was overexpressed after doxycycline induction in clones A and B, but no expression was observed in the absence of doxycycline. The cultures of clone pTRE3G were used as a negative control for *PRDM9* expression. The testis sample was run as a positive control for the expression of *PRDM9* and the examined genes. No changes in the expression of the target genes were seen after the overexpression of *PRDM9*. The 1% agarose gels were run and stained with a pic-green stain to visualise the PCR products, predicted PCR product sizes are shown in parentheses.

4.2.2.5. The influence of *PRDM9* expression on other meiosis genes

The screening of expression profiles for many meiosis-specific genes was also carried out on clones A, B and pTRE3G to check whether the overexpression of *PRDM9* affects the expression of these genes. Moreover, these meiosis genes were also described as cancer testis antigen (CTA) genes. The screening results are shown in Figure 4.7. The expression profile of *HORMAD1* demonstrated a higher expression after 72 hours of induction than in the uninduced cultures of clone A although faint bands were observed in clone pTRE3G. Additionally, the expression of *GAGE* also showed a clear upregulation after 72 hours postinduction of the culture of clone A, but this was not detected in pTRE3G clone. These findings indicate that *GAGE* expression may be activated as a consequence of the overexpression of *PRDM9*.
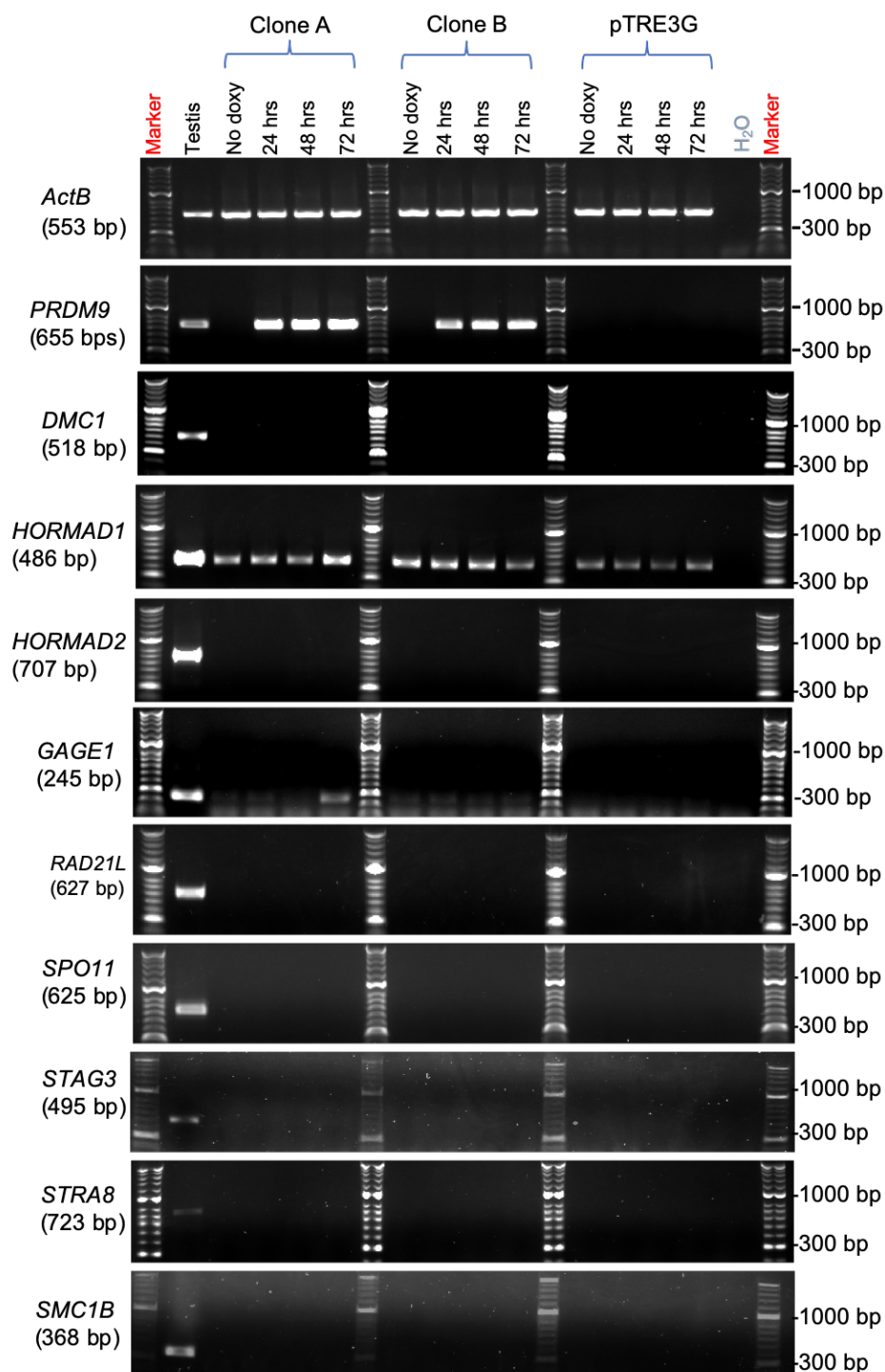
Figure 4. 7. Analysis using RT-PCR demonstrates the expression profile of other meiosis-specific genes after *PRDM9* overexpression in the HeLa Tet-on 3G system. The expression of *ActB* was carried out as a positive control for the quality of the cDNA. *PRDM9* was overexpressed after doxycycline induction in clones A and B, but no expression was observed in the absence of doxycycline. The cultures of clone pTRE3G were used as a negative control for *PRDM9* expression. The testis sample was run as a positive control for the expression of *PRDM9* and the examined genes. The 1% agarose gels were run and stained with a pic-green stain to visualise the PCR products, predicted PCR product sizes are shown in parentheses.

4.2.3. Analysis of histone methyltransferase activity of PRDM9 in HeLa Tet-on 3G cell lines

The histone methyltransferase activity of PRDM9 has been reported, even though these activities and substrate specificity have not been described yet. A recent study demonstrated that PRDM9 can catalyse H3K4 trimethylation (Wu et al., 2013), which is also linked with transcriptional activation (Bernstein et al., 2002; Santos-Rosa et al., 2002), DNA repair (Pena et al., 2008) and the initiation of recombination hotspots (Buard et al., 2009; Borde et al., 2009). In humans, PRDM9 binds DNA regions enriched in the hotspots (Baudat et al., 2010a; Myers et al., 2008). Eram and co-workers have also characterised the ability of PRDM9 to trimethylate H3K4 and H3K36 in HEK293 cells (Eram et al., 2014).

In the current study, we cultured the HeLa Tet-on cells, and *PRDM9* expression was induced for 24, 48 and 72 hours with doxycycline in independent cultures. The cell lysates were extracted to investigate the activity of H3K4 and H3K36 trimethylation, as shown in (Figure 4.8).

The results in Figure 4.8 are an example of the many attempts carried out using different antibodies and different procedures. However, no significant changes of the bands that relate to H3K4me3 or H3K36me3 correlated with the changes in *PRDM9* expression.

A)
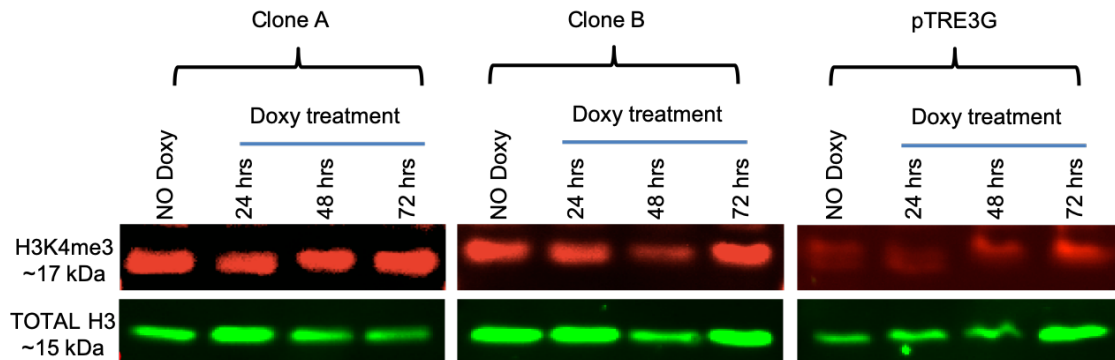
B)
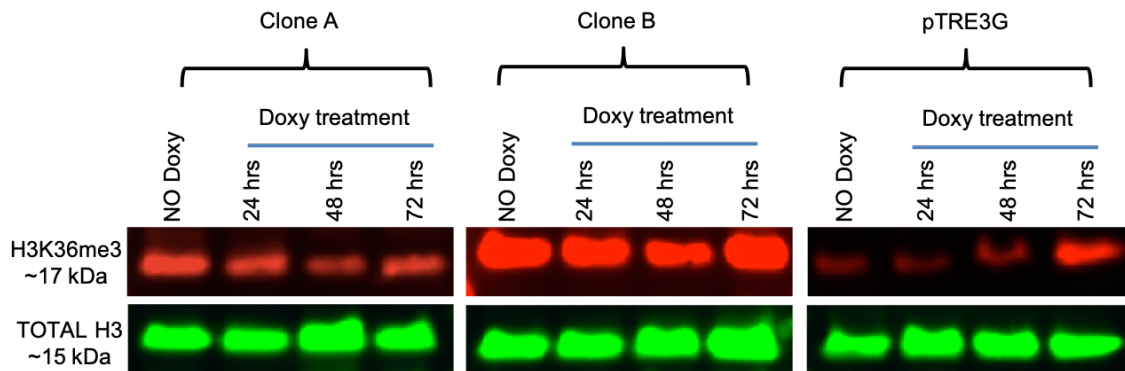
Figure 4. 8. Immunoblotting shows a trimethylation of H3K4 and H3K36 in HeLa Tet-On system cell lines before and after the induction of *PRDM9* expression. Clones A, B and pTRE3G were grown in induced cultures for 24, 48 and 72 hours for each clone, and one culture was not induced so that it could serve as a negative control for doxycycline induction. A) Immunoblot shows the H3K4 trimethylation activity. B) Immunoblot shows the H3K36 trimethylation activity. The anti H3 (Anti-Histone H3) antibody was used as a positive control.

4.2.4. Two point mutations in the integrated *PRDM9* sequence

Mutations are associated with disease progression and help develop genome evolution and architecture. Mutations cause many effects on gene size, organisation and expression level and have the ability to change genetic interactions, hence for *PRDM9* influencing recombination and sex (Lynch, 2005; Rifkin et al., 2005). Additionally, they have direct implications for phenotypic evolution (Nei, 2007). In general, mutations can be categorised into a single nucleotide variation (SNV), insertions/deletions (indel) and rearrangements of chromosomes. SNV mutations can result when a part of the genome is exposed to either endogenous or exogenous mutagens (Friedberg et al., 2004). Insertions and deletions include single base pairs or larger DNA sequences such as entire genes or the larger regions of chromosomes. The location of mutations may occur in coding and noncoding sequences and can be termed lethal, deleterious or neutral mutations, depending on their effects.

Point mutations can be a substitution of one base pair in a codon and functionally categorised into nonsense, missense and silent mutations (Davies, et al., 2002; Li, et al., 2017). Nonsense mutations are a replacement occurring in stop or start codons and result in stop-gain/loss and/or start-gain/loss (Hoeijmakers, 2001; Li et al., 2017). A missense mutation is when a substitution of a base pair leads to an amino acid change, while a silent mutation results in no change in the amino acid. Usually, nonsense and missense mutations may be responsible for changing the properties and functions of the produced protein (Minde, et al., 2011; Li, et al., 2017).

The investigations in the current study showed that the integrated *PRDM9* sequences contain two points of mutations. Both mutations were a substitution of one base pair in two codons that subsequently resulted in changes in the amino acids sequence. The first mutation occurred at the base at position 2008 of the coding sequence and change the amino acid (number# 670), glycine to arginine, and the second mutation was a replacement of the base at position 2042 of the coding region, here resulting in change of an amino acid (number 681) from threonine to serine (see Figure 4.9).

Figure 4. 9. Scheme that represents the two points of mutations in the integrated PRDM9 sequence. The origin template that was constructed for clones A and B contains two mutations.

4.3.1. Discussion

In mammals, PRDM9 identifies the sites of meiotic recombination hotspots (Baudat et al., 2010b; Myers et al., 2010; Parvanov et al., 2010). This protein is produced initially during the early stages of prophase in meiosis (Sun et al., 2015). During this stage the C2H2 zinc-finger (ZF) domain of PRDM9 binds DNA at certain motifs. At the same time, its PR/SET domain trimethylates nearby histone H3 proteins at lysine 4 (H3K4me3) (Hayashi et al., 2005) and lysine 36 (H3K36me3) (Wu et al., 2013; Eram et al., 2014; Powers et al., 2016; Davies et al., 2016; Grey et al., 2017). Trimethylation H3K4me3 is also reported as a mark present in promoters of transcribed genes (Santos-Rosa et al., 2002). At the PRDM9-DNA binding location, SPO11 is recruited to initiate DSBs. The end resection of these DSBs occurs to form a single-stranded DNA, which is the substrate of meiosis specific recombinase protein, DMC1 (Neale & Keeney, 2006; Smagulova et al., 2011; Altemose et al., 2017a).

It has been proposed that the trimethylase activity of PRDM9 plays a role in gene regulation during meiosis (Hayashi et al., 2005; Mihola et al., 2009). However, the importance of this function of PRDM9 during meiosis is unclear considering the recent reports which show full fertility in transgenic mice possessing highly remodelled PRDM9 DNA binding sites (Baker et al., 2014; Davies et al., 2016). Still, the possibility of the fact that PRDM9 protein can behave as a secondary regulator for genes during meiosis is not precluded.

According to Hayashi et al. (2005), the expression of *Rik* (*Morc2b*) gene in mice is transcriptionally regulated by the Prdm9 protein. However, in this current study, the overexpression of *PRDM9* did not appear to influence the expression patterns of human *Rik* (*Morc2b*) orthologues (*MORC1*, *MORC2*, *MORC3* and *MORC4*) in the HeLa Tet-on system. It implies that PRDM9 may not involve in regulation of the *MORC* gene family expression in humans in cancer cells. Moreove, MORC2 showed no signal after 48 hours of treatment which is not expected and might be a result of technical issues.

Furthermore, recent study showed that human PRDM9 binds near a promoter of some genes and then activates histone trimethylation leading to activate their gene expression in HEK293T cells (Altemose et al., 2017). For example, the overexpression

of *PRDM9* in transfected cells results in activation of spermatocytes-specific genes *CTCFL* and *VCX,* compared to untransfected cells. The authors suggested that the effects of PRDM9 on gene expression does not result from its DNA binding function only but also from its trimethylation activity as well (Altemose et al., 2017).

Numerous PRDM family members are able to modify the chromatin state at target gene promoters by which they can regulate the expression of these genes (Hohenauer et al., 2012). In human cancer cells, the role of PRDM proteins in transcription is not fully understood. This current study also raises the question that whether PRDM protein mediates the expression of other meiotic genes in tumour cells. During this study, expression of other genes was assessed to determine if *PRDM9* can affect them in HeLa Tet-on 3G cell lines. The study carried out RT-PCR to study expression of many genes including *PRDM* family genes, *MORC* family genes, CT genes and meiosis-specific genes. In general, the findings of the RT-PCR analysis demonstrate that the overexpression of *PRDM9* was not found to influence the expression of the majority of these genes in HeLa Tet-on 3G cells. It is possible that the RT-PCR analysis is insufficient to investigate if *PRDM9* can transcriptionally activate the expression of these genes. However, four genes showed significant upregulations according to the overexpression of *PRDM9*, and they are *MAGEA1*, *PRDM7*, *PRDM11* and *GAGE1*.

MAGEA1 was described as a CT gene (Simpson et al., 2005; Feichtinger et al., 2012) and belongs to *MAGE* family genes. *MAGEA1* is known as a specific tumour marker and predictor for poor clinical outcomes (Zou et al., 2012). In this study, *MAGEA1* was not detected in pTRE3G clone (negative control) with very faint bands in uninduced cultures of clones A and B. After induction of clones A and B by doxycycline, *MAGEA1* expression was upregulated in similar pattern with *PRDM9* expression, particularly clone B. These findings were confirmed using qRT-PCR showing a significant increase of *MAGEA1* mRNA levels after *PRDM9* overexpression. This result suggests that the overexpression *PRDM9* may influence the expression of *MAGEA1*.

Additionally, overexpression of *PRDM7* was detected with high intensity band, particularly in HeLa Tet-on cell line (clone A), after over expression of *PRDM9*. Because these two genes have similar DNA sequences, it is suggested that this band

might be relating to *PRDM9*. However, the band intensities of *PRDM7* in clone B were faint and it is detectable with very weak signal in uninduced cultures. It is also expected that these two *PRDM* genes are co-expressed in cancer cells. Previous work in McFarlane lab demonstrated that *PRDM9* and *PRDM7* were co-expressed in normal human testis and erythroleukaemic (K-562) cells (Almatrafi, PhD thesis 2014).

Likewise, *PRDM11* is shown to be overexpressed with strong bands in Clone B, correlating to the overexpression of *PRDM9* suggesting that the *PRDM9* may influence the expression of *PRDM11* as well. It has been reported that some members of *PRDM* genes are re-activated and/or co-expressed with other *PRDM* members, for example, the co-expression of *PRDM1* and *PRDM14* is reported in cancer cells (Di Zazzo et al., 2013). Thus, more investigations are required such as, qRT-PCR and western blot, to validate whether *PRDM7* and *PRDM11* are reactivated or co-expressed with *PRDM9* expression.

In this study, we tried to confirm the trimethylation activity of PRDM9 in HeLa Tet-on 3G cells, however, we could not identify any significant correlation between PRDM9 and H3K4me3/ H3K36me3 increases. Although Altemose et al (2017) have now demonstrated that expression of *PRDM9* in HEK293T cells causes histone epigenetic modification linked to the activation of spermatogenesis specific genes *VCX* and *CTCFL.*

These findings may suggest that the integrated *PRDM9* sequence from the original template (that were subcloned in pTRE3G plasmid) contained two substitutions in the zinc finger coding region. This template was amplified originally from cDNA obtained from adult male testis sample. The fertility status of this patient is unknown, but it might be the case that this was a sterile individual and that this is a mutated version of *PRDM9* rather than a natural, functional variant. A remarkable feature of the zinc finger alleles of *PRDM9* is that majority of the polymorphisms in DNA sequences that code for PRDM9 zinc fingers lead to alteration in amino acids which play role in interaction of DNA. Therefore, this leads to changes in motif recognised by PRDM9 and subsequently alterations in DNA-binding properties of PRDM9 (Thomas et al., 2009; Ponting, 2011; Grey et al., 2017) . Moreover, previous study demonstrated that

mutations in mouse Prdm9 has resulted in completely abolished gene activities (Wu et al., 2013). Similarly, other mutations has led to inactive methylation activities of mPRDM9 (Wu et al., 2013). So, the study of the allele we have employed might have value, but in the absence of knowing the status of the patient, this is limited in nature.

4.3.2. Conclusion

PRDM9 has been demonstrated to catalyse H3K4me3 methylation (Hayashi et al., 2005). This histone modification is reported to be enriched at transcription start sites (Barski et al., 2007). This has led to the suggestion that PRDM9 may not be directly involved in transcriptional activities (Wu et al., 2013) but is a key factor in determining the meiotic recombination sites in human and mice (Baudat et al., 2010; Myers et al., 2010; Parvanov et al., 2010). Such role is achieved by the DNA binding properties of its zinc fingers, and it has been demonstrated that PRDM9 binds to specific regions in the genome where its methyltransferase activity leads to a local enrichment of H3K4me3, subsequently, results in the recruitment of the meiotic recombination machinery and gene transcriptional activations (Grey et al., 2011; Altemose et al., 2017). Moreover, the main function PRDM9 zinc finger arrays is to facilitate its DNA-binding (McCarty et al., 2003; Lee et al., 2007). Later, Altemose et al. (2017) identified other functions of this domain such as; forms multimers, activates gene expression and initiates recombination (Altemose et al., 2017). Additionally, the findings that PRDM9 influences the expression of spermatocyte-specific genes; *VCX* and *CTCFL*, suggests that some PRDM9 alleles can positively affect fertility, see (Altemose et al., 2017).

The findings in this study identified two point mutations at the zinc finger exon of integrated PRDM9 sequence. Both mutations lead to changes in amino acids and the produced protein. We suggest that these mutations may lead to changes in DNA-binding specificity of PRDM9. Given that, these mutations may inactivate PRDM9 functions. Thus, our work in the next chapter was carried out to integrate *PRDM9* sequence that is free of mutations.

Chapter 5

Cloning *PRDM9* into mammalian expression system Tet-On 3G

5. Cloning *PRDM9* into mammalian expression system Tet-On 3G

5.1. Introduction

Findings presented in previous chapters indicate that PRDM9 may play a functional role in the transcriptional activity of various genes in cancer cells. To determine the potential function of PRDM9 in cancerous cells, a specific validated antibody is required to detect PRDM9. The use of recombinant proteins is recommended in such cases to determine the presence of PRDM9 protein and study its function in cancer cells (Terpe, 2003).

One of the essential molecular tools and strategies that have been established in this field is the production of recombinant proteins (Morlacchi et al., 2012). A recombinant DNA tool is used in this study to target PRDM9 by incorporating a small peptide sequence of 3-12 amino acids as a tag. Use of a very small sequence as a tag is less likely to affect the biological function, transportation, or post-translational modification of the target protein, which is one of the main advantages of using this technology (Bucher et al., 2002; Gill et al., 1996). Additionally, this tag peptide can be determined using a specific monoclonal antibody, by which the tagged protein can be detected, and many types of assays can be used, such as Western blot. This technology is a valuable tool in studying the expression, localisation, and modification of target proteins and can obtain a high yield of purified protein. Many types of epitope tags are employed, including the Myc and Flag tags used in this study. A Myc tag contains 10 amino acids and is derived from a C-Myc protein, while a Flag tag is composed of eight amino acids that can be incorporated at the C-terminus or N-terminus of the protein of interest (Table 5.1).

Table 5. 1. Sequences of FLAG and Myc tags

Tags	Protein sequence	Nucleotides (5′ – 3′)
FLAG	DYKDDDDK	GAT TAC AAG GAT GAC GAC GAT AAG
MYC	EQKLISEEDL	GAA CAA AAA CTC ATC TCA GAA GAG GAT CTG

The aim of the work described in this chapter was to incorporate tags into the PRDM9 full sequence and then clone it into a pTRE3G plasmid and, therefore, transfected into HeLa Tet-On 3G cell lines to check the effects of PRDM9 overexpression on the activity of cancer cell genes. This work also aims to investigate the specificity of anti-PRDM9 antibody.

5.2. Results

5.2.1. The preparation of a pTRE3G plasmid and amplification of *PRDM9* with different tags.

The tetracycline Tet-On gene expression system is used to regulate the activity of genes in mammalian cells. This system is based on the elements that regulate mechanisms of resistance to tetracycline or its derivatives, such as doxycycline (DOX). The Tet-On 3G transactivator protein binds to tetracycline responsive element (TRE) promoters in the presence of DOX, and in turn, it activates the expression of the target gene (Gossen & Bujard 1992; Vigna et al., 2002; Loew et al., 2010). The Tet-On 3G system is sensitive to DOX and optimised for transfection and target gene expression in human cells (Figure 5.1). In McFarlane Lab, the HeLa Tet-on 3G cells transfected with pCMV-Tet3G plasmid were obtained from Clonetech. A map of the pTRE3G plasmid and its restriction sites is illustrated in Figure 5.2.

To create an inducible clone for *PRDM9*, the full length of human *PRDM9* (NCBI, Gene ID 56979) with a predicted size of 2685 bp was amplified from the constructed clone pGEM-3ZF (+)::*PRDM9* (Named pAMO1; McFarlane Lab). The integrated *PRDM9* sequence in the pAMO1 clone has been sequenced, and we ensured that this sequence was free of mutations prior to amplification. Therefore, the full length of *PRDM9* was amplified using different primers and Phusion high-fidelity PCR Master Mix with a GC buffer (Figure 5.3). The amplification primers contained different tags (N-FLAG, C-FLAG, and C-MYC) in addition to a restriction enzyme (as shown in Table 2.9). Bands of *PRDM9* were excised from the gel, purified, and incubated with the restriction enzymes *Nhe*I and *Bam*HI in a digestion step to facilitate proper cloning.

Similarly, the pTRE3G vector was digested with *Bam*HI and *Nhe*I restriction enzymes and purified, and an undigested pTRE-3G vector was used as a control (Figure 5.4). Fragments of *PRDM9*::C-Myc, *PRDM9*::N-Flag, and *PRDM9*::C-Flag were then ligated into the purified and digested vector pTRE3G using a ratio of 1:6. Ampicillin resistance was used for the successful detection of ligated plasmids in the *E. coli*.
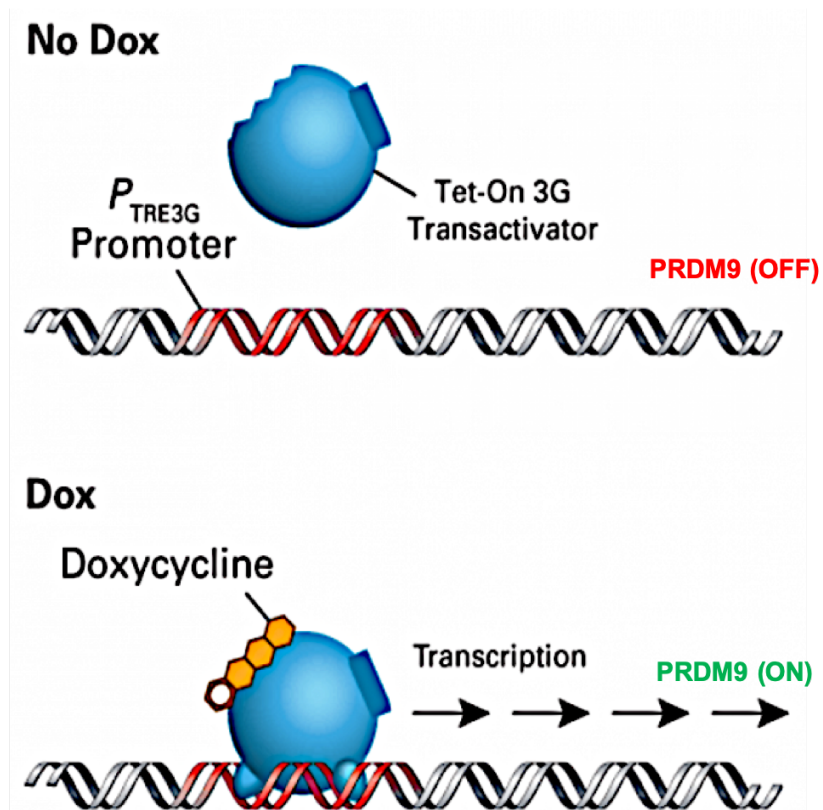
Figure 5. 1. The (ON/OFF) of *PRDM9* expression is regulated by transactivator protein in presence/absence of doxycycline. In presence of doxycycline, the transactivator protein (blue) of the Tet-On 3G system binds to the tet-operato (*tetO*) element (red) at the PTRE3G promoter that activates the expression of *PRDM9*.

Figure 5. 2. Map of pTRE-3G plasmid. The PTRE-3G vector is a 3431-bp inducible expression plasmid system established for use with the Tet-On 3G System. This vector is composed of Tet-responsive promoter-third generation (TRE-3G), SV40 polyA signal, pUC origin of replication, multiple cloning site (MCS), and ampicillin resistance genes (AmpR; β-lactamase). The restriction enzymes *Nhe*I and *Bam*HI were used in this study. This figure was adapted from http:// www.snapgene.com.

Figure 5. 3. PCR amplification of *PRDM9*. The full length of an open reading frame of the *PRDM9* gene was amplified using RT-PCR and visualised on 1.0% agarose gel using peqGREEN DNA dye. Lanes 1-3 show the approximate expected size of *PRDM9* fragments at 2685 bp with C-Myc, N-FLAG, and C-FLAG tags respectively. The marker lane contains 5 µl of HyperLadder 1 Kb.
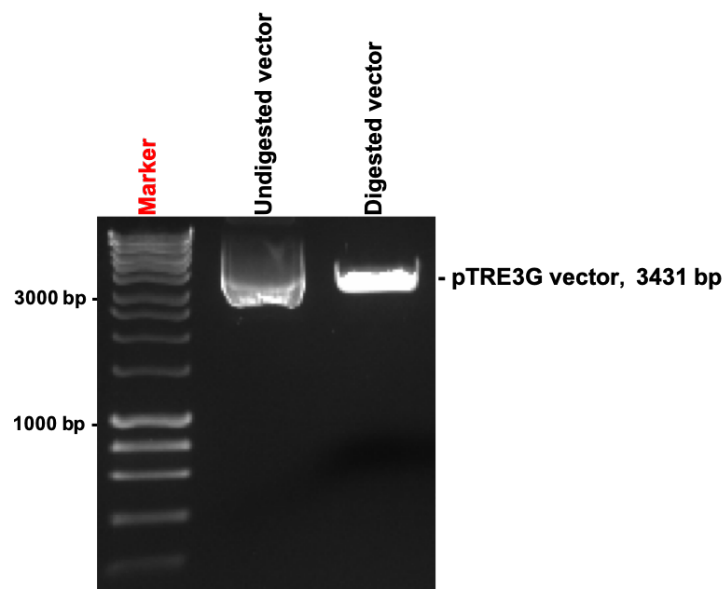
Figure 5. 4. The Digestion and purification of a pTRE3G plasmid. 1% agarose gel was used to visualise an uncut pTRE3G plasmid in Lane 1 as a negative control. Lane 2 shows the linearised plasmid after it was digested by *Nhe*I and *Bam*HI restriction enzymes and then purified. The marker lane contains 5 µl of HyperLadder 1 Kb.

5.2.2. PCR colony screening of *PRDM9* positive clones after transformation into *E. coli*.

An analysis was conducted on *E. coli* colonies after transformation to confirm that the correct colonies were chosen. PCR was conducted using universal primers to ensure that the recombinant plasmid contains the insert *PRDM9*. Only 4 colonies were obtained for pTRE3G::*PRDM9*::C-Myc (colonies from 1–4), while 7 colonies were obtained for pTRE3G::*PRDM9*::N-FLAG culture (colonies from 5–11), and a number of colonies were produced for pTRE3G::*PRDM9*::C-FLAG, and 10 colonies were selected for PCR colony screening (colonies from 12–21). Figure 5.5 shows the positive PCR results for many colonies, which means they had recombinant plasmid pTRE3G::*PRDM9*::C-FLAG, and 4 colonies (13,14, 19, and 20) were chosen for further confirmation. Negative PCR screening results were observed in colonies containing constructed plasmid with inserts *PRDM9*::N-FLAG and *PRDM9*::C-Myc, and one colony was chosen from each culture (colony 9 and colony 3 respectively) for further confirmation.

5.2.3. Restriction digestion of recombinant plasmids using *Nhe*I and *Bam*HI

Colonies with positive PCR results were grown overnight for further investigation. The plasmids were further evaluated by restriction digestion using *Nhe*I and *Bam*HI to validate successful cloning. A digestion restriction analysis of pTRE3G::*PRDM9*::C-Flag confirmed that colonies 13 and 20 were successful clones these plasmids produced two bands (upper for the vector and lower for the insert) as shown in Figure 5.6. Positive clones (#13 and #20) were sent for DNA sequencing analysis to further confirm that the insert was free of mutations and cloned in the correct orientation. The DNA sequencing results confirmed that the *PRDM9* sequence was free from any mutations and inserted in the proper orientation, which indicated that the recombinant plasmid (pTRE3G::*PRDM9*::C-FLAG) was successfully cloned and ready for transfection into HeLa Tet-on 3G cell lines.
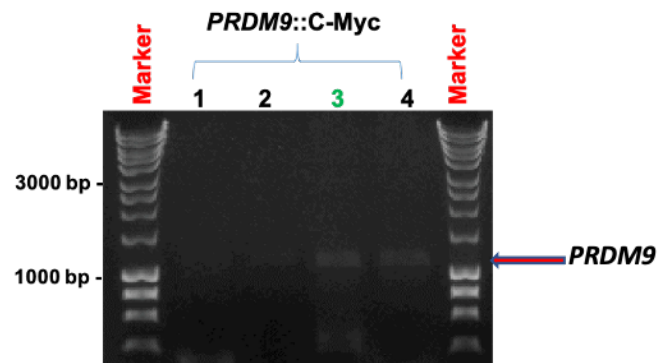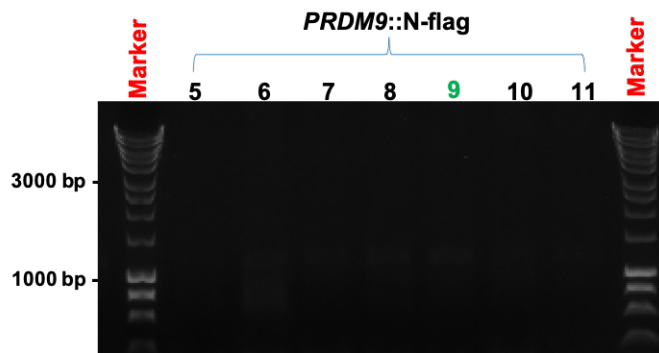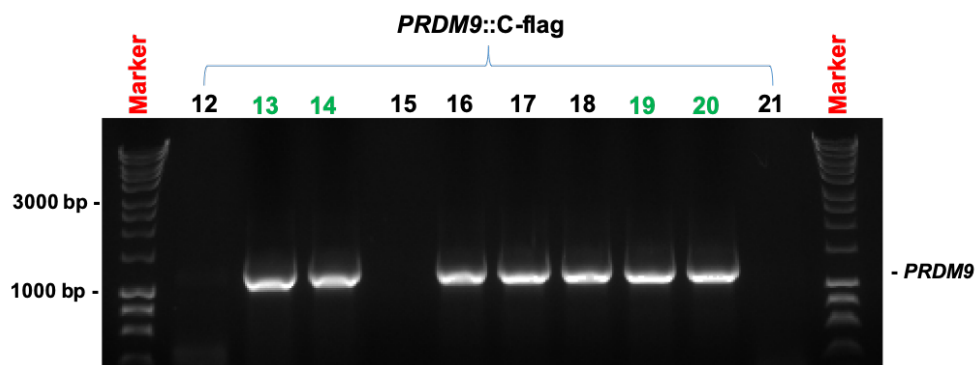
Figure 5. 5. A PCR colony screen of the produced *E. coli* colony after the transformation process was completed. Agarose gel images show the PCR screening results of transformed *E. coli* colonies to detect the recombinant plasmid using internal primers for the *PRDM9* gene. A) Colonies from the cultures transformed with a recombinant plasmid (pTRE3G::*PRDM9*::C-Myc) showed that no insert was detected. B) Colonies from the cultures transformed with a recombinant plasmid (pTRE3G::*PRDM9*::N-FLAG) showed that no insert was detected. C) Colonies from the cultures transformed with a recombinant plasmid (pTRE3G::*PRDM9*::C-FLAG) showed that the insert was detected in many of the chosen colonies. Colonies 3,9,13,14,19, and 20 were chosen for further confirmation. The marker lane contains 5 μl of HyperLadder 1 kb.
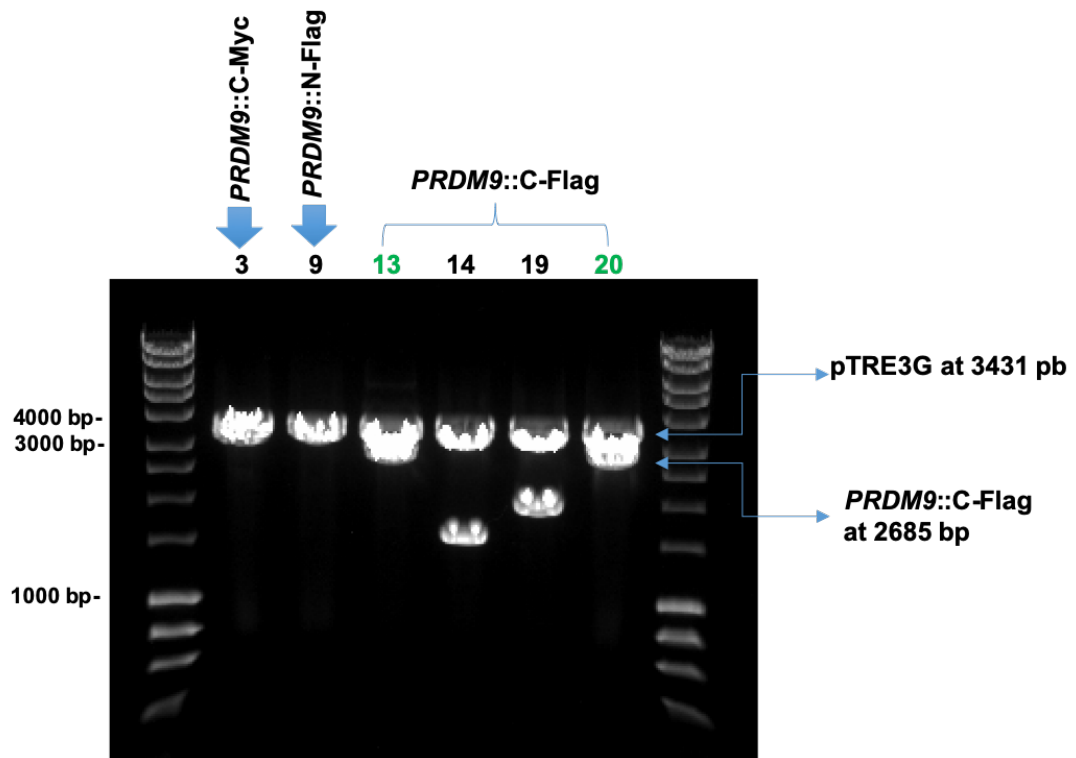
Figure 5. 6. Restriction digestion of recombinant plasmids with *Nhe*I and *Bam*HI restriction enzymes. Agarose gel demonstrates the restriction digestion of purified recombinant plasmids. Lane 1 shows colony #3 for the pTRE3G::*PRDM9*::C-Myc recombinant plasmid with a single band at 3431 bp, which only relates to the vector. Lane 2 shows the colony #9 for pTRE3G::*PRDM9*::N-Flag recombinant plasmid with a single band at 3431 bp, which only relates to the vector. Lanes 3 and 6 show two bands for the recombinant plasmid pTRE3G::*PRDM9*::C-Flag from colonies 13 and 20, respectively. Digestion restriction resulted in two bands at 3431 bp for the pTRE3G plasmid and 2685 bp, which is the expected size for the full length of *PRDM9*. Lanes 4 and 5 are the recombinant plasmid pTRE3G::*PRDM9*::C-Flag from colonies 14 and 19, respectively, showing two bands in each lane; however, the insert fragments were not at the expected size for the full length of *PRDM9*. The marker lanes contain 5 μl of HyperLadder 1 kb.

5.2.4 Establishment of a double-stable Hela Tet-On 3G cell line

One of the major parts of this study was the generation of double-stable Tet-On 3G cell lines capable of inducing *PRDM9* under the regulation of a TRE3G promoter. Establishing this system in cancer cells to control the expression of *PRDM9* (ON/OFF) is important when studying the transcriptional activities of this gene. To establish a double-stable cell line in the Tet-on 3G system to express a target gene, two steps are required. The first step includes the transfection of a pCMV-Tet3G plasmid with cells to constitutively produce the transactivator protein under the selection of a G418 antibiotic. In the McFarlane Lab, the HeLa Tet-on 3G cells transfected with pCMV-Tet3G plasmid were obtained from Clonetech. In the second step, the double-stable cell line was established by co-transfecting HeLa Tet-on 3G cells individually with constructed plasmid pTRE3G::*PRDM9*::C-Flag along with a linear selection marker for the antibiotic puromycin (Figure 5.7). Finally, a selection of double-stable transfected cells that resist puromycin and G418 antibiotics was obtained.

5.2.5. The selection of a double-stable Hela Tet-On 3G cell line

A cell kill curve was established using different puromycin antibiotic concentrations to optimise the minimal inhibition concentration (MIC) of HeLa Tet-on 3G cells prior to transfection. The HeLa Tet-on 3G cells were plated in antibiotic free growth media for 48 hours. Therefore, the cells were exposed to the antibiotic puromycin in different concentrations (0–2.5 µg/ml) for 4–5 days as demonstrated in Figure 5.8. The optimal concentration of puromycin that inhibited the growth of all HeLa Tet-on 3G cells after 5 days was 1.0 µg/ml.

The co-transfection of HeLa Tet-on 3G cells was carried out with either pTRE3G::*PRDM9*-C-Flag or an empty pTRE3G plasmid as a negative control for gene induction, along with a puromycin linear selection marker. The cells were cultured in antibiotic-free media for 4 days and then 1.0 µg/ml of puromycin and 100 µg/ml of G418 were added to the cultures. After 5 days of antibiotic treatments, most cells were killed except cells that were resistant to the puromycin antibiotic, indicating that these cells may have a successful transfection. After two weeks of treating cultures with the optimal concentration of the puromycin antibiotic, large and healthy colonies were

picked up and grown separately in 6-well plates, then 10 cm plates, and finally transferred to T75 flasks.

The resulting colonies were then examined individually through the assessment of *PRDM9* expression in the absence and presence of 1.0 µg/ml doxycycline. High-quality Tet system approved FBS was utilised for cloned cell cultures because it is free of tetracycline and has been functionally tested for this inducible system.
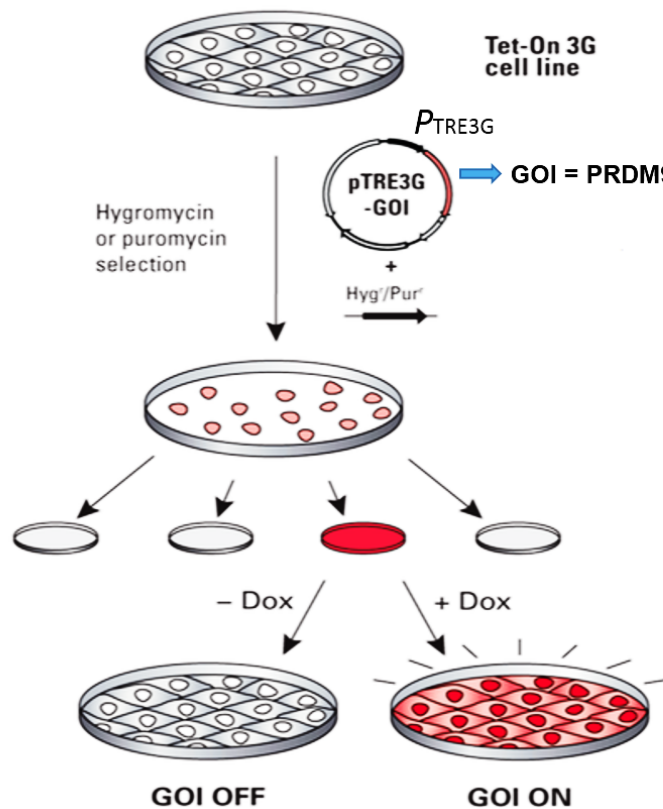
Figure 5. 7. A schematic diagram of the selection of the double Tet-On3G cell line. The tetracycline-inducible gene expression system (Tet-On 3G) regulates the transactivator protein in HeLa Tet-On 3G cells. In the presence of Doxycycline, it binds and activates the TRE3G promoter to express the gene of interest (GOI). HeLa Tet-On 3G cells were transfected with PTRE3G::*PRDM9*::N-Flag along with an antibiotic linear marker of puromycin. The induction of 1 µL/ml Dox results in *PRDM9* overexpression.
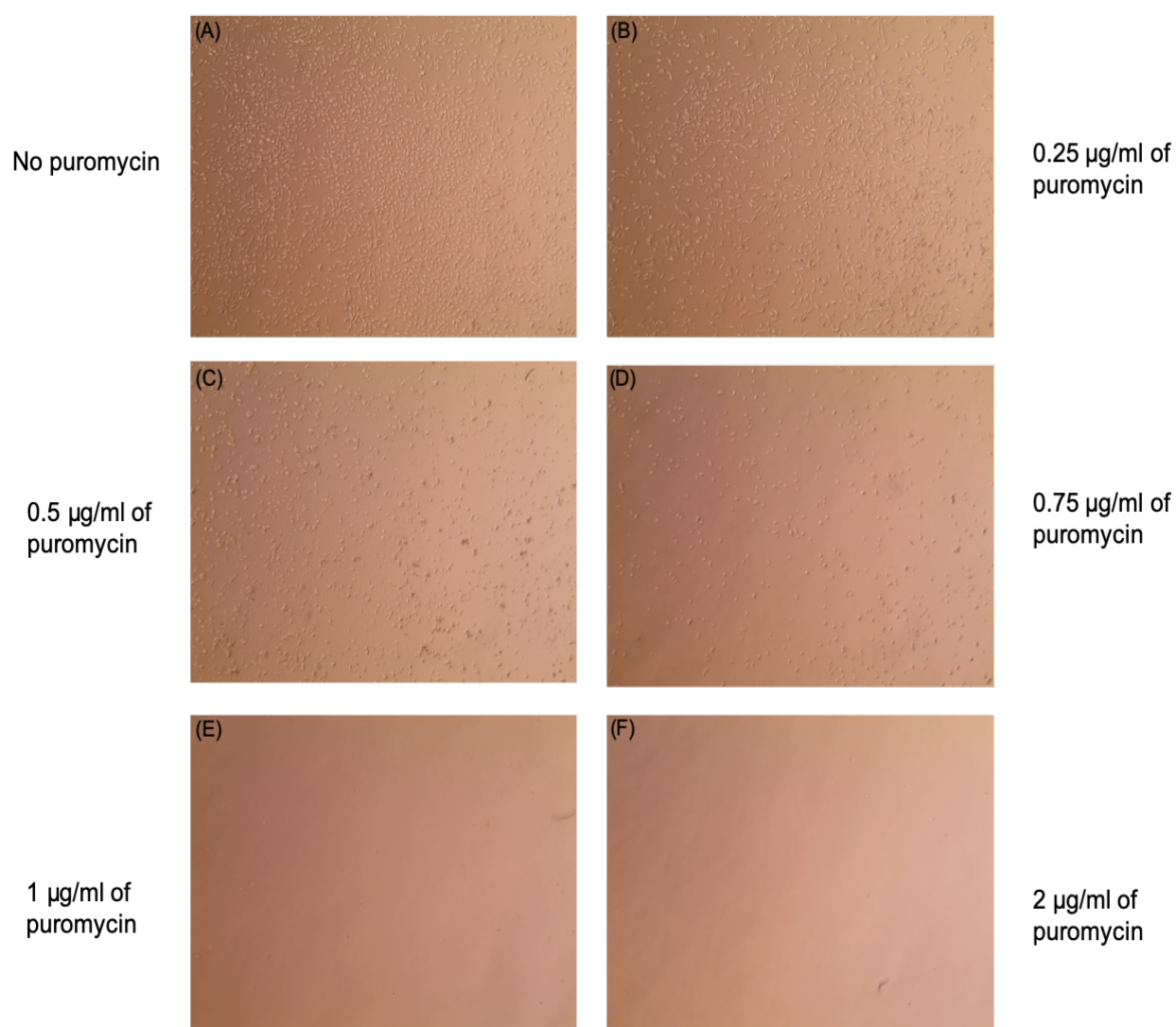
Figure 5. 8. HeLa Tet-On 3G cell kill curve. Untransfected HeLa Tet-On 3G cell lines were grown for 48 hours before the administration of the antibiotic puromycin with different concentrations in each culture to determine the minimal inhibition concentration that would kill cells. Five doses were administered in each culture (0.25–2 µg/mL) and grown for 3–5 days. A concentration of 1 µg/mL was sufficient to kill all HeLa Tet-On 3G cells.

5.2.6. The analysis of *PRDM9* overexpression into double-stable HeLa Tet-On 3G cells using RT-PCR and qRT-PCR.

Healthy colonies were examined to validate the successful integration of *PRDM9* into HeLa Tet-on 3G cells, generating double-stable cell lines. These colonies were cultured in growth media containing 1.0 µg/ml doxycycline for 24 and 48 hours to evaluate the overexpression of *PRDM9* in transfected cells with pTRE3G::*PRDM9*::C-Flag. A portion of each clone was cultured in growth media without doxycycline treatment as a negative control. An additional colony containing only a pTRE3G plasmid was cultured in the presence and absence of 1.0 µg/ml doxycycline.

RT-PCR was conducted first to analyse the expression of *PRDM9* in HeLa Tet-On 3G cell lines prior to the transfection of the recombinant plasmid pTRE3G::*PRDM9*::C-Flag, along with HeLa S3 cancer cell lines showing no expression of the *PRDM9* gene as shown in Figure 5.9. A testis cDNA sample was used as a positive control for *PRDM9* expression. RT-PCR was then carried out on five positive colonies produced after the transfection of the recombinant plasmid pTRE3G::*PRDM9*::C-Flag into HeLa Tet-On 3G cells to assess the expression of *PRDM9* after 1.0 µg/ml doxycycline induction for 0, 24, and 48 hours (Figure 5.10). The results reveal that two clones, #3 and #5, demonstrated significant *PRDM9* expression, whereas clones #1, #2, and #4 did not express *PRDM9*.

Colonies #3 and #5 demonstrated the successful integration of the recombinant plasmid and were labelled AF1 and AF2 clones. These two clones were cultured and re-evaluated again for further confirmation. Each clone was grown in 1.0 µg/ml doxycycline for 24 and 48 hours, along with a culture without doxycycline induction. Additionally, HeLa Tet-On 3G cells with pTRE3G only were grown in the presence and absence of DOX treatment as negative controls. RT-PCR was conducted to evaluate the overexpression of *PRDM9* in clones AF1 and AF2 (Figure 5.11). The results show significant expressions of *PRDM9* in AF1 and AF2 in comparison to the treatment without DOX and only pTRE3G clone cultures.

Further confirmation was conducted using qRT-PCR analysis to determine the levels of *PRDM9* expression in AF1 and AF2 clones with and without DOX induction (Figure

5.12). The results show there were significantly high levels of *PRDM9* mRNA after 1.0 µg/ml DOX induction, but there was no expression in uninduced and pTRE3G clone cultures.
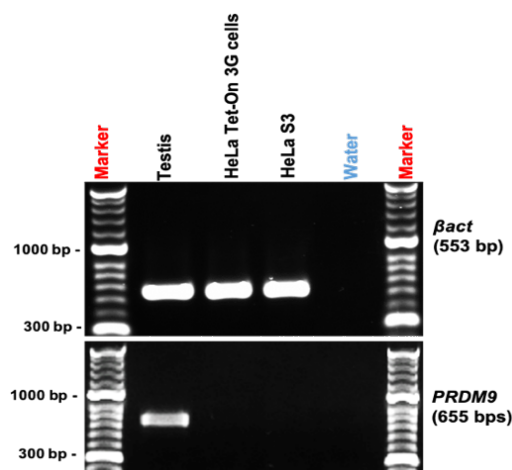
Figure 5. 9. RT-PCR analysis of *PRDM9* expression of HeLa Tet-On 3G cells prior to transfection. 1% agarose gels stained with PeqGREEN DNA dye were run to qualitatively visualise the expression of *PRDM9* in HeLa Tet-On 3G cells and the HeLa S3 cancer cell line, showing no detectable expression in the above gel as shown in lanes 2 and 3, respectively. Lane 1 was a cDNA from a testis sample as a positive control for *PRDM9* expression. The bottom gel was *βact* as a control for cDNA.
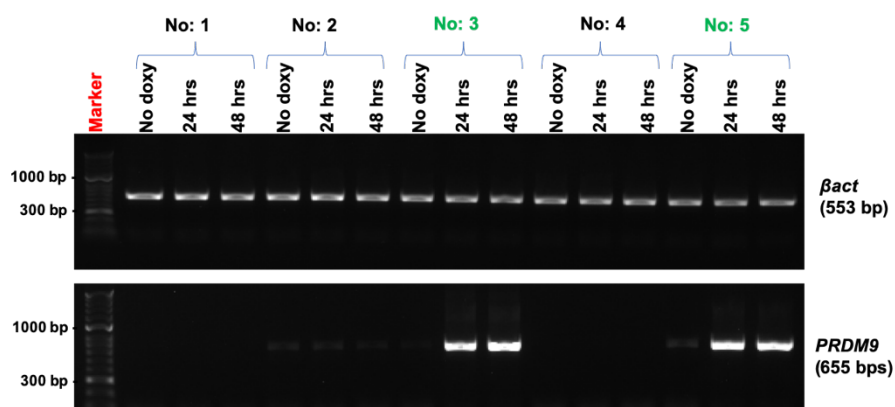
Figure 5. 10. RT-PCR analysis of the *PRDM9* expression of HeLa Tet-On 3G cells after transfection. 1% agarose gels stained with PeqGREEN DNA dye were run to visualise the expression of *PRDM9* in double-stable HeLa Tet-On 3G cells. Five colonies were produced, and each colony was split into three independent cultures as no DOX induction, DOX induction for 24 hours, and DOX induction for 48 hours. The upper gel was conducted for the *βact* gene to evaluate the quality of synthesised cDNA. The bottom gel was run to assess the expression of *PRDM9* in each colony. The significant expression of *PRDM9* was determined in two colonies, #3 and #5. HyperLadder II was used as a marker.
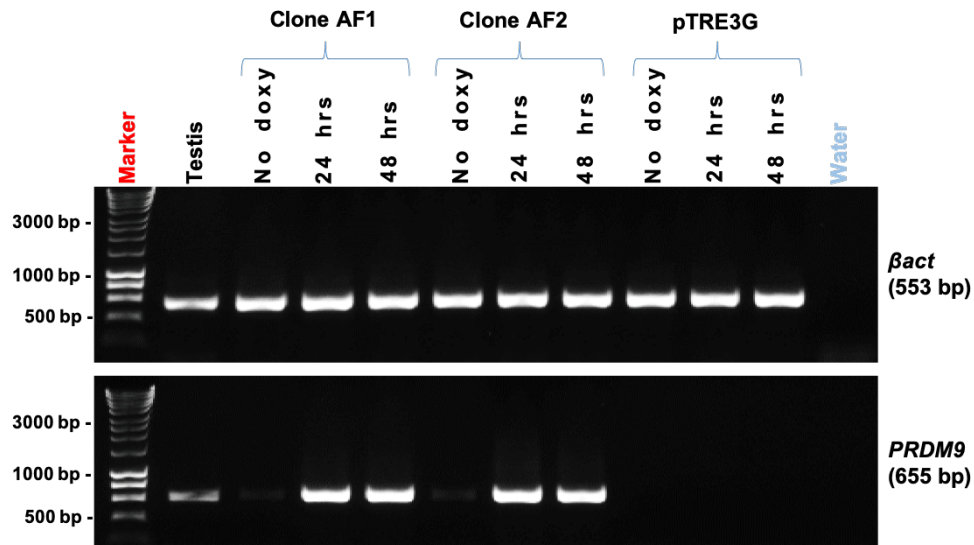
Figure 5. 11. RT-PCR analysis confirming the expression of *PRDM9* in two independent clones (AF1 and AF2). 1% agarose gels stained with PeqGREEN DNA dye were run to visualise the expression of *PRDM9* in two colonies of HeLa Tet-On 3G cells after the transfection of the recombinant plasmid. Cultures from each clone were grown in three conditions: no DOX induction, 24 hours of induction, and 48 hours of DOX induction. A clone that contained only pTRE3G was used as a negative control and a testis sample was used as a positive control for *PRDM9* expression. The upper gel was conducted for the *βact* gene to evaluate the quality of synthesised cDNA. The bottom gel was run to assess the expression of *PRDM9* in each colony. The significant expression of *PRDM9* was determined in AF1 and AF2 clones. HyperLadder II was used as a marker.
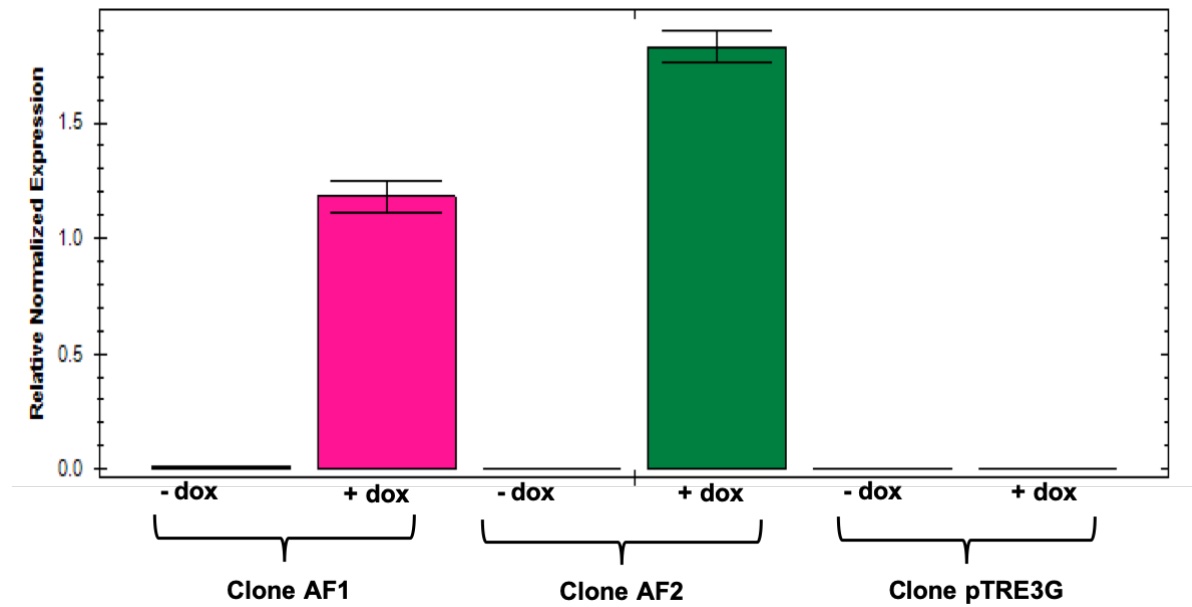
Figure 5. 12. A quantitative qRT-PCR analysis demonstrates the level of *PRDM9* expression in AF1 and AF2 clones. qRT-PCR was carried out to detect the transcript levels of the *PRDM9* gene in HeLa Tet-On 3G cells (clones AF1 and AF2 and pTRE3G) before and after 1 µg/mL DOX induction. Bio-Rad CFX Manager software was used for data analysis. The error bars show the standard error of the mean for the three replicates. The *PRDM9* gene expression levels were normalised to a combination of two endogenous reference genes (*ACTB* and *GAPDH*).

5.2.7. Human *PRDM9* and the transcription activity of other meiosis-specific genes

Findings presented in previous chapters showed that human PRDM9 may act as a transcriptional activator for other meiosis-specific genes. A previous study found that the expression of *PRDM9* can activate the transcription of two spermatocyte-specific genes, *CTCFL* and *VCX* (Altemose et al., 2017). They also observed that the overexpression of *PRDM9* activates an additional 44 genes in transfected HEK293T cells in comparison to untransfected cells. In this study, 15 genes were selected randomly from the 44 genes to be assessed in transfected HeLa Tet-On cells. The overexpression of *PRDM9* was validated in an induced HeLa Tet-On 3G system in two independent clones, AF1 and AF2. Each clone was plated in three cultures as no induction, as well as 24 hours and 48 hours of doxycycline induction. The negative control was HeLa Tet-On 3G cells transfected with the pTRE3G plasmid only and cultured in the same conditions. A testis sample was used as a positive control for the expression of *PRDM9* and examined genes. A set of primers was designed for each gene. Figures 5.13 and 5.14 display the expression profile for each gene, along with the expression of *PRDM9* in Clones AF1 and AF2. The results show that the overexpression of *PRDM9* has no significant influence on the expression of these genes.
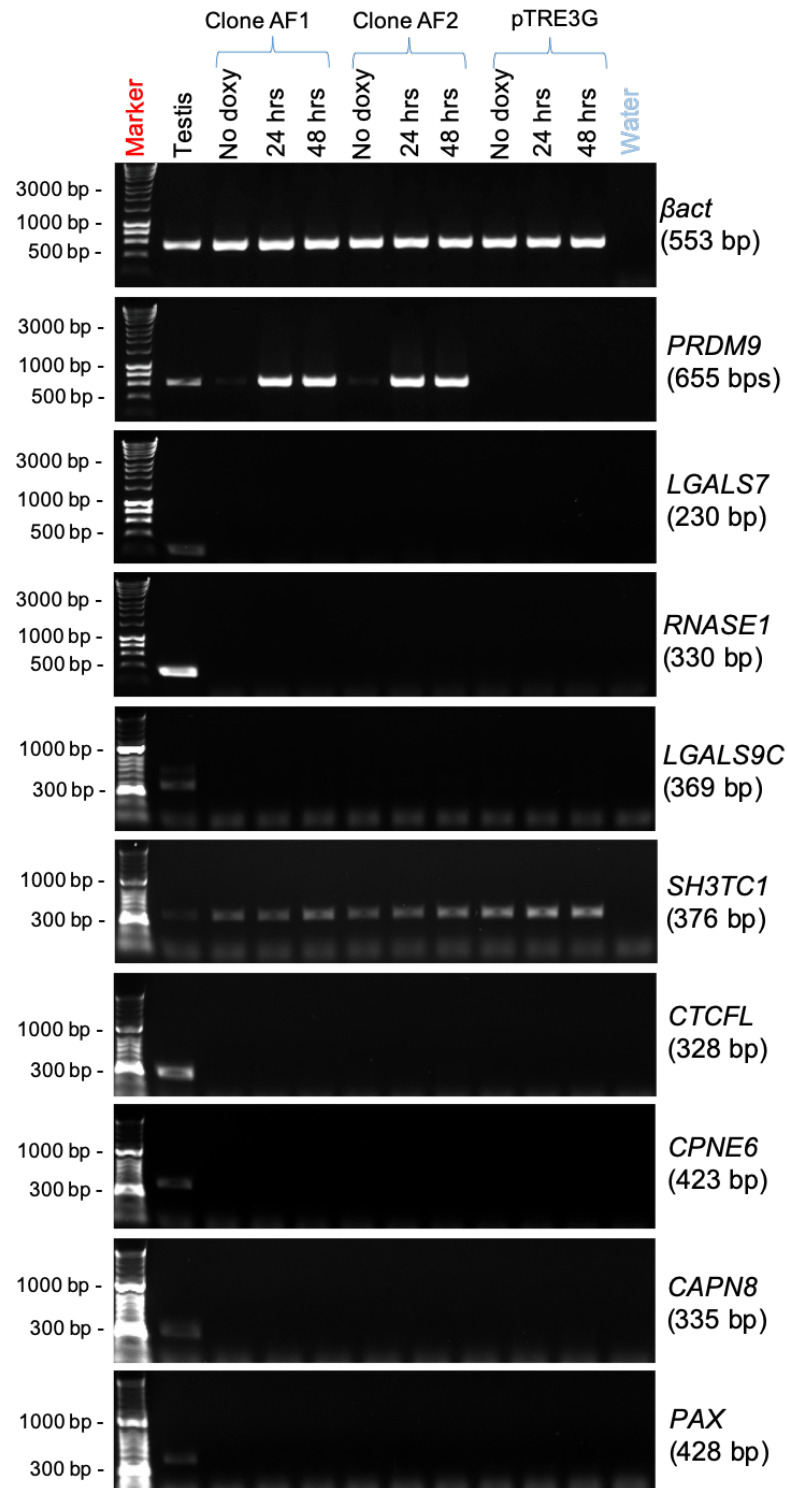
Figure 5. 13. Analysis using RT-PCR demonstrates the expression profile of other genes after *PRDM9* overexpression in the HeLa Tet-on 3G system. The expression of *βAct* was carried out as a positive control for the quality of the cDNA. *PRDM9* was overexpressed after DOX induction in clones AF1 and AF2, but no expression was observed in the absence of DOX. The cultures of clone pTRE3G were used as a negative control for *PRDM9* expression. The testis sample was run as a positive control for the expression of *PRDM9* and the examined genes. The 1% agarose gels were run and stained with a pic-green stain to visualise the PCR products.
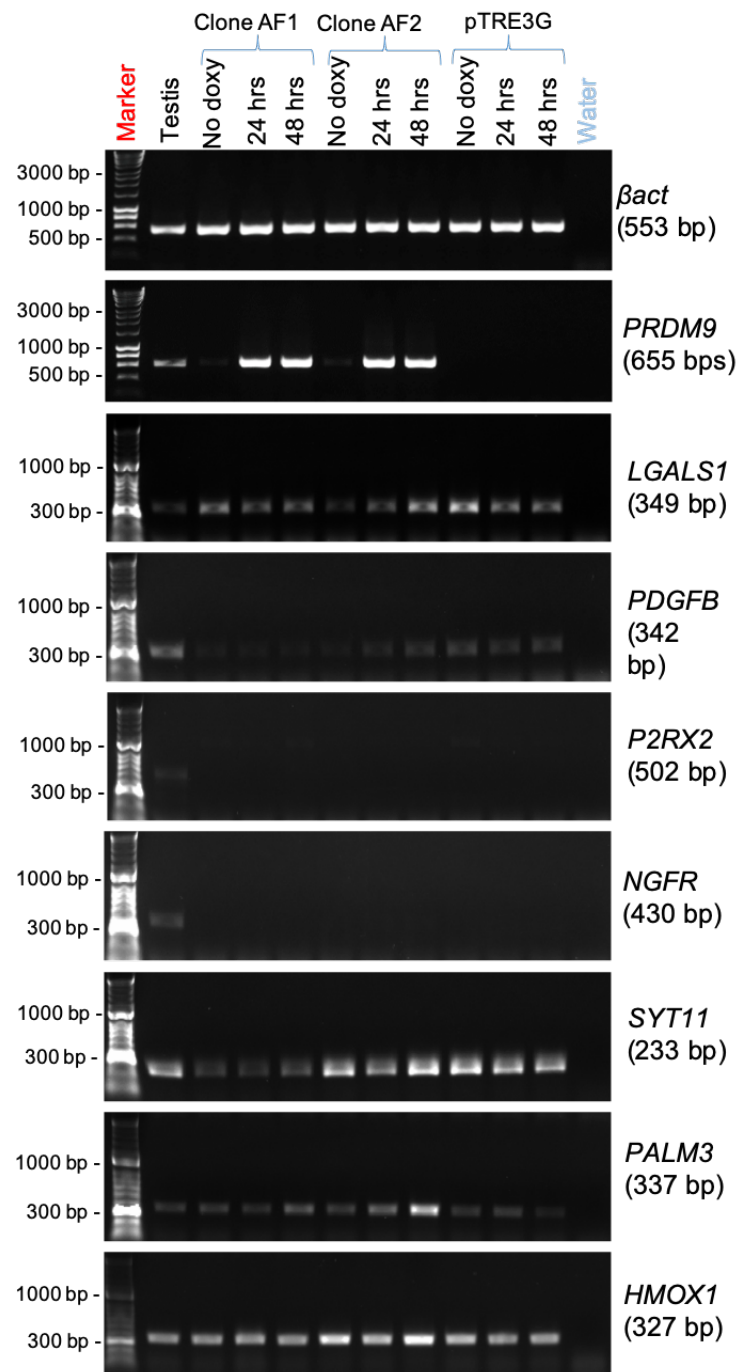
Figure 5. 14. Analysis using RT-PCR demonstrates the expression profile of other genes after *PRDM9* overexpression in the HeLa Tet-on 3G system. The expression of *βAct* was carried out as a positive control for the quality of the cDNA. *PRDM9* was overexpressed after DOX induction in clones AF1 and AF2, but no expression was observed in the absence of DOX. The cultures of clone pTRE3G were used as a negative control for *PRDM9* expression. The testis sample was run as a positive control for the expression of *PRDM9* and the examined genes. The 1% agarose gels were run and stained with a pic-green stain to visualise the PCR products.

127

5.2.8. PRDM9 protein analysis in HeLa Tet-On 3G cells.

Independent colonies with possible tag were evaluated using anti-flag antibodies; monoclonal anti-flag (Sigma; #F1408 and Cell signalling antibody; #8146). The lysates from each individual clone were extracted from cultures that were treated with DOX (1 µg/ml) for 24 and 48 hours, and portion of cells were grown in no DOX. Uninduced cultures were used as negative controls for DOX treatment. Furthermore, HeLa Tet-On 3G cells with only pTRE3G only was used as negative control for this experiment. High-quality Tet system FBS medium which is free of tetracycline was used to grow each culture. All the lysates were probed against anti-flag antibodies using western blot analysis to detect the flag tag that was incorporated into PRDM9. We used PSNF5 cells that were transfected with a constructed clone of BLM gene containing FLAG sequence, as a positive control for anti-FLAG antibody detection. The expected size for BLM::FLAG is 160 kDa. Moreover, lysates from HeLa cell lines were used as a negative control for anti-FLAG antibody.

An example of western blot analysis is shown in Figure 5.15. The results showed that no protein signal is detected at the expected size of PRDM9::C-Flag which is at 104 kDa. It might be considered that the flag protein was not co-expressed with PRDM9 protein or the Tet-On 3G system did not work properly. However, the negative control lysates showed that signals of flag protein is detectable which are not specific. This may indicate that the antibodies are not specific or not working efficiently.
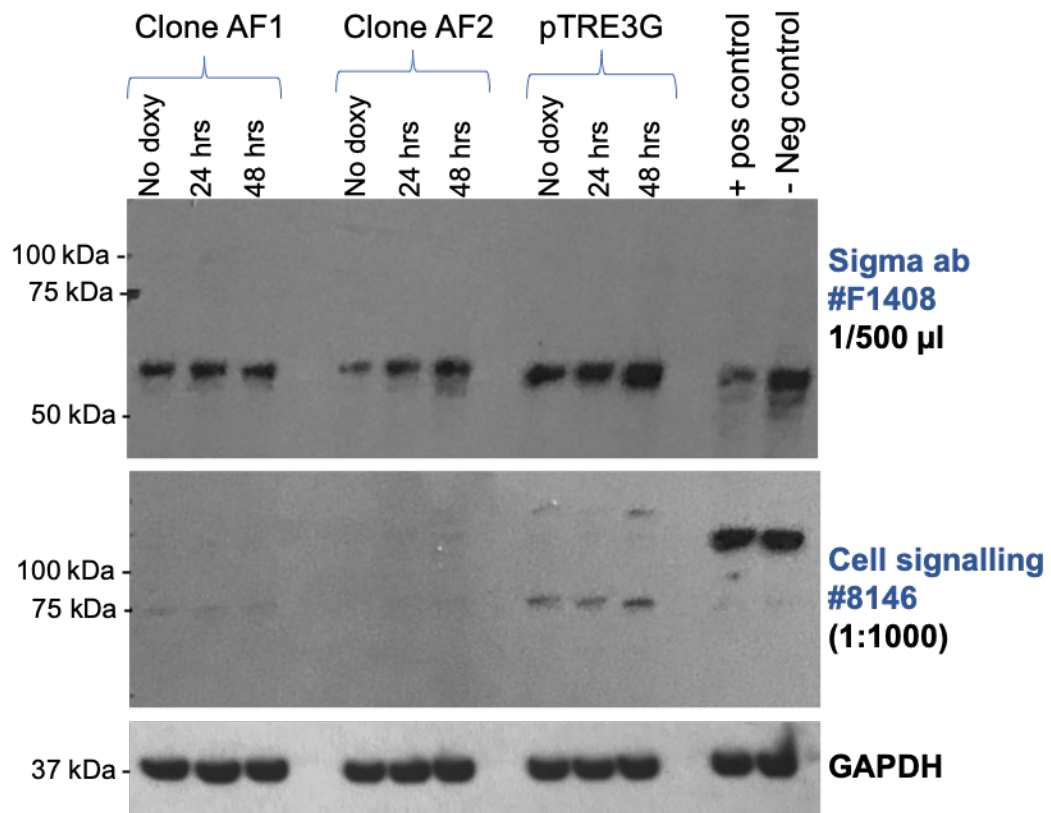
Figure 5. 15. Western blot analysis for C-Flag tag after HeLa Tet-On 3G double stable cells. Two independent clones AF1 and AF2 that contain PRDM9::C-Flag were induced with DOX for 0, 24 and 48 hours. Clones with pTRE3G plasmid only was grown in the same condition as negative controls. Lysates were extracted and probed against two anti-flag antibodies. GAPDH levels was used as a positive loading control. This figure is an example from three biological repeats. No significant signal was detected for flag that was incorporated in PRDM9 at the expected size of 104 kDa. Additionally, positive control (PSNF5 cells) which were transfected with flagged BLM gene did not show signal at expected size of 160 kDa.

5.3. Discussion

PRDM9 is a meiosis-specific gene expressed in the early stages of the meiotic prophase (Sun et al., 2015; Altemose et al., 2017). PRDM9 binds to DNA at specific regions to determine the recombination location or hotspots (Baudat et al., 2010; Myers et al., 2010; Parvanov et al., 2010) by which other proteins (e.g., SPO11) are recruited to carry out the recombination process. However, not all PRDM9 binding sites undergo recombination, and some of these locations are not understood. Recent investigations have reported that PRDM9 binds at the sequences of gene promoters and nearby transcription start sites (TSS), leading to genes being activated. This suggests that PRDM9 may regulate gene transcriptional activities (Altemose et al., 2017). The potential of human PRDM9 to act as a transcriptional activator has been reported, and it has been demonstrated that PRDM9 activates *VCX* and *CTCFL*, two meiosis-specific genes (Altemose et al., 2017). Moreover, the overexpression of transfected *PRDM9* in HEK293T cells results in the activation of some meiotic genes (Altemose et al., 2017), which evidently supports the functional roles of PRDM9 in fertility.

To further study the function of PRDM9, we have integrated the full open-reading frame sequence of *PRDM9* into a cell line that lacks *PRDM9* expression to evaluate its effect on the regulation of other genes and validate the PRDM9 antibody. Therefore, the Flag tag was incorporated at the C-terminus of the PRDM9 sequence to be co-expressed with the PRDM9 protein. Importantly, such tags are designed with a small sequence, which is less likely to interfere with the function of the tagged protein.

Moreover, the Tet-On 3G system is one of the most powerful inducible gene expression systems in eukaryotes that controls the expression of the gene of interest (GOI) in the presence and absence of DOX treatment (Gossen & Bujard, 1992; Urlinger et al., 2000). In this study, two clones of the double-stable HeLa Tet-On 3G cell line were created that contain a recombinant plasmid of pTRE3G::*PRDM9*::C-Flag. The sequence of *PRDM9* was evaluated by DNA sequencing, showing that the integrated sequence was in the correct orientation and free of mutations. The expression of integrated *PRDM9* into HeLa Tet-On 3G cell lines was validated at the transcription level using RT-PCR and qRT-PCR analyses. *PRDM9* transcript levels

were overexpressed following doxycycline induction, but no expression was detected in non-induced HeLa Tet-On 3G cells.

Recombinant DNA tools facilitate the incorporation of a small sequence of tags to identify gene products (proteins) using tag-specific antibodies. In this study, two commercial anti-flag antibodies were used in a Western blot analysis. However, no protein signals were detected, which may suggest that the PRDM9 was not produced or the Tet-On 3G system may not work efficiently. Furthermore, this issue may be related to the quality of the anti-flag antibody, because it is also observed and signal-emerged in negative control lysates.

As the *PRDM9* showed significant expression at transcription levels, we attempted to validate the expression of chosen genes investigated by (Altemose et al., 2017). They observed that the overexpression of *PRDM9* in transfected HEK293T cells results in the activation of 44 genes. However, 15 tested genes in this study showed no significant activation following *PRDM9* overexpression in HeLa Tet-On 3G cells. We suggest that the expression of genes may depend on the nature of the cell's phenotype. Although genomic DNA from these colonies was extracted and successfully sequenced after cloning, the sequence on the genomic DNA after transfection should be considered. Moreover, further investigations of this cloning are required using other stable cell lines, such as HCT116 Tet-On 3G cells transfected with this recombinant plasmid, are also suggested.

Chapter 6

Functional analysis of TEX19 in human cancer cells.

6. Functional analysis of TEX19 in human cancer cells.

6.1 Introduction

Testis Expressed 19 (*TEX19*) is a mammalian-specific gene (Wang et al., 2001; Kuntz et al., 2008). The expression profile of human *TEX19* in a variety of normal and cancer human tissues has been investigated at mRNA and protein levels and demonstrated to be a CTA (Feichtinger et al., 2012; Zhong et al., 2016; Lai et al., 2016; Planells-Palop et al., 2017).

TEX19 orthologues in rodents have been found to be duplicated resulting, in a pair of gene paralogues, *Tex19.1* and *Tex19.2*. (Kuntz et al., 2008). *Tex19.1* expression was observed in early embryo, placenta and adult testis, while *Tex19.2* was expressed in gonadal ridge and adult testis. It has been suggested that the human *TEX19* is the human orthologue for the mouse *Tex19.1* gene, since the two are closely related in terms of their genomic loci, and they have a similar orientation and separation distance from the *UTS2R* gene (see Section 1.5 and Figure 1.10) (Kuntz et al., 2008). *Tex19.1* expression in embryonic stem cells (ESCs) was observed in a pattern similar to *Oct4* expression, suggesting it has a role in stemness (Kuntz et al., 2008). In mice, Tex19.1 protein production was associated with ESC self-renewal (Tarabay et al., 2013) and human TEX19 production was reported to be required for the self-renewal and proliferation of tumour cells (Planells-Palop et al., 2017). Thus, human TEX19 is suggested to play roles in oncogenesis (Planells-Palop et al., 2017).

Tissue-specific promoter DNA methylation regulates the expression of a group of genes encoding for germline genome-defence functions. *Tex19.1* has demonstrated highest sensitivity for methylation amongst these genes that play roles in protecting the genomic DNA of germ cells from transposon activities (Hackett et al., 2012; Reichmann et al., 2013). Furthermore, Tex19.1 interacts with E3 ubiquitin ligase Ubr2, forming a stable complex and the *Tex19.1*-null mouse mutant is similar to the *Ubr2*-deficient mutant in three key defects: meiotic/spermatogenic defects, asynapsis of meiotic chromosomes and embryonic lethality preferentially affecting females (Yang et al., 2010). Recent study showed that *Tex19.1*$^{-/-}$ oocytes demonstrated chromosomal mis-segregation during meiosis, unmaintained chiasmata and aneuploidies (Reichmann et al., 2017). In mitotic somatic cells, the ectopic expression of human

TEX19 was reported to modulate sister chromatid cohesion. Although the association between Tex19.1 protein and cohesion maintenance in postnatal oocytes is indicated, the mechanism of how Tex19.1 protein acts is still poor. The overexpression of *TEX19* in transfected HEK239T cells has been reported to be associate with the increase of a cohesin subpopulation, which is marked by acetylation of the SMC3 subunit. Given that, these findings, it is suggest that TEX19 is specifically regulating an AcSMC3-containing chromatin-associated subpopulation of cohesin (Reichmann et al., 2017).

A previous study identified that *TEX19* is widely expressed in various cancer tissues and cells but not in normal and healthy tissues except germ cells of adult testes and placenta, suggesting that *TEX19* is a potentially oncogenic factor (Feichtinger et al., 2012). Later, Planells-Palop et al. (2017) found that depletion of *TEX19* in cancer cells (such as; SW480 and HCT116 cell lines), resulted in proliferation inhibition and delayed S-phase progression. They suggested that *TEX19* may act as a transcriptional regulator for many genes that promote cancer cell proliferations (Planells-Palop et al., 2017). RNA sequencing analysis was conducted on total RNA obtained from TEX19-depleted cancer cells and compared to untreated cells; the results showed significant changes in transcript levels of 80 genes (Planells-Palop et al., 2017). Additionally, TEX19 appears to differentially regulate the transcript levels of distinct transposable elements (see Planells-Palop et al., 2017).

Cellular growth and proliferation is substantially controlled by specific growth genes that are regulated by various chromatin modifications (Cai et al., 2011). In general, the distinct post-translational modifications in histone tails play regulatory roles in the activation or inactivation of the transcription process (Tessarz et al., 2014). For example, acetylation of histones H3 and H4 has been reported to link with "active" chromatin (Dawson et al., 2012), whereas tri-methylations of H3K27 and H3K9 are identified as repressive histone marks, which result in gene silencing (Chandra & Narita, 2013).

The aim of work in this chapter was firstly to validate TEX19 antibody specificity. As the biological effects of human *TEX19* knockdown on cancer cell proliferation has been studied previously, this work aimed to confirm and extend study using different anti-*TEX19* siRNA molecules and new cancer cell lines (TEX19-HA overexpressing

HCT116 cell lines). Finally, total histone extractions were carried out on TEX19-depleted cancer cells to assess its effect on histone acetylation.

6.2. Results

6.2.1. Validation and optimisation of anti-TEX19 antibody specificity

This experiment was intended to validate the specificity of a newly obtained polyclonal anti-TEX19 antibody (R&D system; # AF6319) in two ways: validation through siRNA transfection and the detection of incorporated tagged sequence of TEX19. The N-terminal of *TEX19* was incorporated with an HA tag and cloned into the pCMV expressing system and subsequently transfected into HCT116 (*TEX19-HA* overexpressing HCT116). These cell clones were established in the McFarlane lab.

HCT116 and *TEX19-HA* overexpressing HCT116 cell lines were depleted of TEX19. The depletion was carried out using an siRNA (purchased from Qiagen) we refer to as siRNA #7 it was chosen because it targets the protein coding region in the second exon of the *TEX19* sequence, as shown in Figure 6.1. A fraction of cells was transfected with a negative control for siRNA to evaluate the depletion of *TEX19*. Knockdown of *TEX19* was achieved after 72 hours of siRNA #7 transfection, and the depletion was evaluated by qRT-PCR analyses, as illustrated in Figure 6.2 A and B. The levels of *TEX19* mRNAs showed significant reductions (by about 60%) compared to negative controls and untreated cells.

The reduction of TEX19 levels was assessed at the protein level using western blot analyses. The *TEX19* sequence was tagged with an HA tag in *TEX19*-HA overexpressing HCT116 cells. These cells were employed in this experiment to determine the specificity of the anti-TEX19 antibody (R&D system; # AF6319) (Figure 6.3). Additionally, the HCT116 cell line was used because it expresses wildtype *TEX19* and western blot using the anti-HA antibody will assess the specificity of the anti-HA antibody too (anti-HA tag monoclonal antibody purchased from cell signalling; #2367). Importantly, the predicted size of human TEX19 is 18.5 kDa, however, in this experiment and downstream western blot analyses, this band migrates at about ~23 kDa (Figure 6.3). It is not known why this species migrates at an apparent higher

molecular weight, however, post-translational modifications (PTMs) of TEX19 might be suggested.

In *TEX19-HA* overexpressing HCT116 cells, three bands were detected when the lysates were blotted against the anti-TEX19 antibody. The highest band (at 25 kDa) had very strong signals in untreated and negative siRNA treated cells; however, the signal intensity was reduced in siRNA-#7-treated cells, indicating that this TEX19 protein originated from the transfected *TEX19-HA* that was overexpressed in untreated and negative control cells. The middle band is detectable at ~23 kDa with a significant reduction of protein levels, following siRNA #7 treatment, suggesting that this band is related to the endogenous TEX19 protein in these cells. Additionally, the lowest molecular weight band (at 21 kDa) with steady levels might be degradation products or non-specific bands. When these lysates were blotted against anti-HA tag antibodies, the western blot showed only one single band at ~25 kDa, which may be related to TEX19-HA (Figure 6.3).

In the HCT116 cell line, double bands emerged when the lysates were blotted against the anti-TEX19 antibody. The higher molecular weight band was detected at ~23 kDa and showed a reduction in TEX19 protein signal in anti-TEX19 siRNA-#7-treated cells, suggesting this band is specific to the TEX19 protein. The lower molecular weight signal showed a higher intensity signal in TEX19-depleted cells, suggesting that these are degradation products from the TEX19 protein. On the other hand, when these lysates were blotted against an anti-HA tag antibody, no signal was detected. These results confirm the specificity of both a polyclonal anti-TEX19 antibody and a monoclonal anti-HA antibody. Moreover, both antibodies confirmed that TEX19 is detectable at ~ 23 kDa, which is higher than the predicted size of human TEX19 at 18.5 kDa. Thus, it is suggested that TEX19 is post-translationally modified.
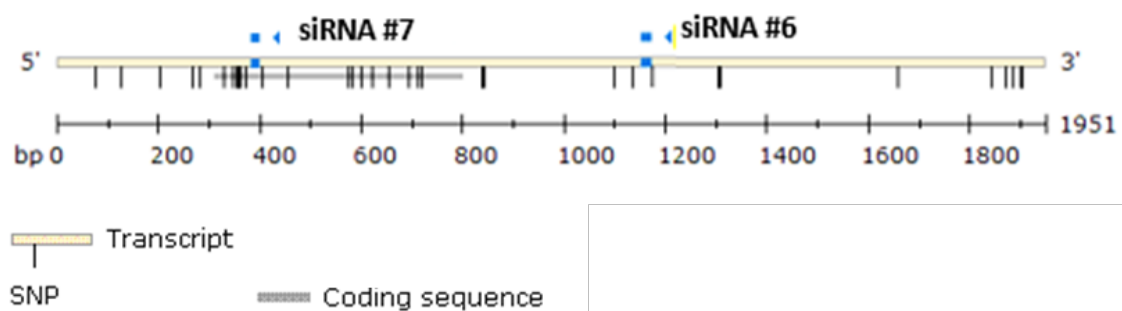
Figure 6. 1. Schematic representation of *TEX19* gene. *TEX19* (NCBI accession number NM_207459, bp 1951) demonstrating the coding region and siRNA target sites. The coding region of *TEX19* is represented with a grey line and is targeted by the siRNA #7 molecule, while siRNA #6 targets *TEX19* mRNAs in the 3′ untranslated region sequence. This figure is adapted from Qiagen. SNP refers to single nucleotide polymorphism.

A) *TEX19-HA* **overexpressing HCT116**
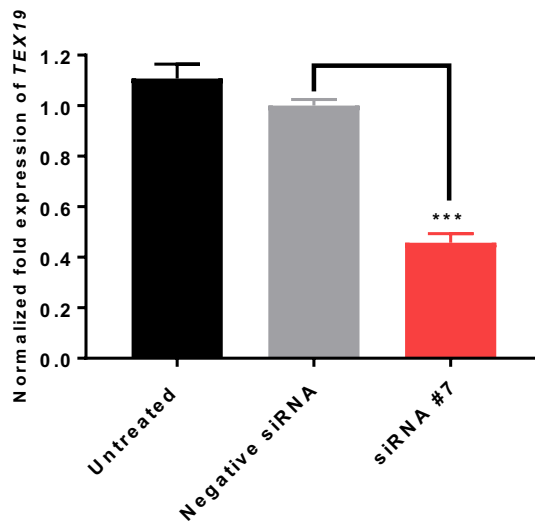
B) HCT116 cell lines
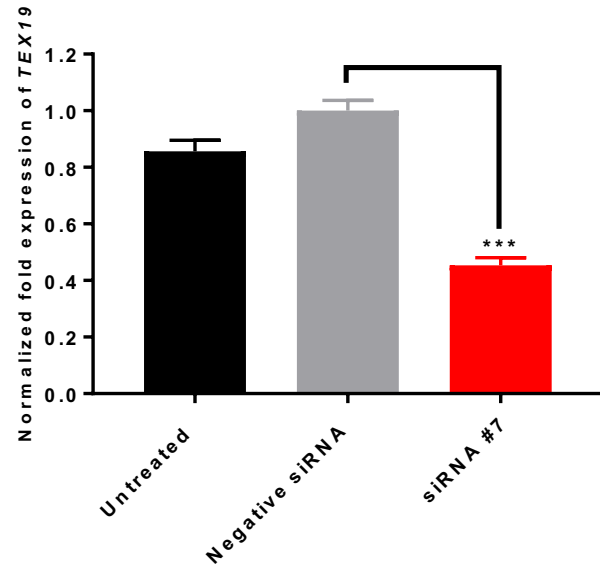
Figure 6. 2. qRT-PCR Analysis of *TEX19* mRNA levels following siRNA #7 transfection (A) *TEX19- HA* **overexpressing HCT116 cells and (B) HCT116 cell lines.** The bar charts show the levels of mRNA transcripts of the *TEX19* gene. Levels were normalised with two reference genes: *GAPDH* and *ACTβ*. The fold change was computed using the ΔΔCt method. Error bars refer to the standard errors of the mean and are obtained from three technical repeats. *P* values were calculated to show significant changes compared to the negative control as (*** *P* < 0.001).
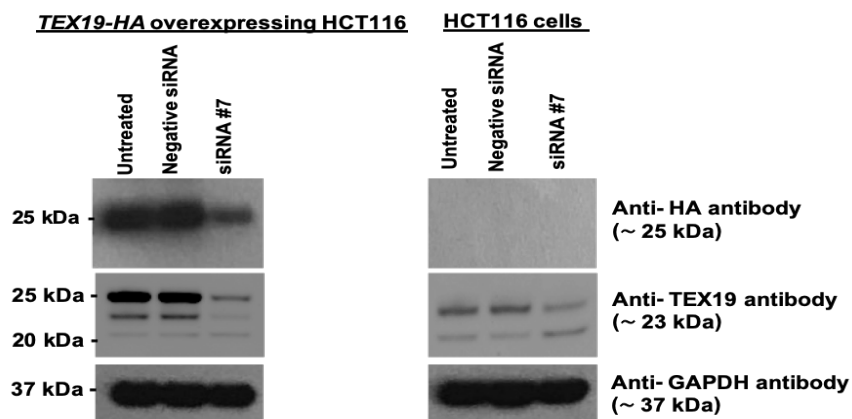
Figure 6. 3. Western blot analysis showing the levels of TEX19 protein after siRNA #7 treatment in HCT116 and *TEX19-HA* overexpressing HCT116 cells. Extracts from untreated, negative siRNA and siRNA #7 cultures were blotted using anti-HA antibody and anti-TEX19 antibody. Anti-GAPDH antibody was used as a loading control. Left figure shows *TEX19-HA* overexpressing HCT116 (transfected with *TEX19-HA* overexpressing plasmid); right Figure shows HCT116 cell lines.

6.2.2. Depletion of TEX19 in colorectal cancer cell lines

Previously, Planells-Palop et al. (2017) demonstrated TEX19 is required to maintain cancer cell proliferation. This work aimed to confirm the biological effects of TEX19 knockdown in colorectal carcinoma cell lines using two siRNAs (#6 and #7) purchased from Qiagen and further investigations were carried out on a *TEX19-HA* overexpressing HCT116 cell line. Figure 6.1 shows that both siRNA molecules target the TEX19 sequence in exon 2, however, the siRNA #7 molecule is complementary to the protein coding sequence, and siRNA #6 in the 3′ UTR. Two cell lines were employed in this study, *TEX19-HA* overexpressing HCT116 and SW480 colorectal carcinoma cell lines, the latter not expressing *TEX19-HA.*

6.2.2.1 TEX19 knockdown in *TEX19-HA* overexpressing HCT116 cell lines

TEX19-HA overexpressing HCT116 cells were cultured and transfected for 72 hours with two siRNAs (#6 and #7), along with negative siRNA as a transfection control. Total mRNA and protein were extracted from each independent culture to evaluate the efficiency of the knockdown. Figures 6.4 A and B illustrated the analyses of qRT-PCR and western blot after TEX19 knockdown in *TEX19-HA* overexpressing HCT116 cell lines. Cultures transfected with siRNAs #6 and #7 showed significant reductions in mRNA levels (P < 0.0001) of *TEX19* compared to the negative siRNA culture, as shown in figure 6.4 A. The efficiency of knockdown of *TEX19* levels were calculated in each culture in comparison to negative control culture levels as; siRNA #6 was 83%, siRNA #7 was 89%.

At the protein level, three detectable bands were emerged as previously observed, as shown in Figure 6.4 B. The highest molecular weight band at ~25 kDa exhibited only a very slight reduction of signal intensity in siRNA #6 and siRNA #7- treated cells compared to negative siRNA cultures. The second band at ~23 kDa shows a clear reduction of protein levels in siRNA #6 treated cells, and non-detectable signal in siRNA #7 treated cells compared to negative control cultures. The reduction of TEX19 levels in siRNA #6 treated cells might because of that this molecule did not directly target protein coding region. This band is suggested to be specific to endogenous TEX19 protein in TEX19-HA overexpressing HCT116 cells. The lowest molecular weight band is detectable at ~21 kDa with increased signal intensities in TEX19-depleted cultures, suggesting that these are degradation products of TEX19 protein.

A)
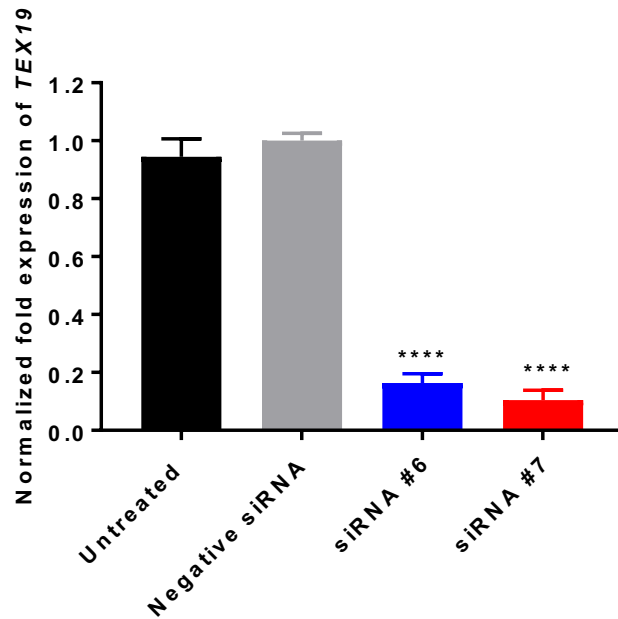
B)
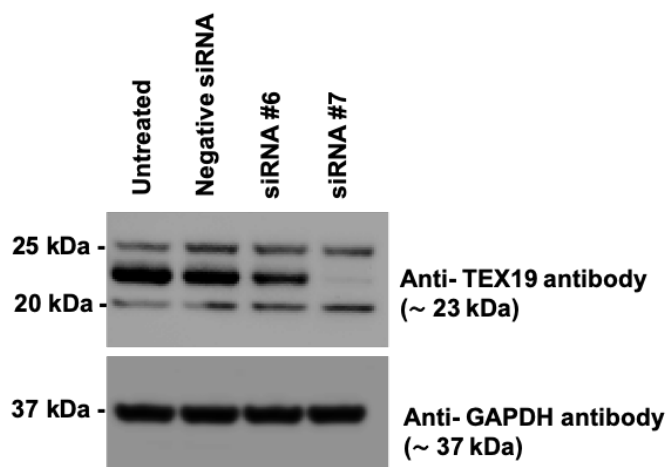
Figure 6. 4. Analysis of the depletion of TEX19 in *TEX19-HA* overexpressing HCT116 cells using two siRNAs, #6 and #7. After 72 hrs of siRNA transfection, total RNA and protein were extracted. A) The bar charts show the levels of mRNA transcripts of the *TEX19* gene using qRT-PCR analysis. Levels were normalised with two reference genes: *GAPDH* and *ACTβ*. The fold change was computed using the ΔΔCt method. Error bars refer to the standard errors of the mean and are statistically obtained from three technical repeats. P values were calculated to show significant changes compared to the negative siRNA control as (**** *P* < 0.0001). B) The western blot shows reduced TEX19 proteins in siRNA-#7/#6 treated culture. Anti-GAPDH was used as a loading control.

6.2.2.2 TEX19 knockdown in SW480 cell lines

The depletion of TEX19 was also investigated in a colorectal cancer cell line, SW480, using two siRNAs, #6 and #7, along with negative siRNA as a control. Each fraction of cell cultures was transfected with a subsequent siRNA for 72 hours, then total mRNAs and protein were extracted. The knockdown efficiency was evaluated at mRNA transcript and protein levels as shown in Figure 6.5.

Figure 6.5 A demonstrates the qRT-PCR analysis of *TEX19* mRNAs in SW480 cell lines after the depletion of *TEX19* mRNA. The results show significantly reduced *TEX19* mRNA levels in positive siRNAs-treated cells compared to negative control (P < 0.001) with 81% in level reductions in both positive treated cultures.

Figure 6.5 B shows the western blot analysis of the TEX19 protein in *TEX19* mRNA depleted SW480 cell lines. The results show that dual bands had emerged—one with a size of 23 kDa. This band was clearly eradicated after the treatment of both siRNAs #6 and #7. This may indicate that this band is specific to the TEX19 protein. Although this band was retained in *TEX19-HA* overexpressing HCT116 cells in cultures transfected with siRNA #6, but not SW480 cells transfected with siRNA #6, the disappearance of this signal in SW480 cells could be explained by the fact that the eradication of all produced *TEX19* mRNAs was achieved, and that depends on the ratio of transfected siRNA concentration to the number of cultured cells or mRNA molecules. Moreover, the discrepancy of the intensity of this band between cell lines may depend on the cell line phenotypes. The lower molecular weight band is detectable below the TEX19 band, which is possibly produced as a degradation product.
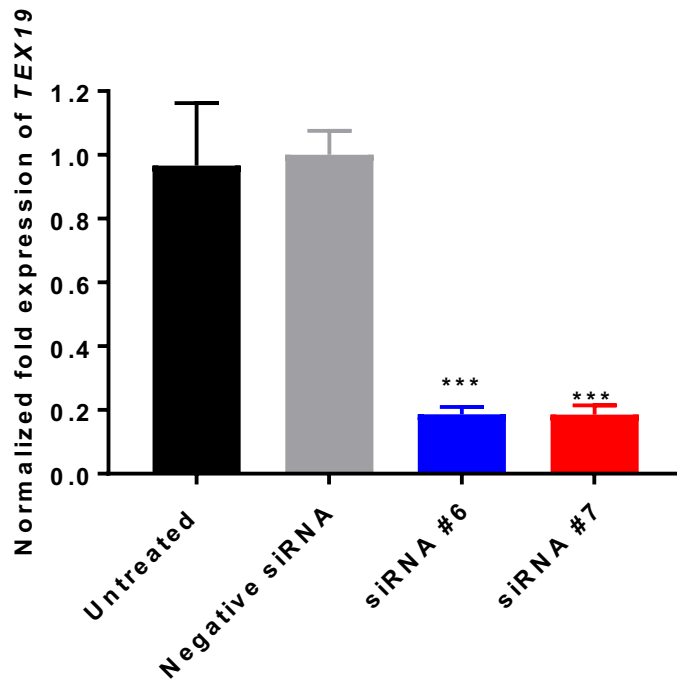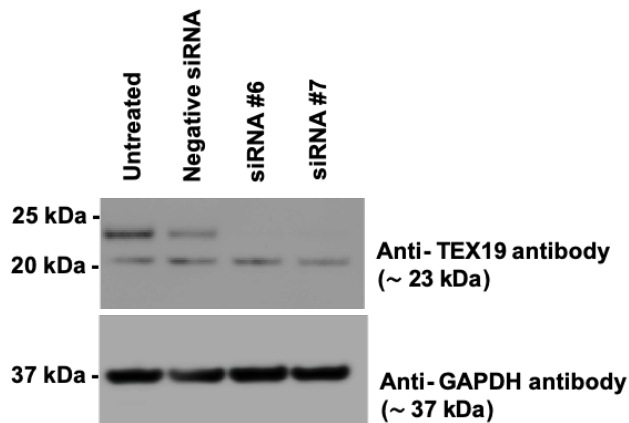
Figure 6. 5. Analysis for depletion of TEX19 in SW480 colorectal carcinoma cells using two siRNAs, #6 and #7. After 72 hours of siRNA transfection, total RNA and protein were extracted. A) The bar charts show the levels of mRNA transcripts of the *TEX19* gene using qRT-PCR analysis. Levels were normalised with two reference genes: *GAPDH* and *ACTβ*. The fold change was computed using the ΔΔCt method. Error bars refer to the standard errors of the mean and are statistically obtained from three technical repeats. P values were calculated to show significant changes compared to the negative control as (*** $P < 0.001$). B) The western blot shows a reduced TEX19 protein in both siRNA #6- and #7-treated cultures. Anti-GAPDH was used as a loading control.

6.2.3 TEX19 depletion influences the cancer cell proliferation

The successful knockdown of TEX19 in cancer cell lines was extended further to assess its effects on cellular proliferation. Two cell lines were selected in this experiment: *TEX19-HA* overexpressing HCT116 and SW480 cell lines. The cell proliferation curves were established for seven days of transfections of siRNA #6 and siRNA #7, along with negative siRNA and untreated cells as a negative control.

In *TEX19-HA* overexpressing HCT116 cells, the cultures transfected with siRNA #7 demonstrated a significant decrease ($P < 0.0001$) in cell counts from day 3 compared to untreated and/or negative siRNA transfected cultures. However, anti-*TEX19* siRNA #6 transfected cultures showed a lesser, but significant reduction in cell counts from day 4, as shown in Figure 6.6. The cell count in siRNA-#6-treated cultures was clearly higher than in siRNA-#7-treated cultures with larger variation in each repetition. This can be explained by the fact that the siRNA #6 molecule is not the protein coding sequence target; in addition, these cells have an additional *TEX19-HA* overexpressing plasmid integrated into the genome. Thus, the siRNA #6 molecule may require a long transfection time to ultimately affect cell proliferation. Figures 6.7 shows the analysis of *TEX19* mRNA depletion from select days during this experiment that were applied using qRT-PCR.

Similarly, *TEX19*-depleted SW480 cells using siRNA #6 and #7 resulted in significant proliferation inhibitions ($P < 0.001$) from days 4 and 5, respectively, in comparison to negative control cultures (Figure 6.8). Furthermore, the efficiency of *TEX19* mRNA depletions were confirmed from different selected days using qRT-PCR analysis (Figure 6.9).

TEX19-HA overexpressing HCT116 cells
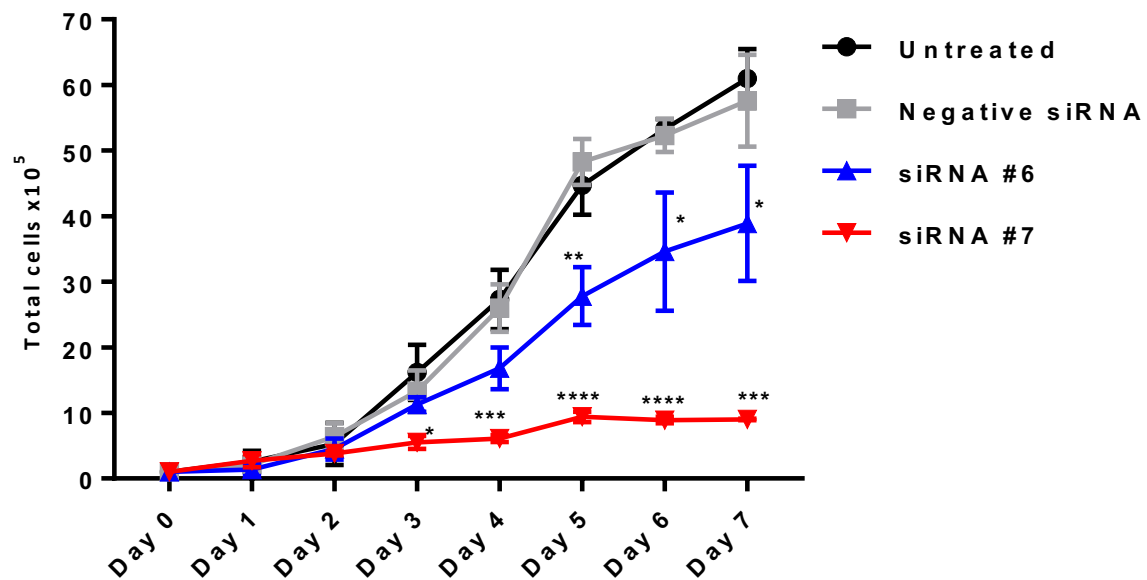
Figure 6. 6. _TEX19-HA_ overexpressing HCT116 cell growth curve after _TEX19_ knockdown. The cell growth curve was established for different independent cultures of _TEX19-HA_ overexpressing HCT116 cells. An untreated culture was used as a negative control culture, while negative siRNA culture was used as a negative control for treatment. Both siRNA #6- and #7-treated cultures showed significant proliferation inhibitions, from three biological repeats and stars refer to P values. P values: (* P < 0.05, ** P <0.01, *** P < 0.001 and **** P < 0.0001).

A) Day 1
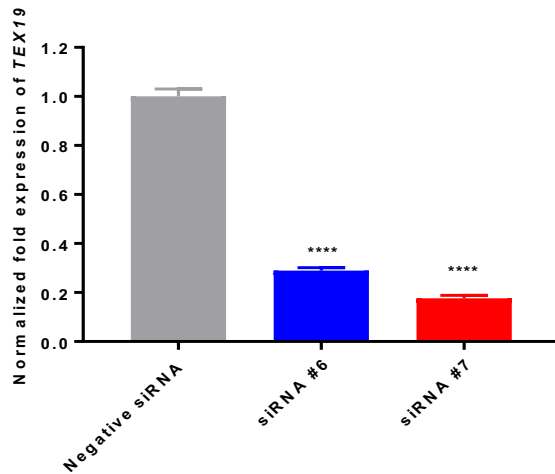
B) Day 3
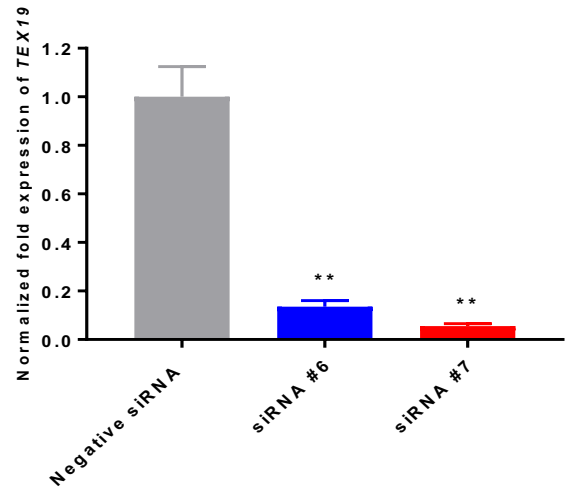
C) Day 5
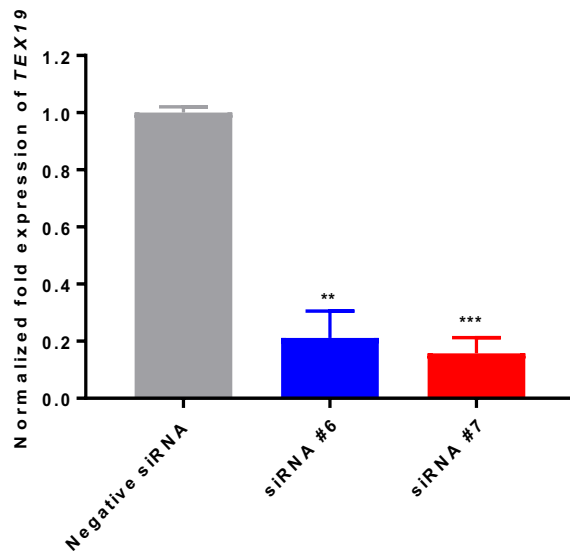
D) Day 7
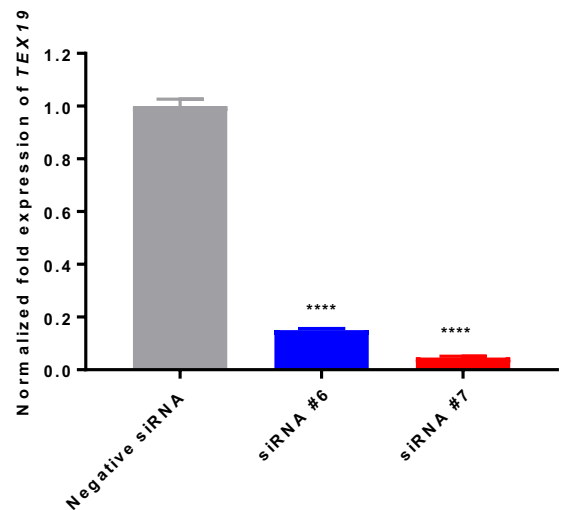
Figure 6. 7. qRT-PCR analysis for TEX19 mRNAs in *TEX19-HA* overexpressing HCT116 cell during cell growth curve experiment. The efficiency of *TEX19* mRNA depletion was evaluated using qRT-PCR analysis for the chosen days during the previous experiment. The levels of *TEX19* mRNA were normalised to two endogenous genes *ACTB* and *GAPDH*. Error bars represent the standard errors to the mean of three technical replicates. The results showed significant reductions of *TEX19* mRNA levels in siRNA #6 and #7- treated cultures compared to a negative siRNA culture as a negative control. Total RNAs were extracted from independent cultures and analyses were conducted separately as shown A) day 1, B) day 3, C) day 5 and D) day 7. P values: (* P < 0.05, ** P <0.01, *** P < 0.001 and **** P < 0.0001).

SW480 cells
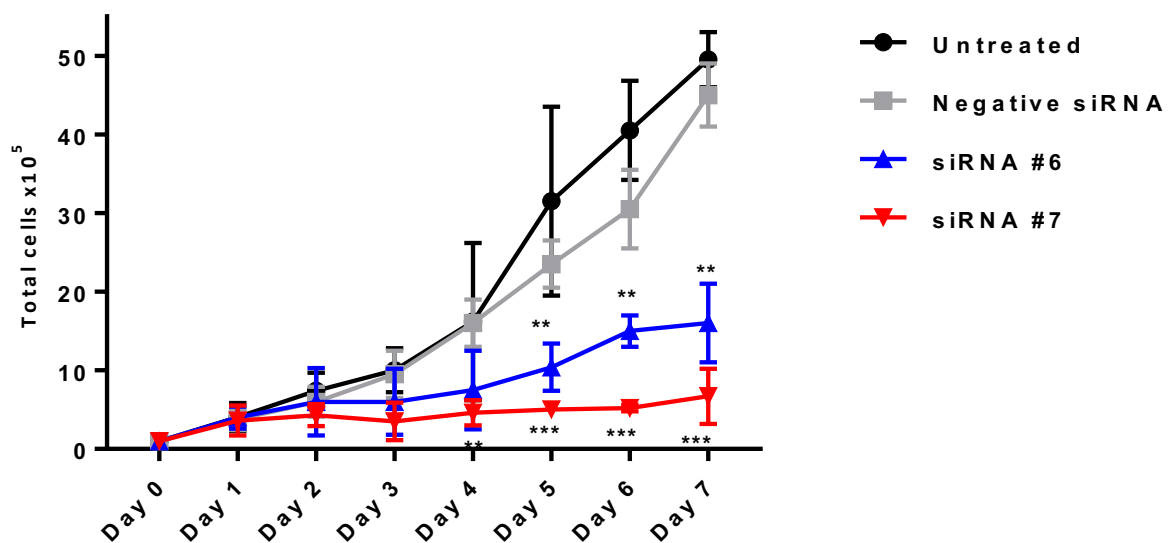
Figure 6. 8. *SW480* **cell growth curve after** *TEX19* **knockdown.** A cell growth curve was established for different independent cultures of SW480 cell lines. An untreated culture was used as a negative control culture while negative siRNA culture was used as a negative control for treatment. Both siRNA #6- and #7-treated cultures showed significant proliferation inhibitions, and stars refer to P values: (* $P < 0.05$, ** $P < 0.01$, *** $P < 0.001$ and **** $P < 0.0001$). The error bars refer to the standard deviation for the mean of three biological replicates.
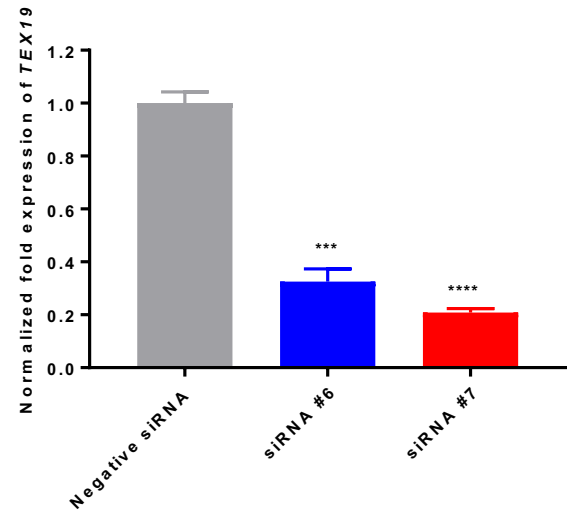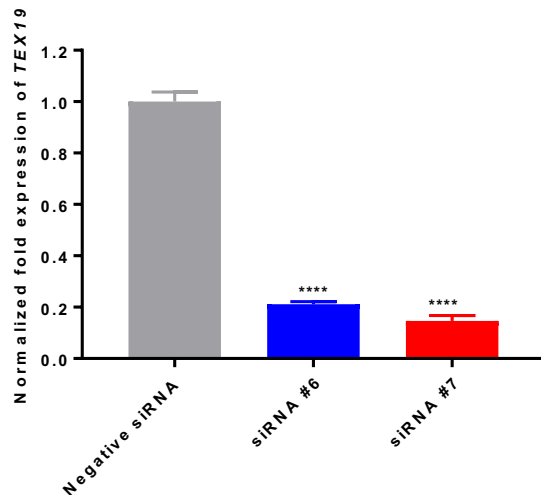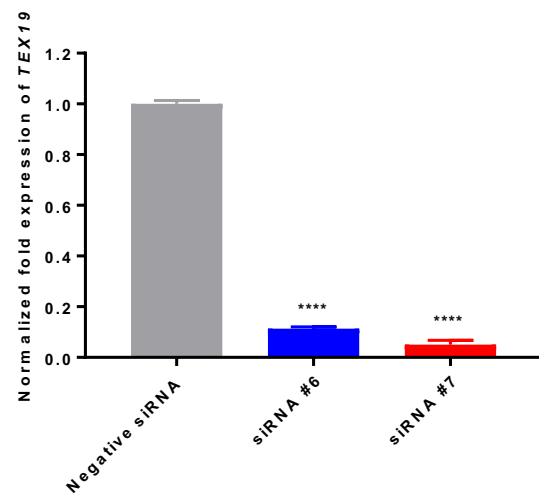
Figure 6. 9. qRT-PCR analysis for TEX19 mRNAs in SW480 cells during cell growth curve experiment. The efficiency of *TEX19* mRNA depletion was evaluated using qRT-PCR analysis for the chosen days during the previous experiment. The levels of *TEX19* mRNA were normalised to two endogenous genes *ACTB* and *GAPDH*. Error bars represent the standard errors to the mean of three technical replicates. The results showed significant reductions of *TEX19* mRNA levels in siRNA #6 and #7- treated cultures compared to a negative siRNA culture as a negative control. Total RNAs were extracted from independent cultures and analyses were conducted separately as shown A) day 1, B) day 3, C) day 5 and D) day 7. P values: (* P < 0.05, ** P <0.01, *** P < 0.001 and **** P < 0.0001).

6.2.4 The correlation between TEX19 depletion and Histone acetylation within cancer cells

A previous study that suggested that role of TEX19 in promoting cancer cell proliferation might be associated with its transcriptional regulatory of specific genes important for cell cycle and cellular proliferation (Planells-Palop et al., 2017). Histone modifications play regulatory roles in altering transcriptional activities (Tessarz & et al., 2014) and the most frequent histone modification that is linked with "active" chromatin is histone acetylation (Dawson et al., 2012). Additionally, a preliminary study from a co-worker (L. Alqahtani), demonstrated that TEX19 might regulate histone H3K9 acetylation, as H3K9 acetylation was reduced in TEX19-depleted cancer cells. This required verification and assessment in the *TEX19-HA* overexpressing HCT116 cell line.

The *TEX19-HA* overexpressing HCT116 cells and SW480 cell lines were independently transfected with two siRNAs (#6 and #7), along with a negative control (negative siRNA), and the total histone was extracted from each independent culture. Western blot analysis was conducted to assess the acetylated H3 at lysine 9 using a specific antibody, anti-H3K9-Ac, from Abcam (ab12179). Anti-Histone H3 antibody (Abcam, #ab10799) was used as a loading control by assessing total histone H3 levels.

Figure 6.10 demonstrates that the histone H3 acetylation at K9 was slightly reduced following the TEX19 depletion in *TEX19-HA* overexpressing HCT116 cells treated with anti-TEX19 siRNA #7 only (Figure 6.10 A). SW480 cells that were treated with anti-TEX19 siRNA #7 showed a clear reduction of histone acetylation (H3K9) compared to negative siRNA treated cultures (Figure 6.10 B).

For further confirmation, histone extractions were previously carried out on fractions from the cultured cells (*TEX19-HA* overexpressing HCT116 cells and HCT116 cells) in Section 6.2.1. We blotted these lysates using the anti-H3K9-Ac antibody to assess the levels of H3 acetylation at K9, and the results are shown in Figure 6.11. These cells were transfected with siRNA #7, along with negative siRNA. In both cells, the levels of acetylated H3 were reduced after the depletion of TEX19 using siRNA #7

molecule. These findings suggest that TEX19 may play a key role in histone acetylation in cancerous cells.

A) *TEX19-HA* overexpressing HCT116 cells

B) SW480 cell lines
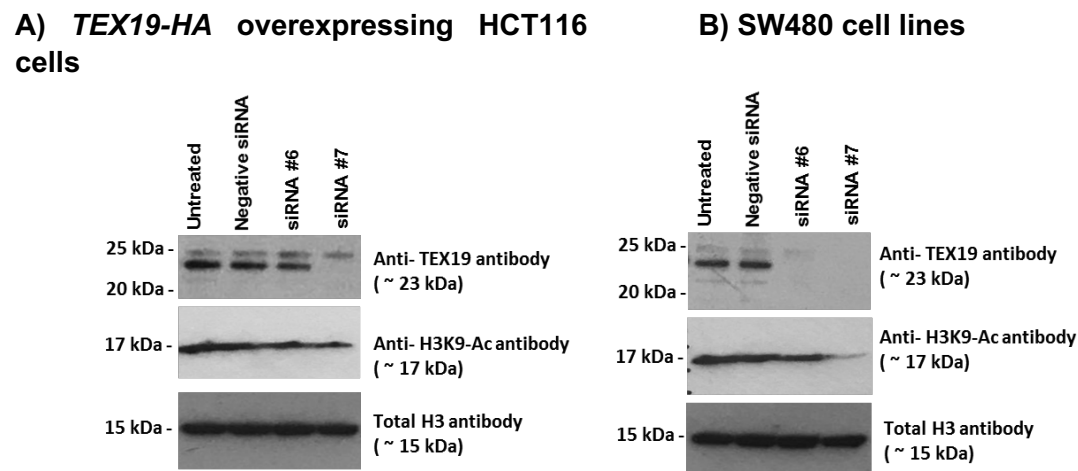
Figure 6. 10. Analysis of H3K9-Ac in cancer cells after TEX19 depletion using siRNA #6 and #7. The total histone was extracted from cells after 72 hours of siRNA transfections. A) Histone extraction from *TEX19-HA* overexpressing HCT116 cells were analysed to confirm TEX19 protein depletion and the levels of acetylated H3 at K9 using the anti-H3K9-Ac antibody. Total H3 antibody was used as loading control. B) Histone extractions from SW480 cells after TEX19 depletion. The H3K9-Ac antibody shows a reduced acetylated H3 in siRNA-#7-treated SW480 cells.

A) *TEX19-HA* overexpressing HCT116 cells

B) HCT116 cell lines
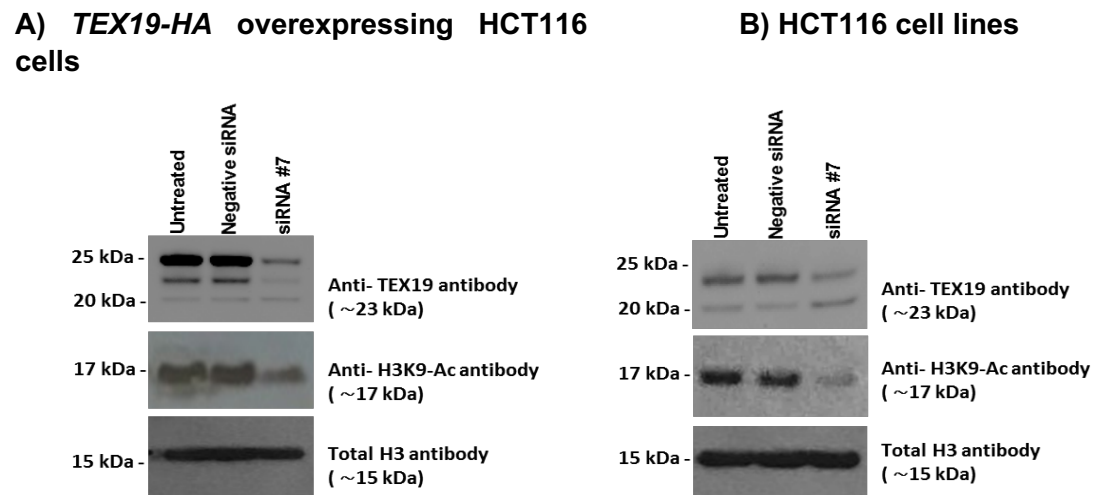
Figure 6. 11. Analysis of acetylated H3K9-Ac in cancer cells after TEX19 depletion using siRNA #7. Total histone was extracted from cells after 72 hours of siRNA transfections. A) Histone extraction from *TEX19-HA* overexpressing HCT116 cells were analysed to confirm TEX19 protein depletion and the levels of acetylated H3 at K9 using anti-H3K9-Ac antibody. Total H3 antibody was used as loading control. B) Histone extractions from HCT116 cells after TEX19 depletion. H3K9-Ac antibody shows a reduced acetylated H3 in siRNA-#7-treated SW480 cells.

6.3. Discussion

Self-renewal potential is one of the main features that characterises cancer cells and stem cells. It has been proposed that cancer cells may undergo a soma-to-germline transition or initiate programmes that orchestrate the germ-like state (McFarlane et al., 2014; Feichtinger et al., 2014; McFarlane et al., 2015). The hallmarks of cancers, such as metastasis, invasiveness and uncontrolled proliferative potentials are common biological features in cancer cells and germ cells (Hanahan & Weinberg, 2011; Fratta et al., 2011; Maine et al., 2016). This has led to the suggestion that the reactivation of germline genes in cancer cells contributes to these activities (e.g., ectopic expression of germline genes). SPANX-A/B/C are associated with development and poor clinical prognosis in breast cancers (Maine et al., 2016). Moreover, aggressive and metastatic features of lung cancer have been linked to the re-activation of many germline genes that can be used in approaches that are beneficial to diagnoses and therapies (Rousseaux et al., 2013). Other germline genes that are known to regulate meiosis have been reported to drive oncogenesis (Cho et al., 2014). Thus, it is become clear that germline genes are required for cancer initiation, progression and maintenance.

Human *TEX19* expression has been found in a wide range of cancer cells but is restricted to germ cells in the placenta and adult male testes from normal tissues (Feichtinger et al., 2012). This expression profile has led to the suggestion that TEX19 may drive oncogenesis and is required to maintain the proliferation and development of cancerous cells (Planells-Palop et al., 2017). In mice, loss of *Tex19.1*, which is an orthologue of human *TEX19*, has resulted in spermatogonia cells entering apoptosis (Tarabay et al., 2013). In another study, human cancer cells that were depleted of TEX19 showed an accumulation of cells in the S-phase (Planells-Palop et al., 2017). Our findings here demonstrated that TEX19 depletion is significantly linked with proliferation inhibition in cancer cells. Colorectal carcinoma SW480 cells showed slow or stopped proliferation after treatment of two anit-*TEX19* siRNAs, which is consistent with the results of western blot analysis that showed significant depletions of protein signals. Although *TEX19-HA* overexpressed HCT116 produces excessive TEX19 protein, the proliferation was significantly reduced in positive siRNA treated cultures. These results appear to confirm that TEX19 plays an important role in cancer cell proliferations.

In epigenetics, one of the most frequent post-translational modification is acetylation. The extent of acetylation is controlled by the dynamic balance between acetylation by histone acetyltransferases (HATs) and deacetylation by histone deacetylases (HDACs). Importantly, acetylation can occur in non-histone proteins, as was first report when researchers were investigating high mobility group proteins and acetylation on transcription factor and tumour suppressor p53 (Sterner et al., 1979; Gu & Roeder, 1997). Acetylated non-histone proteins act as silencers or activators of entities related to transcription (Dekker & Haisma, 2009). The mechanism of acetylation in transcriptional factors is based on the fact that acetylation induces protein-DNA binding affinity, resulting in the facilitation of gene transcription. On the other hand, deacetylation plays a role in reducing ubiquitination, thereby influencing the level and stability of protein (Caron et al., 2005). The most (de)acetylation in the transcriptional factors occurs in lysine and is catalysed by HATs or HDACs. Narita et al. briefly described different mechanisms and roles of acetylation in non-histone proteins (Narita et al., 2018). For example, acetylation acts as a regulator of gene transcription, and acetylated proteins are located in the nucleus, where they influence the process of transcription either directly or indirectly through nuclear receptors, co-activators and transcription factors. An example of non-histone proteins is SMC3, and its acetylation plays regulatory roles in sister chromated cohesin and non-cohesion function (Kawasumi et al., 2017). Cohesion function is important for the cell cycle, DNA damage repair, gene transcription and sister chromatid stabilization in the S phase of the replication process (Ben-Shahar et al., 2008; Ünal et al., 2008; Zhang et al., 2008; Deardorff et al., 2012). Interestingly, it has been reported that TEX19 regulates acetylated SMC3, which mediates sister chromatid cohesion (Reichmann et al., 2017). Furthermore, from the identified possible rules of TEX19, for example, transcriptional regulation (Planells-Palop et al., 2017), meiotic chromosome synapsis regulation (Yang et al., 2010), meiosis and sister chromatid cohesion (Reichmann et al., 2017), it is possible to speculate that these roles could be achieved through the involvement of TEX19 in histone modification, or histone chaperoning.

In support of this view, TEX19 has key features of a histone chaperone. Firstly, it is predicted to be highly acidic. Secondly, it is intrinsically disordered. This hypothesis remaining untested.

Distinct post-translation modifications (PTMs) are epigenetic mechanisms that could occur at histone tails and subsequently remodel chromatin structure resulting in altered transcriptional states (active or inactive) (Tessarz et al., 2014). Acetylation is one of the PTMs that takes place at H3 and H4 and has been found to associate with active chromatin marks (Dawson et al., 2012). Here, we extended a preliminary observation from the McFarlane group and found that total histone H3K9 acetylation was reduced following TEX19 protein depletion in cancerous cells. These findings suggest that the overexpression of *TEX19* is correlated with H3K9 acetylation and is associated with active chromatin. Given that TEX19 appears to be involved in histone acetylation, this contribution is possibly responsible for potential of TEX19 to act as a transcriptional regulator and promote proliferation in cancer cells. To date, this experiment has been limited due to time constraints, and extended analyses (such as; acetylation markers and other histone modifications) are required.

6.4. Concluding remarks

The work in this chapter focused on the functional analysis of TEX19 on cancer cell proliferation and its involvement in histone acetylation. This study has demonstrated that the polyclonal anti-TEX19 antibody (R&D system; # AF6319) is specific for TEX19 protein. Although the predicted size of human TEX19 is 18.5 kDa, this protein was detected at ~ 23 kDa during this study. The reason for the increased molecular weight is not known, however, it can be hypothesised by that a post-translation modification might occur following TEX19 production in cancerous cells. Depletion of TEX19 results in a clear inhibition of cancer cell proliferation, suggesting that the aberrant expression might be required for cancer progression and proliferation. Moreover, extended analyses found that TEX19-depleted cancer cells showed reduced levels of acetylated H3K9. These findings suggest that TEX19 is possibly involved in histone acetylation. Give that TEX19 acts as a transcriptional regulator protein (Planells-Palop et al., 2017), in addition to proliferative potentials of TEX19 in cancer cells, it could be proposed that these potentials of TEX19 might be consequences of its contribution to histone acetylation.

Chapter 7

Final discussion and summary

7. Final discussion and further studies

7.1 Summary of findings

There is apparent similarities and common features between the gametogenesis process in both sexes and tumorigenesis. Such features include that cancers are characterised by the expression or re-activation of genes that are specific for meiotic cells in gametogenic tissues. It has been proposed that this aberrant expression of specific-meiosis genes in tumours indicates that cancer cells might undergo soma-to-germline transition (Whitehurst, 2014; McFarlane et al., 2014; 2015; Gjerstorff et al., 2015) or attempt a meiotic entry, which is a programmed germ line event. These suggestions were supported by the findings that identified aberrant reactivation of meiotic genes in a wide range of cancer types and some of these genes were found to act as oncogenic drivers (see McFarlane & Wakeman, 2017; Feichtinger & McFarlane, 2019). Moreover, many studies on several cancer types reported that the ectopic reactivation of meiosis-specific genes and other germline gens plays important roles during oncogenesis, such as the initiation and maintenance of cancerous state (Simpson et al., 2005; Fratta et al., 2011; Rousseaux et al., 2013; Lafta et al., 2014; McFarlane et al., 2014; 2015; Whitehurst, 2014; Nielsen & Gjerstorff, 2016). Because of this, studying the molecular roles of meiosis-specific genes in cancer development is attractive in the fields of cancer prognosis, diagnosis and treatment (Simpson et al., 2005; Feichtinger et al., 2012; Whitehurst, 2014).

Meiotic specific genes that are abnormally reactivated in several cancer types are a subclass of cancer testis genes (CT). CT genes are those genes whose expression is normally restricted to adult male testis but aberrantly expressed in cancers (Simpson et al., 2005; Whitehurst, 2014; Gibbs & Whitehurst, 2018). Examples of meiosis-specific genes that were defined as CT genes include, the meiotic DSB initiator, *SPO11*, and the histone methyltransferase activator of meiotic recombination hotspots, *PRDM9* (Koslowski et al., 2002; Feichtinger et al., 2012). Thus far, there have been no clear indications regarding the oncogenic function(s) of human SPO11; however, important seminal work in *Drosophila melanogaster* provides remarkable insights into its possible oncogenic functions (Janic et al., 2010; Rossi et al., 2017). The formation of *D. melanogaster* brain tumour can be initiated in presence of temperature-sensitive alleles of the *l(3) mbt* gene resulting in the activation of a large

number of germline genes. Moreover, transcriptional profiling of l(3) mbt tumours has suggested that most of these activated genes are required for tumour development (Janic et al., 2010). Interestingly, Feichtinger and co-worker reported that many human cancers showed expression of a similar gene profiling (Feichtinger et al., 2014). The *D. melanogaster* orthologues of human *SPO11* (called *mei-W68*) and *TOPOVIBL* (called *mei-P22*) are the two fly genes that are essential for the formation of l(3)mbt tumours (Rossi et al., 2017). Extended research showed that ionizing irradiation could result in some suppression of the oncogenic ability of the *D. melanogaster SPO11* (*Mei-W68*) mutant, to form tumour and this suggests that there is a relationship between the DSB mediating function of Mei-W68 and oncogenesis (Rossi et al., 2017). How DSBs could be driving oncogenesis is unclear, but it might be the case that they drive general oncogenic genome instability. This said, another non-DSB associated function for *Mei-W68* cannot be ruled out.

Human *PRDM9* is a meiosis-specific gene with methyltransferase activities, which has been reported to be re-expressed in a wide range of cancer types (Feichtinger et al., 2014). Meisetz, which is the murine orthologue of PRDM9, has been defined as a meiotic recombination activator that also regulates transcriptional activities for other meiosis specific genes (Hayashi et al., 2005). Overexpression of transfected PRDM9 in HEK293T cells has led to upregulation of many human genes showing that the transcriptional landscape of human cells can be altered as a result of a single meiosis-specific epigenetic regulator expression (Altemose et al., 2017). Given that, this raises possibilities that one meiotic regulatory gene has potentials to deregulate transcriptional landscape in cancer cells.

PRDM9 contributes to activation of meiotic recombination hotspot sites (Baudat et al., 2010; Myers et al., 2010; Parvanov et al., 2010). However, recent studies reported that meiotic recombination hotspot sequences are significantly linked to genomic stability (Houle et al., 2018; Kaiser & Semple, 2018). Zinc fingers of PRDM9 protein facilitate its binding to specific sequences within the genome (Grey et al., 2018; Paigen & Petkov, 2018). By analysing PRDM9 binding sites in human cancers, it can be suggested that there is a relationship between these sites and the sites of genome rearrangements in cancers (Houle et al., 2018; Kaiser & Semple, 2018). Given that, it can be also proposed that they generate a site for chromosomal instabilities in the form of a SPO11-TOPOVIBL mediated break; however, for this to occur, several meiosis-specific factors (such as SPO11 and PRDM9) have to collaboratively work

towards generating a break. Nonetheless, another more reasonable explanation, is that PRDM9 binds to chromatin regions resulting in changing chromatin state with other factors, this leads to random blocking of DNA replication, which could be responsible for the initiation of genome instability and cancer development (Blumenfeld et al., 2017; Zhang et al., 2019). An alternative is that epigenetic mechanisms normally controlling proper gene expression in the cell becomes oncogenically altered by PRDM9 (Nottke et al., 2009; Meikar et al., 2013). According to this, the activation of master germline genes (specifically those behind the direct regulation of genome demethylation) could cause a gametogenic process to activate at the time of tumourigenesis. Thus, cancer in somatic tissues might be initiated as a result of activation of silenced CT genes (Old et al., 2001; Simpson et al., 2005).

It has been suggested that methyltransferase activities of PRDM9 allow this protein to act not only as hotspot activator, but also as a transcriptional regulator for many meiosis proteins. This is supported by the evidence that the expression of the testis-specific *RIK* gene (namely, Morc2b) was directly regulated by *Prdm9* in mice (Hayashi et al., 2005). In this current study, the overexpression of transfected *PRDM9* into HeLa Tet-On cell lines has led to a slight upregulation of two genes from *MORC* family (*MORC3* and *MORC4*). Moreover, this study demonstrated that human *PRDM9* may act as a transcriptional regulator for many genes; such as, meiosis-specific genes (*HORMAD1* and *SYCE2*), PRDM family genes (*PRDM7* and *PRDM11*), and CT genes (*MAGEA1* and *GAGE*). Thus, we suggested that *PRDM9* might act as a transcriptional regulator for other human genes in cancer cells. Moreover, our study demonstrated the presence of PRDM9 in many cancer cell lines such as; MCF7, NTERA2, and K562, suggesting its functional roles in cancer cells. This thesis also found that the depletion of *PRDM9* transcripts maight reduce the proliferative potentials of cancerous cells, which proposes that *PRDM9* is required for carcinogenesis maintenance.

PRDM9 consists of a PR/SET domain, which is comprising of histone methyltransferase activity, in addition to the multiple zinc finger arrays and the KRAB (Kruppel-association box) protein-protein binding domain (Fumasoni et al., 2007; Baudat et al., 2013). It has been identified that the PR/SET domain of mouse Prdm9 catalyses H3K4 trimethylation, which has a significant influence on transcriptional activity landscape (Hayashi et al., 2005). Furthermore, Eram and co-workers have also characterised the ability of human PRDM9 to trimethylate H3K4 and H3K36 in transfected HEK293 cells (Eram et al., 2014). However, in this current study, the

overexpression of transfected *PRDM9* into HeLa Tet-on system did not show any measurable changes of trimethylated H3K4 and/or H3K36 activity. This might because protein analysis did not confirm the production of PRDM9 protein during this study, suggesting that the overexpressing system (pTRE3G system) was not working properly. The used antibodies from Abcam (ab85654 and ab178531) showed that they work at first, but the different batchs did not work. It is clear that among of the issues we faced during this work were related to the antibodies. Batch-to-batch variability could result in different findings, even in using same cells and experiment conditions. Even more problematic is that the antibodies may recognise and detect other proteins in addition to the intended ones to be targrted (Baker et al., 2015). To improve the reproducibility and reliability of antibodies, it has been argued that spicifity of these antibodies must be defined by using expressed recombinant proteins in cell lines, (more details reviewd in Bradbury & Plückthun, 2015).

Another example of meiosis-specific gene that has been defined as a CT gene is human TEX19. TEX19 regulates SPO11-mediated recombination and demonstrates significant roles in cancer cell proliferations (Planells-Palop et al., 2017). Researchers are yet to discover the functions of human TEX19 in oncogenesis; however, its aberrant activation has been reported in a wide variety of cancer types (Feichtinger et al., 2012; Zhong et al., 2016). *Tex19.1* and *Tex19.2* are the two *TEX19* orthologues present in the mouse, but it is considered that Tex19.1 is the functional orthologue of human TEX19 (Kuntz et al., 2008; Öllinger et al., 2008). In murine germ cells, Tex19.1 has been reported to interact with the murine Ubr2 E3 ubiquitin ligase, allowing it to control many biological functions, such as initiating Spo11 meiotic recombination and regulating LINE1 transposition (Yang et al., 2010; Reichmann et al., 2013; Tarabay et al., 2013; Crichton et al., 2017; MacLennan et al., 2017). Although the previous study on *D. melanogaster* l(3)mbt tumours does not shed light on a mammalian specific gene, TEX19, and its contribution on tumour formation, a recent study has determined that this gene is activated in early stages of cancers and is required to maintain cancer cell proliferation, suggesting that TEX19 might play important roles during early stages of oncogenic process. Additionally, TEX19 has been suggested to act as a protein coding gene transcriptional regulator in cancer cells (Planells-Palop, et al., 2017). In McFarlane lab, a preliminary study from a co-worker (L. Alqahtani) has hypothesised that TEX19 might regulate histone H3K9 acetylation, as H3K9 acetylation was

reduced in TEX19-depleted cancer cells. In this study, we verified that H3K9 is significantly reduced in TEX19-depleted cancer cells.

7.2 Further directions

The results of this work provide insight into the uncharacterised functions of PRDM9 and TEX19 proteins in cancerous cells. For further directions and investigations on PRDM9 work, a stable *PRDM9* knockout cell line could be established using, for example, Clustered Regularly Interspaced Short Palindromic Repeats (CRISPR/Cas9), which might shed light on the functional analysis of PRDM9 in cancer cells. Furthermore, another tags such as HA and C-MYC should be incorporated with PRDM9 and transfected into Tet-On 3G inducing system stable cell line that could be tested at different concentrations of doxycycline to determine the influence of *PRDM9* overexpression on cell proliferation. Different techniques such as shRNA and siRNA should be performed to confirm knockdown of *PRDM9* in cancer cells, and thereafter, further analyses are required, such as; fluorescent-activated cell sorting (FACS) analysis and RNA sequencing analysis. RNAseq analysis is also required on overexpressing PRDM9 HeLa Tet-On 3G cells to validate its transcriptional activities.

Further experiments are required to determine whether PRDM9 has effects on cell proliferation *in vivo* (mouse model) using shRNA techniques. Ultimately, small molecular PRDM9 inhibitors could be established to evaluate the potentials of PRDM9 as cancer drug target.

This current work on TEX19 demonstrated that TEX19 protein was detected at a higher molecular weight, suggesting that this protein might be exposed to a posttranslational modification (PTM). For further investigations, we suggest that TEX19 protein could be isolated (by co-immunoprecipitation) using a specific antibody. Therefore, the isolated protein should be analysed against other covalently attached proteins such as ubiquitin and could be further analysed using mass spectrometric analysis. HaloTag cloning is proposed to be carried out to determine whether TEX19 was disabling any protein interactions. We also suggest investigating the RNA/DNA binding capacity of TEX19 to validate whther TEX19 is a transcriptional regulator and whether it interacts with the genome.

7. References

Aarts, M., Linardopoulos, S. & Turner, N.C. 2013. Tumour selective targeting of cell cycle kinases for cancer treatment. *Current opinion in pharmacology,* 13 (4), pp. 529-535.

Abbotts, R., Thompson, N. & Madhusudan, S. 2014. DNA repair in cancer: emerging targets for personalized therapy. *Cancer management and research,* 6 pp. 77.

Adair, S.J. & Hogan, K.T. 2009. Treatment of ovarian cancer cell lines with 5-aza-2′-deoxycytidine upregulates the expression of cancer-testis antigens and class I major histocompatibility complex-encoded molecules. *Cancer immunology, immunotherapy,* 58 (4), pp. 589-601.

Akers, S.N., Odunsi, K. & Karpf, A.R. 2010. Regulation of cancer germline antigen gene expression: implications for cancer immunotherapy. *Future oncology,* 6 (5), pp. 717-732.

Akhavan-Niaki, H. & Samadani, A.A. 2013. DNA methylation and cancer development: molecular mechanism. *Cell biochemistry and biophysics,* 67 (2), pp. 501-513.

Almatrafi, A., Feichtinger, J., Vernon, E.G., Escobar, N.G., Wakeman, J.A., Larcombe, L.D. & McFarlane, R.J. 2014. Identification of a class of human cancer germline genes with transcriptional silencing refractory to the hypomethylating drug 5-aza-2′-deoxycytidine. *Oncoscience,* 1 (11), pp. 745.

Altemose, N., Noor, N., Bitoun, E., Tumian, A., Imbeault, M., Chapman, J.R., Aricescu, A.R. & Myers, S.R. 2017. A map of human PRDM9 binding provides evidence for novel behaviors of PRDM9 and other zinc-finger proteins in meiosis. *Elife,* 6 pp. e28383.

Aly, H.A. 2012. Cancer therapy and vaccination. *Journal of immunological methods,* 382 (1-2), pp. 1-23.

Arnoult, N. & Karlseder, J. 2014. ALT telomeres borrow from meiosis to get moving. *Cell,* 159 (1), pp. 11-12.

Autier, P. 2016. Age at cancer diagnosis and interpretation of survival statistics. *The Lancet Oncology,* 17 (7), pp. 847-848.

Bagci, O. & Kurtgöz, S. 2015. Amplification of cellular oncogenes in solid tumors. *North American journal of medical sciences,* 7 (8), pp. 341.

Baker, C.L., Kajita, S., Walker, M., Saxl, R.L., Raghupathy, N., Choi, K., Petkov, P.M. & Paigen, K. 2015. PRDM9 drives evolutionary erosion of hotspots in Mus musculus through haplotype-specific initiation of meiotic recombination. *PLoS genetics,* 11 (1), pp. e1004916.

Baker, C.L., Walker, M., Kajita, S., Petkov, P.M. & Paigen, K. 2014. PRDM9 binding organizes hotspot nucleosomes and limits Holliday junction migration. *Genome research,* 24 (5), pp. 724-732.

Ballestar, E. 2011. An introduction to epigenetics. In: Anon*Epigenetic Contributions in Autoimmune Disease.* Springer. pp. 1-11.

Bannister, A.J. & Kouzarides, T. 2011. Regulation of chromatin by histone modifications. *Cell research,* 21 (3), pp. 381.

Barneda-Zahonero, B. & Parra, M. 2012. Histone deacetylases and cancer. *Molecular oncology,* 6 (6), pp. 579-589.

Barski, A., Cuddapah, S., Cui, K., Roh, T., Schones, D.E., Wang, Z., Wei, G., Chepelev, I. & Zhao, K. 2007. High-resolution profiling of histone methylations in the human genome. *Cell,* 129 (4), pp. 823-837.

Baudat, F., Buard, J., Grey, C., Fledel-Alon, A., Ober, C., Przeworski, M., Coop, G. & De Massy, B. 2010. PRDM9 is a major determinant of meiotic recombination hotspots in humans and mice. *Science,* 327 (5967), pp. 836-840.

Baudat, F., Imai, Y. & De Massy, B. 2013. Meiotic recombination in mammals: localization and regulation. *Nature Reviews Genetics,* 14 (11), pp. 794.

Beaupre, D.M. & Kurzrock, R. 1999. RAS and leukemia: from basic mechanisms to gene-directed therapy. *Journal of Clinical Oncology,* 17 (3), pp. 1071.

Ben-Shahar, T.R., Heeger, S., Lehane, C., East, P., Flynn, H., Skehel, M. & Uhlmann, F. 2008. Eco1-dependent cohesin acetylation during establishment of sister chromatid cohesion. *Science,* 321 (5888), pp. 563-566.

Berg, I.L., Neumann, R., Lam, K.G., Sarbajna, S., Odenthal-Hesse, L., May, C.A. & Jeffreys, A.J. 2010. PRDM9 variation strongly influences recombination hot-spot activity and meiotic instability in humans. *Nature genetics,* 42 (10), pp. 859.

Berg, I.L., Neumann, R., Sarbajna, S., Odenthal-Hesse, L., Butler, N.J. & Jeffreys, A.J. 2011. Variants of the protein PRDM9 differentially regulate a set of human meiotic recombination hotspots highly active in African populations. *Proceedings of the National Academy of Sciences,* 108 (30), pp. 12378-12383.

Bergerat, A., de Massy, B., Gadelle, D., Varoutas, P., Nicolas, A. & Forterre, P. 1997. An atypical topoisomerase II from Archaea with implications for meiotic recombination. *Nature,* 386 (6623), pp. 414.

Berlin, A., Lalonde, E., Sykes, J., Zafarana, G., Chu, K.C., Ramnarine, V.R., Ishkanian, A., Sendorek, D.H., Pasic, I. & Lam, W.L. 2014. NBN gain is predictive for adverse outcome following image-guided radiotherapy for localized prostate cancer. *Oncotarget,* 5 (22), pp. 11081.

Bernstein, B.E., Humphrey, E.L., Erlich, R.L., Schneider, R., Bouman, P., Liu, J.S., Kouzarides, T. & Schreiber, S.L. 2002. Methylation of histone H3 Lys 4 in coding regions of active genes. *Proceedings of the National Academy of Sciences,* 99 (13), pp. 8695-8700.

Billings, T., Parvanov, E.D., Baker, C.L., Walker, M., Paigen, K. & Petkov, P.M. 2013. DNA binding specificities of the long zinc-finger recombination protein PRDM9. *Genome biology,* 14 (4), pp. R35.

Birtle, Z. & Ponting, C.P. 2006. Meisetz and the birth of the KRAB motif. *Bioinformatics,* 22 (23), pp. 2841-2845.

Blanchard, T., Srivastava, P.K. & Duan, F. 2013. Vaccines against advanced melanoma. *Clinics in dermatology,* 31 (2), pp. 179-190.

Blazer, L.L., Lima-Fernandes, E., Gibson, E., Eram, M.S., Loppnau, P., Arrowsmith, C.H., Schapira, M. & Vedadi, M. 2016. PR domain-containing protein 7 (PRDM7) is a histone 3 lysine 4 trimethyltransferase. *Journal of Biological Chemistry,* 291 (26), pp. 13509-13519.

Blumenfeld, B., Ben-Zimra, M. & Simon, I. 2017. Perturbations in the replication program contribute to genomic instability in cancer. *International journal of molecular sciences,* 18 (6), pp. 1138.

Bolcun-Filas, E., Speed, R., Taggart, M., Grey, C., de Massy, B., Benavente, R. & Cooke, H.J. 2009. Mutation of the mouse Syce1 gene disrupts synapsis and suggests a link between synaptonemal complex structural components and DNA repair. *PLoS genetics,* 5 (2), pp. e1000393.

Borde, V., Robine, N., Lin, W., Bonfils, S., Geli, V. & Nicolas, A. 2009. Histone H3 lysine 4 trimethylation marks meiotic recombination initiation sites. *The EMBO journal,* 28 (2), pp. 99-111.

Bordeaux, J., Welsh, A.W., Agarwal, S., Killiam, E., Baquero, M.T., Hanna, J.A., Anagnostou, V.K. & Rimm, D.L. 2010. Antibody validation. *BioTechniques,* 48 (3), pp. 197-209.

Bourc'his, D. & Bestor, T.H. 2004. Meiotic catastrophe and retrotransposon reactivation in male germ cells lacking Dnmt3L. *Nature,* 431 (7004), pp. 96.

Bradbury, A. & Plückthun, A. 2015. Reproducibility: Standardize antibodies used in research. *Nature News,* 518 (7537), pp. 27.

Brasseur, F., Rimoldi, D., Liénard, D., Lethé, B., Carrel, S., Arienti, F., Suter, L., Vanwijck, R., Bourlond, A. & Humblet, Y. 1995. Expression of MAGE genes in primary and metastatic cutaneous melanoma. *International journal of cancer,* 63 (3), pp. 375-380.

Brick, K., Smagulova, F., Khil, P., Camerini-Otero, R.D. & Petukhova, G.V. 2012. Genetic recombination is directed away from functional genomic elements in mice. *Nature,* 485 (7400), pp. 642.

Brown, P.R., Miki, K., Harper, D.B. & Eddy, E.M. 2003. A-kinase anchoring protein 4 binding proteins in the fibrous sheath of the sperm flagellum. *Biology of reproduction,* 68 (6), pp. 2241-2248.

Buard, J., Barthès, P., Grey, C. & De Massy, B. 2009. Distinct histone modifications define initiation and repair of meiotic recombination in the mouse. *The EMBO journal,* 28 (17), pp. 2616-2624.

Bucher, M.H., Evdokimov, A.G. & Waugh, D.S. 2002. Differential effects of short affinity tags on the crystallization of Pyrococcus furiosus maltodextrin-binding protein. *Acta Crystallographica Section D: Biological Crystallography,* 58 (3), pp. 392-397.

Caballero, O.L. & Chen, Y. 2009. Cancer/testis (CT) antigens: potential targets for immunotherapy. *Cancer science,* 100 (11), pp. 2014-2021.

Cahoon, C.K. & Hawley, R.S. 2016. Regulating the construction and demolition of the synaptonemal complex. *Nature structural & molecular biology,* 23 (5), pp. 369.

Cai, L., Sutter, B.M., Li, B. & Tu, B.P. 2011. Acetyl-CoA induces cell growth and proliferation by promoting the acetylation of histones at growth genes. *Molecular cell,* 42 (4), pp. 426-437.

Campos-Perez, J., Rice, J., Escors, D., Collins, M., Paterson, A., Savelyeva, N. & Stevenson, F.K. 2013. DNA fusion vaccine designs to induce tumor-lytic CD8 T-cell attack via the immunodominant cysteine-containing epitope of NY-ESO 1. *International journal of cancer,* 133 (6), pp. 1400-1407.

Cappell, K.M., Sinnott, R., Taus, P., Maxfield, K., Scarbrough, M. & Whitehurst, A.W. 2012. Multiple cancer testis antigens function to support tumor cell mitotic fidelity. *Molecular and cellular biology,* 32 (20), pp. 4131-4140.

Caron, C., Boyault, C. & Khochbin, S. 2005. Regulatory cross-talk between lysine acetylation and ubiquitination: role in the control of protein stability. *Bioessays,* 27 (4), pp. 408-415.

Celebi, C., Van Montfoort, A., Skory, V., Kieffer, E., Kuntz, S., Mark, M. & Viville, S. 2012. Tex 19 paralogs exhibit a gonad and placenta-specific expression in the mouse. *Journal of Reproduction and Development,* pp. 1203020441.

Chambers, I., Colby, D., Robertson, M., Nichols, J., Lee, S., Tweedie, S. & Smith, A. 2003. Functional expression cloning of Nanog, a pluripotency sustaining factor in embryonic stem cells. *Cell,* 113 (5), pp. 643-655.

Chandra, T. & Narita, M. 2013. High-order chromatin structure and the epigenome in SAHFs. *Nucleus,* 4 (1), pp. 23-28.

Cheema, Z., Hari-Gupta, Y., Kita, G., Farrar, D., Seddon, I., Corr, J. & Klenova, E. 2014. Expression of the cancer-testis antigen BORIS correlates with prostate cancer. *The Prostate,* 74 (2), pp. 164-176.

Chen, Y., Güre, A.O., Tsang, S., Stockert, E., Jäger, E., Knuth, A. & Old, L.J. 1998. Identification of multiple cancer/testis antigens by allogeneic antibody screening of a melanoma cell line library. *Proceedings of the National Academy of Sciences,* 95 (12), pp. 6919-6923.

Chen, Y., Scanlan, M.J., Sahin, U., Türeci, Ö, Gure, A.O., Tsang, S., Williamson, B., Stockert, E., Pfreundschuh, M. & Old, L.J. 1997. A testicular antigen aberrantly expressed in human cancers detected by autologous antibody screening. *Proceedings of the National Academy of Sciences,* 94 (5), pp. 1914-1918.

Chen, Y., Venditti, C.A., Theiler, G., Stevenson, B.J., Iseli, C., Gure, A.O., Jongeneel, C.V., Old, L.J. & Simpson, A.J. 2005. Identification of CT46/HORMAD1, an immunogenic cancer/testis antigen encoding a putative meiosis-related protein. *Cancer Immun,* 5 (9), .

Cheng, Y., Wong, E.W. & Cheng, C.Y. 2011. Cancer/testis (CT) antigens, carcinogenesis and spermatogenesis. *Spermatogenesis,* 1 (3), pp. 209-220.

Choi, J.D. & Lee, J. 2013. Interplay between epigenetics and genetics in cancer. *Genomics & informatics,* 11 (4), pp. 164.

Choudhary, C., Kumar, C., Gnad, F., Nielsen, M.L., Rehman, M., Walther, T.C., Olsen, J.V. & Mann, M. 2009. Lysine acetylation targets protein complexes and co-regulates major cellular functions. *Science,* 325 (5942), pp. 834-840.

Choudhury, J.D., Kumar, S., Mayank, V., Mehta, J. & Bardalai, D. 2012. A review on apoptosis and its different pathway. *International Journal of Biological and Pharmaceutical Research,* 3 pp. 848-861.

Clapp, R.W., Jacobs, M.M. & Loechler, E.L. 2008. Environmental and occupational causes of cancer: new evidence 2005-2007. *Reviews on environmental health,* 23 (1), pp. 1-38.

Clift, D. & Marston, A.L. 2011. The role of shugoshin in meiotic chromosome segregation. *Cytogenetic and genome research,* 133 (2-4), pp. 234-242.

Colaiácovo, M.P., MacQueen, A.J., Martinez-Perez, E., McDonald, K., Adamo, A., La Volpe, A. & Villeneuve, A.M. 2003. Synaptonemal complex assembly in C. elegans is dispensable for loading strand-exchange proteins but critical for proper completion of recombination. *Developmental cell,* 5 (3), pp. 463-474.

Coleman-Derr, D. & Zilberman, D. 2012. Deposition of histone variant H2A. Z within gene bodies regulates responsive genes. *PLoS genetics,* 8 (10), pp. e1002988.

Cooper, T.J., Garcia, V. & Neale, M.J. 2016. Meiotic DSB patterning: A multifaceted process. *Cell Cycle,* 15 (1), pp. 13-21.

Costa, F.F., Le Blanc, K. & Brodin, B. 2007. Concise review: cancer/testis antigens, stem cells, and cancer. *Stem Cells,* 25 (3), pp. 707-711.

Crichton, J.H., Playfoot, C.J., MacLennan, M., Read, D., Cooke, H.J. & Adams, I.R. 2017. Tex19. 1 promotes Spo11-dependent meiotic recombination in mouse spermatocytes. *PLoS genetics,* 13 (7), pp. e1006904.

Croce, C.M. 2008. Oncogenes and cancer. *New England journal of medicine,* 358 (5), pp. 502-511.

Daniel, K., Lange, J., Hached, K., Fu, J., Anastassiadis, K., Roig, I., Cooke, H.J., Stewart, A.F., Wassmann, K. & Jasin, M. 2011a. Meiotic homologue alignment and its quality surveillance are controlled by mouse HORMAD1. *Nature cell biology,* 13 (5), pp. 599.

Davies, B., Hatton, E., Altemose, N., Hussin, J.G., Pratto, F., Zhang, G., Hinch, A.G., Moralli, D., Biggs, D. & Diaz, R. 2016. Re-engineering the zinc fingers of PRDM9 reverses hybrid sterility in mice. *Nature,* 530 (7589), pp. 171.

Davies, H., Bignell, G.R., Cox, C., Stephens, P., Edkins, S., Clegg, S., Teague, J., Woffendin, H., Garnett, M.J. & Bottomley, W. 2002. Mutations of the BRAF gene in human cancer. Nature, 417 (6892), pp. 949.

Davuluri, R.V., Grosse, I. & Zhang, M.Q. 2001. Computational identification of promoters and first exons in the human genome. *Nature genetics,* 29 (4), pp. 412.

Dawson, M.A. & Kouzarides, T. 2012. Cancer epigenetics: from mechanism to therapy. Cell, 150 (1), pp. 12-27.

De Backer, O., Arden, K.C., Boretti, M., Vantomme, V., De Smet, C., Czekay, S., Viars, C.S., De Plaen, E., Brasseur, F. & Chomez, P. 1999. Characterization of the GAGE genes that are expressed in various human cancers and in normal testis. Cancer research, 59 (13), pp. 3157-3165.

De Ruijter, A.J., Van Gennip, A.H., Caron, H.N., Stephan, K. & Van Kuilenburg, A.B. 2003. Histone deacetylases (HDACs): characterization of the classical HDAC family. *Biochemical Journal,* 370 (3), pp. 737-749.

De Smet, C. & Loriot, A. 2013. DNA hypomethylation and activation of germline-specific genes in cancer. In: AnonEpigenetic Alterations in Oncogenesis. Springer. pp. 149-166.

de Vries, F.A., de Boer, E., van den Bosch, M., Baarends, W.M., Ooms, M., Yuan, L., Liu, J., van Zeeland, A.A., Heyting, C. & Pastink, A. 2005. Mouse Sycp1 functions in synaptonemal complex assembly, meiotic recombination, and XY body formation. *Genes & development,* 19 (11), pp. 1376-1389.

Deal, R.B. & Henikoff, S. 2011. Histone variants and modifications in plant gene regulation. *Current opinion in plant biology,* 14 (2), pp. 116-122.

Deardorff, M.A., Bando, M., Nakato, R., Watrin, E., Itoh, T., Minamino, M., Saitoh, K., Komata, M., Katou, Y. & Clark, D. 2012. HDAC8 mutations in Cornelia de Lange syndrome affect the cohesin acetylation cycle. *Nature,* 489 (7415), pp. 313.

Dekker, F.J. & Haisma, H.J. 2009. Histone acetyl transferases as emerging drug targets. *Drug discovery today,* 14 (19-20), pp. 942-948.

Di Zazzo, E., De Rosa, C., Abbondanza, C. & Moncharmont, B. 2013. PRDM proteins: molecular mechanisms in signal transduction and transcriptional regulation. *Biology,* 2 (1), pp. 107-141.

Diagouraga, B., Clément, J.A., Duret, L., Kadlec, J., De Massy, B. & Baudat, F. 2018. PRDM9 methyltransferase activity is essential for meiotic DNA double-strand break formation at its binding sites. *Molecular cell,* 69 (5), pp. 85-865. e6.

Dillon, S.C., Zhang, X., Trievel, R.C. & Cheng, X. 2005. The SET-domain protein superfamily: protein lysine methyltransferases. *Genome biology,* 6 (8), pp. 227.

Dokmanovic, M., Clarke, C. & Marks, P.A. 2007. Histone deacetylase inhibitors: overview and perspectives. *Molecular cancer research,* 5 (10), pp. 981-989.

Dray, E., Dunlop, M.H., Kauppi, L., San Filippo, J., Wiese, C., Tsai, M., Begovic, S., Schild, D., Jasin, M. & Keeney, S. 2011. Molecular basis for enhancement of the meiotic DMC1 recombinase by RAD51 associated protein 1 (RAD51AP1). *Proceedings of the National Academy of Sciences,* .

Egel, R. & Lankenau, D. 2007. *Recombination and Meiosis: Crossing-over and disjunction.* Springer Science & Business Media.

Eram, M.S., Bustos, S.P., Lima-Fernandes, E., Siarheyeva, A., Senisterra, G., Hajian, T., Chau, I., Duan, S., Wu, H. & Dombrovski, L. 2014. Trimethylation of histone H3 lysine 36 by human methyltransferase PRDM9. *Journal of Biological Chemistry,* pp. jbc. M113. 523183.

Esteller, M. & Herman, J.G. 2002. Cancer as an epigenetic disease: DNA methylation and chromatin alterations in human tumours. *The Journal of Pathology: A Journal of the Pathological Society of Great Britain and Ireland,* 196 (1), pp. 1-7.

Feichtinger, J. & McFarlane, R.J. 2019. Meiotic gene activation in somatic and germ cell tumours. *Andrology,* .

Feichtinger, J., Aldeailej, I., Anderson, R., Almutairi, M., Almatrafi, A., Alsiwiehri, N., Griffiths, K., Stuart, N., Wakeman, J.A. & Larcombe, L. 2012. Meta-analysis of clinical data using human meiotic genes identifies a novel cohort of highly restricted cancer-specific marker genes. *Oncotarget,* 3 (8), pp. 843.

Feichtinger, J., Larcombe, L. & McFarlane, R.J. 2014. Meta-analysis of expression of l (3) mbt tumor-associated germline genes supports the model that a soma-to-germline transition is a hallmark of human cancers. *International journal of cancer,* 134 (10), pp. 2359-2365.

Feinberg, A.P., Ohlsson, R. & Henikoff, S. 2006. The epigenetic progenitor origin of human cancer. *Nature reviews genetics,* 7 (1), pp. 21.

Ferguson, L.R., Chen, H., Collins, A.R., Connell, M., Damia, G., Dasgupta, S., Malhotra, M., Meeker, A.K., Amedei, A. & Amin, A. 2015. Genomic instability in human cancer: Molecular insights and opportunities for therapeutic attack and prevention through diet and nutrition. *Seminars in cancer biology.* Elsevier. pp. S.

Fiedler, S.E., Dudiki, T., Vijayaraghavan, S. & Carr, D.W. 2013. Loss of R2D2 proteins ROPN1 and ROPN1L causes defects in murine sperm motility, phosphorylation, and fibrous sheath integrity. *Biology of reproduction,* 88 (2), pp. 41, -10.

Filippakopoulos, P., Picaud, S., Mangos, M., Keates, T., Lambert, J., Barsyte-Lovejoy, D., Felletar, I., Volkmer, R., Müller, S. & Pawson, T. 2012. Histone recognition and large-scale structural analysis of the human bromodomain family. *Cell,* 149 (1), pp. 214-231.

Flachs, P., Mihola, O., Šimeček, P., Gregorová, S., Schimenti, J.C., Matsui, Y., Baudat, F., de Massy, B., Pialek, J. & Forejt, J. 2012. Interallelic and intergenic incompatibilities of the Prdm9 (Hst1) gene in mouse hybrid sterility. *PLoS genetics,* 8 (11), pp. e1003044.

Flavahan, W.A., Gaskell, E. & Bernstein, B.E. 2017a. Epigenetic plasticity and the hallmarks of cancer. *Science,* 357 (6348), pp. eaal2380.

Fledel-Alon, A., Leffler, E.M., Guan, Y., Stephens, M., Coop, G. & Przeworski, M. 2011. Variation in human recombination rates and its genetic determinants. *PloS one,* 6 (6), pp. e20321.

Fog, C.K., Galli, G.G. & Lund, A.H. 2012. PRDM proteins: important players in differentiation and disease. *Bioessays,* 34 (1), pp. 50-60.

Folco, H.D., Chalamcharla, V.R., Sugiyama, T., Thillainadesan, G., Zofall, M., Balachandran, V., Dhakshnamoorthy, J., Mizuguchi, T. & Grewal, S.I. 2017. Untimely expression of gametogenic genes in vegetative cells causes uniparental disomy. *Nature,* 543 (7643), pp. 126.

Fratta, E., Coral, S., Covre, A., Parisi, G., Colizzi, F., Danielli, R., Nicolay, H.J.M., Sigalotti, L. & Maio, M. 2011a. The biology of cancer testis antigens: putative function, regulation and therapeutic potential. *Molecular oncology,* 5 (2), pp. 164-182.

Fraune, J., Schramm, S., Alsheimer, M. & Benavente, R. 2012. The mammalian synaptonemal complex: protein components, assembly and role in meiotic recombination. *Experimental cell research,* 318 (12), pp. 1340-1346.

Friedberg, E.C., McDaniel, L.D. & Schultz, R.A. 2004. The role of endogenous and exogenous DNA damage and mutagenesis. *Current opinion in genetics & development,* 14 (1), pp. 5-10.

Fumasoni, I., Meani, N., Rambaldi, D., Scafetta, G., Alcalay, M. & Ciccarelli, F.D. 2007. Family expansion and gene rearrangements contributed to the functional specialization of PRDM genes in vertebrates. *BMC evolutionary biology,* 7 (1), pp. 187.

Gao, Y. & Tollefsbol, T.O. 2015. Cancer Chemoprotection Through Nutrient-mediated Histone Modifications. *Current medicinal chemistry,* 22 (17), pp. 2051.

Garcia-Cruz, R., Roig, I. & Caldés, M.G. 2009. Maternal origin of the human aneuploidies. Are homolog synapsis and recombination to blame? Notes (learned) from the underbelly. In: Anon*Meiosis.* Karger Publishers. pp. 128-136.

Gerton, J.L. & Hawley, R.S. 2005. Homologous chromosome interactions in meiosis: diversity amidst conservation. *Nature Reviews Genetics,* 6 (6), pp. 477.

Ghafouri-Fard, S. & Modarressi, M. 2012. Expression of cancer–testis genes in brain tumors: implications for cancer immunotherapy. *Immunotherapy,* 4 (1), pp. 59-75.

Gibbs, Z.A. & Whitehurst, A.W. 2018. Emerging contributions of Cancer/Testis antigens to neoplastic behaviors. *Trends in cancer,* .

GILL, J., ELLIS, B., BOGUSLAWSKI, S. & TANG, P. 1996. Direct Western blot detection of HA epitope-tagged proteins using Anti-HA-peroxidase. *Biochemica,* 1 pp. 41-43.

Gjerstorff, M.F., Andersen, M.H. & Ditzel, H.J. 2015. Oncogenic cancer/testis antigens: prime candidates for immunotherapy. *Oncotarget,* 6 (18), pp. 15772.

Gnoni, A., Licchetta, A., Scarpa, A., Azzariti, A., Brunetti, A., Simone, G., Nardulli, P., Santini, D., Aieta, M. & Delcuratolo, S. 2013. Carcinogenesis of pancreatic adenocarcinoma: precursor lesions. *International journal of molecular sciences,* 14 (10), pp. 19731-19762.

Gossen, M. & Bujard, H. 1992. Tight control of gene expression in mammalian cells by tetracycline-responsive promoters. *Proceedings of the National Academy of Sciences,* 89 (12), pp. 5547-5551.

Gray, S. & Cohen, P.E. 2016. Control of meiotic crossovers: from double-strand break formation to designation. *Annual Review of Genetics,* 50 pp. 175-210.

Greten, T.F. & Jaffee, E.M. 1999. Cancer vaccines. *Journal of Clinical Oncology,* 17 (3), pp. 1047.

Greve, K.B., Lindgreen, J.N., Terp, M.G., Pedersen, C.B., Schmidt, S., Mollenhauer, J., Kristensen, S.B., Andersen, R.S., Relster, M.M. & Ditzel, H.J. 2015. Ectopic expression of cancer/testis antigen SSX2 induces DNA damage and promotes genomic instability. *Molecular oncology,* 9 (2), pp. 437-449.

Grey, C., Barthès, P., Chauveau-Le Friec, G., Langa, F., Baudat, F. & De Massy, B. 2011. Mouse PRDM9 DNA-binding specificity determines sites of histone H3 lysine 4 trimethylation for initiation of meiotic recombination. *PLoS biology,* 9 (10), pp. e1001176.

Grey, C., Baudat, F. & de Massy, B. 2018. PRDM9, a driver of the genetic map. *PLoS genetics,* 14 (8), pp. e1007479.

Grey, C., Clément, J.A., Buard, J., Leblanc, B., Gut, I., Gut, M., Duret, L. & De Massy, B. 2017. In vivo binding of PRDM9 reveals interactions with noncanonical genomic sites. *Genome research,* 27 (4), pp. 580-590.

Grunstein, M. 1997. Histone acetylation in chromatin structure and transcription. *Nature,* 389 (6649), pp. 349.

Guillon, H., Baudat, F., Grey, C., Liskay, R.M. & De Massy, B. 2005. Crossover and noncrossover pathways in mouse meiosis. *Molecular cell,* 20 (4), pp. 563-573.

Guo, L., Sang, M., Liu, Q., Fan, X., Zhang, X. & Shan, B. 2013. The expression and clinical significance of melanoma-associated antigen-A1,-A3 and-A11 in glioma. *Oncology letters,* 6 (1), pp. 55-62.

Hackett, J.A., Reddington, J.P., Nestor, C.E., Dunican, D.S., Branco, M.R., Reichmann, J., Reik, W., Surani, M.A., Adams, I.R. & Meehan, R.R. 2012. Promoter DNA methylation couples genome-defence mechanisms to epigenetic reprogramming in the mouse germline. *Development,* 139 (19), pp. 3623-3632.

Hanahan, D. & Weinberg, R.A. 2011. Hallmarks of cancer: the next generation. *Cell,* 144 (5), pp. 646-674.

Hanahan, D. & Weinberg, R.A. 2000. The hallmarks of cancer. *Cell,* 100 (1), pp. 57-70.

Handel, M.A. & Schimenti, J.C. 2010. Genetics of mammalian meiosis: regulation, dynamics and impact on fertility. *Nature Reviews Genetics,* 11 (2), pp. 124.

Hartl, F.U., Bracher, A. & Hayer-Hartl, M. 2011. Molecular chaperones in protein folding and proteostasis. *Nature,* 475 (7356), pp. 324.

Hatzimichael, E. & Crook, T. 2013. Cancer epigenetics: new therapies and new challenges. *Journal of drug delivery,* 2013.

Hayashi, K. & Matsui, Y. 2006. Meisetz, a novel histone tri-methyltransferase, regulates meiosis-specific epigenesis. *Cell Cycle,* 5 (6), pp. 615-620.

Hayashi, K., Yoshida, K. & Matsui, Y. 2005. A histone H3 methyltransferase controls epigenetic events required for meiotic prophase. *Nature,* 438 (7066), pp. 374.

He, Y., Wang, M., Dukowic-Schulze, S., Zhou, A., Tiang, C., Shilo, S., Sidhu, G.K., Eichten, S., Bradbury, P. & Springer, N.M. 2017. Genomic features shaping the landscape of meiotic double-strand-break hotspots in maize. *Proceedings of the National Academy of Sciences,* 114 (46), pp. 12231-12236.

Henderson, K.A. & Keeney, S. 2004. Tying synaptonemal complex initiation to the formation and programmed repair of DNA double-strand breaks. *Proceedings of the National Academy of Sciences,* 101 (13), pp. 4519-4524.

Hess, R.A. & De Franca, L.R. 2009. Spermatogenesis and cycle of the seminiferous epithelium. In: Anon*Molecular mechanisms in spermatogenesis.* Springer. pp. 1-15.

Hinch, A.G., Tandon, A., Patterson, N., Song, Y., Rohland, N., Palmer, C.D., Chen, G.K., Wang, K., Buxbaum, S.G. & Akylbekova, E.L. 2011. The landscape of recombination in African Americans. *Nature,* 476 (7359), pp. 170.

Hoeijmakers, J.H. 2001. Genome maintenance mechanisms for preventing cancer. *Nature,* 411 (6835), pp. 366.

Hofmann, O., Caballero, O.L., Stevenson, B.J., Chen, Y., Cohen, T., Chua, R., Maher, C.A., Panji, S., Schaefer, U. & Kruger, A. 2008. Genome-wide analysis of cancer/testis gene expression. *Proceedings of the National Academy of Sciences,* 105 (51), pp. 20422-20427.

Hohenauer, T. & Moore, A.W. 2012. The Prdm family: expanding roles in stem cells and development. *Development,* 139 (13), pp. 2267-2282.

Holthausen, J.T., Wyman, C. & Kanaar, R. 2010. Regulation of DNA strand exchange in homologous recombination. *DNA repair,* 9 (12), pp. 1264-1272.

Hosoya, N., Okajima, M., Kinomura, A., Fujii, Y., Hiyama, T., Sun, J., Tashiro, S. & Miyagawa, K. 2012. Synaptonemal complex protein SYCP3 impairs mitotic recombination by interfering with BRCA2. *EMBO reports,* 13 (1), pp. 44-51.

Hou, S., Sang, M., Geng, C., Liu, W., Lü, W., Xu, Y. & Shan, B. 2014. Expressions of MAGE-A9 and MAGE-A11 in breast cancer and their expression mechanism. *Archives of Medical Research,* 45 (1), pp. 44-51.

Houghton, A.N., Gold, J.S. & Blachere, N.E. 2001. Immunity against cancer: lessons learned from melanoma. *Current opinion in immunology,* 13 (2), pp. 134-140.

Houle, A.A., Gibling, H., Lamaze, F.C., Edgington, H.A., Soave, D., Fave, M., Agbessi, M., Bruat, V., Stein, L.D. & Awadalla, P. 2018. Aberrant PRDM9

expression impacts the pan-cancer genomic landscape. *Genome research,* 28 (11), pp. 1611-1620.

Hrabeta, J., Stiborova, M., Adam, V., Kizek, R. & Eckschlager, T. 2014. Histone deacetylase inhibitors in cancer therapy. A review. *Biomedical Papers,* 158 (2), pp. 161-169.

Hunder, N.N., Wallen, H., Cao, J., Hendricks, D.W., Reilly, J.Z., Rodmyre, R., Jungbluth, A., Gnjatic, S., Thompson, J.A. & Yee, C. 2008. Treatment of metastatic melanoma with autologous CD4 T cells against NY-ESO-1. *New England Journal of Medicine,* 358 (25), pp. 2698-2703.

Hunter, N. 2015. Meiotic recombination: the essence of heredity. *Cold Spring Harbor perspectives in biology,* pp. a016618.

Hussin, J., Sinnett, D., Casals, F., Idaghdour, Y., Bruat, V., Saillour, V., Healy, J., Grenier, J., De Malliard, T. & Busche, S. 2013. Rare allelic forms of PRDM9 associated with childhood leukemogenesis. *Genome research,* 23 (3), pp. 419-430.

Ibrahim, A.E., Arends, M.J., Silva, A., Wyllie, A.H., Greger, L., Ito, Y., Vowler, S.L., Huang, T.H., Tavaré, S. & Murrell, A. 2011. Sequential DNA methylation changes are associated with DNMT3B overexpression in colorectal neoplastic progression. *Gut,* 60 (4), pp. 499-508.

Imai, Y., Baudat, F., Taillepierre, M., Stanzione, M., Toth, A. & De Massy, B. 2017. The PRDM9 KRAB domain is required for meiosis and involved in protein interactions. *Chromosoma,* 126 (6), pp. 681-695.

Ishiguro, K., Kim, J., Fujiyama-Nakamura, S., Kato, S. & Watanabe, Y. 2011. A new meiosis-specific cohesin complex implicated in the cohesin code for homologous pairing. *EMBO reports,* 12 (3), pp. 267-275.

Jagadish, N., Parashar, D., Gupta, N., Agarwal, S., Sharma, A., Fatima, R., Suri, V., Kumar, R., Gupta, A. & Lohiya, N.K. 2016. A novel cancer testis antigen target A-kinase anchor protein (AKAP4) for the early diagnosis and immunotherapy of colon cancer. *Oncoimmunology,* 5 (2), pp. e1078965.

Jacoby, E., Nguyen, S.M., Fountaine, T.J., Welp, K., Gryder, B., Qin, H., Yang, Y., Chien, C.D., Seif, A.E., Lei, H. and Song, Y.K., 2016. CD19 CAR immune pressure induces B-precursor acute lymphoblastic leukaemia lineage switch exposing inherent leukaemic plasticity. Nature communications, 7(1), pp.1-10.

Janic, A., Mendizabal, L., Llamazares, S., Rossell, D. & Gonzalez, C. 2010. Ectopic expression of germline genes drives malignant brain tumor growth in Drosophila. *Science,* 330 (6012), pp. 1824-1827.

Jeffreys, A.J., Kauppi, L. & Neumann, R. 2001. Intensely punctate meiotic recombination in the class II region of the major histocompatibility complex. *Nature genetics,* 29 (2), pp. 217.

Jemal, A., Siegel, R., Ward, E., Hao, Y., Xu, J. & Thun, M.J. 2010. CA: a cancer journal for clinicians. *Cancer statistics,* 60 (5), pp. 277-300.

Jørgensen, A. & Rajpert-De Meyts, E. 2014. Regulation of meiotic entry and gonadal sex differentiation in the human: normal and disrupted signaling. *Biomolecular concepts,* 5 (4), pp. 331-341.

Jungbluth, A.A., Stockert, E., Chen, Y.T., Kolb, D., Iversen, K., Coplan, K., Williamson, B., Altorki, N., Busam, K.J. & Old, L.J. 2000. Monoclonal antibody MA454 reveals a heterogeneous expression pattern of MAGE-1 antigen in formalin-fixed paraffin embedded lung tumours. *British journal of cancer,* 83 (4), pp. 493.

Jungbluth, A.A., Ely, S., DiLiberto, M., Niesvizky, R., Williamson, B., Frosina, D., Chen, Y., Bhardwaj, N., Chen-Kiang, S. & Old, L.J. 2005. The cancer-testis antigens CT7 (MAGE-C1) and MAGE-A3/6 are commonly expressed in multiple myeloma and correlate with plasma-cell proliferation. *Blood,* 106 (1), pp. 167-174.

Kagawa, W. & Kurumizaka, H. 2010. From meiosis to postmeiotic events: Uncovering the molecular roles of the meiosis-specific recombinase Dmc1. *The FEBS journal,* 277 (3), pp. 590-598.

Kaiser, V.B. & Semple, C.A. 2018. Chromatin loop anchors are associated with genome instability in cancer and recombination hotspots in the germline. *Genome biology,* 19 (1), pp. 101.

Kalejs, M. & Erenpreisa, J. 2005. Cancer/testis antigens and gametogenesis: a review and" brain-storming" session. *Cancer cell international,* 5 (1), pp. 4.

Katzke, V.A., Kaaks, R. & Kühn, T. 2015. Lifestyle and cancer risk. *The Cancer Journal,* 21 (2), pp. 104-110.

Kawasumi, R., Abe, T., Arakawa, H., Garre, M., Hirota, K. & Branzei, D. 2017. ESCO1/2's roles in chromosome structure and interphase chromatin organization. *Genes & development,* 31 (21), pp. 2136-2150.

Keeney, S., Giroux, C.N. & Kleckner, N. 1997. Meiosis-specific DNA double-strand breaks are catalyzed by Spo11, a member of a widely conserved protein family. *Cell,* 88 (3), pp. 375-384.

Keeney, S., Lange, J. & Mohibullah, N. 2014. Self-organization of meiotic recombination initiation: general principles and molecular pathways. Annual Review of Genetics, 48 pp. 187-214.

Kim, D., Kim, M. & Kwon, H. 2003. Histone deacetylase in carcinogenesis and its inhibitors as anti-cancer agents. *BMB Reports,* 36 (1), pp. 110-119.

Kim, R., Kulkarni, P. & Hannenhalli, S. 2013. Derepression of Cancer/testis antigens in cancer is associated with distinct patterns of DNA hypomethylation. *BMC cancer,* 13 (1), pp. 144.

Kim, S. 2015. New and emerging factors in tumorigenesis: an overview. *Cancer management and research,* 7 pp. 225.

Klein, F., Mahr, P., Galova, M., Buonomo, S.B., Michaelis, C., Nairz, K. & Nasmyth, K. 1999. A central role for cohesins in sister chromatid cohesion, formation of axial elements, and recombination during yeast meiosis. *Cell,* 98 (1), pp. 91-103.

Koh-Stenta, X., Poulsen, A., Li, R., Wee, J.L.K., Kwek, P.Z., Chew, S.Y., Peng, J., Wu, L., Guccione, E. & Joy, J. 2017. Discovery and characterisation of the automethylation properties of PRDM9. *Biochemical Journal,* pp. BCJ20161067.

Koslowski, M., Bell, C., Seitz, G., Lehr, H., Roemer, K., Müntefering, H., Huber, C., Sahin, U. & Türeci, Ö 2004. Frequent nonrandom activation of germ-line genes in human cancer. *Cancer research,* 64 (17), pp. 5988-5993.

Koslowski, M., Türeci, Ö, Bell, C., Krause, P., Lehr, H., Brunner, J., Seitz, G., Nestle, F.O., Huber, C. & Sahin, U. 2002. Multiple splice variants of lactate dehydrogenase C selectively expressed in human cancer. *Cancer research,* 62 (22), pp. 6750-6755.

Kouzarides, T. 2007. Chromatin modifications and their function. *Cell,* 128 (4), pp. 693-705.

Kronja, I. & Orr-Weaver, T.L. 2011. Translational regulation of the cell cycle: when, where, how and why? Philosophical Transactions of the Royal Society B: Biological Sciences, 366 (1584), pp. 3638-3652.

Kuntz, S., Kieffer, E., Bianchetti, L., Lamoureux, N., Fuhrmann, G. & Viville, S. 2008. Tex19, a mammalian-specific protein with a restricted expression in pluripotent stem cells and germ line. *Stem cells,* 26 (3), pp. 734-744.

Kuo, K., Chou, T., Hsu, H., Chen, W. & Wang, L. 2012. Prognostic significance of NBS1 and Snail expression in esophageal squamous cell carcinoma. *Annals of surgical oncology,* 19 (3), pp. 549-557.

Kurashige, T., Noguchi, Y., Saika, T., Ono, T., Nagata, Y., Jungbluth, A., Ritter, G., Chen, Y., Stockert, E. & Tsushima, T. 2001. Ny-ESO-1 expression and immunogenicity associated with transitional cell carcinoma: correlation with tumor grade. *Cancer research,* 61 (12), pp. 4671-4674.

Lafta, I.J., Bryant, H.E. & Goldman, A.S. 2014. 'Sex'in the cancer cell. *Oncotarget,* 5 (18), pp. 7984.

Lai, T., Wu, Y., Wang, Y., Chen, M., Wang, P., Chen, T., Wu, Y., Chiang, H., Kuo, P. & Lin, Y. 2016. SEPT12–NDC1 Complexes Are Required for Mammalian Spermiogenesis. *International journal of molecular sciences,* 17 (11), pp. 1911.

Lajmi, N., Luetkens, T., Yousef, S., Templin, J., Cao, Y., Hildebrandt, Y., Bartels, K., Kröger, N. & Atanackovic, D. 2015. Cancer-testis antigen MAGEC 2 promotes proliferation and resistance to apoptosis in Multiple Myeloma. *British journal of haematology,* 171 (5), pp. 752-762.

Lam, I. & Keeney, S. 2015. Nonparadoxical evolutionary stability of the recombination initiation landscape in yeast. *Science,* 350 (6263), pp. 932-937.

Lee, J. & Hirano, T. 2011. RAD21L, a novel cohesin subunit implicated in linking homologous chromosomes in mammalian meiosis. *The Journal of cell biology,* 192 (2), pp. 263-276.

Lee, K.K. & Workman, J.L. 2007. Histone acetyltransferase complexes: one size doesn't fit all. *Nature reviews Molecular cell biology,* 8 (4), pp. 284.

Lee, S., Lee, J., Hah, H., Kim, Y., Ahn, J., Bae, C., Yang, J. & Hahn, M. 2007. PIAS1 interacts with the KRAB zinc finger protein, ZNF133, via zinc finger motifs and regulates its transcriptional activity. *Experimental & molecular medicine,* 39 (4), pp. 450.

Lee, T.S., Kim, J.W., Kang, G.H., Park, N.H., Song, Y.S., Kang, S.B. & Lee, H.P. 2006. DNA hypomethylation of CAGE promotors in squamous cell carcinoma of uterine cervix. *Annals of the New York Academy of Sciences,* 1091 (1), pp. 218-224.

Levine, A.J., Puzio-Kuter, A.M., Chan, C.S. & Hainaut, P. 2016. The role of the p53 protein in stem-cell biology and epigenetic regulation. *Cold Spring Harbor perspectives in medicine,* 6 (9), pp. a026153.

Li, G., Miles, A., Line, A. & Rees, R.C. 2004. Identification of tumour antigens by serological analysis of cDNA expression cloning. *Cancer Immunology, Immunotherapy,* 53 (3), pp. 139-143.

Li, M., Goncearenco, A. & Panchenko, A.R. 2017. Annotating mutational effects on proteins and protein interactions: designing novel and revisiting existing protocols. In: Anon*Proteomics.* Springer. pp. 235-260.

Li, R., Pang, X., Chen, W., Li, L., Tian, W. & Zhang, X. 2012. Gastric cancer cell lines AGS before and after CD40 signal activating. Molecular biology reports, 39 (6), pp. 6615-6623.

Li, X., Li, L., Pandey, R., Byun, J.S., Gardner, K., Qin, Z. & Dou, Y. 2012. The histone acetyltransferase MOF is a key regulator of the embryonic stem cell core transcriptional network. Cell stem cell, 11 (2), pp. 163-178.

Lichten, M. & Goldman, A.S. 1995. Meiotic recombination hotspots. *Annual Review of Genetics,* 29 (1), pp. 423-444.

Lin, W., Jin, H., Liu, X., Hampton, K. & Yu, H. 2011. Scc2 regulates gene expression by recruiting cohesin to the chromosome as a transcriptional activator during yeast meiosis. *Molecular biology of the cell,* 22 (12), pp. 1985-1996.

Lindsey, S.F., Byrnes, D.M., Eller, M.S., Rosa, A.M., Dabas, N., Escandon, J. & Grichnik, J.M. 2013. Potential role of meiosis proteins in melanoma chromosomal instability. *Journal of skin cancer,* 2013.

Linley, A.J., Mathieu, M.G., Miles, A.K., Rees, R.C., McArdle, S.E. & Regad, T. 2012. The helicase HAGE expressed by malignant melanoma-initiating cells is required for tumor cell proliferation in vivo. *Journal of Biological Chemistry,* 287 (17), pp. 13633-13643.

Liu, S., Sang, M., Xu, Y., Gu, L., Liu, F. & Shan, B. 2016. Expression of MAGE-A1,-A9,-A11 in laryngeal squamous cell carcinoma and their prognostic significance: a retrospective clinical study. *Acta Oto-Laryngologica,* 136 (5), pp. 506-513.

Loew, R., Heinz, N., Hampf, M., Bujard, H. & Gossen, M. 2010. Improved Tet-responsive promoters with minimized background expression. *BMC biotechnology,* 10 (1), pp. 81.

Longhese, M.P., Bonetti, D., Guerini, I., Manfrini, N. & Clerici, M. 2009. DNA double-strand breaks in meiosis: checking their formation, processing and repair. *DNA repair,* 8 (9), pp. 1127-1138.

Longhese, M.P., Guerini, I., Baldo, V. & Clerici, M. 2008. Surveillance mechanisms monitoring chromosome breaks during mitosis and meiosis. *DNA repair,* 7 (4), pp. 545-557.

Lynch, M. 2005. The origins of eukaryotic gene structure. *Molecular biology and evolution,* 23 (2), pp. 450-468.

Ma, L., O'Connell, J.R., VanRaden, P.M., Shen, B., Padhi, A., Sun, C., Bickhart, D.M., Cole, J.B., Null, D.J. & Liu, G.E. 2015. Cattle sex-specific recombination and genetic control from a large pedigree analysis. *PLoS genetics,* 11 (11), pp. e1005387.

MacLennan, M., Garcia-Canadas, M., Reichmann, J., Khazina, E., Salvador-Palomeque, C., Mann, A., Peressini, P., Sanchez, L., Playfoot, C.J. & Read, D. 2017. Tex19. 1 Restricts LINE-1 Mobilisation in Mouse Embryonic Stem Cells. *bioRxiv,* pp. 102442.

MacQueen, A.J., Colaiácovo, M.P., McDonald, K. & Villeneuve, A.M. 2002. Synapsis-dependent and-independent mechanisms stabilize homolog pairing during meiotic prophase in C. elegans. *Genes & development,* 16 (18), pp. 2428-2442.

Maine, E.A., Westcott, J.M., Prechtl, A.M., Dang, T.T., Whitehurst, A.W. & Pearson, G.W. 2016. The cancer-testis antigens SPANX-A/C/D and CTAG2 promote breast cancer invasion. *Oncotarget,* 7 (12), pp. 14708.

Małuszek, M. 2015. Multifunctionality of MDM2 protein and its role in genomic instability of cancer cells. *Postepy biochemii,* 61 (1), pp. 42-51.

Mariño-Ramírez, L., Spouge, J.L., Kanga, G.C. & Landsman, D. 2004a. Statistical analysis of over-represented words in human promoter sequences. *Nucleic acids research,* 32 (3), pp. 949-958.

Marks, P.A. & Xu, W. 2009. Histone deacetylase inhibitors: Potential in cancer therapy. *Journal of cellular biochemistry,* 107 (4), pp. 600-608.

Marston, A.L. & Amon, A. 2005. Meiosis: cell-cycle controls shuffle and deal. *Nature Reviews Molecular Cell Biology,* 6 (10), pp. 818.

Maus, M.V. and June, C.H., 2016. Making better chimeric antigen receptors for adoptive T-cell therapy.

Maxfield, K.E., Taus, P.J., Corcoran, K., Wooten, J., Macion, J., Zhou, Y., Borromeo, M., Kollipara, R.K., Yan, J. & Xie, Y. 2015. Comprehensive functional characterization of cancer–testis antigens defines obligate participation in multiple hallmarks of cancer. *Nature communications,* 6 pp. 8840.

McCarty, A.S., Kleiger, G., Eisenberg, D. & Smale, S.T. 2003. Selective dimerization of a C2H2 zinc finger subfamily. *Molecular cell,* 11 (2), pp. 459-470.

McFarlane, R.J., Feichtinger, J. & Larcombe, L. 2015. Germline/meiotic genes in cancer: new dimensions. *Cell Cycle,* 14 (6), pp. 791.

McFarlane, R.J., Feichtinger, J. & Larcombe, L. 2014. *Cancer germline gene activation: friend or foe?.*

McFarlane, R.J. & Wakeman, J.A. 2017. Meiosis-like Functions in Oncogenesis: A New View of Cancer. *Cancer research.*

Mecklenburg, I., Sienel, W., Schmid, S., Passlick, B. & Kufer, P. 2017. A Threshold of Systemic MAGE-A Gene Expression Predicting Survival in Resected Non–Small Cell Lung Cancer. *Clinical Cancer Research,* 23 (5), pp. 1213-1219.

Meikar, O., Da Ros, M. & Kotaja, N. 2013. Epigenetic regulation of male germ cell differentiation. In: Anon*Epigenetics: Development and Disease.* Springer. pp. 119-138.

Mellman, I., Coukos, G. & Dranoff, G. 2011. Cancer immunotherapy comes of age. *Nature,* 480 (7378), pp. 480.

Mengus, C., Schultz-Thater, E., Coulot, J., Kastelan, Z., Goluza, E., Coric, M., Spagnoli, G.C. & Hudolin, T. 2013. MAGE-A10 cancer/testis antigen is highly expressed in high-grade non-muscle-invasive bladder carcinomas. *International journal of cancer,* 132 (10), pp. 2459-2463.

Meuwissen, R.L., Offenberg, H.H., Dietrich, A.J., Riesewijk, A., van Iersel, M. & Heyting, C. 1992. A coiled-coil related protein specific for synapsed regions of meiotic prophase chromosomes. *The EMBO journal,* 11 (13), pp. 5091-5100.

Mihola, O., Trachtulec, Z., Vlcek, C., Schimenti, J.C. & Forejt, J. 2009. A mouse speciation gene encodes a meiotic histone H3 methyltransferase. *Science,* 323 (5912), pp. 373-375.

Miller, M.P., Amon, A. & Ünal, E. 2013. Meiosis I: when chromosomes undergo extreme makeover. *Current opinion in cell biology,* 25 (6), pp. 687-696.

Minde, D.P., Anvarian, Z., Rüdiger, S.G. & Maurice, M.M. 2011. Messing up disorder: how do missense mutations in the tumor suppressor protein APC lead to cancer? *Molecular cancer,* 10 (1), pp. 101.

Mirandola, L., J. Cannon, M., Cobos, E., Bernardini, G., Jenkins, M.R., Kast, W.M. & Chiriva-Internati, M. 2011. Cancer testis antigens: novel biomarkers and targetable proteins for ovarian cancer. *International reviews of immunology,* 30 (2-3), pp. 127-137.

Moller, H., Flatt, G. & Moran, A. 2011. High cancer mortality rates in the elderly in the UK. *Cancer epidemiology,* 35 (5), pp. 407-412.

Morgan, R.A., Yang, J.C., Kitano, M., Dudley, M.E., Laurencot, C.M. and Rosenberg, S.A., 2010. Case report of a serious adverse event following the administration of T cells transduced with a chimeric antigen receptor recognizing ERBB2. Molecular Therapy, 18(4), pp.843-851.

Morlacchi, S., Sciandra, F., Bigotti, M.G., Bozzi, M., Hübner, W., Galtieri, A., Giardina, B. & Brancaccio, A. 2012. Insertion of a myc-tag within α-dystroglycan

domains improves its biochemical and microscopic detection. *BMC biochemistry,* 13 (1), pp. 14.

Morris, L.G. & Chan, T.A. 2015. Therapeutic targeting of tumor suppressor genes. *Cancer,* 121 (9), pp. 1357-1368.

Myers, S., Bottolo, L., Freeman, C., McVean, G. & Donnelly, P. 2005. A fine-scale map of recombination rates and hotspots across the human genome. *Science,* 310 (5746), pp. 321-324.

Myers, S., Bowden, R., Tumian, A., Bontrop, R.E., Freeman, C., MacFie, T.S., McVean, G. & Donnelly, P. 2010. Drive against hotspot motifs in primates implicates the PRDM9 gene in meiotic recombination. *Science,* 327 (5967), pp. 876-879.

Myers, S., Freeman, C., Auton, A., Donnelly, P. & McVean, G. 2008. A common sequence motif associated with recombination hot spots and genome instability in humans. *Nature genetics,* 40 (9), pp. 1124.

Nakazawa, T., Kondo, T., Ma, D., Niu, D., Mochizuki, K., Kawasaki, T., Yamane, T., Iino, H., Fujii, H. & Katoh, R. 2012. Global histone modification of histone H3 in colorectal cancer and its precursor lesions. *Human pathology,* 43 (6), pp. 834-842.

Narita, T., Weinert, B.T. & Choudhary, C. 2018. Functions and mechanisms of non-histone protein acetylation. *Nature Reviews Molecular Cell Biology,* pp. 1.

Nassar, D. & Blanpain, C. 2016. Cancer stem cells: basic concepts and therapeutic implications. *Annual Review of Pathology: Mechanisms of Disease,* 11 pp. 47-76.

Neale, M.J. & Keeney, S. 2006. Clarifying the mechanics of DNA strand exchange in meiotic recombination. *Nature,* 442 (7099), pp. 153.

Negrini, S., Gorgoulis, V.G. & Halazonetis, T.D. 2010. Genomic instability—an evolving hallmark of cancer. *Nature reviews Molecular cell biology,* 11 (3), pp. 220.

Nei, M. 2007. The new mutation theory of phenotypic evolution. *Proceedings of the National Academy of Sciences,* 104 (30), pp. 12235-12242.

Nielsen, A. & Gjerstorff, M. 2016. Ectopic expression of testis germ cell proteins in cancer and its potential role in genomic instability. *International journal of molecular sciences,* 17 (6), pp. 890.

Nielsen, A.L., Oulad-Abdelghani, M., Ortiz, J.A., Remboutsika, E., Chambon, P. & Losson, R. 2001. Heterochromatin formation in mammalian cells: interaction between histones and HP1 proteins. *Molecular cell,* 7 (4), pp. 729-739.

Nishikawa, H., Maeda, Y., Ishida, T., Gnjatic, S., Sato, E., Mori, F., Sugiyama, D., Ito, A., Fukumori, Y. & Utsunomiya, A. 2012. Cancer/testis antigens are novel targets of immunotherapy for adult T-cell leukemia/lymphoma. *Blood,* pp. bloo-379982.

Nishikawa, N., Toyota, M., Suzuki, H., Honma, T., Fujikane, T., Ohmura, T., Nishidate, T., Ohe-Toyota, M., Maruyama, R. & Sonoda, T. 2007. Gene amplification and overexpression of PRDM14 in breast cancers. *Cancer research,* 67 (20), pp. 9649-9657.

Nottke, A., Colaiácovo, M.P. & Shi, Y. 2009. Developmental roles of the histone lysine demethylases. *Development,* 136 (6), pp. 879-889.

Nowick, K., Carneiro, M. & Faria, R. 2013. A prominent role of KRAB-ZNF transcription factors in mammalian speciation? *Trends in Genetics,* 29 (3), pp. 130-139.

O'Shea, J.J., Kanno, Y. & Chan, A.C. 2014. In search of magic bullets: the golden age of immunotherapeutics. *Cell,* 157 (1), pp. 227-240.

Öllinger, R., Childs, A.J., Burgess, H.M., Speed, R.M., Lundegaard, P.R., Reynolds, N., Gray, N.K., Cooke, H.J. & Adams, I.R. 2008. Deletion of the pluripotency-associated Tex19. 1 gene causes activation of endogenous retroviruses and defective spermatogenesis in mice. *PLoS genetics,* 4 (9), pp. e1000199.

Orkin, S.H., Kazazian, H.H., Antonarakis, S.E., Goff, S.C., Boehm, C.D., Sexton, J.P., Waber, P.G. & Giardina, P.J. 1982. Linkage of β-thalassaemia mutations and β-globin gene polymorphisms with DNA polymorphisms in human β-globin gene cluster. *Nature,* 296 (5858), pp. 627-631.

Ovalle, W.K. & Nahirney, P.C. 2013. *Netter's Essential Histology E-Book.* Elsevier Health Sciences.

Page, S.L. & Hawley, R.S. 2004. The genetics and molecular biology of the synaptonemal complex. *Annu.Rev.Cell Dev.Biol.,* 20 pp. 525-558.

Pagotto, A., Caballero, O.L., Volkmar, N., Devalle, S., Simpson, A.J., Lu, X. & Christianson, J.C. 2013. Centrosomal localisation of the cancer/testis (CT) antigens NY-ESO-1 and MAGE-C1 is regulated by proteasome activity in tumour cells. *PloS one,* 8 (12), pp. e83212.

Paigen, K. & Petkov, P. 2010. Mammalian recombination hot spots: properties, control and evolution. *Nature Reviews Genetics,* 11 (3), pp. 221.

Paigen, K. & Petkov, P.M. 2018. PRDM9 and its role in genetic recombination. *Trends in Genetics.*

Pal, S. & Sif, S. 2007. Interplay between chromatin remodelers and protein arginine methyltransferases. *Journal of cellular physiology,* 213 (2), pp. 306-315.

Pan, J., Sasaki, M., Kniewel, R., Murakami, H., Blitzblau, H.G., Tischfield, S.E., Zhu, X., Neale, M.J., Jasin, M. & Socci, N.D. 2011. A hierarchical combination of factors shapes the genome-wide topography of yeast meiotic recombination initiation. *Cell,* 144 (5), pp. 719-731.

Pâques, F. & Haber, J.E. 1999. Multiple pathways of recombination induced by double-strand breaks in Saccharomyces cerevisiae. *Microbiology and molecular biology reviews,* 63 (2), pp. 349-404.

Parvanov, E.D., Petkov, P.M. & Paigen, K. 2010. Prdm9 controls activation of mammalian recombination hotspots. *Science,* 327 (5967), pp. 835.

Parvanov, E.D., Tian, H., Billings, T., Saxl, R.L., Spruce, C., Aithal, R., Krejci, L., Paigen, K. & Petkov, P.M. 2017. PRDM9 interactions with other proteins provide a link between recombination hotspots and the chromosomal axis in meiosis. *Molecular biology of the cell,* 28 (3), pp. 488-499.

Patel, A., Horton, J.R., Wilson, G.G., Zhang, X. & Cheng, X. 2016. Structural basis for human PRDM9 action at recombination hot spots. *Genes & development,* 30 (3), pp. 257-265.

Patel, A., Zhang, X., Blumenthal, R.M. & Cheng, X. 2017. Structural basis of human PRDM9 allele C specific recognition of its cognate DNA sequence. *Journal of Biological Chemistry,* pp. jbc. M117. 805754.

Pousette, Å., Leijonhufvud, P., Arver, S., Kvist, U., Pelttari, J. and Höög, C., 1997. Presence of synaptonemal complex protein 1 transversal filament-like protein in human primary spermatocytes. Human reproduction, 12(11), pp.2414-2417.

Peinado, H., Ballestar, E., Esteller, M. & Cano, A. 2004. Snail mediates E-cadherin repression by the recruitment of the Sin3A/histone deacetylase 1 (HDAC1)/HDAC2 complex. *Molecular and cellular biology,* 24 (1), pp. 306-319.

Pena, P.V., Hom, R.A., Hung, T., Lin, H., Kuo, A.J., Wong, R., Subach, O.M., Champagne, K.S., Zhao, R. & Verkhusha, V.V. 2008. Histone H3K4me3 binding is required for the DNA repair and apoptotic activities of ING1 tumor suppressor. *Journal of Molecular Biology,* 380 (2), pp. 303-312.

Petes, T.D. 2001. Meiotic recombination hot spots and cold spots. *Nature Reviews Genetics,* 2 (5), pp. 360.

Petronczki, M., Siomos, M.F. & Nasmyth, K. 2003. Un menage a quatre: the molecular biology of chromosome segregation in meiosis. *Cell,* 112 (4), pp. 423-440.

Planells-Palop, V., Hazazi, A., Feichtinger, J., Jezkova, J., Thallinger, G., Alsiwiehri, N.O., Almutairi, M., Parry, L., Wakeman, J.A. & McFarlane, R.J. 2017. Human germ/stem cell-specific gene TEX19 influences cancer cell proliferation and cancer prognosis. *Molecular cancer,* 16 (1), pp. 84.

Ponting, C.P. 2011. What are the genomic drivers of the rapid evolution of PRDM9? *Trends in Genetics,* 27 (5), pp. 165-171.

Powers, N.R., Parvanov, E.D., Baker, C.L., Walker, M., Petkov, P.M. & Paigen, K. 2016. The meiotic recombination activator PRDM9 trimethylates both H3K36 and H3K4 at recombination hotspots in vivo. *PLoS genetics,* 12 (6), pp. e1006146.

Prabhu, V.V., Hong, B., Allen, J.E., Zhang, S., Lulla, A., Dicker, D.T. & El-Deiry, W.S. 2016. Small molecule prodigiosin restores p53 tumor suppressor activity in chemoresistant colorectal cancer stem cells via c-Jun-mediated ΔNp73 inhibition and p73 activation. *Cancer research,* pp. canres. 2430.2014.

Pratto, F., Brick, K., Khil, P., Smagulova, F., Petukhova, G.V. & Camerini-Otero, R.D. 2014. Recombination initiation maps of individual human genomes. *Science,* 346 (6211), pp. 1256442.

Qiu, Z., Wang, J. & Wu, Y. 2018. The Landscape of Histone Modification in Cancer Metastasis. In: Anon*Cancer Metastasis.* IntechOpen.

Ramakrishnan, S., Ku, S., Ciamporcero, E., Miles, K.M., Attwood, K., Chintala, S., Shen, L., Ellis, L., Sotomayor, P. & Swetzig, W. 2016. HDAC 1 and 6 modulate cell invasion and migration in clear cell renal cell carcinoma. *BMC cancer,* 16 (1), pp. 617.

Ramos, C.A., Savoldo, B. and Dotti, G., 2014. CD19-CAR trials. Cancer journal (Sudbury, Mass.), 20(2), p.112.

Rajagopalan K, Mooney SM, Parekh N, Getzenberg RH, Kulkarni P: A majority of the cancer/testis antigens are intrinsically disordered proteins. J Cell Biochem. 2011, 112 (11): 3256-3267. 10.1002/jcb.23252.

Reichmann, J., Dobie, K., Lister, L.M., Best, D., Crichton, J.H., MacLennan, M., Read, D., Raymond, E.S., Hung, C. & Boyle, S. 2017. Tex19. 1 regulates acetylated SMC3 cohesin and prevents aneuploidy in mouse Oocytes. *bioRxiv,* pp. 102285.

Reichmann, J., Reddington, J.P., Best, D., Read, D., Öllinger, R., Meehan, R.R. & Adams, I.R. 2013. The genome-defence gene Tex19. 1 suppresses LINE-1 retrotransposons in the placenta and prevents intra-uterine growth retardation in mice. *Human molecular genetics,* 22 (9), pp. 1791-1806.

Remeseiro, S., Cuadrado, A., Carretero, M., Martínez, P., Drosopoulos, W.C., Cañamero, M., Schildkraut, C.L., Blasco, M.A. & Losada, A. 2012. Cohesin-SA1 deficiency drives aneuploidy and tumourigenesis in mice due to impaired replication of telomeres. *The EMBO journal,* 31 (9), pp. 2076-2089.

Ren, B., Wei, X., Zou, G., He, J., Xu, G., Xu, F., Huang, Y., Zhu, H., Li, Y. & Ma, G. 2016. Cancer testis antigen SPAG9 is a promising marker for the diagnosis and treatment of lung cancer. *Oncology reports,* 35 (5), pp. 2599-2605.

Renkvist, N., Castelli, C., Robbins, P.F. & Parmiani, G. 2001. A listing of human tumor antigens recognized by T cells. *Cancer Immunology, Immunotherapy,* 50 (1), pp. 3-15.

Rifkin, S.A., Houle, D., Kim, J. & White, K.P. 2005. A mutation accumulation assay reveals a broad capacity for rapid evolution of gene expression. *Nature,* 438 (7065), pp. 220.

Rivera, M., Wu, Q., Hamerlik, P., Hjelmeland, A.B., Bao, S. & Rich, J.N. 2015. Acquisition of meiotic DNA repair regulators maintain genome stability in glioblastoma. *Cell death & disease,* 6 (4), pp. e1732.

Robert, T., Nore, A., Brun, C., Maffre, C., Crimi, B., Guichard, V., Bourbon, H. & de Massy, B. 2016. The TopoVIB-Like protein family is required for meiotic DNA double-strand break formation. *Science,* 351 (6276), pp. 943-949.

Rodenhuis, S. 1992. ras And human tumors. *Seminars in cancer biology.* pp. 241.

Romanienko, P.J. & Camerini-Otero, R.D. 2000. The mouse Spo11 gene is required for meiotic chromosome synapsis. *Molecular cell,* 6 (5), pp. 975-987.

Rosa, A.M., Dabas, N., Byrnes, D.M., Eller, M.S. & Grichnik, J.M. 2012. Germ cell proteins in melanoma: prognosis, diagnosis, treatment, and theories on expression. *Journal of skin cancer,* 2012.

Rossi, F., Molnar, C., Hashiyama, K., Heinen, J.P., Pampalona, J., Llamazares, S., Reina, J., Hashiyama, T., Rai, M. & Pollarolo, G. 2017. An in vivo genetic screen in Drosophila identifies the orthologue of human cancer/testis gene SPO11 among a network of targets to inhibit lethal (3) malignant brain tumour growth. *Open biology,* 7 (8), pp. 170156.

Roth, S.Y., Denu, J.M. & Allis, C.D. 2001. Histone acetyltransferases. *Annual Review of Biochemistry,* 70 (1), pp. 81-120.

Rousseaux, S., Debernardi, A., Jacquiau, B., Vitte, A., Vesin, A., Nagy-Mignotte, H., Moro-Sibilot, D., Brichon, P., Lantuejoul, S. & Hainaut, P. 2013a. Ectopic activation of germline and placental genes identifies aggressive metastasis-prone lung cancers. *Science translational medicine,* 5 (186), pp. 186ra66.

Roy, N.K., Bordoloi, D., Monisha, J., Anip, A., Padmavathi, G. & Kunnumakkara, A.B. 2017. Cancer—An Overview and Molecular Alterations in Cancer. In: Anon*Fusion Genes And Cancer.* World Scientific. pp. 1-15.

Sammut, S.J., Feichtinger, J., Stuart, N., Wakeman, J.A., Larcombe, L. & McFarlane, R.J. 2014. A novel cohort of cancer-testis biomarker genes revealed through meta-analysis of clinical data sets. *Oncoscience,* 1 (5), pp. 349.

Sandor, C., Li, W., Coppieters, W., Druet, T., Charlier, C. & Georges, M. 2012. Genetic variants in REC8, RNF212, and PRDM9 influence male recombination in cattle. *PLoS genetics,* 8 (7), pp. e1002854.

Santos-Rosa, H., Schneider, R., Bannister, A.J., Sherriff, J., Bernstein, B.E., Emre, N.T., Schreiber, S.L., Mellor, J. & Kouzarides, T. 2002. Active genes are tri-methylated at K4 of histone H3. *Nature,* 419 (6905), pp. 407.

Sawan, C. & Herceg, Z. 2010. Histone modifications and cancer. In: Anon*Advances in genetics.* Elsevier. pp. 57-85.

Scanlan, M.J., Altorki, N.K., Gure, A.O., Williamson, B., Jungbluth, A., Chen, Y. & Old, L.J. 2000. Expression of cancer-testis antigens in lung cancer: definition of bromodomain testis-specific gene (BRDT) as a new CT gene, CT9. *Cancer letters,* 150 (2), pp. 155-164.

Schild-Prüfert, K., Saito, T.T., Smolikov, S., Gu, Y., Hincapie, M., Hill, D.E., Vidal, M., McDonald, K. & Colaiácovo, M.P. 2011. Organization of the synaptonemal complex during meiosis in Caenorhabditis elegans. *Genetics,* pp. genetics. 111.132431.

Schramm, S., Fraune, J., Naumann, R., Hernandez-Hernandez, A., H   g, C., Cooke, H.J., Alsheimer, M. & Benavente, R. 2011. A novel mouse synaptonemal complex protein is essential for loading of central element proteins, recombination, and fertility. *PLoS genetics,* 7 (5), pp. e1002088.

Ségurel, L. 2013. The complex binding of PRDM9. *Genome biology,* 14 (4), pp. 112.

Shang, B., Gao, A., Pan, Y., Zhang, G., Tu, J., Zhou, Y., Yang, P., Cao, Z., Wei, Q. & Ding, Y. 2014. CT45A1 acts as a new proto-oncogene to trigger tumorigenesis and cancer metastasis. *Cell death & disease,* 5 (6), pp. e1285.

Sharma, S., Kelly, T.K. & Jones, P.A. 2010. Epigenetics in cancer. *Carcinogenesis,* 31 (1), pp. 27-36.

Shin, Y., Choi, Y., Erdin, S.U., Yatsenko, S.A., Kloc, M., Yang, F., Wang, P.J., Meistrich, M.L. & Rajkovic, A. 2010a. Hormad1 mutation disrupts synaptonemal complex formation, recombination, and chromosome segregation in mammalian meiosis. *PLoS genetics,* 6 (11), pp. e1001190.

Siciliano, V., Caliendo, F. and Dukhinova, M., 2019. Engineered cell-based therapeutics: synthetic biology meets immunology. Frontiers in Bioengineering and Biotechnology, 7, p.43.

Siegel, R.L., Miller, K.D. & Jemal, A. 2017. Cancer statistics, 2017. *CA: a cancer journal for clinicians,* 67 (1), pp. 7-30.

Siegel, R., DeSantis, C., Virgo, K., Stein, K., Mariotto, A., Smith, T., Cooper, D., Gansler, T., Lerro, C. & Fedewa, S. 2012. Cancer treatment and survivorship statistics, 2012. *CA: a cancer journal for clinicians,* 62 (4), pp. 220-241.

Silkworth, W.T. & Cimini, D. 2012. Transient defects of mitotic spindle geometry and chromosome segregation errors. *Cell division,* 7 (1), pp. 19.

Simpson, A.J., Caballero, O.L., Jungbluth, A., Chen, Y. & Old, L.J. 2005. Cancer/testis antigens, gametogenesis and cancer. *Nature Reviews Cancer,* 5 (8), pp. 615.

Singh, A.M. & Dalton, S. 2014. Cell cycle regulation of pluripotent stem cells. *Stem cells: from basic research to therapy: basic stem cell biology, tissue formation during development, and model organisms,* 1 (3)

Sjögren, C. & Nasmyth, K. 2001. Sister chromatid cohesion is required for postreplicative double-strand break repair in Saccharomyces cerevisiae. *Current Biology,* 11 (12), pp. 991-995.

Skibbens, R.V., Colquhoun, J.M., Green, M.J., Molnar, C.A., Sin, D.N., Sullivan, B.J. & Tanzosh, E.E. 2013. Cohesinopathies of a feather flock together. *PLoS genetics,* 9 (12), pp. e1004036.

Smagulova, F., Gregoretti, I.V., Brick, K., Khil, P., Camerini-Otero, R.D. & Petukhova, G.V. 2011. Genome-wide analysis reveals novel molecular features of mouse recombination hotspots. *Nature,* 472 (7343), pp. 375.

Smolikov, S., Eizinger, A., Schild-Prufert, K., Hurlburt, A., McDonald, K., Engebrecht, J., Villeneuve, A.M. & Colaiácovo, M.P. 2007. SYP-3 restricts synaptonemal complex assembly to bridge paired chromosome axes during meiosis in C. elegans. *Genetics.*

Smolikov, S., Schild-Prüfert, K. & Colaiacovo, M.P. 2009. A yeast two-hybrid screen for SYP-3 interactors identifies SYP-4, a component required for synaptonemal

complex assembly and chiasma formation in Caenorhabditis elegans meiosis. *PLoS genetics,* 5 (10), pp. e1000669.

Solit, D.B., Garraway, L.A., Pratilas, C.A., Sawai, A., Getz, G., Basso, A., Ye, Q., Lobo, J.M., She, Y. & Osman, I. 2006. BRAF mutation predicts sensitivity to MEK inhibition. *Nature,* 439 (7074), pp. 358.

Song, M., Kim, Y., Lee, J., Lee, C. & Lee, S. 2016. Cancer/testis antigen NY-SAR-35 enhances cell proliferation, migration, and invasion. *International journal of oncology,* 48 (2), pp. 569-576.

Sonnenschein, C. & Soto, A.M. 2013. The aging of the 2000 and 2011 Hallmarks of Cancer reviews: a critique. *Journal of Biosciences,* 38 (3), pp. 651-663.

Soper, S.F., van der Heijden, Godfried W, Hardiman, T.C., Goodheart, M., Martin, S.L., de Boer, P. & Bortvin, A. 2008. Mouse maelstrom, a component of nuage, is essential for spermatogenesis and transposon repression in meiosis. *Developmental cell,* 15 (2), pp. 285-297.

Soriano, A.O., Yang, H., Faderl, S., Estrov, Z., Giles, F., Ravandi, F., Cortes, J., Wierda, W.G., Ouzounian, S. & Quezada, A. 2007. Safety and clinical activity of the combination of 5-azacytidine, valproic acid, and all-trans retinoic acid in acute myeloid leukemia and myelodysplastic syndrome. *Blood,* 110 (7), pp. 2302-2308.

Sorrentino, A., Federico, A., Rienzo, M., Gazzerro, P., Bifulco, M., Ciccodicola, A., Casamassimi, A. & Abbondanza, C. 2018. PR/SET Domain Family and Cancer: Novel Insights from The Cancer Genome Atlas. *International journal of molecular sciences,* 19 (10), pp. 3250.

Souhami, R. & Tobias, J.S. 2008. *Cancer and its management.* John Wiley & Sons.

Sterner, D.E. & Berger, S.L. 2000. Acetylation of histones and transcription-related factors. *Microbiology and Molecular Biology Reviews,* 64 (2), pp. 435-459.

Sterner, R., Vidali, G. & Allfrey, V.G. 1979. Studies of acetylation and deacetylation in high mobility group proteins. Identification of the sites of acetylation in HMG-1. *Journal of Biological Chemistry,* 254 (22), pp. 11577-11583.

Storlazzi, A., Tessé, S., Gargano, S., James, F., Kleckner, N. & Zickler, D. 2003. Meiotic double-strand breaks at the interface of chromosome movement, chromosome remodeling, and reductional division. *Genes & development,* 17 (21), pp. 2675-2687.

Strahl, B.D. & Allis, C.D. 2000. The language of covalent histone modifications. *Nature,* 403 (6765), pp. 41.

Stratton, M.R., Campbell, P.J. & Futreal, P.A. 2009. The cancer genome. *Nature,* 458 (7239), pp. 719.

Stubbs, M. & Suleyman, N. 2015. *Cell Biology and Genetics.* Mosby.

Sun, F., Fujiwara, Y., Reinholdt, L.G., Hu, J., Saxl, R.L., Baker, C.L., Petkov, P.M., Paigen, K. & Handel, M.A. 2015. Nuclear localization of PRDM9 and its role in

meiotic chromatin modifications and homologous synapsis. *Chromosoma,* 124 (3), pp. 397-415.

Sura, W., Kabza, M., Karlowski, W.M., Bieluszewski, T., Kus-Slowinska, M., Pawełoszek, Ł, Sadowski, J. & Ziolkowski, P.A. 2017. Dual role of the histone variant H2A. Z in transcriptional regulation of stress-response genes. *The Plant Cell,* 29 (4), pp. 791-807.

Surget, S., Khoury, M.P. & Bourdon, J. 2014. Uncovering the role of p53 splice variants in human malignancy: a clinical perspective. *OncoTargets and therapy,* 7 pp. 57.

Tarabay, Y., Kieffer, E., Teletin, M., Celebi, C., Van Montfoort, A., Zamudio, N., Achour, M., El Ramy, R., Gazdag, E. & Tropel, P. 2013. The mammalian-specific Tex19. 1 gene plays an essential role in spermatogenesis and placenta-supported development. *Human reproduction,* 28 (8), pp. 2201-2214.

Tauchi, H. 2000. Positional cloning and functional analysis of the gene responsible for Nijmegen breakage syndrome, NBS1. *Journal of radiation research,* 41 (1), pp. 9-17.

Terpe, K. 2003. Overview of tag protein fusions: from molecular and biochemical fundamentals to commercial systems. *Applied Microbiology and Biotechnology,* 60 (5), pp. 523-533.

Tessarz, P. & Kouzarides, T. 2014. Histone core modifications regulating nucleosome structure and dynamics. *Nature reviews Molecular cell biology,* 15 (11), pp. 703.

Thoma, C.R., Toso, A., Meraldi, P. & Krek, W. 2011. Mechanisms of aneuploidy and its suppression by tumour suppressor proteins. *Swiss medical weekly,* 141 pp. w13170.

Thomas, J.H., Emerson, R.O. & Shendure, J. 2009. Extraordinary molecular evolution in the PRDM9 fertility gene. *PloS one,* 4 (12), pp. e8505.

Tock, A.J. & Henderson, I.R. 2018. Hotspots for initiation of meiotic recombination. *Frontiers in genetics,* 9.

Tokarew, N., Ogonek, J., Endres, S., von Bergwelt-Baildon, M. and Kobold, S., 2019. Teaching an old dog new tricks: next-generation CAR T cells. British journal of cancer, 120(1), pp.26-37.

Tortora, G.J. & Derrickson, B.H. 2008. *Principles of anatomy and physiology.* John Wiley & Sons.

Trego, K.S., Groesser, T., Davalos, A.R., Parplys, A.C., Zhao, W., Nelson, M.R., Hlaing, A., Shih, B., Rydberg, B. & Pluth, J.M. 2016. Non-catalytic roles for XPG with BRCA1 and BRCA2 in homologous recombination and genome stability. *Molecular cell,* 61 (4), pp. 535-546.

Türeci, Ö, Sahin, U., Zwick, C., Koslowski, M., Seitz, G. & Pfreundschuh, M. 1998. Identification of a meiosis-specific protein as a member of the class of cancer/testis antigens. *Proceedings of the National Academy of Sciences,* 95 (9), pp. 5211-5216.

Ünal, E., Heidinger-Pauli, J.M., Kim, W., Guacci, V., Onn, I., Gygi, S.P. & Koshland, D.E. 2008. A molecular determinant for the establishment of sister chromatid cohesion. *Science,* 321 (5888), pp. 566-569.

Urlinger, S., Baron, U., Thellmann, M., Hasan, M.T., Bujard, H. & Hillen, W. 2000. Exploring the sequence space for tetracycline-dependent transcriptional activators: novel mutations yield expanded range and sensitivity. *Proceedings of the National Academy of Sciences,* 97 (14), pp. 7963-7968.

van der Bruggen, P., Traversari, C., Chomez, P., Lurquin, C., De Plaen, E., Van den Eynde, B., Knuth, A. & Boon, T. 1991. A gene encoding an antigen recognized by cytolytic T lymphocytes on a human melanoma. *Science,* 254 (5038), pp. 1643-1647.

Vervoort, M., Meulemeester, D., Béhague, J. & Kerner, P. 2015. Evolution of Prdm genes in animals: insights from comparative genomics. *Molecular biology and evolution,* 33 (3), pp. 679-696.

Vigna, E., Cavalieri, S., Ailles, L., Geuna, M., Loew, R., Bujard, H. & Naldini, L. 2002. Robust and efficient regulation of transgene expression in vivo by improved tetracycline-dependent lentiviral vectors. *Molecular therapy,* 5 (3), pp. 252-261.

Vogelstein, B. & Kinzler, K.W. 2004. Cancer genes and the pathways they control. Nature medicine, 10 (8), pp. 789.

Walczak, C.E., Cai, S. & Khodjakov, A. 2010. Mechanisms of chromosome behaviour during mitosis. *Nature reviews Molecular cell biology,* 11 (2), pp. 91.

Wang, C., Gu, Y., Zhang, K., Xie, K., Zhu, M., Dai, N., Jiang, Y., Guo, X., Liu, M. & Dai, J. 2016a. Systematic identification of genes with a cancer-testis expression pattern in 19 cancer types. Nature communications, 7 pp. 10499.

Wang, H., Cao, R., Xia, L., Erdjument-Bromage, H., Borchers, C., Tempst, P. & Zhang, Y. 2001. Purification and functional characterization of a histone H3-lysine 4-specific methyltransferase. *Molecular cell,* 8 (6), pp. 1207-1217.

Wang, P.J., McCarrey, J.R., Yang, F. & Page, D.C. 2001. An abundance of X-linked genes expressed in spermatogonia. *Nature genetics,* 27 (4), pp. 422.

Wang, Y., Miao, X., Liu, Y., Li, F., Liu, Q., Sun, J. & Cai, L. 2014. Dysregulation of histone acetyltransferases and deacetylases in cardiovascular diseases. Oxidative medicine and cellular longevity, 2014.

Ward, A., Hopkins, J., Mckay, M., Murray, S. & Jordan, P.W. 2016. Genetic interactions between the meiosis-specific cohesin components, STAG3, REC8 and RAD21L. *G3: Genes, Genomes, Genetics,* pp. g3. 116.029462.

Washio, M., Mori, M., Mikami, K., Miki, T., Watanabe, Y., Nakao, M. & Tamakoshi, A. 2016. Risk Factors for Upper and Lower Urinary Tract Cancer Death in a Japanese Population: Findings from the Japan Collaborative Cohort Study for Evaluation of Cancer Risk (JACC Study. *Asian Pac J Cancer Prev,* 17 pp. 3545-3549.

Watkins, J., Weekes, D., Shah, V., Gazinska, P., Joshi, S., Sidhu, B., Gillett, C., Pinder, S., Vanoli, F. & Jasin, M. 2015. Genomic complexity profiling reveals that

HORMAD1 overexpression contributes to homologous recombination deficiency in triple-negative breast cancers. *Cancer discovery,* 5 (5), pp. 488-505.

Weiderpass, E. 2010. Lifestyle and cancer risk. *J Prev Med Public Health,* 43 (6), pp. 459-471.

Weinberg, R. 2013. *The biology of cancer.* Garland science.

Welch, J.S., Ley, T.J., Link, D.C., Miller, C.A., Larson, D.E., Koboldt, D.C., Wartman, L.D., Lamprecht, T.L., Liu, F. & Xia, J. 2012. The origin and evolution of mutations in acute myeloid leukemia. *Cell,* 150 (2), pp. 264-278.

Whitehurst, A.W. 2014. Cause and consequence of cancer/testis antigen activation in cancer. *Annual Review of Pharmacology and Toxicology,* 54 pp. 251-272.

Wischnewski, F., Friese, O., Pantel, K. & Schwarzenbach, H. 2007. Methyl-CpG binding domain proteins and their involvement in the regulation of the MAGE-A1, MAGE-A2, MAGE-A3, and MAGE-A12 gene promoters. *Molecular Cancer Research,* 5 (7), pp. 749-759.

Wojtasz, L., Daniel, K., Roig, I., Bolcun-Filas, E., Xu, H., Boonsanay, V., Eckmann, C.R., Cooke, H.J., Jasin, M. & Keeney, S. 2009. Mouse HORMAD1 and HORMAD2, two conserved meiotic chromosomal proteins, are depleted from synapsed chromosome axes with the help of TRIP13 AAA-ATPase. *PLoS genetics,* 5 (10), pp. e1000702.

Wood, A. & Shilatifard, A. 2004. Posttranslational modifications of histones by methylation. In: Anon*Advances in protein chemistry.* Elsevier. pp. 201-222.

Wright, W.D., Shah, S.S. & Heyer, W. 2018. Homologous recombination and the repair of DNA double-strand breaks. *Journal of Biological Chemistry,* 293 (27), pp. 10524-10535.

Wu, C. & Bekaii-Saab, T. 2012. CpG island methylation, microsatellite instability, and BRAF mutations and their clinical application in the treatment of colon cancer. *Chemotherapy Research and Practice,* 2012.

Wu, H., Mathioudakis, N., Diagouraga, B., Dong, A., Dombrovski, L., Baudat, F., Cusack, S., de Massy, B. & Kadlec, J. 2013. Molecular basis for the regulation of the H3K4 methyltransferase activity of PRDM9. *Cell reports,* 5 (1), pp. 13-20.

Yamada, S., Kim, S., Tischfield, S.E., Jasin, M., Lange, J. & Keeney, S. 2017. Genomic and chromatin features shaping meiotic double-strand break formation and repair in mice. *Cell Cycle,* 16 (20), pp. 1870-1884.

Yamada, T. & Ohta, K. 2013. Initiation of meiotic recombination in chromatin structure. *The Journal of Biochemistry,* 154 (2), pp. 107-114.

Yamaji, M., Seki, Y., Kurimoto, K., Yabuta, Y., Yuasa, M., Shigeta, M., Yamanaka, K., Ohinata, Y. & Saitou, M. 2008. Critical function of Prdm14 for the establishment of the germ cell lineage in mice. *Nature genetics,* 40 (8), pp. 1016.

Yan, J., Jiang, J., Lim, C.A., Wu, Q., Ng, H. & Chin, K. 2007. BLIMP1 regulates cell growth through repression of p53 transcription. *Proceedings of the National Academy of Sciences,* 104 (6), pp. 1841-1846.

Yang, F., Cheng, Y., An, J.Y., Kwon, Y.T., Eckardt, S., Leu, N.A., McLaughlin, K.J. & Wang, P.J. 2010. The ubiquitin ligase Ubr2, a recognition E3 component of the N-end rule pathway, stabilizes Tex19. 1 during spermatogenesis. *PloS one,* 5 (11), pp. e14017.

Yang, P., Huo, Z., Liao, H. & Zhou, Q. 2015. Cancer/testis antigens trigger epithelial-mesenchymal transition and genesis of cancer stem-like cells. *Current pharmaceutical design,* 21 (10), pp. 1292-1300.

Yoshida, K. & Miki, Y. 2004. Role of BRCA1 and BRCA2 as regulators of DNA repair, transcription, and cell cycle in response to DNA damage. *Cancer science,* 95 (11), pp. 866-871.

Yuan, H. & Marmorstein, R. 2013. Histone acetyltransferases: Rising ancient counterparts to protein kinases. *Biopolymers,* 99 (2), pp. 98-111.

Zhang, B.N., Venegas, A.B., Hickson, I.D. & Chu, W.K. 2019. DNA replication stress and its impact on chromosome segregation and tumorigenesis. *Seminars in cancer biology.* Elsevier. pp. 61.

Zhang, J., Shi, X., Li, Y., Kim, B., Jia, J., Huang, Z., Yang, T., Fu, X., Jung, S.Y. & Wang, Y. 2008. Acetylation of Smc3 by Eco1 is required for S phase sister chromatid cohesion in both human and yeast. *Molecular cell,* 31 (1), pp. 143-151.

Zhang, K. & Dent, S.Y. 2005. Histone modifying enzymes and cancer: going beyond histones. *Journal of cellular biochemistry,* 96 (6), pp. 1137-1148.

Zhang, S., Zhou, L., Hong, B., van den Heuvel, A Pieter J, Prabhu, V.V., Warfel, N.A., Kline, C.L.B., Dicker, D.T., Kopelovich, L. & El-Deiry, W.S. 2015. Small molecule NSC59984 restores p53 pathway signaling and anti-tumor effects against colorectal cancer via p73 activation and degradation of mutant p53. *Cancer research,* pp. canres. 1079.2013.

Zhang, S., Zhai, X., Wang, G., Feng, J., Zhu, H., Xu, L., Mao, G. & Huang, J. 2015. High expression of MAGE-A9 in tumor and stromal cells of non-small cell lung cancer was correlated with patient poor survival. *International journal of clinical and experimental pathology,* 8 (1), pp. 541.

Zhao, L., Mou, D., Leng, X., Peng, J., Wang, W., Huang, L., Li, S. & Zhu, J. 2004. Expression of cancer-testis antigens in hepatocellular carcinoma. *World journal of gastroenterology: WJG,* 10 (14), pp. 2034.

Zhong, J., Chen, Y., Liao, X., Li, J., Wang, H., Wu, C., Zou, X., Yang, G., Shi, J. & Luo, L. 2016. Testis expressed 19 is a novel cancer-testis antigen expressed in bladder cancer. *Tumor Biology,* 37 (6), pp. 7757-7765.

Zickler, D. & Kleckner, N. 1998. The leptotene-zygotene transition of meiosis. *Annual Review of Genetics,* 32 (1), pp. 619-697.

Zickler, D. 2006. From early homologue recognition to synaptonemal complex formation. *Chromosoma,* 115 (3), pp. 158-174.

Zou, C., Shen, J., Tang, Q., Yang, Z., Yin, J., Li, Z., Xie, X., Huang, G., Lev, D. & Wang, J. 2012. Cancer-testis antigens expressed in osteosarcoma identified by

gene microarray correlate with a poor patient prognosis. *Cancer,* 118 (7), pp. 1845-1855.

9. Appendix

9.1.
A) PRDM9 sequence

MSPEKSQEESPEEDTERTERKPMVKDAFKDISIYFTKEEWAEMGDWEKTRYRNVKRNYNALI
TIGLRATRPAFMCHRRQAIKLQVDDTEDSDEEWTPRQQVKPPWMALRVEQRKHQKGMPKASF
SNESSLKELSRTANLLNASGSEQAQKPVSPSGEASTSGQHSRLKLELRKKETERKMYSLRER
KGHAYKEVSEPQDDDYLYCEMCQNFFIDSCAAHGPPTFVKDSAVDKGHPNRSALSLPPGLRI
GPSGIPQAGLGVWNEASDLPLGLHFGPYEGRITEDEEAANNGYSWLITKGRNCYEYVDGKDK
SWANWMRYVNCARDDEEQNLVAFQYHRQIFYRTCRVIRPGCELLVWYGDEYGQELGIKWGSK
WKKELMAGREPKPEIHPCPSCCLAFSSQKFLSQHVERNHSSQNFPGPSARKLLQPENPCPGD
QNQEQQYPDPHSRNDKTKGQEIKERSKLLNKRTWQREISRAFSSPPKGQMGSCRVGKRIMEE
ESRTGQKVNPGNTGKLFVGVGISRIAKVKYGECGQGFSVKSDVITHQRTHTGEKLYVCRECG
RGFSWKSHLLIHQRIHTGEKPYVCRECGRGFSWQSVLLTHQRTHTGEKPYVCRECGRGFSRQ
SVLLTHQRRHTGEKPYVCRECGRGFSRQSVLLTHQRRHTGEKPYVCRECGRGFSWQSVLLTH
QRTHTGEKPYVCRECGRGFSWQSVLLTHQRTHTGEKPYVCRECGRGFSNKSHLLRHQRTHTG
EKPYVCRECGRGFRDKSHLLRHQRTHTGEKPYVCRECGRGFRDKSNLLSHQRTHTGEKPYVC
RECGRGFSNKSHLLRHQRTHTGEKPYVCRECGRGFRNKSHLLRHQRTHTGEKPYVCRECGRG
FSDRSSLCYHQRTHTGEKPYVCREDE

B) PRDM7 sequence

MSPERSQEESPEGDTERTERKPMVKDAFKDISIYFTKEEWAEMGDWEKTRYRNVKMNYNALI
TVGLRATRPAFMCHRRQAIKLQVDDTEDSDEEWTPRQQVKPPWMAFRGEQSKHQKGMPKASF
NNESSLRELSGTPNLLNTSDSEQAQKPVSPPGEASTSGQHSRLKLELRRKETEGKMYSLRER
KGHAYKEISEPQDDDYLYCEMCQNFFIDSCAAHGPPTFVKDSAVDKGHPNRSALSLPPGLRI
GPSGIPQAGLGVWNEASDLPLGLHFGPYEGRITEDEEAANSGYSWLITKGRNCYEYVDGKDK
SSANWMRYVNCARDDEEQNLVAFQYHRQIFYRTCRVIRPGCELLVWSGDEYGQELGIRSSIE
PAESLGQAVNCWSGMGMSMARNWASSGAASGRKSSWQGENQSQRSIHVPHAVWPFQVKNFSV
NMWNAITPLRTSQDHLQENFSNQRIPAQGIRIRSGNILIHAAVMTKPKVKRSKKGPNS